From the Sea into the Sky

A Research into the Feasibility of Floating High-rise Structures

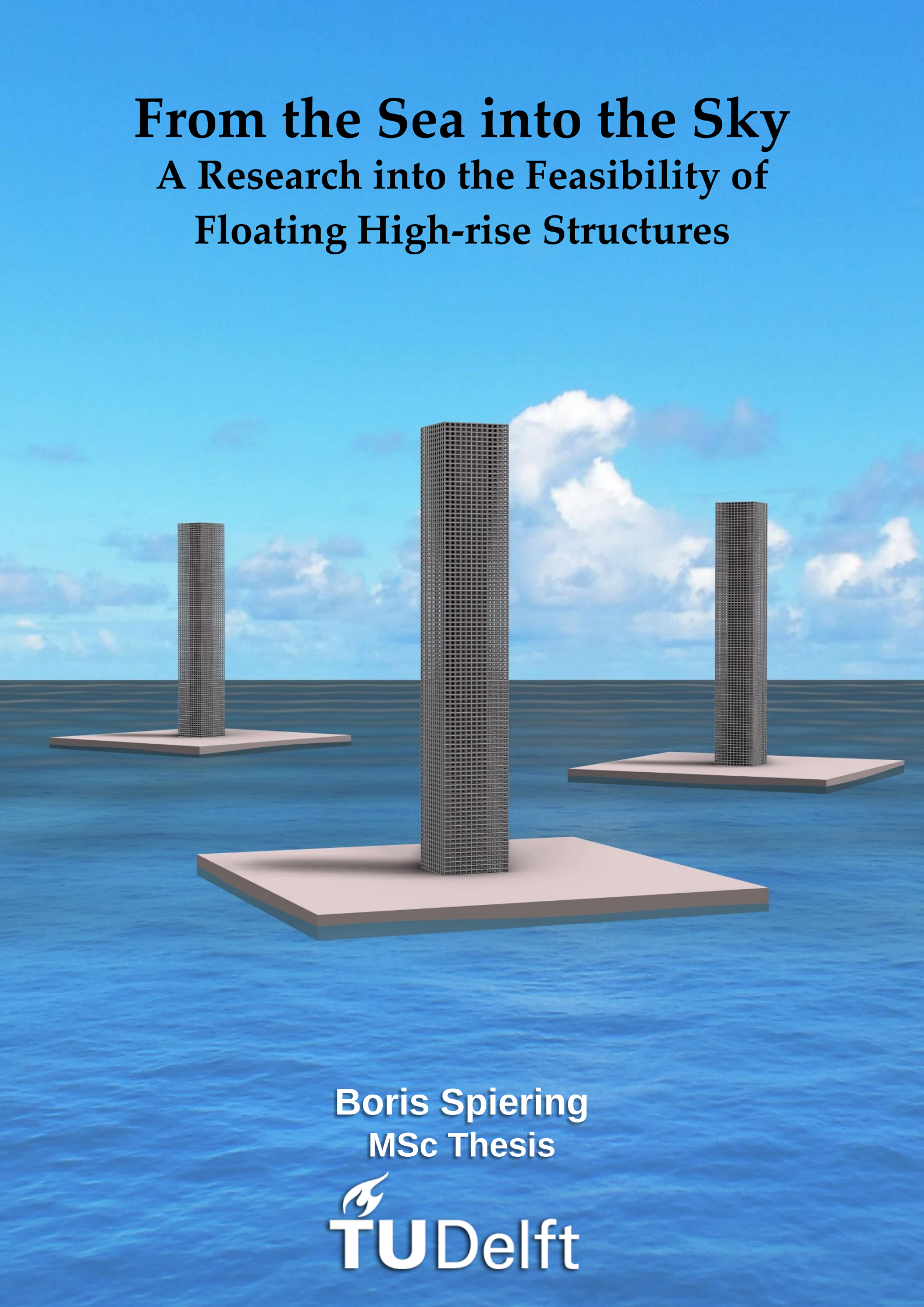

Boris Spiering

MSc Thesis

TU Delft

FROM THE SEA INTO THE SKY

A RESEARCH INTO THE FEASIBILITY OF FLOATING HIGH-RISE STRUCTURES

A master thesis

by

Boris Spiering

Student number: 4489535

MSc. Building Engineer – Structural Design
Delft University of Technology
Faculty of Civil engineering and Geosciences

April 2022

Thesis committee:

Dr.ir. H.R. Schipper	TU Delft, chair
ir. H. Alkisaei	TU Delft
ir. P.H. Ham	TU Delft
ir. P.A. Korswagen Eguren	TU Delft

Delft University of Technology

PREFACE

This master thesis research is the final part of my study Civil Engineering at the Delft University of Technology at the Faculty of Civil Engineering and Geosciences, where I followed both my Bachelor Civil Engineering and my Master Building Engineering-Structural Design Track.

This research came about as a result of my interest in buildings and especially tall buildings, which I have had since I was a child. Never did I doubt about the path in education that I would take to eventually combine my interest and passion with the knowledge I had gained to do research on this intriguing branch of the building industry. To this day, I do not understand why I combined high-rise building with a form of hydraulic engineering with many dynamic aspects, since this was much less of my interest. It is a result of the interest in parametric design and innovative projects in the world of sustainability that led me to investigate floating structures. By combining this with high-rise building, a research has been carried out which for many seems a utopia. But for me it seemed the opportunity to use my specific knowledge and learn many new skills about the aspects of Civil Engineering that are less known to me in order to make this utopia a little more realistic.

Using the knowledge I have gained would not have been possible without all the teachers who have helped me in the various subjects throughout my years of study to acquire this knowledge. Thanks to all of you. Special thanks go to my committee members; Ir. H (Hussein) Alkisaei, Ir. P.H. (Pieter) Ham, Ir. P.A. (Paul) Korswagen Eguren and Dr.ir. H.R. (Roel) Schipper for all advice, feedback, suggestions and help but especially for your patience when I once again came up with a totally new subject for this research, and for kindly forcing me to choose this specific subject because it showed my passion best. Without you, I would still be wandering around looking for a new topic. And with all due respect, I hope I never have to see your living rooms or home offices in the background again as we can meet normally at the faculty.

Apart from my committee members and teachers, I would like to thank my friends, fellow students and housemates for all the support in these tough pandemic times to do a graduation project. Thank you for listening to all my complaints about failed calculations and for listening carefully to the results I found, which sometimes went beyond your comprehension. And of course, thanks to my family who have always supported me throughout not only my studies but my whole life. Without you, I would never have got here. Thank you and I love you.

SUMMARY

Due to global warming and the subsequent rise of the sea level, scarcity of land to build on, the continues increase of the world's population and a shift in population from rural areas to the city, there is a need for innovative projects to tackle or deal with the increase of needed liveable area. One of the solutions is life on the water. Something that has been done on a (very) small scale for hundreds of years, but which has been given a boost to be applied on a large scale by the problems faced today. So that not only houses, but entire cities will be built on floating platforms on the seas or oceans. One component of a modern city is high-rise buildings. High-rise is an advantageous option to deal with the limited availability of ground surface on the floating platforms. The question is whether it is possible to realise these floating high-rise structures.

This research investigates whether it is possible to realise high-rise buildings on floating platforms with limited dimensions on the sea or ocean regarding stability. And if it is feasible, what the requirements are for the general dimensions of both the platform and the high-rise building. For this purpose, conditions were used from the following three representative locations:

- North Sea
- North of the Atlantic Ocean
- Atlantic Ocean around the equator

At these three locations, the floating high-rise is tested for four different wave situations:

- Tsunami.
- Growing waves. For example a developing storm.
- Most extreme wave. A regular wave with the highest possible wave height.
- Irregular wave field. A combination of waves with different frequencies and heights.

The platform and building are tested whether the structure could meet the various requirements and regulations. These are divided into three forms of stability:

- Buoyancy
- Static stability
- Dynamic stability

The most important of the requirements are that:

- The platform does not submerge
- The entire structure is stable
- The accelerations in the entire building are below the determined limits.

In this study, for both the platform and the building a square cross-section is used and both are prismatic in the direction of the height. The platform and building can be seen in Figure 1. The platform and the core of the building are made of concrete. Apart from the four parameters: height of the building and width, height and depth of the platform all other parameters are based on these four parameters. No stability systems in the building were used (except the core), nor methods to keep the platform in place, such as mooring systems.

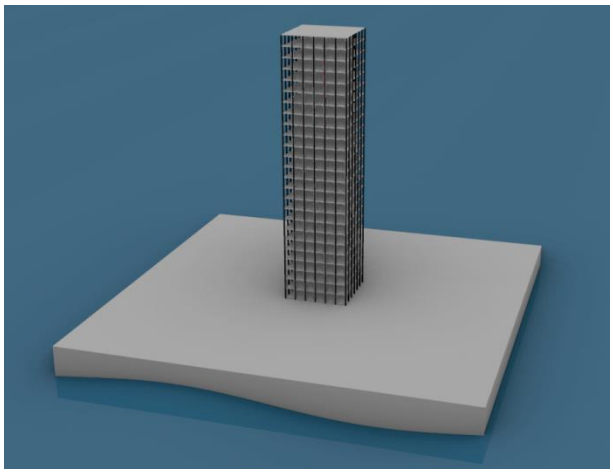

Figure 1 - Render of the platform and building.

For the buoyancy, mainly the relation between the mass and the depth of the platform is determined. This is a relationship that has been used extensively in static and dynamic stability. The mass of the building and platform pose few problems for staying afloat. In fact, extra ballast water can easily be used to make the platform heavier in order to achieve the desired mass or depth.

For the static stability a combination of hand calculations based on the GM-method and a model that can include deformations in the calculations as well is used. A linear relationship was found between the height of the building and the width of the platform for which the floating high-rise is stable. The floating high-rise is stable if the following inequality formula is fulfilled:

$$Height\ building \leq\ 2.3936 * Width\ platform - 44.817 \tag{0.1}$$

The model is used to determine the minimum platform depth and height, as well as the rotation for different building heights and platform widths. It follows that there are platform widths for which the vertical force is minimal. This is when the width of the platform is equal to the wavelength of the wave or a multiple of it. In addition, there are platform widths for which the moment due to the wave force on the platform is minimal. These values are called "zero moment widths" because for these widths the wave moment, regardless of position or time, is approximately equal to 0 kNm. Therefore the rotation is minimal when these zero moment widths are used for the platform width. These widths are only optimal for the specific wavelength for which they are calculated. If the wavelength is different, the zero moment widths will be different.

For the dynamic stability, a model consisting of three point masses distributed over the height connected with a beam was used. Figure 2 shows the schematization. The platform is included in the lower mass. The three point masses each have three degrees of freedom: vertical and horizontal translation and rotation. With this model the accelerations of the three possible motions for different heights of the building, platform widths and platform masses (this can be adjusted by

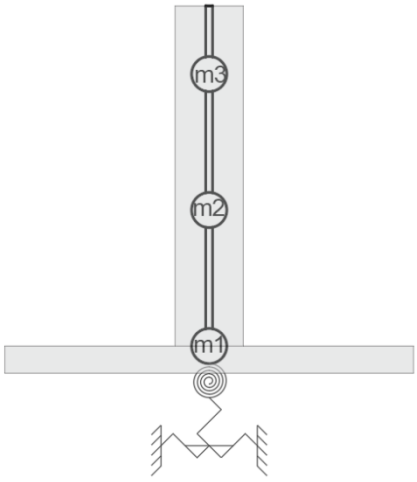

Figure 2 - Multiple mass model of the dynamic stability.

including ballast water) are calculated. It follows that:

- The tsunami and the growing wave are not a problem and the most extreme wave or the irregular wave field is normative.
- The vertical acceleration is minimal when the width of the platform is equal to the wave-length or a multiple of it.
- The vertical acceleration is only normative for small building heights and platform widths, whereas it is the biggest cause of seasickness.
- The horizontal acceleration at the top of the building due to both the horizontal motion and the rotation is almost always normative. It is largely caused by the rotation of the platform.
- If the zero moment widths are used for the width of the platform, the rotation and thus the horizontal acceleration is minimal. This does not mean that the accelerations are below the limit.

In order to avoid resonance in the motion, and thus extreme accelerations, of the floating high-rise with an irregular wave field, graphs are made were the combination of the height of the building and the width of the platform that result in resonance are shaded. An example is shown in Figure 3. In addition to the frequency limits, the depth limit is shown as well. This is the limit for which the depth of 20 m is still possible. Finally, the previously obtained stability limit is shown. These graphs do not say anything about the accelerations and even if a combination of parameters is chosen outside the shaded area, the acceleration may be too high.

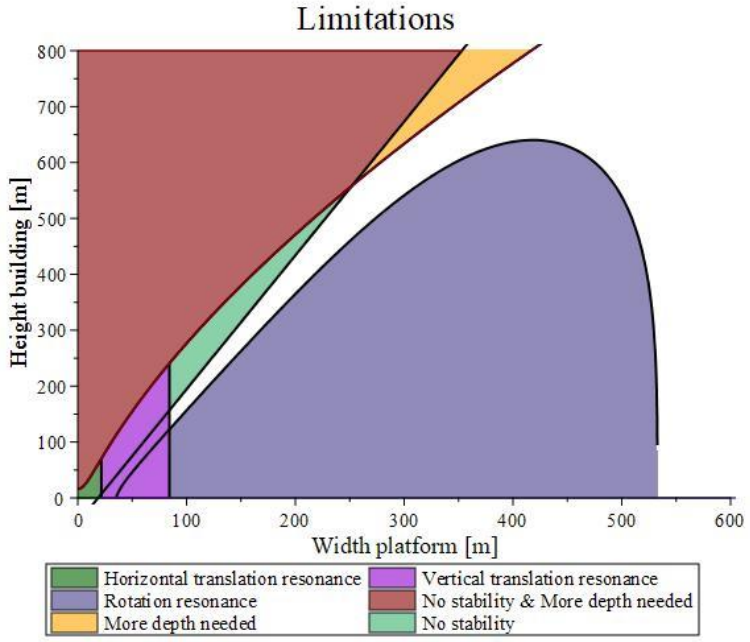

Figure 3 – A graph of different limitations. The shaded areas are not usable. This graph is an example. It is applicable for the North Sea location, for a platform with a depth of 20m. Note: The shaded areas can overlap, this is not visible.

Using the results of the static and dynamic analysis and a few case studies, it can be concluded that with the design choices and simplifications used, it is not possible to realise floating high-rise buildings on platforms with limited dimension at the North Sea and the North of the Atlantic ocean due to too extreme condition causing too high accelerations, especially in the horizontal

motion. The static stability and the buoyancy are less of a problem. If one of these locations is chosen, platforms over 600 m wide are required that are so stable that the rotation of the platform is minimal and no resonance occurs in the rotation motion. In this case, the conditions are similar to those on land and the wind force becomes the governing factor. In those cases, the same approach and measures should be used as for high-rise buildings on land. Even with these sizes, it is advised to use the zero moment widths to limit the rotation as much as possible.

The location on the Atlantic Ocean around the equator is the only location that is promising. The results show that several building heights are possible on different platform dimensions for the highest wave, as long as the platforms have the zero moment widths dimensions. However, it appears that the accelerations become too high when these sizes for the building and platform are tested with different wave frequencies with lower wave heights. Therefore, this option might not be suitable either, but it is not excluded in this research. One option is found that meets the regulations for all possible wave frequencies is a 50 m building on a platform 223 m wide (a zero moment width) and 22.7 m deep for the location around the equator. This proves that it is possible to construct high-rise buildings on platforms of limited size with the design choices used, but that it is very difficult and the options are limited.

Despite the conclusion that it is almost impossible with the design choices, floating high-rise buildings on limited platforms are still expected to be possible as the design can be improved. The first next steps to investigate are other, better shapes for the platform and building to increase stability and reduce overall forces. In addition, it is recommended that other methods of increasing stability and reducing motion, such as building stabilisation systems and tuned mass dampers, are investigated. With these improvements floating high-rise is more feasible than found in this research.

LIST OF SYMBOLS

a Added mass

c Damping value

d Depth platform

g Gravitational acceleration ($9.81\ m/s^2$ is used)

h_b Height of the building

h_p Height platform

k Spring stiffness

m Mass

mv Motion vector

q Distributed force

r Distance between the centre of gravity and the surface of the water

t Time

u Horizontal displacement

u_{10} Wind speed at reference height of 10 m.

u_{wind} Wind speed

v_b Wind speed at reference height

w Vertical displacement

w_b Width of the building

w_c Width core

w_p Width platform

z Depth of the water

A Area

A_w Cross-section of the platform at the height of the water

B Centre of buoyancy

COG Centre of gravity

DOF Degree of freedom

E Young's modules (E-modules)

EI Bending moment

EM eigenmode

F Force

G Centre of gravity

GM GM value

$H_{5\%}$ Wave height with 5% probability of exceedance

H_s Significant wave height

H_{wave}/H_w Wave height

I Second moment of area

J Mass moment of inertia

K Keel position

L Length between two point masses

L_{wave} Wave length

M Meta centre

M Moment

T_w Either wave or wind period

T_{wave} Wave period

T_{wind} Wind period

V_{sub} Submerged volume

S Energy density

W Weight

ζ Damping ratio

η Vertical displacement of the water

θ	Rotation
ρ_{water}	Density of water
φ	Phase shift
ϕ	Rotation
ω	Frequency
ω_0	Eigenfrequency
ω_e	Natural frequency
ω_p	Peak frequency
ω_w	Either wind or wave frequency
ω_{wave}	Wave frequency
ω_{wind}	Wind frequency

TABLE OF CONTENT

1. INTRODUCTION

1.1 BACKGROUND INFORMATION

The building and construction industry is always changing. New challenges arise and new techniques and designs are created to overcome them. A subject which could be a solution for many challenges is building on water, and although this has been done for decades, there is a renewed and increased interest. This is due to the current challenges such as global warming and the subsequent rise of the sea level. A report by the IPCC predicts a rise of between 0.29m and 1.1m in the global mean sea level. Depending on the location, this rise could be up to 30% higher locally (Oppenheimer et al, 2019). Since most cities are located near the sea, this is a potentially disastrous increase. As this will result in much higher risk of flooding of land areas.

A second challenge is scarcity of land to build on. The world's population continues to grow and more and more land is needed to live on, grow food on and extract raw materials of. Especially for the urban (build) environment, space is limited. In addition, there is a shift in population from rural areas to the city in many countries. This increases the pressure on cities that already have many inhabitants (Flikkema et al, 2021). Various functionalities, including infrastructure, compete for the limited space available (Jonkers, 2019). According to IPCC reports 70% of the global, ice-free land surface is already being used by mankind and this will only increase. 1% of this is used for infrastructure (Shukla et al, 2019). This value is even higher in densely populated countries such as the Netherlands where 69% of the land surface is used for agriculture and 17% for infrastructure (Centraal Bureau voor de Statistiek, 2020). The decrease in natural areas has the effect of increasing global warming (natural areas convert greenhouse gases, act as a sink for greenhouse gases and increase the reflection and absorption of heat) and decreasing biodiversity. This decline in diversity results in declines in ecosystem functioning and ecosystem stability (Naeem, et al, 2009). The increase in human population and the struggle for land use results, among other things, in the challenge of housing shortages. Finally, there is a rise in offshore activities that is leading to an increase in life on the water (Flikkema et al, 2021).

Another less pressing challenge has more to do with an urge for humanity to search for the limit. In construction, one of those limits is the possible height of a building. And thus the question is raised “How high can we go?” Answering this question is fuelled by the prestige gained when the height record is broken. Therefore, new research is done and new ingenious designs are being created to tackle the problems that accompany higher building heights. The highest building at the moment is the Burj Khalifa extending 828 m above the ground, increasing the record for highest tower with 62 % but even higher buildings are being planned.

A possible solution to all of the before mentioned challenges is building on water. This is already being done in several countries and comes in many forms. One of these forms is the building of floating structures. These floating structures are not founded on piles, but are held up by the buoyant force. Often this involves a house that is moored at the quay of a river, but there are floating villages as well. For example the modern and sustainable floating district of Schoonschip in Amsterdam, but also older villages in poorer counties such as the floating villages in Tonle Sap Lake, Cambodia. If more and more people will live on the water, this will even lead to floating cities.

Floating cities provide the possibility of new land to build on an thus offer the opportunity for housing, food production, producing energy and creating living environments (Rui, Boogaard & Sazonov, 2020) and have a lower total environmental and local impact as floating cities can be moved easily. (Flikkema et al, 2021). If the floating buildings are designed to withstand the conditions on the water, the rise of the sea level will no longer be a problem for the city. The floating city will simply float higher. In addition, a floating city creates better possibilities for offshore workers, housing, tourism and the sea is a more effective location for generating wind energy (Flikkema et al, 2021).

To make the floating villages and cities, buildings are placed on (multiple) floating platforms. This does give a different and perhaps more difficult set of boundary condition and challenges for the design of a building than on land. This means that other decisions will be made and different solutions need to be found in the design process. With the advent of cities come high-rise buildings. As on land, high-rise buildings on floating platforms have the advantage that they use little surface area and they house many people and provide many services. This can be advantageous as the platform area can be smaller or it can be used for other functions such as agriculture or leisure. As mentioned, the floating aspect poses potential problems, and the same applies to floating high-rise buildings. Therefore, high-rise buildings should be rethought and the influence of floating on high-rise buildings should be investigated. This changes the previously asked question about high-rise to "how high can we float?"

When thinking in extremes the question can perhaps simply be answered. When the floating platform is extremely wide and deep it will result in the same conditions as on land and therefore the buildings can become just as high as on land. According to Flikkema et al. (2021) "*The challenge for floating islands is in achieving a technical solution that resembles onshore conditions as much as possible*." There are several different ideas for floating cities, but they can be sorted into two groups: Cities on one big platform and cities on multiple smaller platforms. There are already some projects in the second group that have been investigated, designed and planned. This option seems the more likely option for the near future and the more problematic for the realisation of high-rise buildings. Therefore, the design aspects of high-rise buildings when placed on a platform of limited size should be studied.

1.2 RESEARCH DESCRIPTION

The research description consists of the research aim, which explains the direction of this research. This is followed by the research questions. From these research questions, the research objectives are determined. For these objectives, sub-questions are formulated. The research description ends with the description of the research approach and the methodology.

1.2.1 RESEARCH AIM

This study attempts to form an understanding of the influences of floating on high-rise buildings placed on a floating platform of limited size. Platform of limited size are platforms with dimensions for which floating has an impact on the requirements of the building. This will ultimately help to determine what is required in the design of the building and the platform to achieve a certain building height and to estimate the limits of this height. In this research, the stability of the building, and thus the entire floating high-rise, is examined as the stability is often normative in both high-rise structures and floating buildings. The stiffness is partly investigated, especially its influence on the stability. No research is being done into the strength of the building.

In order to determine the influences of floating on stability the conditions at different locations where a floating city can be built, will be investigated. This will result in the forces acting on a floating platform and on the high-rise building. Calm and extreme locations will be used to determine whether the floating high-rise can be realised in different conditions and to investigate the difference in requirements. Regulations and other limitations will be used to determine the possibility of floating high-rise and the maximum possible height of the building at these locations.

To investigate the stability, three aspects will be examined. These are the buoyancy, the static stability and the dynamic stability. For all three, the influences are examined, the limitations are determined and the limits calculated, in order to compare and conclude what is normative.

All this should lead to a determination of the requirements for the building and for the platform for certain building heights for different locations. This will determine whether the floating high-rise is feasible from a standpoint of stability and what the possible heights of the building on a platform with a limited size are.

1.2.2 RESEARCH QUESTION

The following two research questions follow from this research aim:

Research question 1:

Is it structurally feasible to construct high-rise buildings on floating platforms which are limited in size regarding stability?

Research question 2:

What are the requirements for both the platform and the building regarding the stability of a floating high-rise building for different building heights?

1.2.3 RESEARCH OBJECTIVES AND SUB-QUESTIONS

The two main research questions can be divided into five objectives. Each objective has its own set of sub-questions. These questions help to answer the main research questions. The research consists of the following five objects:

1. Examining the various topics that form a basis for this research. These are the following topics: Floating buildings, floating cities, high-rise buildings, locations and conditions and regulations and limitations. These topics all have their own sub-question:
   - What are floating buildings?
   - What has been researched so far about floating cities?
   - What are high-rise buildings?
   - On which locations can floating high-rise be realised and what are the conditions on these locations?
   - What are the different extreme conditions to be investigated?
   - What are the different regulations and limitations for floating high-rise buildings?
   - What are the assumptions that have to be made for this research?

2. Investigating the buoyancy of a floating high-rise building.
   - What is static buoyancy?

- How is the buoyancy determined?
- What parameters influence the buoyancy?

3. Investigating the static stability of a floating high-rise building.
   - What is static stability?
   - How is static stability determined?
   - What are the influence parameters and what influence do they have?
   - What are the requirements for the platform and for the building for different building heights in terms of static stability at different locations?

4. Investigating the dynamic stability of a floating high-rise building.
   - What is dynamic stability?
   - How is the dynamic stability determined?
   - What are the influence parameters and what influence do they have?
   - What are the requirements for the platform and for the building for different building heights when it comes to the dynamic stability at different locations?

5. Testing, assessing and drawing conclusions about the results found with a case study.
   - How should the results found be used in a case study?
   - Are the results from the case study according to expectations when compared to the results and conclusions of the research?
   - What can be concluded about the research questions with the results of the case study?

1.2.4 Research Approach and Methodology

The three phases of the research can be identified from the objectives: The context phase, in which research is carried out into floating construction. The exploration phase, in which research is carried out into buoyancy, static stability and dynamic stability, and the testing phase, in which a case study is used to test and asses the found results and to draw conclusions about the research questions.

Phase 1: The context phase.

In the context phase, the floating of buildings and cities is investigated. This is done with a study of literature on floating and on high-rise buildings, researches done on floating buildings and cities and a study of different possible locations by determining the condition and thus the availability for the floating buildings and cities. The characteristics of waves and wind are investigated and the most extreme cases are determined to be used in the calculations in the next phase. In addition, using regulations and research, limits are set for buoyancy, static stability and dynamic stability. This will all be in chapter 2. Subsequently in chapter 3, the assumptions for this research will be made and described together with the case parameters. This is a standard set of values for the different parameters that will be used in the next phase.

Phase 2: The exploration phase.

In this phase, both static and dynamic stability are investigated. To examine these two, it is necessary to look at buoyancy as well. The study of buoyancy will then serve primarily as a form of input for static and dynamic stability at will be done in chapter 4. In this chapter no results will

be shown or conclusion drawn, these will be incorporated in the results of the static stability as buoyancy is a form of static stability. Chapter 5 will consist of the static stability and chapter 6 of the dynamic stability. Because these stabilities differ substantially from each other, they have their own methodology. This is described below for both.

Static stability

For the static stability, it is determined, with the aid of literature, how stability can be determined. This involves researching and determining which calculations should be used. With the help of these calculations, it can be determined which parameters play a role and how they are related. Subsequently, the formulas that are necessary to calculate the parameters or to determine the relationship between the parameters are determined.

Then the calculations can be done. For the static stability this is done with the help of Grasshopper/Rhino including the plugin Karamba. This programme is used because it works parametrically. This means that the parameters can be used as input, the calculation can be done with the corresponding result and then the parameters can be changed. This has the advantage that the behaviour under different values of the important parameters; height of the building and width of the platform can be examined and optimised.

Dynamic stability

For the dynamics, first the different motions that the building can undergo are investigated and it is determined which are the most important to investigate. Then the calculations are done for these different motions to determine the behaviour of the motions and the accelerations. This is done by using different models/schematizations that build up in complexity. At first, one point mass with one degree of freedom is used, in this research it is called the single-mass model. This is to investigate how the individual motions work and which parameters play a role in this motion. To investigate the influence of these parameters, the calculations are carried out with a fixed set of "standard" parameters, except for one parameter, which will be variable. With these calculations, graphs are made from which the influence of the parameters can be described. In addition, the relations between the parameters will be used in order to leave only the height of the building and the width of the platform as changeable parameters, which are the two most important parameters. The relations will follow from the literature or assumptions that are made. This will allow a better investigation of the actual values of the parameters and the corresponding motions and accelerations.

After looking at the motions separately, the whole is schematized as one point mass with several degrees of freedom (and thus several motions). This gives the same results as when the motions are considered one by one, but it is a necessary step to extend the model to a multiple mass model with multiple degrees of freedom, in this research called the multi-mass model. It is determined how many point masses are needed and with this number of masses the investigation into the influence of parameters is repeated. Subsequently, the results of the single-mass model and the multi-mass model are compared.

For the dynamic stability, manual calculations are used instead of modelling software. The reason for this is that Grasshopper/Karamba does not have a dynamics component, which means that this software cannot be used. Also no other modelling software has been used because these lack the parametric aspect. If the parameters would change, the whole model would have to be

modified. This is too much work to be advantageous. The calculations are done in the Maple software. This is a programming language that can be used to work symbolically, in addition to numerically. This helps in understanding the consequences of changing parameters. The programme is useful for solving differential equations. Something that often has to be done in a dynamic analysis. However, the software DIANA is used as well. This is a Finite Element Analysis solver that, besides actual constructions, has a more conceptual aspect in the form of point masses as well. This software is used to validate the calculations and to investigate the number of masses that should be used.

Phase 3: The test phase

In the test phase, the results, advice and conclusions from the exploration phase are used to illustrate what they mean in the situation of designing a floating high-rise structure. For this purpose, in addition to the results of the exploration phase, the calculations described in this phase for the chosen/determined parameters in the case study are done as well. These are not only meant to illustrate how the results can be used but also to check how reliable they are. In addition, the case study is used to draw conclusions about the different possibilities of the floating high-rise.

2. LITERATURE REVIEW

In this literature review, the first three paragraphs discuss floating homes, floating cities and high-rise buildings. The fourth paragraph is about information needed for this research. This consists of the locations, properties of the waves and wind and the different possible forms of waves that the floating high-rise must be tested for. Finally, paragraph 5 discusses the regulations and limits that the floating high-rise must comply with.

2.1 FLOATING BUILDINGS

The first villages and towns in history were built near rivers, lakes and seas. The water brings numerous advantages necessary for survival. It provides drinking water and food in the form of fish and other animals attracted by it. It also creates fertile land. It offers possibilities for transportation and trade, natural protection, it moderates the climate and the land is often flat. The water is so important that in the course of the centuries houses were not only built next to the water but also on the water.

Many centuries ago fishermen built their own floating village by the sea in southeast Fujian province of Luoyuan Bay, China. In South America on Lake Titicaca floating islands were created by the indigenous people of Peru and Bolivia (Lin, Spijkers & Van der Plank, 2020). In Cambodia on Tonle Sap Lake the Khmer civilization started building floating villages between the 11th and 13th century (Lau-Bignon, A.W, 2015). Living on water is still done here to this day.

Figure 4 – Floating homes in Luoyuan Bay, in south-eastern China's Fujian province (left). Image: Daily mail (Thornhill, 2022). Floating home on Tonle Sap Lake (right). Image: Angela Altus (Altus, 2022).

Life on water in these examples is mainly due to the convenience of living close to the source of food or income. Many of the inhabitants are fishermen. But it is not only in these, poorer, parts of the world that people live on water. In the western world, too, there is a history of living on water. There are examples of floating homes in the United States. For example in Seattle there is a big cluster of houseboats, a tradition that dates back over more than a hundred years. And there are many more examples all over Europe. One country that has a rich history, and present, in floating homes is The Netherlands.

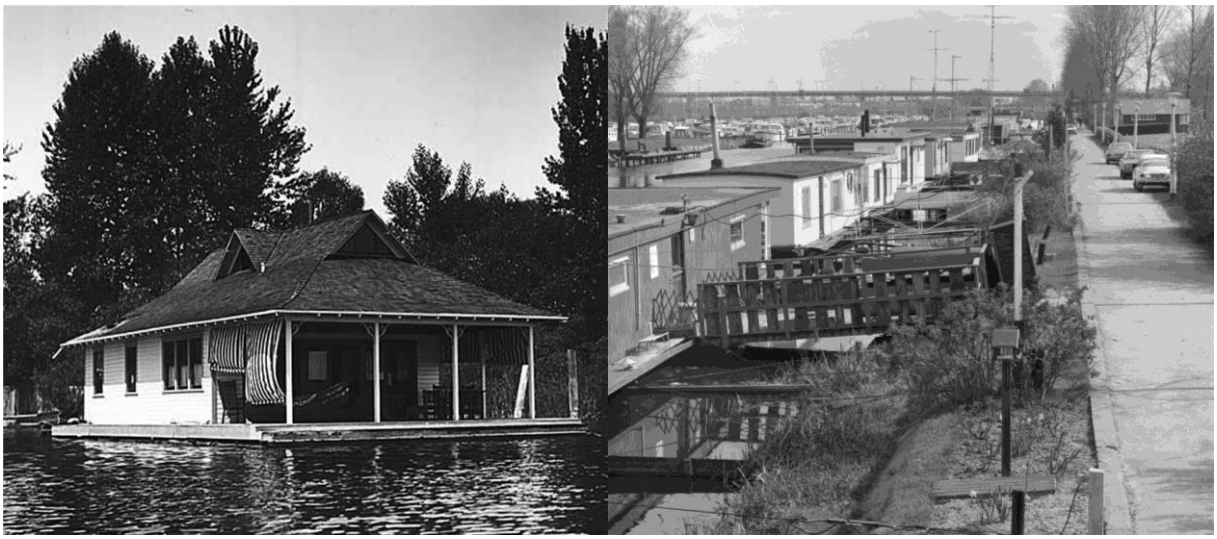

Figure 5 - Houseboat in Seattle, USA from 1905 (left). Image: Mohai (Blecha, 2010). Floating homes (woonschepen) Noorderkanaal, Rotterdam, Netherlands (right). Image: Gemeente Rotterdam.

In addition to the long history of living on water, there are many modern and future projects in The Netherlands, such as the floating neighbourhood in IJburg, Amsterdam and the floating homes of the Nassauhaven in Rotterdam. See Figure 6.

Figure 6 - Floating neighbourhood Ijburg, Amsterdam (left). Image: Marcel van der Burg. Floating lofts Nassauhaven, Rotterdam (right). Image: Gemeente Rotterdam.

Besides floating houses, there are projects of other floating constructions such as the floating pavilion and the floating office in the Rijnhaven, Rotterdam and the floating farm in the Merwe-Vierhaven, Rotterdam. There are also bigger projects, for example Sebitseom in Seoul. This is an art gallery build on three floating islands. See Figure 7.

Figure 7 - Floating office Rijnhaven, Rotterdam (left). image: Powerhouse Company. Sebitseom, Floating island on the Han River in Seoul, South Korea (right). Image: Haeahn Architecture.

2.2 FLOATING CITIES AND HIGH-RISE

These floating projects are the introduction to a new form of floating where the floating structures do not only house people but can have different and multiple functions: Floating Cities. According to Blue 21 founder De Graaf, it is *"time for a blue revolution"* and cities must be built on water as it is a solution to the scarcity of space and reduces the vulnerability of floods and other extreme weather events (De Graaf, 2021). In Figure 8 two of Blue 21's plans are shown. With the blue revolution as a goal, Blue 21 aims to design floating cities that are fully self-sufficient. One might wonder why the cities have to float and why the ground is not raised to make it dry or why it is not founded on piles that reach to the bottom. This is not always a solution as it is not feasible to create artificial islands that are fixed to the bottom when the bottom is deeper than 20 to 25 m (Flikkema et al, 2021). For deeper seas and oceans floating is a solution.

Figure 8 - Blue revolution plan (left). Seasteading implementation plan (right). Images: Blue21.

To achieve floating cities there are multiple projects investigating every aspect of it. For example the Space@sea project. The aim is to design a workspace at sea which is both sustainable and affordable. Four applications for the floating city have been investigated as they were deemed especially interesting; energy hub, transport and logistics, aquaculture and living. All with their own requirements (Czapiewska, K, 2021). In one of the deliverables of the project an exploration is done into the design of modular floating platforms. Initially, it was tried with triangular platforms. It was concluded that this is possible but that square platforms are better for spatial distribution and usable space. Therefore, they switched to square platforms. Two designs were made: a platform with sides of 45 m, that needs a depth of approximately 10 to 11 m, and a platform with sides of 90 m. The latter was better for the North Sea because of the conditions at this location (Zanon, et al, 2017). The platforms can be connected to form a city, see Figure 9 for one of the concepts.

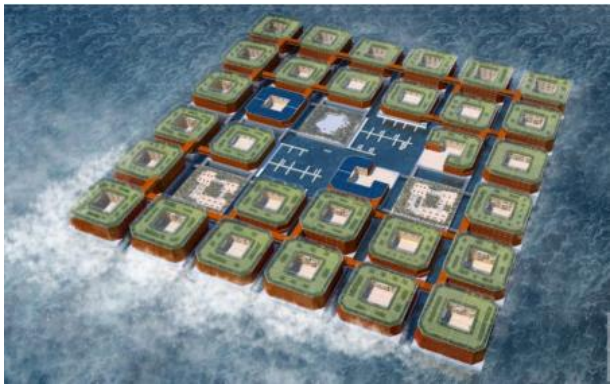

Figure 9 - Fortress concept of Space@sea. Image form Zanon, et al, 2017.

Another project that is attracting a lot of attention is the "Oceanix city", see Figure 10. A collaboration between the BIG-Bjarke Ingels Group, UN-Habitat's New Urban Agenda, Massachusetts Institute of Technology (MIT) and the Busan Metropolitan City in South Korea. A plan that is supported by the UN. The following info is obtained from Oceanix Ltd (2021): The city will be able to accommodate 10,000 people on 75 hectares of platform and will be self-sufficient in terms of energy, water, food and waste processing. Creating a blueprint for a modular maritime metropolis. The city is made up of neighbourhoods. These are communities of up to 300 people on a hexagon-shaped platform. Each district has a mixed-use space for living, working and leisure. The buildings in the districts are kept below seven storeys to create a low centre of gravity. The neighbourhoods are clustered in groups of six to form a village with a central protected harbour, as shown in Figure 11. These villages can house up to 1,650 people. These villages can also be linked together to create a city with a protected harbour at its centre. The city is designed to withstand natural disasters such as floods, tsunamis and hurricanes (Myers, 2021).

Figure 10 – Oceanix city. Image: OCEANIX/BIG-Bjarke Ingels Group

Figure 11 - Plan view of the Oceanix city. Image: OCEANIX/BIG-Bjarke Ingels Group

These are just a few examples of designs and research on floating cities. Often with modular platforms with buildings of a few floors high. However, the image on the right of Figure 8 shows a large tower in the floating city as well. The Space@sea project has not yet reached the subject of higher buildings, but there are other studies and projects on floating high-rise buildings. These will be discussed here.

Ko (2015) investigated whether it was at all possible to realise a floating city. Hexagonal shaped platforms were used with sides of 60m and a depth of 6m, connected to each other. Each platform was schematised as an infinite stiff block. The result was that it is technically feasible to realise floating cities with modular platforms. In his research a small study was done into higher buildings on the floating platforms. Ko (2015) investigated whether it was possible to realise high-rise buildings on these floating platforms. The starting point of the research was a rectangular building with a height of 50 m centred on the hexagonal shaped platform. After calculating the stability the conclusion of the research was that the platform will ensure stability for a building of this height. Than calculations were made to investigate how high the building can become before it will result in instability. The findings are that a height of 141 m can be reached. It is noted in the research that simplifications are made in wind action and that the building cross-section is constant over the height. When the building would become more slender with height, the centre of gravity would be lower and thus the floating module would be more stable.

Another study on floating high-rise buildings is the paper "*A study on stability of floating architecture and its design methodology*" (Nakajima, Saito & Umeyama, 2020). It describes the calculations that need to be done to get a good estimate of the dimensions of the platform. These will be used as a guide for the static stability chapter. One of the cases used is the "Singapore Water City" where three 51-storey towers are built on a floating platform. The buoyancy and static stability is described and calculated for a floating high-rise. The location is however not at the open sea or ocean but in a bay like area.

There is even a study that has questioned how high we can float. In Van Winkelen's research “How high can we float?” a design was made for a floating hotel with calculations for buoyancy, static stability and dynamic stability (Van Winkelen, 2007). This was located in a protected area near the quay as well.

This paragraph ends with a final, very ambitious plan. The "Green float". A collaboration with, among others, Blue 21. The design is for a circular platform with a diameter of 3 km. With a 1 km high tower in the middle, see Figure 12. Besides liveability, sustainability and other issues, the

safety of the project was also considered. For example, the green float is balanced by 400 million tonnes of ballast water. The designers expect that with the dimensions of the whole, the normal sea, strong wind waves and tsunamis will have almost no influence on the structural safety. Inside the building there are evacuation areas that are safer than other parts of the building, there is vibration-reduction equipment to counteract the strong wind forces and there is a wave buffering mechanism to counteract high waves. The green float will not be held in place but will move with the tide around the equator (Shimizu corporation, 2020). However, this project is still in its infancy and much more calculation is needed on the actual possibilities, but the ideas and concepts can certainly be used in this research.

Figure 12 - Green float. Image left from Takeuchi & Yoshida (2020). Image right from Shimizu corporation (2020).

These studies and projects form the basis of this study. In this study, the static and dynamic stability is further examined for multiple building heights with a focus on the building. In the previous studies the focus was mainly on the platform and the input was either a specific size of the platform or a specific height of the building. In these previous studies infinitely stiff buildings are used and the dynamics are reduced to some simple formulas that belong to a simplified single-mass model. In this study, the flexibility of the building and the platform will be included in the stability calculations and a dynamic calculation will be done with multiple masses to better approximate the dynamic behaviour of the building. In addition, other locations will be examined. In the two studies where high-rise buildings were designed, the locations have calm water and are near land. This research will focus on locations with much rougher conditions in the middle of the sea or ocean.

2.3 HIGH-RISE

High-rise can be described as a building with many floors. However, there is no specific boundary between low-rise and high-rise buildings. In the Dutch building code (NEN-EN 1990, 2021), high-rise is classified as a building higher than 70 m. However, high-rise buildings are often referred to as such when the height is above 25 m or when there is a lift. In this study, the minimum height of the high-rise is 50 m. All heights above 50 m will be covered by the term high-rise in this research.

Like all buildings, high-rise buildings must be tested for ultimate limit state and serviceability limit state. These consist of: Strength, stiffness, static stability and dynamic stability. Figure 13 shows when which parts are normative (on land). In most high-rise buildings, it is the static sta-

bility, stiffness and dynamic stability (Nijsse, 2019). These problems are amplified by placing a high-rise building on a floating platform. Due to the rotation of the platform, the stability of both the platform and the building will be endangered. In addition, a rotation creates many 2nd order moments in the building, that can lead to severe deformations. Finally, the platform will rotate back and forth, which can cause a lot of motion. This also affects the requirements for the strength of the building. In this study, the strength of the building is not further investigated.

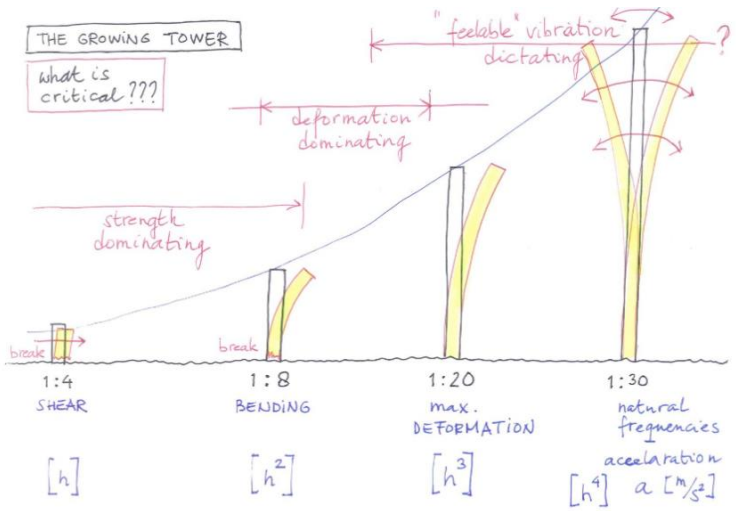

Figure 13 – Critical failure of the growing tower. Image: Nijsse (2019)

To ensure sufficient stiffness and stability and to reduce motion, stability systems are widely used in high-rise buildings. These ensure that the large horizontal forces caused by the wind can be transferred to the ground without the building deforming too much or falling over. There are different forms of stability systems, see Figure 14, that work for different heights.

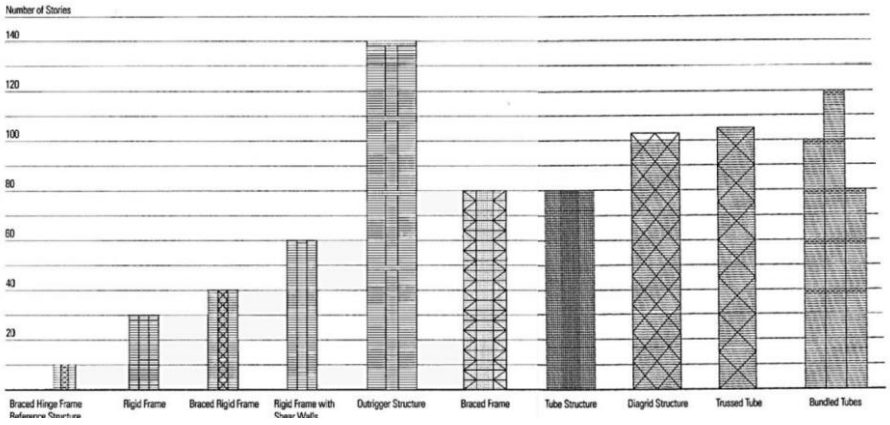

Figure 14 - Stability systems. Image from Ching (2014).

2.4 LOCATION AND CONDITIONS

This paragraph discusses the conditions at various selected locations where the floating high-rise is tested for. The locations are discussed first. Then the characteristics of the waves and wind are discussed. This paragraph ends with the extreme cases. It discusses the various scenarios that can be normative and for which the floating structure must be tested.

2.4.1 LOCATIONS

To determine the stability of a floating high-rise, the conditions on the water must first be described. These conditions can vary greatly from location to location and not every location is equally suitable. Therefore, three locations were chosen for this research to test the floating high-rise; the North Sea in between the Netherlands and Great Britten, the middle of the North Atlantic at the latitude of Spain and the middle of the Atlantic Ocean around the equator, In Appendix I the locations are shown on a map.

The three locations are chosen for different reasons. The location around the equator is the calmest area on the ocean and thus has the best conditions. The North Atlantic is a lot less calm as the wave height is substantial. It is however, a location closer to rich first world countries. As this project will be expensive and only needed when not enough space on land is available, it seems that only these countries will be interested in the near future. Also other parts of the world's oceans have similar conditions and this location can thus serve as an example. The final location is the North Sea. This location is chosen as it is close to land and therefor easier to realise. This location has limited depth giving different boundaries for the platform and it is known for its high wind speeds.

The conditions for all three locations have been determined[1] . These are Significant wave height (H_s), 5% wave height ($H_{5\%}$), Wave (peak) period (T_w), wind speed at reference height of 10 m (u_{10}) and the depth of the sea or ocean. The values are shown in Table 1 below.

Table 1 - Conditions at the different locations.

Location	H_s [m]	$H_{5\%}$ [m]	T_w [s]	u_{10} [m/s]	Depth [m]
North Sea	7.95	9.73	9.8	50	30
North Atlantic	16	19.58	14	40	-*
Equator	4	4.90	10	20	-*

* These depths are so large they have no influence.

To describe the extreme wave heights, the significant wave height is often used. This is the height with a 13.5% probability of ever being exceeded. However, in the Eurocode forces have a probability of exceeding of only 5%. Therefore, the significant wave height is converted to the 5% wave height ($H_{5\%}$) using the formula for the probability of exceeding of Bezuyen, Stive, Vaes, Vrijling & Zitman (2011). The calculation is shown in Appendix I.

2.4.2 CONDITIONS

Wave

To investigate the stability of a floating high-rise, waves will be described. Waves create large forces on the platform and it has a strong asymmetric and dynamic character.

[1] Caires, Groeneweg, & Sterl, (2006). Holthuijsen et al., (1995). Young. (1999). Young, Vinoth, Zieger & Babanin. (2012).

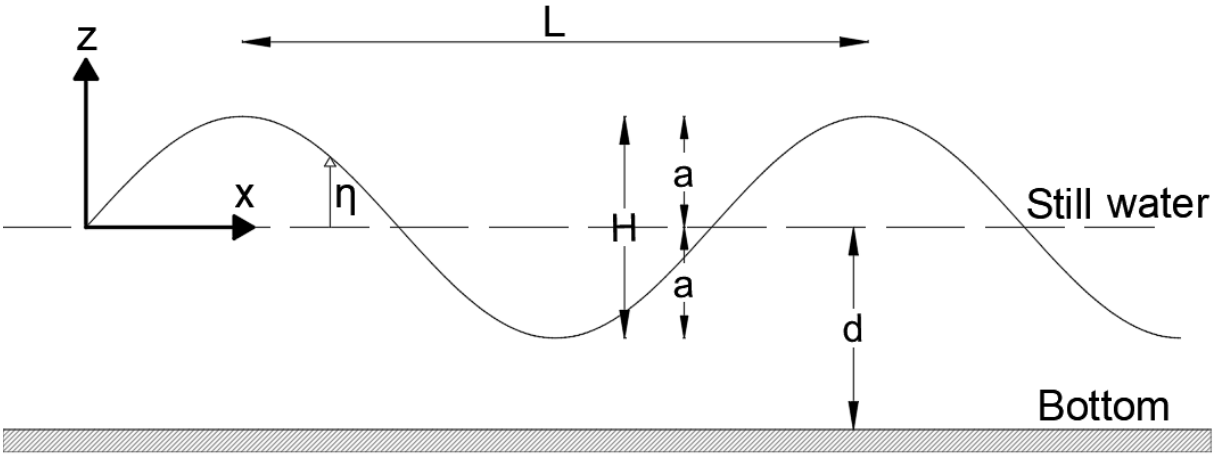

Figure 15 - Sinusoidal wave. (Based on figure 3-28, Bezuyen, Stive, Vaes, Vrijling & Zitman (2011)

A standard, most simple wave can be described as a sinusoid with the amplitude equal to half of the wave height. Figure 15 shows such a wave with the different parameters used in the formula to describe the wave. The height of the wave varies in both place and time. Therefor the formula is expressed in these two variables. The formula for the wave height is as follows:

$$\eta(x,t) = \frac{H_w}{2}\sin\left(\frac{2\pi x}{L_{wave}} - \frac{2\pi t}{T_{wave}}\right) \quad [2] \tag{2.1}$$

Where:

η is the vertical displacement of the water level [m]

H_w is the wave height [m]

x is the distance in the direction of the wave propagation [m]

L_{wave} is the wave length [m]

t is the time

T_{wave} is the wave period [s]

Often in this research the variable x "distance in the direction of the wave propagation" part of the formula is either omitted as it does not matter what the exact locations of the platform is for the most extreme situation. If the platform would be 100m further the most extreme condition will simply occur earlier or later but will be the same. Or the variable is used to convert the 2D wave formula in a 1D force or moment.

For the different locations the wave height and wave period are known. The wave length can then be calculated by the formula:

$$L_{wave} = \frac{g * T_{wave}^{\,2}}{2\pi}\tanh\left(\frac{2\pi z}{L}\right) \quad [2] \tag{2.2}$$

Where:

g is the gravitational constant (9.81 m/s^2)

[2] Bezuyen et al, 2011

z is the depth of the water [m]

As the wave length is both on the left and the right side of the equation it has to be solved with multiple iterations. However, the depth of the water in the ocean is so great that the tangent hyperbolic will approach 1 so that the wave length is only dependent on the wave period. Note, this doesn't apply to the North sea where the depth is not that large. For the calculation of the wavelength of the North Sea see Appendix I.

To include the waves in a calculation, the wave height must be translated into a force. To do this, the wave height can be multiplied by the "force of the water" which is equal to the density of the water times the gravitational acceleration:

$$F_{wave}(x,t) = \frac{H_w}{2}\sin\left(\frac{2\pi x}{L_{wave}} - \frac{2\pi t}{T_{wave}}\right) * \rho_{water} * g \tag{2.3}$$

Although the term "wave force" is used, this is the buoyancy force that is no longer equally distributed over the platform because the height of the water is no longer equal. The buoyancy force is described in detail in chapter 4. To model the wave, however, the "wave force" is used. The force is equal to the buoyancy force of the difference in water height of the wave with the still water. This means that the wave force can be negative (work downwards). Because of the still water buoyancy force that is always present the total force will not be negative. Appendix II shows the calculations that coverts the formula of the height of the wave to the distributed wave force and to the moment of the wave.

In reality this sinus wave does not occur, waves are rather made up of multiple sinusoidal waves (Bezuyen et al, 2011). Which gives a rather irregular wave pattern as can be seen in the typical random wave time history of Figure 16. These random waves or irregular wave field can cause problems as it has multiple frequencies. However, it is a complicated collection of several sinusoids and there are an infinite number of possible combinations. It is therefore impossible to describe them all. Therefore, this research focuses on the possible frequencies that can occur in an irregular wave field. The irregular waves will be considered as an extreme case that can cause problems. This will be discussed in more detail later in the chapter.

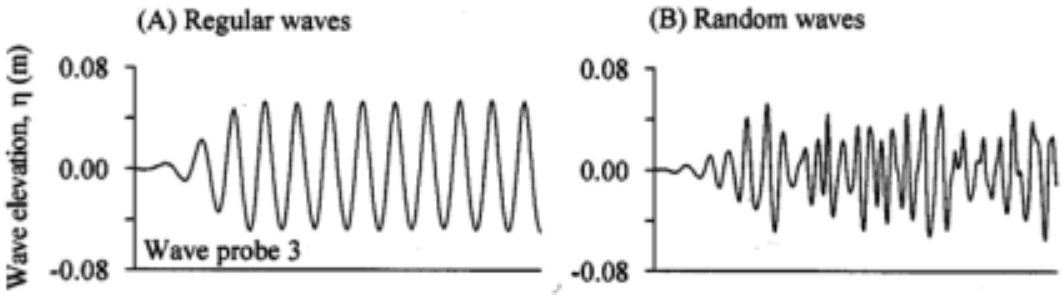

Figure 16 - Typical regular and random wave time histories, (Based on figure 4, Balaji, Sannasiraj, & Sundar. (2007))

Because of the huge influences the waves have on the building, floating breakwaters will have to be used. In the Floating Forest research by Wang et al. (2020) a floating breakwater was designed and tested for a coastal zone in Australia. The resulting transmission of waves is below 50% for a wave period lower than 30 s. The transmission is even lower for shorter wave peri-

ods. For this research a transmission factor of 0.5 is used for all locations. This changes the values of Table 1 to the values in Table 2. The wave height with breakwater is denoted as H_w and is used in all the forthcoming calculations.

Table 2 - Wave height with a breakwater with transmission of 0.5. H_w is the wave height with breakwaters

Location	H_s [m]	$H_{5\%}$ [m]	H_w [m]
North Sea	7.95	9.73	4.87
North Atlantic	16	19.58	9.79
Equator	4	4.90	2.45

Wind

For the calculation of the wind force on the building the NEN-EN 1991-1-4 code is used together with assumptions and simplifications. For the input for the wind force calculation, the wind speed at a reference height of 10 meters is used with a return period of 100 years. The wind will have the distribution as described in the code which can be seen in Figure 17. In Appendix I the calculation is shown to calculate the maximum wind speed (u_{max}) based on the wind speed at a reference height of 10 m (u_{10}). The calculation of the wind force and the moment due to the wind can be seen in Appendix II.

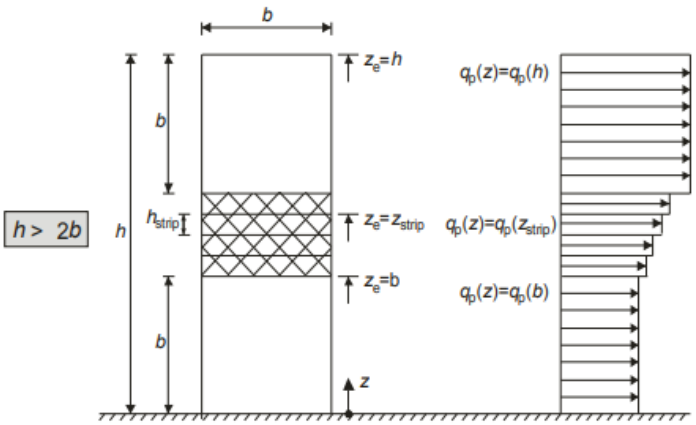

Figure 17 - Distribution of the wind force.

To include the wind in the dynamic analysis, the dynamic behaviour of the wind will have to be studied and described. For the dynamics it is necessary to be able to describe the wind over a certain time period. Wind has a dynamic character as illustrated by a graph of wind speed measurements for a mast in Figure 18. The wind speed, and thus the wind force, can vary greatly in a short time and is thus quite chaotic. Therefore, it is difficult to accurately describe the behaviour of the wind in one formula. To be able to include the dynamic aspect of the wind in the models for the motion, the wind is modelled as one sine function.

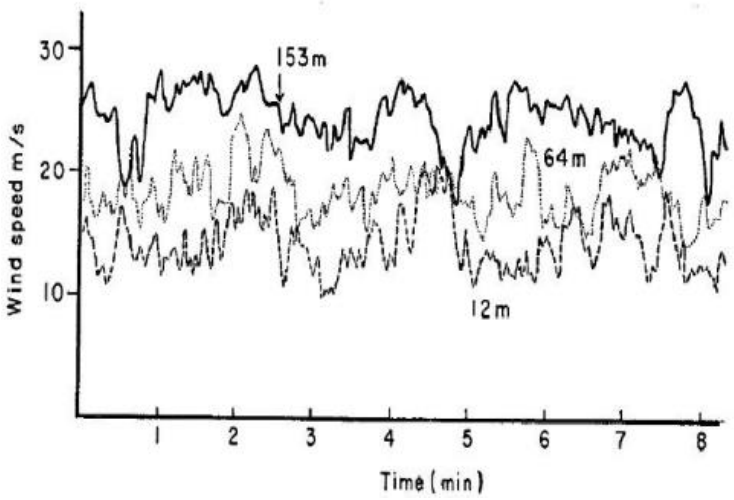

Figure 18 - Record of wind speed at three heights on a 153 m mast in open terrain. From Solari, Carassale & Tubino (2007).

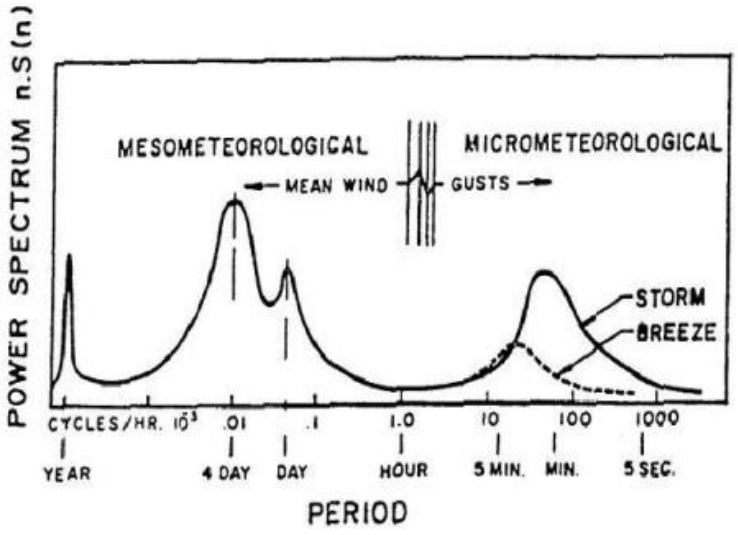

Figure 19 - Wind spectrum. From Solari, Carassale & Tubino (2007)

Figure 19 is used to determine the period of the wind. The graph in this figure shows the intensity of the wind for different periods. For the dynamic response of the structure, the peak on the right-hand side, between 3 seconds and 5 minutes, is particularly interesting. The biggest problem is when the waves and the wind have the same period. Then the two forces will reinforce each other. Therefore, for the calculations in this study, the wind period is equated with the wave period. This is always in the time range of 3 seconds and 5 minutes.

The waves fluctuate between an equilibrium level of the still water. Since the buoyancy force is considered a separate force, the equilibrium position will therefore produce 0 kN of force. Figure 18 shows that this does not apply to the wind. Therefore, an equilibrium position of $u_{max} - 5$ m/s with an amplitude of 5 m/s is used, based on this figure. The formula for the wind speed will be as follows:

$$u_{wind}(t) = (u_{max} - 5) + 5 * \sin\left(\frac{2\pi}{T_{wind}} * t\right)[m] \tag{2.4}$$

Where

u_{max} is the maximum wind speed

T_{wind} is the period of the wind

This means that the speed fluctuates between with 5 m/s. This amplitude is the most important for dynamics, since the constant force does not cause any acceleration. The constant value of the force will not be taken into account when determining the motion. Therefore the function is the same for each location:

$$u_{wind}(t) = 5 * \sin\left(\frac{2\pi}{T_{wind}} * t\right)[m] \tag{2.5}$$

2.4.3 EXTREME CASES

For the determination of whether the floating high-rise building is stable, it must meet the requirement. To determine whether they meet the requirement, the most extreme cases must be taken into account. Previously, the maximum height of a wave is described. In a storm these highest waves do not suddenly start. The waves of maximum height will develop over time and not emerge from the calm water all at once. The emergence of a wave from calm water does exist and is caused by an earthquake and is called a tsunami. A third "case" is the irregular wave field. This in facts always is the case with waves but because of the difficulty in describing it, as it is complex and there are infinite many possibilities, it is seen as a separate case. These three cases are described below. The fourth case is the case of extreme waves. This is a wave with one frequency as described previously with the most extreme wave height.

Growing waves

The waves on the ocean are so-called "wind waves" that are caused by the wind blowing small ridges in the water surface. These ridges then have a surface that the wind can push against, making the ridges grow. This eventually results in the large waves that the floating building must be able to withstand. The heights of the waves grow exponentially over time. For the wave heights used in this study, a time of 40 hours is needed to reach the maximum height (Curriculum Research & Development Group, 2015). This growing of the waves has a great influence on the dynamic reaction of the floating high-rise building. The homogeneous solution of the equation of motion can be enormous and cause extreme accelerations. When the homogeneous solution already damp out after each small increase in time this part of the solution will be neglectable. This ensures that only the particular solution has to be used for this situation. For the single-mass models in the chapter on dynamic stability, only the particular solution is used for the maximum acceleration at the maximum wave height. It is only proven in the paragraph about the multi-mass models that the homogeneous solution is indeed negligible.

Tsunami

The emergence of a wave of substantial height from a situation of calm sea does exist and is caused by an underwater earthquake. Such a wave is called a tsunami. They occur mainly in the Pacific Ocean and the Indian Ocean due to the presence of fault lines. None of the three locations used for this research lies in either of these oceans. Nevertheless, the research looks at the reaction of the floating building to a tsunami in the open ocean as the two locations on the open

ocean can be used as a guide for other locations with similar conditions where these tsunami can occur. For the location at the North Sea there the tsunami is not considered. There are location in the world with condition similar to the North Sea where there is a possibility of extreme tsunamis. For these locations an extra study will have to be done. It is not done in this research as these locations are here for not deemed suitable.

The wavelengths and periods of tsunamis vary. As the wave gets closer to the shore, it slows down. This makes the wavelength smaller and the height of the wave higher. The depth of the seabed has a great influence on the characteristics of the wave. For this research, a depth of 2000 m is assumed. According to the International Tsunami Information Centre (2021), a tsunami has a wavelength of 151 km at this depth. Using the formula to determine the wavelength, the period can be calculated. This is 1080 seconds.

It is difficult to predict the exact extreme value of possible tsunamis. These are too dependent on the location and characteristics of the earthquake. In order to test the floating building, the amplitude of the tsunamis of December 24, 2004 in the Indian Ocean and March 11, 2011 in the Pacific Ocean are examined. These two were chosen because they were extreme events with a big tsunami. The National Oceanic and Atmospheric Administration Center (2021) for Tsunami Research (NOAA) has done research on the tsunami amplitude across the oceans. A maximum wave height of 50 cm was determined on the basis of mapped amplitudes. This is the highest amplitude at substantial distance from the earthquake and the coast. These earthquakes often take place near the coast, the floating high-rise will only be useful when placed at a distance from the coast, so it will never float near the centre of an earthquake. Earthquakes take place on fault lines which run under the oceans. However, these produce less severe tsunamis (Howe et al, 2019). This study assumes that the location of the floating high-rise is such a distance from these fault lines that the impact of the subsequent tsunami is comparable to that of a tsunami caused by an earthquake near the coast. If, in the future, the placing of floating high-rise buildings at specific locations is considered, more research will have to be done into the danger and behaviour of a tsunami at the location.

A tsunami usually consists of a large wave followed by smaller waves. Sometimes there are small waves that precede the largest wave. This research only looks at the response to the largest wave as if from nowhere, this is the most disadvantageous as it causes the biggest response. This is equal to the first quarter of the standard wave's period. Furthermore, the wind load is neglected in this case. According to the Eurocode this load should have a reduced value due to the tsunami being an accidental load but since the load is substantially lower than the wave load it is not considered at all.

For the tsunami situation, an approximation of a sine function is used. The problem with the normal sine function is that the derivative is not equal to zero when time is equal to zero. In fact, the derivative is maximal at this time. For the normal sine, this means that the slope is maximum at this time. However, when the tsunami wave reaches the platform, this slope will not be maximum. There is a small "growth moment" from a calm ocean to the tsunami wave. This can be seen in Figure 20. This is a graph from the work of Song & Cho (2020) with measurements of wave height in time after an earthquake. The blue line shows the height of a tsunami at a location far away from the epicentre. As can be seen, the very first wave has a smooth transition from water with height 0 m and speed of 0 m/s to a sine function. (The location of the measurements is close to the coast, hence the higher waves than previously determined as maxi-

mum). To approximate this behaviour, curve fitting is performed in which a function is used to approximate the situation at time zero and the sine function as closely as possible. To do this, the first half of the sine is approximated by a Gaussian function. This has the following form:

$$f(x) = ae^{-b(x-c)^2} \tag{2.6}$$

The constant "a" is equal to the maximum wave height. The constant "b" is calculated so that the wave has a height of 0.1% at time zero. And the constant "c" is equal to a quarter of the wavelength, this value ensures that the function is shifted so that the function is not maximum at time zero but at a quarter of the wave period, just like a sine. The result is the following formula:

$$H_{wave}(t) = 0.5 * e^{-9.5*10^{-5}(t-270)^2} \tag{2.7}$$

This formula has the advantage over the sine that it has a smooth transition, however, determining a suitable particular solution to the equation of motion (a differential equation) is required. Therefore, this function is again approximated, this time by a polynomial. This is again done with curve fitting. The function is approximated by calculating ten sets of coordinates and entering them in the curve fitting calculation. The sets of coordinates that are used occur before the function reaches its top, otherwise it cannot be approximated properly. The polynomial is of 3rd degree and is has the following function:

$$H_{wave}(t) = 0.00101 * t - 2.3048 * 10^{-5} * t^2 + 4.4987 * 10^{-7} * t^3 \tag{2.8}$$

In Figure 21 the wave as a sine function is plotted together with the Gaussian approximation and the polynomial approximation. From the figure it can be seen that the polynomial approximation is only valid up to 100 s.

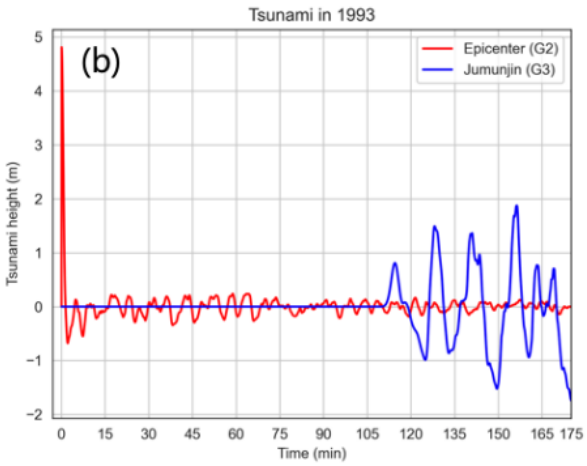

Figure 20 - Time series of tsunami heights at epicenter and Jumunjin port by tsunami in 1993. (Song & Cho, 2020)

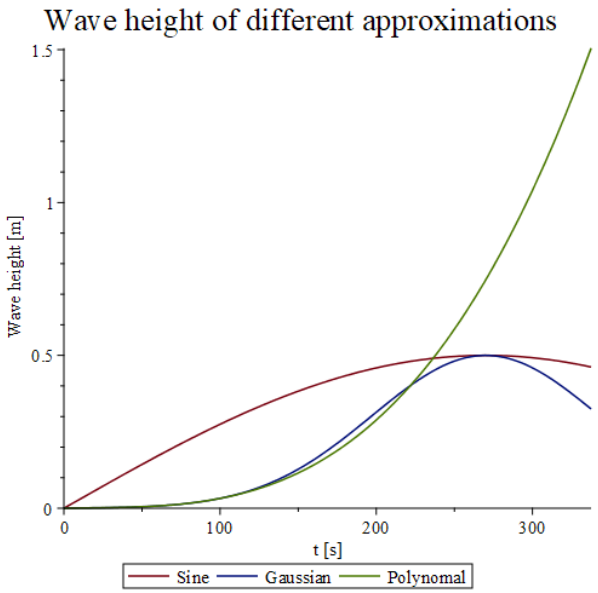

Figure 21 - The wave height as a sine function and the approximations.

Irregular waves

As mentioned, the waves that occur in reality cannot be described by a single sine wave function. One must use the so-called Fourier analysis of waves (Bezuyen et al, 2011). A Fourier analysis is an approximation of an irregular function or data set by means of the sum of several or infinitely many sine functions (Boyce & DiPrima, 2010). For waves, a data set of measurements of wave height is used. Since in this research not a data set of wave heights is used and not one situation is investigated but the most extreme out of several possible wave fields, the Pierson-Moskovitz spectrum is used which gives the energy density as a function of frequency (Bezuyen et al, 2011).

$$S(\omega) = \frac{\alpha g^2}{2\pi\omega^5} e^{-\frac{5}{4}*(\frac{\omega}{\omega_p})^{-4}} \tag{2.9}$$

Where

α equals 0.081 for storms

ω is the frequency

ω_p is the peak frequency

The peak frequency can be calculated with the previously determined wave periods (Table 1). The wave with the peak frequency has the largest share in the total wave field. The other frequencies will have a lesser share. If the floating high-rise building can handle this peak frequency (as is tested in the growing wave / most extreme wave), it can handle the other frequencies in terms of the total force acting on the structure. However, another problem may arise: resonance. When one of the motions of the floating high-rise is equal to the frequency of one of the sine waves that make up the total wave, the motion can cause the most extreme displacement even if the share of this wave is not that big relative to the peak wave. It must therefore be ensured that the floating high-rise does not have a single motion frequency that falls within the range that strong resonance can occur. Since this function is infinite, the limits of the wave frequency are chosen so that 5% of the wave energy lie above or below this limit. This 5% value is chosen be-

cause it is often used for the exceeding probability of a load (De Vries, Fennis & Pasterkamp, 2013). The calculation of these limit frequencies and thus the frequency width of the wave is shown in Appendix I. The table below shows the wave frequency widths that can cause resonance for the three different locations.

Table 3 - Frequency width of the wave for the three locations.

Location	Frequency width [rad/s]
North Sea	0.43 – 1.44
North Atlantic	0.30 – 1.01
Equator	0.42 – 1.42

Since the energy for frequencies other than the peak frequencies is lower, so is the wave height. Normally, the energy is determined from an irregular wave field. From this, the significant wave height and the peak period are extracted. Since no wave field was investigated in this study, these two must be used as input to determine the energy density function. To translate this into a wave height, the relation between the energy and the height of the wave is used. This relation is $E_w = a * H_w^2$ (where a is an unknown constant) (Bezuyen et al, 2011). With this relation the height of the wave is determined for the different frequencies. The calculation is shown in Appendix I.

2.5 Regulations and limitations

This paragraph deals with the regulations and limits that floating high-rise buildings must meet. These are divided into regulations and limits for the buoyancy and static stability and for the dynamic stability.

2.5.1 Serviceability limit state – Buoyance and static stability

The most standard criteria that the floating high-rise has to meet, is that it must remain afloat. In the construction world, this can be seen as a serviceability limit state. Since floating construction is not often used, the Eurocode does not yet have a code for this. Therefore other codes must be looked at that can be used. One of these is the Dutch technical agreement NTA 8111 (2011) (Dutch code for floating structures). This code is mainly useful for small floating buildings. The code states that *"floating structures to which the rules apply:*

- *Have consequence class CC1 or CC2, according to the Eurocode;*
- *Have up to 3 storeys above the waterline.*

For structures that do not meet the above characteristics, a safety assessment must be prepared." (NTA 8111, 2011). High-rise buildings fall into the CC3 class in the Eurocode and have more than 3 floors. Therefore, the regulations are not applicable. Nevertheless, some regulations from the NTA 8111 (2011) used.

The regulation regarding buoyancy from the NTA 8111 (2011) that is used is;

- The minimum distance between the top of the platform and the water must be at least 0.3 m. This is to prevent water from getting onto the platform.

This regulation will be interpreted so that at all times and at all possible positions the height of the wave will be 0.3 m lower than the top of the platform. Thus the height of the wave and the translation and rotation of the platform are taken into account when determining if the platform meets this regulation.

A second regulation, one that does not appear in the code but should be used to avoid unwanted results in this study, is that;

- The depth of the platform must be large enough so that the trough of the wave is not lower than the platform.

When this happens there is a "chasm" next to the platform and the platform will rotate substantially. This must be avoided at all times as this produces large rotations in the platform. However, this extra rotation will not follow from the modelling, due to the way of modelling. Therefore, it is considered as a regulation.

To meet the requirements, additional ballast water can be used in the platform. This provides more depth. With more depth, a higher platform is required to meet the regulations. The two discussed regulations are more often used in this research as input than for controlling the output. Often the two parameters; height of the building and width of the platform will be chosen. With the two regulations, together with the two parameters, a minimum depth and height of the platform can be determined. These can then be used as input. In this way they are input parameters but they are also dependent on the two previously mentioned parameters.

For static stability, the following regulations from NTA 8111 (2011) will be relevant:

- The GM value (for explanation, see chapter static stability) must be at least 0.25 m.

This regulation ensures that the floating high-rise is stable.

A final regulation is that

- The building has an angle of maximum 4^0.

2.5.2 SERVICEABILITY LIMIT STATE - ACCELERATION

As for the statics of a building, there is a serviceability limit state for the dynamics. Although these are not mandatory limits from the regulations, they are always taken into account for high buildings. There are two types of consequences of the motion of buildings. The first type is a decreased health, decreased comfort and a perception of the motion. These take place with motions between 0.5 Hz and 80 Hz. According to the ISO code 2631-1 (1997) "*effects of long-term high-intensity whole-body vibration indicates an increased health risk to the lumbar spine and the connected nervous system of the segments affected"* and *"With a lower probability, the digestive system, the genital/urinary system, and the female reproductive organs are also assumed to be affected."* The second consequence of motion is motion sickness. It occurs with motions between 0.1 Hz and 0.5 Hz and the probability increases with longer duration of motion exposure (ISO - 2631-1, 1997).

There are various codes with guidelines for dynamic behaviour. These are often maximum permissible values for the acceleration. In the NTA 8111 (2011) reference is made to the SBR guideline B ("hinder voor personen in gebouwen"). In this guideline a limiting value of 0.4 m/s^2 is

used. For buildings, ISO standards are often used. There are, however, different standards in the ISO regarding dynamics. None of which seems directly applicable to floating high-rise. For the Space@Sea project an investigation was done into the limitations of the accelerations, based on the ISO standard and other research (Lin, Czapiewska, Iorga, Totolici & Koning, 2019). This resulted in a table with the maximum acceleration for different return periods and different urban function. For both residential as Office/retail the maximum acceleration with a return period of once every 100 year is 0.4 m/s^2. As the floating building can move in multiple ways, it can also move in multiple frequencies, but not every frequency is equally bad for human perception and motion sickness. Lin et al. (2019) states that "Human perception however is quite different to motions and vibrations. Motions with frequencies from 0.1 to 1 Hz, and in particular at frequencies around 0.2 Hz, are likely to cause disorientation, nausea and result in motion- or seasickness". Two graphs are used in their deliverables, see Figure 22. The first is for frequencies up to 1 Hz and varies with the time a person is exposed to it. The second graph is for frequencies above 1 Hz and deals with continuous motions over a long period of time. For the second, the red line (Offices and Residences) is used. Note that the vertical axis is expressed as a percentage of gravity. To translate this into an acceleration, the value can be divided by 9.81.

However, translation is not the only thing that can occur. The floating building can rotate as well. Rotation is mentioned in the ISO code as a possible contributor to motion sickness. However, there was not enough data to include it in the 1997 ISO code (ISO 2631-1, 1997). Part 2 from 2003 does not address this either (ISO 2631-2, 1997). The fourth part of the ISO code 2631 does talk about rotation (roll and pitch) but this is about vehicles. *"The frequency range of motions expected to impact ride comfort significantly in conventional rail vehicles includes 0,1 Hz to 2 Hz on curve transitions (roll) ... roll (bank) angle and roll velocity (roll rate) should be considered in assessing the effects of motion on comfort.*" (ISO 2631-4, 1997). According to Wertheim, Bos & Bles (1998), rotations are not a cause of motion sickness when they occur without translation. However, when the rotation is accompanied by a small vertical translation, which in itself would not cause motion sickness, there is a 'sickness-inducing potential'. This goes against the studies that existed until then, which concluded that seasickness came from the vertical component of motion with little effect or no effects from rotation. For example O'Hanlon & McCauley (1973), and Lawther & Griffin (1987) which are often used in maritime environment. Since there is no limiting value for angular acceleration in the codes and since it causes seasickness to a much lesser extent, the value will not be limited. However, the value is related to the accelerations of displacements, which are limited.

The figures show that acceptable acceleration varies with frequency. In order to keep the limitation as simple as possible, a limitation of 0.55 m/s^2 for offices and residences is used in this study. More research is needed into the specific limitations for the motion of the floating high-rises and thus into the consequences of these motions. The 0.4 m/s^2 mentioned above has not been used because measures can be taken specifically for these high-rise structures so that if a storm that occurs once every 100 years happens, the occupants are moved to a place within the building where the least acceleration occurs. In the study where the limit of 0.4 m/s^2 was determined, there are only low-rise buildings and everything will move just about the same and therefore have the same acceleration. This is not the case with the floating high-rise buildings.

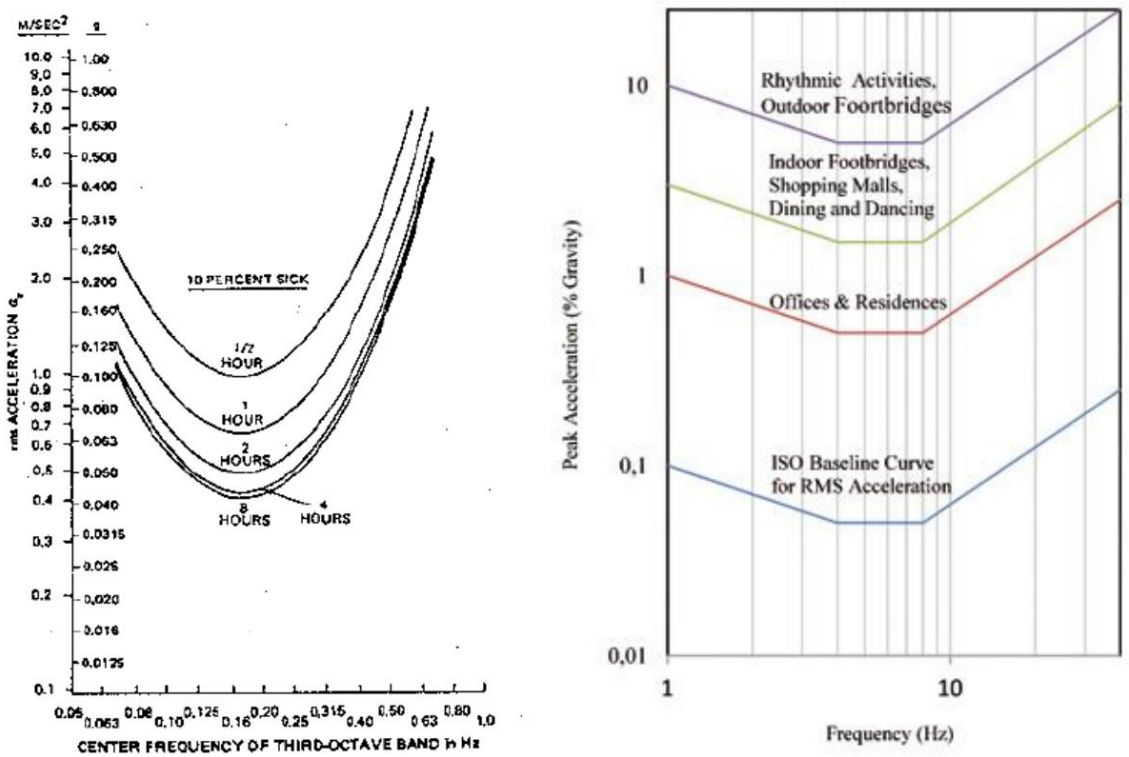

Figure 22 - Acceleration limits for different frequencies of the motion of a building. Left image source: March & Palo, (1998). Right image source: ISO 2631-2 (1989).

3. ASSUMPTIONS

In this chapter the different assumptions are discussed used for the high-rise building and for the platform. First, the models are briefly discussed. This is because the modelling method is the reason why the assumptions are needed. The models are discussed in more detail in the relevant chapters. After the models, first the assumptions of the building are discussed and then those of the platform. This chapter is concluded with a paragraph in which a set of standard values are given. These will be used in example calculations.

3.1 MODELS AND CALCULATIONS

For both the static and the dynamic stability, a form of parametric design is used. According to Starink (2019) parametric design is "*a design process in which a design can be generated on the basis of data and relationships between parts of a structure. […] Parametric design also offers possibilities to make changes in a responsive model until a late stage in the design process. This process enables offices to generate models quickly and performance-driven, to test different interventions and scenario and to make performance transparent.*" Parametric design is thus the calculation of a structure based on a base of data. These are conditions and chosen variable parameters. These parameters are thus the input for the calculations. What makes it parametric is that the value of these input parameters can be changed at any time in the design process. Also when all the calculations are done. This ensures that, when all calculations have been made in the model, the input parameters can be changed and the results of the new parameters follow directly from the model.

In this study, the advantage of being able to test many different possibilities is the reason for using parametric models. Because it is not only possible to test one possibility, but all possible combinations of the chosen input parameters. The calculations are therefore all based on two parts; the basis of data and the relationship between parts of the structure. The basis of the data are the condition values discussed in Chapter 2. Besides these conditions, there are the basic parameters. These parameters will be the parameters investigated in this research. The more basic parameters are chosen, the heavier and longer the calculations become. Therefore it is decided to use two to four basic parameters. The two that are always variable are:

- Building height
- Width of the platform

In addition to these two, it can be chosen use:

- The depth of the platform;
- the height of the platform;
- the mass of the extra ballast;

as variable input. Chapter 4 shows the relationship between the depth of the platform and the extra ballast. If one of the two is used as a variable input parameter, the other follows from that value.

In addition to the basis of data, a parametric model uses the relationship between parts of the structure. These will be discussed in this chapter, and partly in chapter 4. These relationships are mostly assumptions.

A parametric model will lead to too large calculations/models if it is a 3D model with elements as close to the real elements as possible. Therefore it was decided to keep the model 2D. This is often done in preliminary investigations as a first step and this will also suffice for this preliminary investigation. The building and the platform will be modelled as 1D elements. A 2D model with 1D elements is a lot smaller and can be used more easily in a parametric way. It is also often a good first estimate of reality. However, it does mean that various aspects are not taken into account. This will be explained later in the chapters on the various stabilities. Also, many assumptions and relations are needed for different values of the building and platform. For example, the stiffness of the building cannot be determined from the model but will have to be determined via a relation with the input parameters. These relations will be discussed further in this chapter.

3.2 BUILDING

The building will be modelled as a 1D element with only dimension "height building" as input. The building can be seen as a cantilever beam, clamped by the foundation (the foundation is the platform), see Figure 23. The stability will therefore only come from the core of the building and no stabilising elements such as outriggers have been used. This approach causes the following parameter to be determined based on the variable input parameters:

- Building width
- Building stiffness
- Building mass
- Mass moment of inertia

All these parameters are discussed in this paragraph.

Figure 23 - The building as 1D element.

This paragraph will only discuss what the parameters are based on and what the results are. The determinations and calculations are shown in Appendix III.

3.2.1 BUILDING WIDTH

For the cross-section of the building, a square shape is used in this study. This is a standard shape that is very useful in a 2D model with 1D elements because of its symmetry. So there is only one value for the width of the building. This parameter has an influence on results as a larger width results in a larger total weight of and vertical load on the building and a larger wind load on the building.

Normally, this is a freely chosen parameter, although it always depends to some extent on the height of the building. In this study it was decided to make this parameter completely dependent on the height of the building in order to eliminate it as a variable parameter. This requires an assumption for the relation between the width of the building and the height of the building. For the assumption, three reference buildings are used; the Twin Towers of the World Trade Centre (New York), Zalmhaven Tower (Rotterdam) and the New Orleans (Rotterdam). These are chosen as they have different heights and widths and a square cross-section. Curve fitting is used to create a formula linking the two parameters, explained in more detail in Appendix III. The formula is as follows:

$$w_b = \frac{17}{3475290} * h_b^2 + \frac{421523}{3475290} * h_b + \frac{104225}{8911} \ [m] \tag{3.1}$$

Where

w_b is the width of the building [m]

h_b is the height of the building [m]

3.2.2 CORE STIFFNESS

In high-rise buildings, various stability systems can be used. To model the building as a 1D element, only a core can be used as a stabilising element. However, a core will not be enough for buildings above 120m. Other stability system have to be used. These other methods are not used in this research to keep the problem simple. In order to include heights above 120 m, the deflection limit in the Eurocode is used as an input rather than a regulation to comply with. This code states that the deflection may not be greater than the height divided by 500. For the deflection of a cantilever, a forget-me-not can be used. Combining this with the deflection limit gives the following formula for the stiffness:

$$EI_{core} = \frac{500}{8} * q * {h_b}^3 \ [\mathrm{N/mm}] \tag{3.2}$$

Where

q is the distributed load over the height [N/mm].

A class C60/75 concrete will be used for the core. This has an E-modulus of 39000 N/mm^2. Because the stiffness of concrete decreases when it cracks, a stiffness of 1/3 times the initial stiffness is used.

The previous chapter discussed wind and wind load. Inserting the expression of the wind load into formula (3.2) yields the following formula for the bending stiffness of the building expressed in the height of the building, width of the building and the wind speed:

$$\begin{aligned} EI_{building} = \ & 0.7132958138 * vb^2 * w_b * {h_b}^3 \\ & * \left(148.8202864 + 18.61828598 * ln(h_b) + ln(h_b)^2 + 18.61828598 \right. \\ & \left. * ln(w_b) + ln(w_b)^2\right) \end{aligned} \tag{3.3}$$

Where

vb is the wind speed

The formula consists of three different parameters. The previous paragraph showed how the width of the building can be expressed in terms of the height of the building. The wind speed is a constant based on the location. And so, as desired, only the height of the building remains as a variable parameter. In this study, the moment of inertia of the building is used as well, without the E-modules. This can be calculated by dividing the expression of the bending stiffness of the building by the E-modules of the building.

3.2.3 BUILDING MASS

The mass of the building is difficult to approximate as it depends on many design choices. It was decided to use a standard weight per floor area. In the research of Nakajima, Saito & Umeyama (2020) a weight of 13.04 kN/m^2 was used. This value will be used in this study.

The number of floors will be equal to the height of the building divided by 4 m (approximately the height of a floor level) rounded to an integer. All together this gives the following formula for the weight of the building:

$$W_b = 13.04 * \ w_b^2 * int(\frac{h_b}{4}) \text{ [kN]} \tag{3.4}$$

Where

W_b is the weight of the building m].

This is a very rough approximation. When a 3D model of the floating high-rise is made in the future, it will be possible to get a better approximation of the weight. In the chapter on dynamic stability, the influence of changing this weight on the behaviour will be examined. The mass of the building can be calculated by dividing the weight by 9.81.

Since the floating high-rise is tested for stability the safety factors of a serviceability limit state apply. According to the building code on floating structure the safety factors are equal to 1 (NTA8111, 2011). For the mass, no further research was done into live loads in the building. The assumption of a specific weight without live loads in the building is rather small. Therefore, in chapter 6 on the dynamic stability, the influence of changing the mass is investigated.

3.2.4 MASS MOMENT OF INERTIA FOR THE BUILDING

For the dynamic stability calculation the mass moment of inertia of the building must be used. The mass moment of inertia is a difficult value to determine for a building. All elements in the building influence this value. In this study, no specific research is done into this value. To be able to use values close to the truth, a reference project is used. In the numerical example of Liu, Chiang, Hwang & Chu (2008) it is calculated that in a building with a width and depth of 40 m and floors of 4 m high, each floor has a mass moment of inertia of $1.31 * 10^8$ kgm^2. For this study, linear interpolation is used between no width and thus no mass moment of inertia and the $1.31 * 10^8$ kgm.

$$J_{per\ floor} = \frac{w_b}{40} * 1.31 * 10^8 \ [kgm^2] \tag{3.5}$$

Where

J is the mass moment of inertia.

To calculate the total mass moment of inertia of (a part of) the building, the number of stories must be multiplied by the mass moment of inertia of one floor.

3.3 PLATFORM

In the calculations and models, the platform is modelled as a 0D (point mass) or a 1D element. Therefore, for the platform, as for the building, some assumptions and approximations have to be made. A square box platform is used (the length and width are the same but the height is different). This is not the most advantageous shape for the platform but it is the simplest one for

the calculations. To improve the stability, other shapes for the platform can be considered in the future.

3.3.1 PLATFORM STIFFNESS

In order to approximate the stiffness of the platform an approximation is done using the program Grasshopper with the plugin Karamba. Because there are no deformation limits for the platform as there are for the building. This model is used to translate the properties of a 3D platform into a 1D beam. For this purpose, the platform is modelled in 3D. The material for the platform will be concrete C60/75 and the platform will consist of cubes of 5 by 5 by 5 metres. In other words, the platform will not only have walls, a floor and a roof on the outside but also internal walls and floors. This can be seen in Appendix III. The stiffness was then calculated for different platform widths and heights. From this a formula was derived to determine the moment of inertia with the parameters height of the platform and width of the platform, this can also be seen in Appendix III. The formula is as follows:

$$I_p = \left(0.01198 * h_p^3 - 0.05448 * h_p^2 + 1.1877 * h_p - 1.099\right) * w_p \; [m^4] \tag{3.6}$$

Where

I_p is the second moment of area of the platform.

h_p is the height of the platform [m].

w_p is the width of the platform [m].

3.3.2 PLATFORM MASS

For the weight, the same model is used as for the stiffness and the following formula is determined:

$$W_p = \frac{h_p}{5} * \left(\frac{w_p^3}{6000} + 2.45 * w_p^2 + 43\frac{1}{3} * w_p - 2000\right) \; [kN] \tag{3.7}$$

Where

W_p is the weight of the platform.

3.3.3 MOORING SYSTEM

Due to the many horizontal forces on a floating high-rise, the platform can move a great distance in the course of time. One solution could be to attach the building to the bottom with steel cables to keep it in place, a mooring system. According to Ko (2015), a mooring system does not help to prevent motion and displacement, even if the cable were very stiff. The only use of the cable is to hold the floating platform somewhat in place (so even with a cable, horizontal motions can occur). In addition, it follows from the study by Flikkema et al. (2021) that the conditions on the North Sea are already too rough for a mooring system. It is possible, however, in the Mediterranean Sea. It is clear that a good solution is needed for keeping the platform in place, but this is not a challenge that will be tackled in this study. Using Ko's conclusion, the assumption is made

that a mooring system can always be used without affecting the motion of the platform. Therefore, a mooring system is not taken into account.

3.4 STANDARD USED VALUES FOR THE PARAMETERS

In the research into the influence of parameters, a standard set of values for the parameters is used. The parameter under investigation is variable and the others constant. Even if the parameter would actually change. For example if the platform becomes wider, the depth would decrease. The standard parameters are given in Table 4.

Table 4 - Set of standard values for the parameters of a floating high-rise.

Parameter	Symbol	Value
Building height	h_b	100 m
Building width	w_b	23.87 m
Core width	w_c	11.06 m
Platform height	h_p	5.29 m
Platform width	w_b	100 m
Platform depth	d	2.49m
GM value	GM	294 m
Centre of gravity	COG	42 m
Zeta (damping)	ζ	0.1 [-]

4. BUOYANCY

This chapter discusses the buoyancy. This is a short chapter explaining what the buoyancy is and which formulas it involves. Then the limits are discussed and how the buoyancy is used in the coming chapters.

The first thing a floating building must comply with is that it must remain afloat. To stay afloat, the platform needs to submerge enough in order for the displaced fluid to create an upwards buoyancy force equal to the gravity force on the structure (Journee & Massie, 2015). In Figure 24 a sketch of the forces can be seen. When these vertical forces are equal there is a vertical state of equilibrium and the object will not move up or down and it will thus float.

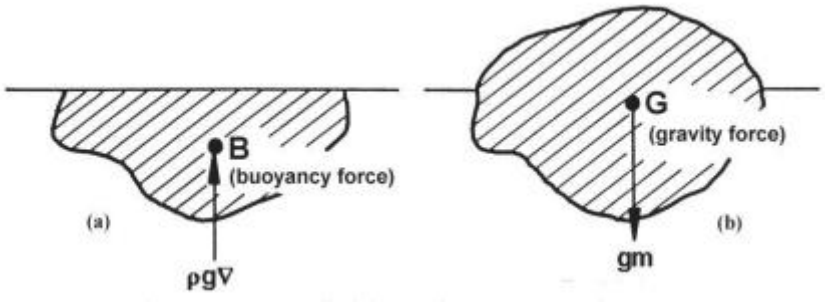

Figure 24 - Buoyancy force (B) and gravity force (G) of a floating object. (Journee & Massie, 2015).

The equality between the upward buoyancy force and the downward gravity force is known as Archimedes' law and has the following equation form:

$$m * g = \rho * g * V_{sub} \tag{4.1}$$

Where

m is the mass of the object [kg]

g is the acceleration of gravity (9.81 m/s).

ρ is the density of water (1.025 kg/m^3 for salt water).

V_{sub} is the submerged volume [m^3].

Instead of the mass times the acceleration of gravity, the weight (W [N]) of the object can be used. As the platform used in this study is a square box, the submerged volume (V_{sub}) can be calculated by the length times the width times the depth of the platform. And since a square has length equal to width the calculation can be simplified to:

$$V_{sub} = w_p^2 * d \ [m^3] \tag{4.2}$$

Where

w_p is the width of the platform.

d is the depth of the platform under the water line. (Also known as draft in marine engineering.)

As mentioned in the paragraph on regulations and limits, there are two buoyancy requirements that the platform must meet. Firstly, the height of the platform should be such that the top of the platform should be 0.3 m higher than the height of the crest of the wave. And secondly the depth of the platform must be large enough so that the trough of the wave is not lower than the platform. Because of these two requirements, the platform must have a minimum depth and a minimum height. The height of the platform is a parameter that can be adjusted to meet the requirement. However, the depth follows from equation (4.1) and formula (4.2). When the mass of the object increases, and the dimensions of the object remain the same, the depth of the platform increases. Thus, an additional weight can be added to reach the desired depth. This extra weight comes in the form of ballast water that can be stored in the platform.

In the static and dynamic stability calculations, depth is used both as an initial parameter and as a dependent parameter (meaning that either the value is choses or it follows from other parameters and conditions). If it is used as a dependent parameter, the requirement is used to determine the depth. A calculation is then made as to how much additional ballast is required in order to achieve the desired depth. If the weight of the platform and the high-rise together is large enough to achieve the desired depth, no extra ballast is used.

For the height of the platform the requirement is always used. The height of the platform will therefore follow from the depth of the platform and the height of the wave. As described in the paragraph assumptions and case parameters, the height of the platform changes the weight and thus the depth. Calculating the depth and height so that both conditions are met is an iterative process.

5. STATIC STABILITY

This chapter is about static stability. The first paragraph explains what static stability is. The second paragraph introduces the meta centre and metacentric height, along with other centres and standard distances used in the calculation of the stability. The metacentric height is abbreviated to GM and is used extensively in this study. The third paragraph discusses the Grasshopper model used for the static stability calculations. The results of the calculations are discussed in the fourth paragraph. This chapter ends with a conclusion on the static stability.

5.1 STABILITY

For the possibility of floating high-rise buildings, the static stability must be investigated. The dynamic aspect may also lead to instability, but only the static forces will be considered in this chapter. The static stability of a floating object is about the return of the object to equilibrium when it is brought out of balance by a force or moment (Nakajima, Saito & Umeyama, 2020). A moment causes the building to rotate around its centre of gravity. Figure 24 shows the two forces; buoyancy force and gravity force. The buoyancy force passes through the centre of buoyancy which is equal to the centre of submerged volume (Journee & Massie, 2015). The gravity force goes through the centre of gravity of the whole object. If no other forces or moment are acting on the object, these two centres are located on the same vertical line and the object is in equilibrium. When the object starts to rotate because of an external moment (heeling moment), the object will rotate and the submerged volume will be distributed differently (the total remains the same), shifting the centre of buoyancy, see Figure 25. Now the centre of buoyancy and gravity are no longer on one vertical line and thus the forces will provide a moment. This moment is called the righting moment. The object is stable when this righting moment cancels the heeling moment. In other words, it is equal to the heeling moment in the opposite direction. If this is the case, when the heeling moment disappears, the object will return to the equilibrium position. If the righting moment does not cancel out the heeling moment, the building will be unstable and will not return to equilibrium and so it will "fall over".

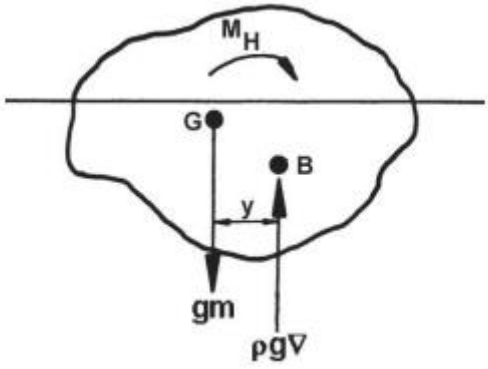

Figure 25 - Shift of the centre of buoyancy due to a heeling moment. Source: (Journee & Massie, 2015).

5.2 META CENTRE AND METACENTRIC HEIGHT (GM)

The righting moment should thus be equal and opposite to the heeling moment. This is the case when the centre of gravity is positioned lower than the so-called meta centre. The rotation of the object not only causes the buoyancy and gravity centres to no longer be on the same vertical line,

but also causes the direction of the forces to no longer be the same as the central axis of the object. (The central axis is the vertical line on which both centres lie when there is no heeling moment acting on it), see Figure 26b. At the place where the direction of the buoyancy force intersects the central axis, after a rotation, is the meta centre (denoted as M). The distance between the centre of gravity (denoted as G) and the meta centre is called the metacentric height and is noted as $\overline{GM}$ as seen in Figure 26a (Beyond this paragraph GM will be referred to without the dash that is used to indicate that it is a distance between two points.) If the $\overline{GM}$ value is greater than 0, the righting moment cancels out the heeling moment and therefore there is stability. In the chapter on regulations it is described that this $\overline{GM}$ value must be greater than 0.25 m according to the code.

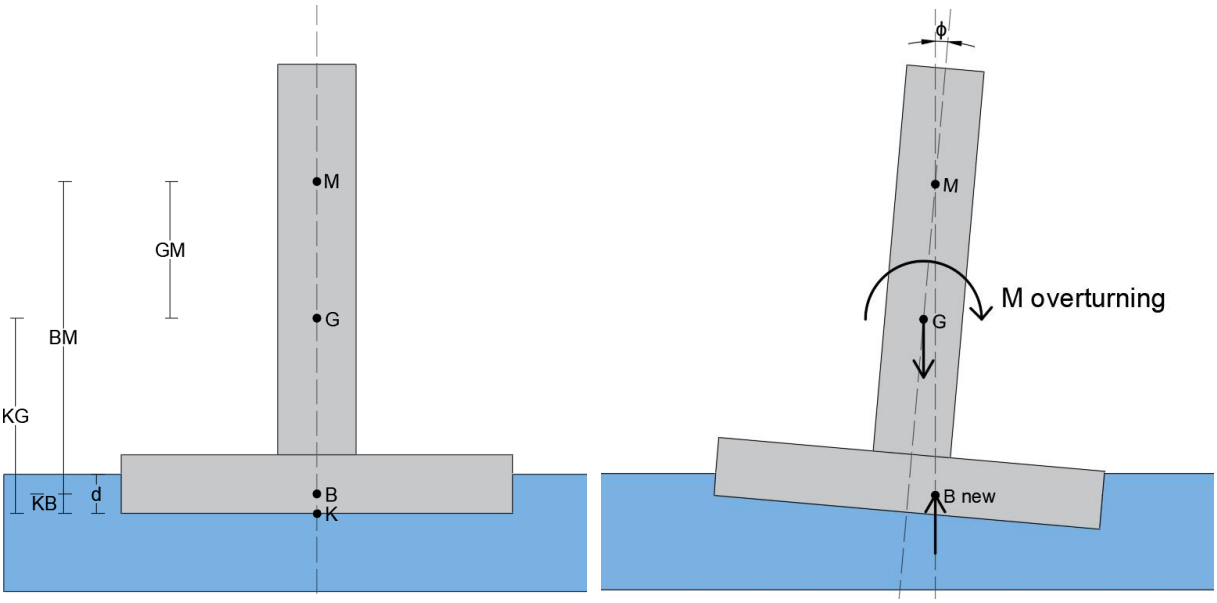

Figure 26 – Different centres and distances used in the calculation of the static stability of a floating structure. a) Upright position. b) Heeling position.

As explained, the metacentric height is the distance between the centre of gravity (G) and the meta centre (M) denoted as $\overline{GM}$. Figure 26a shows a picture of the important centres covered in this paragraph and the distances between some of them. The metacentric height can be calculated by using the distance between the keel (K) and the centre of gravity denoted as $\overline{KG}$, the distance between the keel and the centre of buoyancy (B) denoted as $\overline{KB}$ and the distance between the centre of buoyancy and the metacentre denoted as $\overline{BM}$. Figure 26 shows that when $\overline{KG}$ is subtracted from $\overline{BM}$ plus $\overline{KB}$ you obtain the value of $\overline{GM}$:

$$\overline{GM} = \overline{BM} + \overline{KB} - \overline{KG} \ [m] \ ^{3} \tag{5.1}$$

$\overline{BM}$ can be calculated with the Scribanti Formula. This formula is applicable for a wall-sided structure with a heeling angle of less than 10^0 (Journee & Massie, 2015). The platform is box-shaped and thus is wall-sided. It must be checked whether the floating high-rise has a rotation of less than 10^0, since this is a considerable rotation, it is provisionally assumed that the rotation will be less and the formula is applied. The Scribanti Formula is as follows:

$$\overline{BM} = \frac{I_i}{V_{sub}} \ [m] \ ^{3} \tag{5.2}$$

Where

I_i is the second moment of inertia of the cross-section of the waterline [m^4]

V_{sub} is the submerged volume [m^3]

The second moment of inertia of the cross-section of the waterline I_i can be calculated for this platform with the formula:

$$I_i = \frac{1}{12} * w_p^4 \, [m^4] \tag{5.3}$$

The distance between the keel and the centre of buoyancy $\overline{KB}$ can be calculated with the following formula:

$$\overline{KB} = d - \frac{1}{3} * (\frac{d}{2} + \frac{V_{sub}}{A_w}) \, [m] \, ^3 \tag{5.4}$$

Where

d is the depth of the platform [m]

A_w is the cross-section of the platform at the height of the water [m^2]

For the box-shaped platform used, the cross-section of the platform at the height of the water is equal to the width of the platform squared. When using the formulas for V_{sub} and A_w the formula can be simplified for a box-shaped platform to:

$$\overline{KG} = \frac{1}{2} d \, [m] \tag{5.5}$$

The distance between the keel $\overline{KG}$ can be calculated by calculating the position of the centre of gravity with the bottom of the platform as reference line. This will give the following formula:

$$\overline{KG} = \frac{m_b * \left(\frac{1}{2} * h_b + h_p\right) + m_p * \left(\frac{1}{2} * h_p\right)}{m_b + m_p} \, [m] \tag{5.6}$$

Where

h_b is the height of the building [m]

h_p is the height of the platform [m]

m_b Is the mass of the building [kg]

m_p is the mass of the platform (with extra ballast) [kg]

[3] Journee & Massie, 2015

The value of GM can not only be used to determine whether the object is stable, it can also be used to give the relationship between the heeling moment and the rotation. This relationship is used in the formula for the healing moment:

$$M_{heeling} = W_{total} * \sin(\phi) * \overline{\overline{GM}}\ [kNm]\ ^{4} \tag{5.7}$$

Where

W_{total} is the total weight, thus the weight of the platform and the weight of the building.

ϕ is the rotation of the floating high-rise as can be seen in Figure 26.

5.3 THE MODEL

Although the calculation of the GM value is very convenient and easy, the crucial assumption is made that the object is infinitely stiff. With ships, for example, this is a reasonable assumption due to their dimensions. However, with floating high-rise buildings, this cannot be assumed. Both the relatively thin platform and the relatively thin tower can deform substantially. This can cause a strong change in the calculation of the stability. To include this flexibility in the calculations, the total calculation must be started from the beginning.

A model is used for the calculations. This will be created in the Rhino and Grasshopper programme with the Karamba plugin. In this model the flexibility will be taken into account. The purpose of the model is to give a more realistic result than the GM method. To validate the model, the elements in the model can be made infinitely stiff. With these elements, the results of the model and the GM method should be the same. Then, with the realistic values for the stiffness's (as described earlier in chapter 3) the new calculations can be done.

How all parts of the model work is explained next. But before going into these details, the model will be discussed globally.

The model has three goals: Firstly, to determine the minimum platform width for which the whole is stable for different building heights. The stability is not only determined by this width, but it is by far the largest influence factor. This goal is to understand the stability and to find minimum required values. The second goal is to determine the minimum height and depth of the platform for different heights of the building and for different platform widths. This second goal is to get a notion of the behaviour of the stability of the building. The last goal of the model is to compare the results with flexible elements with the manual calculations of the GM method. The GM method is thus used to validate the model when infinitely stiff elements are used and to determine the difference when realistic stiffnesses are used. The latter goal is to determine whether "flexible" elements are needed for determining the stability and minimum dimensions.

To achieve these goals, four input parameters were used in addition to the location conditions. These are:

- Building height
- Width of the platform
- Height of the platform
- Depth of the platform

[4] Journee & Massie, 2015

By using the parametric programme, these parameters are variable and can be adjusted at any time. In this way, the parameters will be adjusted to meet the checks. Actually, there are three parameters that can be freely chosen. In addition to the height of the building and the width of the platform, this is the extra ballast that can be used to make the whole heavier and thus to create more depth. Because this is not a convenient input parameter, it was decided to use the depth as input parameter. In the calculations, the extra ballast needed to reach this depth is calculated and used. The height of the platform follows from the depth of the platform and the wave height. However, because, like the width, the minimum necessary value of the height is investigated, it will also be used as input.

The major difference with the manual calculations (GM method) are the flexible elements. These flexible elements ensure that an extra component is needed in the model compared to the hand calculations; multiple iterations for the second order moment. When a very tall building deforms as well as rotates, a large second order moment is created. This will cause a larger deformation and rotation. Because these can be substantial, the second order moment will increase again. In order to calculate the final deformation and rotation as good as possible, several iterations will be made.

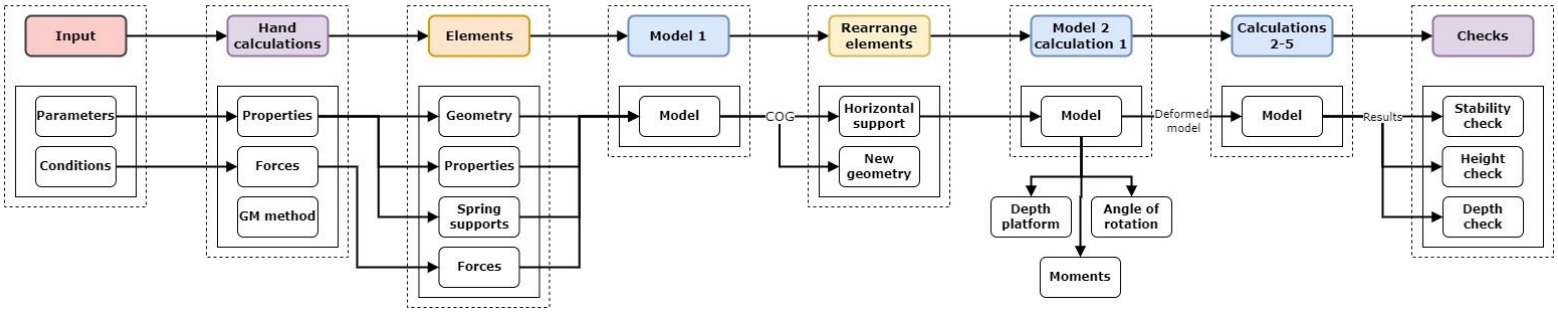

Figure 27 - Flow diagram of the static stability model.

Now that the model has been globally described, we will now turn to the content. The diagram in Figure 27 was created for this purpose. This diagram shows the 8 steps that the model follows and which parts are included in these steps. The various steps are discussed one by one below with the exception of the first two: the input and the hand calculations. The contents of these are discussed in chapters 2 and 3. In these steps, it is mainly about the values that are going to be used, for example: The weight of the building. In the second step, besides calculating the properties and forces for the model, the calculations are done using the GM method as explained earlier. The calculated forces, depth of the platform and rotation of this GM method will be used to validate the model.

5.3.1 ELEMENTS

The third step is to create the elements for the model. The four parts in this step are: The geometry, the properties, the spring supports and the forces. These are described below.

Geometry: The model in Rhino/ Grasshopper will be 2D with two 1D elements; platform and building. This choice for the model is explained in chapter 3. The main reason is to keep the amount of calculations limited in order to do a proper parametric analysis.

The 1D elements are placed in the middle of the original object, see Figure 28. This causes the building to no longer be attached to the platform. Therefore an extra height of half the height of the platform has been added to the building element. This part has an infinite stiffness. The two elements are then divided into small elements. This creates nodes between these small elements where the supports and the forces can be attached. Both the platform and the building will be divided into 100 elements. This is enough to model both the forces and the supports accurately enough.

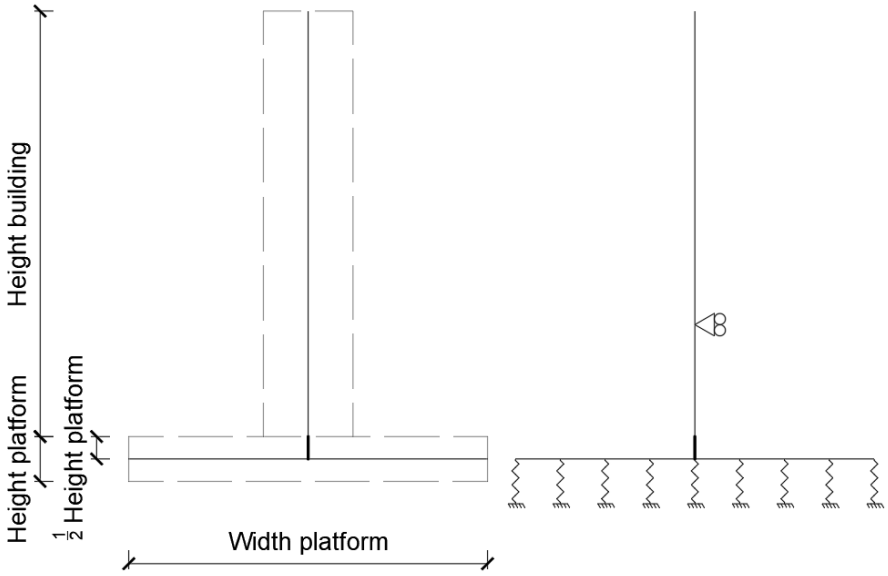

Figure 28 - Schematisation of the model where de elements are modelled in 1D (shown as a line). a) With the contour of the building and platform. b) With the supports.

Properties: Again, there is a heading "properties" (just as in step 2). This step is about applying the properties to the elements. These are values based on the variable input parameters, as determined in chapter 3. In this step an option is added to make all elements infinitely stiff, or to give them the realistic stiffness. Making the elements infinitely stiff ensures that the model can be validated with the GM method.

Spring supports: The platform is supported by springs with a spring stiffness of 10.055 kN/m^3. This represent the upward buoyancy force in salt water. In the program Karamba, no spring supports are available, only spring elements. These spring elements are distributed over the length and at one side attached to the platform and on the other side clamped, in order for them to act as spring supports. This can be seen in Figure 28b. The spring forces are scaled, taking into account the distance between the springs and the length and width of the platform in order for the total spring force to be equal to 10.055 kN/m^3. Although in reality the water can be seen as a continues spring, multiple springs distributed over the length gives the same results when enough spring elements are used. In this model 101 springs are used which is more than enough. This can also be concluded later when it is shown that the GM method gives the same results as the model.

Forces: Four different forces have been modelled;

- Dead weight
- Wind force

- Wave force
- Second order moment.

Figure 29 shows three of them (the dead weight speaks for itself). All forces are modelled as point loads. This is necessary because the distributed load of the wind and waves is not equally distributed but differs per position. To be able to apply this in Grasshopper, the forces have to be modelled as point loads with each point load having its specific value. There are 101 point loads for the wind and for the wave (the elements are split into 100 creating 101 nodes). The point loads represent a piece of distributed load, the point loads at the ends of the elements represent only half of what the other point loads represent. Therefore they are separately added with a reduced value. This is perhaps an exaggeration because the margin of error when this is not done is probably very small, but it is done anyway to be able to validate the model as well as possible. The same is done for the spring supports. How the wind and wave force is determined has already been described in chapter 2. A small addition must be made about the wave force. In the paragraph on location and conditions it can be seen that the wave is variable over the direction of the wave and in time. The latter causes the wave force and thus the moment through the wave to change in time. For the static stability the most extreme static situation has to be examined Therefore, an additional calculation has been added (in step 2) that calculates for each situation the time for which the moment of the wave is at its maximum, and therefore the most negative. This moment in time is used for the calculations.

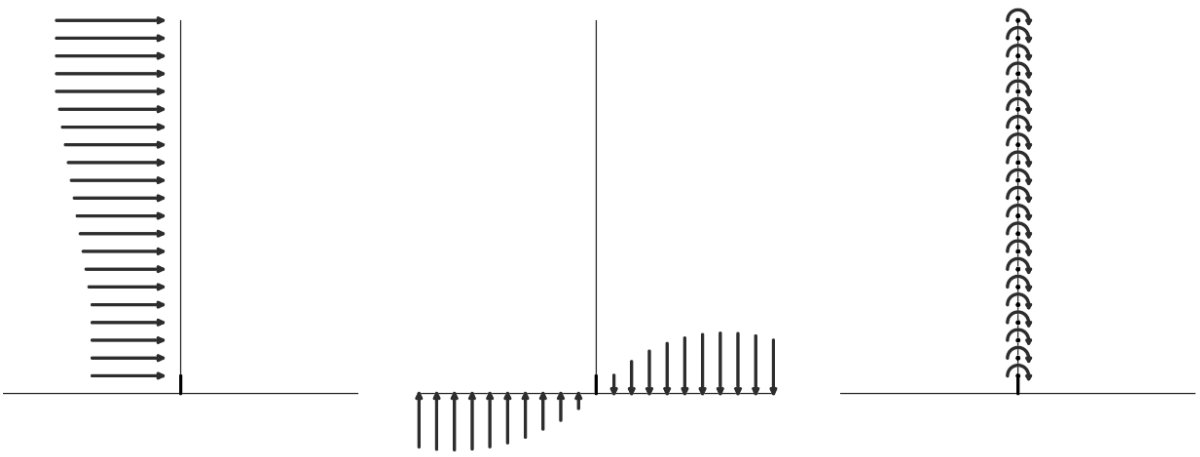

Figure 29 - Modelled forces. a) Wind force. b) Wave force. c) Second order bending moments.

5.3.2 MODEL 1 AND THE REARRANGEMENT OF ELEMENTS

The elements can now be used to create a model. There is only one crucial element missing, so that no equilibrium can be found when the calculations are made: a horizontal support. A fixed support does not exist in reality and the floating high-rise can move horizontally and is, just like vertically, held back by the water which can be modelled as springs. These springs are not added to this model because they have little added value and they are difficult to model correct with the 1D platform element. To prevent the horizontal displacement a horizontal support is added. To ensure that it does not influence the results, it should be applied at the height of the centre of gravity, see Figure 28b. To do this, the centre of gravity is determined in step "model 1". This

centre of gravity is then added as a node in the next step "rearranging the elements". As this node was not yet present it has to be created in the elements.

5.3.3 MODEL 2 AND THE CALCULATIONS

With the horizontal support, the model can now be calculated. Two load cases are calculated. The first is with only the own weight. From this, the depth of the platform can be determined. This was an input parameter and so it can be checked here whether this depth is also achieved. The second load case is with the wind and wave forces but without the second order moment. With the resulting support forces and moments in the elements, the total wind and wave moments can be determined. These can be validated by the hand calculations of step 2 in order to check whether the forces are correctly modelled and applied. The rotation cannot yet be validated as the GM method includes a second order moment. This will therefore also have to be applied in the model. This can now be done with the results of the first calculation.

For the second order moment the deformation of each point of the building, obtained from the first calculation, is determined and multiplied by its representing gravity force. This gives the bending moment due to the second order. These moments are added at the positions of the points in the model, see Figure 29c. A moment was used because the vertical force, due to its own weight, is already in the model and was otherwise taken into account twice. This method is used instead of only one bending moment at the centre of gravity as this method is more accurate when taking into account the deformation of the building.

When this second-order moment is applied, the calculation can again be done. When infinitely stiff elements are chosen, this second calculation can be used to validate the model, the rotation of the model must now be equal to the rotation of the GM method. When the elements are not infinitely stiff, the rotation will be different.

As mentioned, several iterations are used to calculate the final displacement and rotation if flexible elements are used. In the second calculation, the deformation of the first calculation will be used to determine the second order moment as just described. In the third calculation, the deformation of the second calculation will be used, etc. The calculation is done five times. In this chapter, the difference of these five calculations will not be discussed and the last calculation will be used as output. During the calculation, for each iteration it is determined how much the rotation varies with respect to the previous iteration in order to check whether the difference is small enough to use it as the final result.

5.3.4 CHECKS

The result of the last iteration is used to check whether the regulations are met. The first check is whether the floating high-rise is stable. This can be seen in the results, when it is not stable, the model will translate endlessly and therefore give no (normal) results. The second check is whether the depth of the platform is enough to ensure that the wave is not lower than the platform, see Figure 30. This is checked for the situation without translation of the floating structure and for the situation with translation (Because these are static calculations, it is not known how much the floating structure has been translated at which moment in time. Therefore, these two extremes are taken. It is assumed here that if the checks complies with these two situations, it complies with all situations). To determine whether the check is satisfied, the wave, like the plat-

form, is divided into 101 nodes. Next, it is checked per node whether the node of the bottom of the platform is lower than the node of the wave. The third check is whether the top of the platform is 0.3 m higher than the wave. This is done in the same way for the two situations. When one of the checks is not satisfied the input will have to be changed and the whole calculation is repeated.

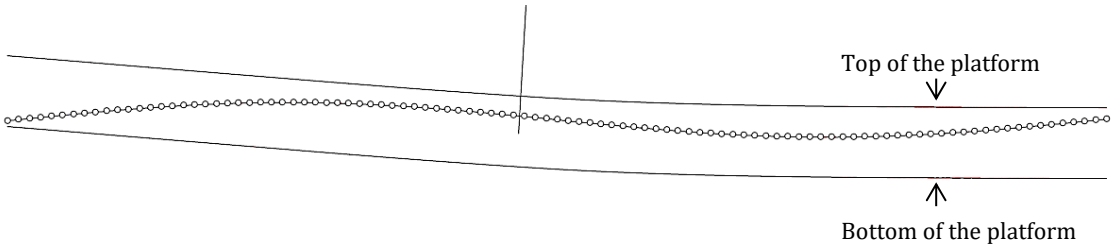

Figure 30 - Check whether the wave is within de top and the bottom of the platform.

5.3.5 FLAW IN THE MODEL

The validation of the model has revealed a flaw in the model. When the value of GM from the GM method is low or negative, the model gives incorrect result. This is due to the iterations that have to be done. The smaller the GM value, the larger the rotation. And the larger the rotation, the more iterations are required to arrive at the final equilibrium. When the rotation is very large, it takes too many iterations to calculate. Even after 30 iterations (usually 5 are enough) the difference per iteration is still more than 5% and the rotation is only half of what it should be. When the GM value is negative, and therefore there is no stability, the model does give results. This is to be expected because the lack of stability of the building means that very little equilibrium will be found when doing infinite iterations. However, it is not possible to see the difference in the model between needing many iterations to reach the equilibrium as necessary with a low GM value or not being able to find an equilibrium because the GM value is negative. For all results in the next paragraph, it is tested whether the model is accurate when rigid elements are used. Usually 5 iterations are used. If this is not sufficient, it can be scaled up to a maximum of 30 iterations.

5.4 RESULTS

In this paragraph, the results of the model are discussed and compared with the manual calculations based on the GM method. Many results have been obtained, but only a few are shown for illustrative purposes. Some results are used as input for the dynamic calculations.

5.4.1 MINIMUM PLATFORM WIDTH

Because of the flaw mentioned, the first goal of the model, the determination of the minimum width of the platform for stability, cannot be achieved with the model. In order to achieve this goal, the GM method is used. In theory, the flexibility of the elements should not make any difference to the stability of the whole and therefore the model should give the same stability limit as the GM method. The depth and height of the platform must comply with the two regulations explained above. However, this can only be determined correctly in the model and not in the GM method. Therefore, the depth used is the depth that the floating high-rise would have without additional ballast until the depth would be less than half the wave height. For those values, extra ballast was used to make the depth equal to half the wave height. This would also have been done if it had been assumed that the building could not move. In this way the depth is not a vari-

able parameter which ensures that the limiting values due to static stability is solely expressed in the height of the building and the width of the platform.

Excel was used to determine the minimum possible width of the platform for different building heights. In Excel the following steps are made:

- All the values required for calculating the GM value are determined or calculated according to chapter 3, 4 and 5.
- Than the GM value is calculate for platform widths of 50 m to 500 m for one specific building height.
- From that list, the smallest platform width is extracted that provides stability. This is the width that has the lowest positive GM value for that specific height.
- This process is repeated for multiple building heights between 100 m and 800 m with steps of 25 m.

In Appendix IV an example is given of the spreadsheet of the calculations. The results for minimum platform width are shown in Figure 31. The calculation does not take the location into account as the GM value is not dependent on the conditions at the location. So it does not (yet) consider how much the building rotates and whether it is partly submerged, but only whether it is stable.

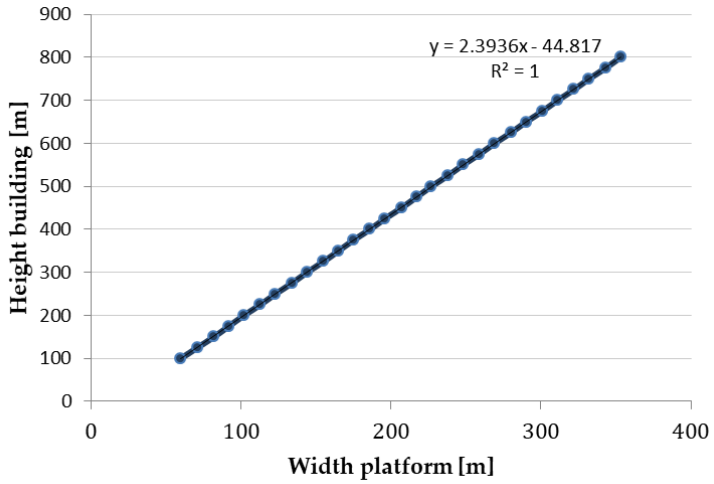

Figure 31 – Resulting graph of the static stability calculations. The line shows the value of the platform width that only just gives stability for a certain building height. Sets of parameters below the line give a stable structure, sets of parameters above the line give instable buildings.

As can be seen, the graph is completely linear. The formula for minimum platform width is determined by means of curve fitting and is

$$Height\ building = 2.3936 * Width\ platform - 44.817 \quad (5.8)$$

To determine whether a floating high-rise is stable, the following inequality formula must therefore be fulfilled:

$$Height\ building \leq 2.3936 * Width\ platform - 44.817 \quad (5.9)$$

This purely linear graph seems to be the result of very simple calculations, but this is not the case and the result is also somewhat surprising. It is probably due to the assumption of the different parameters. In the end, all parameters are based on the height of the building and the width of the platform. Apparently in such a way that a linear result comes out of the minimum required platform width. To show that the calculation of the value from GM is quite extensive and to show that the results are correct, the same calculation was done in Maple to determine the formula and to make the 3D plot with both the height of the building as the platform width as a variable. In this plot you can also see that there is a linear relationship. The formula and 3D plot can be seen in Appendix IV. In spite of the flaw in the model, the minimum required platform width was also determined with the results of the model. These are not shown, because they are not exact, but the results were in the end little different from those of the GM method.

5.4.2 MINIMUM PLATFORM HEIGHT AND DEPTH

The second goal of the model is to calculate the minimum height and depth of the platform for different building heights and platform widths and to get a notion of the behaviour of the stability of the building. For this goal the Grasshopper model is used, and thus the flexibility of both the building and platform is taken into account.

For different combinations of building height and platform width values, the minimum height and depth of the platform is calculated. In order not to get too many calculations and data, it was decided to take only heights of 100 m, 300 m and 500 m for the building and platform width ranging from the first platform width for which it is stable up to 600 m with steps of 25 m.

After the height and depth of the platform are determined, the following results are obtained from the model:

- Angle of rotation at the middle of the platform
- 2nd order moment
- Wind and wave moment
- Deflection at the top of the building
- Ratio between the model and the GM method
- Change in the angle at the fifth iteration of the model

The results for all three location can be seen in Appendix IV. The rotation in the centre of the platform from the model is compared with the expected rotation of the GM-method. This shows how different the rotation is. Also when the infinite stiff elements are used the rotation should be the same. The wind and wave moments of the model and of the GM model are compared in order to check if they are the same and thus correct.

5.4.3 INFLUENCES OF THE PARAMETERS

In this subparagraph the influences of the different parameters are discussed. These are based on the results of the determination of the minimum depth and height of the platform. For illustrative purposes some results are shown. Other results can be seen in Appendix IV.

The height and depth of the platform depends on several factors. Therefore, it is difficult to say why a certain set of parameters gives a certain height and depth. The minimum height and depth depend strongly on the width of the platform. Widening of the platform can have both positive and negative effects on the minimum dimensions. The different ways in which an increase in the width of the platform affects these dimensions are as follows:

- The rotation of the platform becomes less because the GM value increases. This is a positive effect as the maximum tilt will be less. In addition, the ends of the platform will translate less vertically due to rotation from the centre of the platform. This reduces the risk of the end of the platform being flooded. This last advantage can also be a disadvantage. Due to more stability, the platform moves less with the waves. Figure 32 shows that this can lead to problems.
- Secondly, the total forces on the platform will increase. This may cause more rotation. With more rotation there is more chance that the end of the platform will submerge and thus a change in the necessary platform height and depth will be needed.
- Thirdly, the value of the moment due to the wave fluctuates with wider platforms. This means that a narrower platform may cause less rotation than a wider platform because it has substantially less moment. This will be discussed later in this subparagraph.
- Lastly, the stiffness of the platform will increase. It is to be noted that the increase in forces is (relatively) larger than the increase in stiffness and thus a wider platform deforms more. This deformation can be favourable or unfavourable. The building in the centre of the platform gives the platform a banana shape where the ends are pushed up relative to the centre, see Figure 33a. This can reduce the needed height of the platform. However, the sagging in the middle of the platform can result in a need for more depth, see Figure 33b. If more depth is required, the height of the platform will also need to be increased. It must be said that if the platform is very wide and the height is not very high, the platform also deforms a lot due to the wave force or the weight of the building and it will have less of a banana shape. In this case the local deformation can cause problems to the amount of rotation of the building but not for the minimum needed height and depth of the platform.

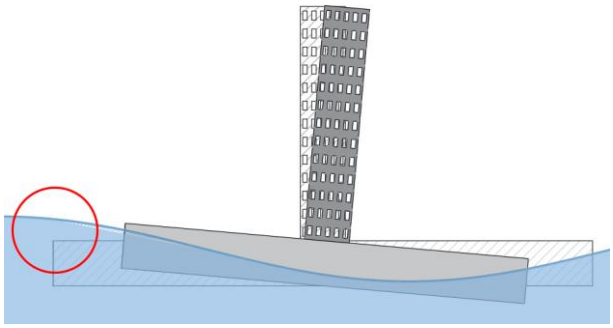

Figure 32 – An example of the possible negative influence of more platform width. The bigger platform rotates less which can cause it to be below the wave.

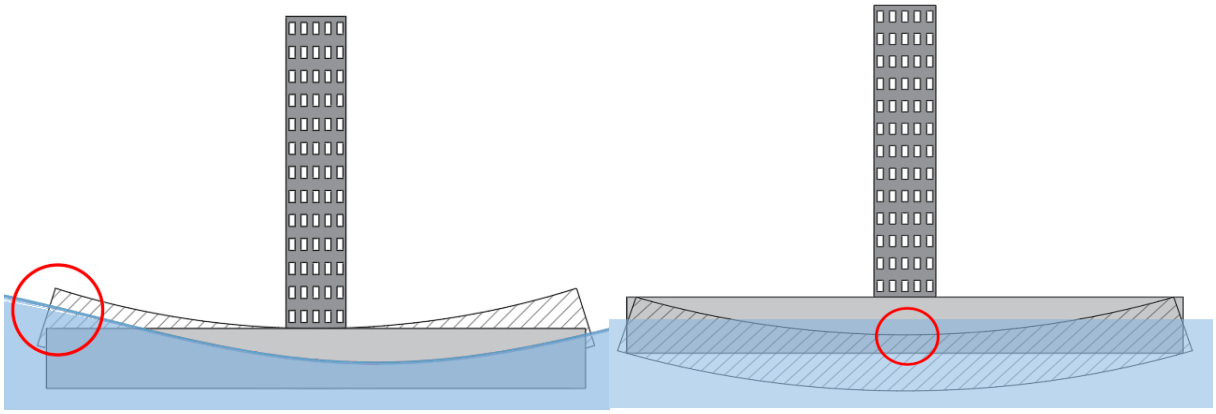

Figure 33 - Positive and negative influence of the deformation of the platform into a banana shape. In the left figure the deformation is positive as the outer edges rise above the wave. In the right figure the influence is negative as the middle of the platform sinks below the water.

In addition to the width of the platform, the height of the building also affects the minimum platform height and depth. As the height of the building increases, so does its weight. This increases the deformation in the middle of the platform. This in turn can have a positive or negative effect on the minimum depth and height of the platform as explained before and shown in Figure 33.

Although it is difficult to determine why there are certain results as they are very complicated, patterns can be discovered. The graph for the height of the platform and the depth of the platform are very similar and both can be divided into three phases. To illustrate, the graph of the platform depth for a building with height of 100 m at the location of the equator is given in Figure 34. In the first phase the minimum platform width decreases sharply until the width of the platform has a certain value. What this value represents is unknown. It is always lower than the wave length. In the second phase, the minimum depth increases slightly and then decreases again until it has a second local minimum. This minimum happens when the platform width is equal to a multiple of the wavelength. There may be several of these minima in the graphs. In this case, there are two. The third phase is the phase in which the platform is so wide that it hardly rotates. As a result, the depth of the platform should be approximately equal to half the wave height for all platform widths. The graph will therefore be constant. This third phase will occur at bigger platform width values if there is a higher and thus heavier building. This is because of the sagging of the platform.

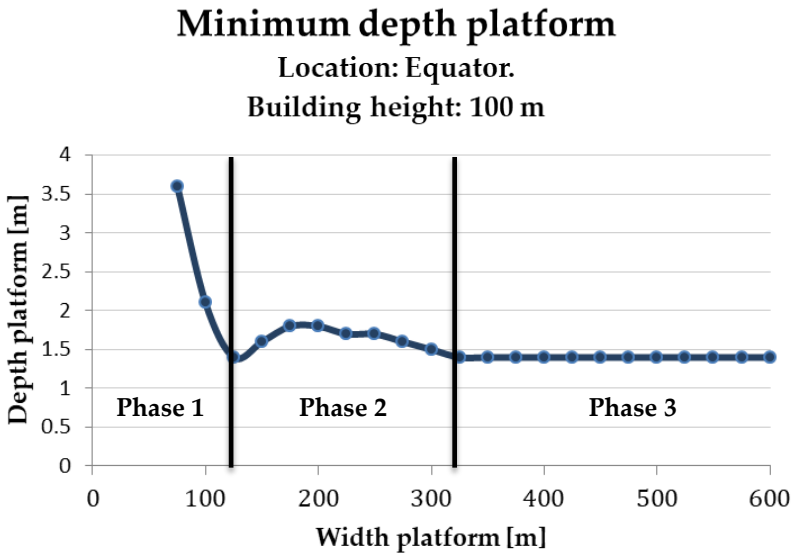

Figure 34 – Minimum needed platform depth for a floating high-rise building with a height of 100m at the location of the equator. The graph is divided in three phases. Phase 1 were the needed depth decreases with increasing platform width. The second phase were the needed depth increases and decreases again. And the third phase were the platform is so stable that there is no rotation anymore and the minimum depth of the platform is equal to half the height of the wave.

For the rotation, a graph was made for both the model and the results of the GM method calculations (which is equal to an infinite stiff building in the model). In Figure 35 the results are shown for a building of 100m and 300 m for the North Sea location,

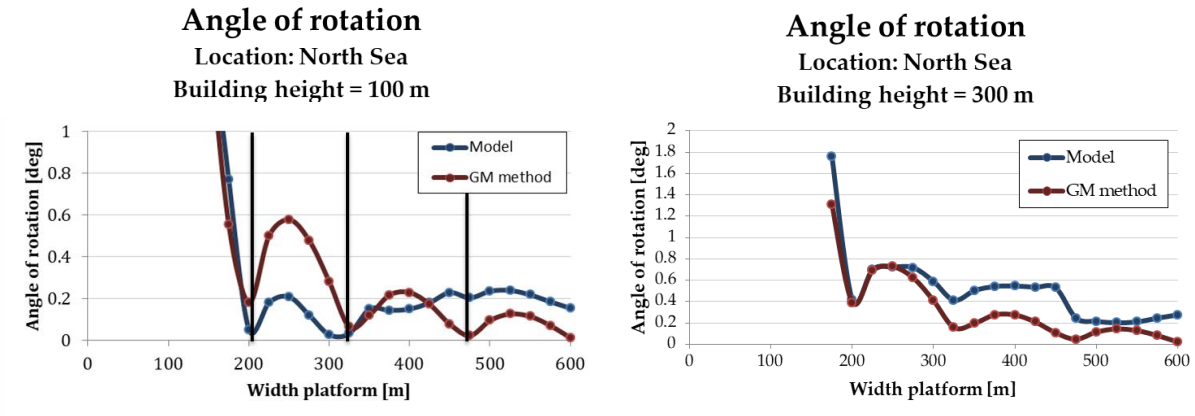

Figure 35 - Angle of rotation in the middle of the platform for different widths of the platform from the model and calculated with the GM method. The left graph is for a building height of 100 m. The black lines indicate the minimums. Right graph is for a building height of 300 m. Both graphs are for the North Sea location

The rotation calculated with the GM method shows minimum values for certain platform widths. Research into these platform widths shows that these are platform widths for which the total moment due to the waves is minimal. In Figure 36 the moment due to the wave is shown for the North Sea location. Earlier in this chapter it was mentioned that for these static calculations a calculation is done for the most "negative" time. That is the time for which the moment through the waves is at its maximum. For these platform widths the wave moment is minimal regardless of the time. These are clearly important widths as there is substantially less rotation. That is why these widths have been given a name in this study. The so-called "zero moment widths". In Appendix V a more extensive study and explanation of these zero moment widths can be found.

The zero moment widths depend on the wavelength and are therefore different for each location.

Figure 35 also shows that the rotation for these zero moment widths decreases when the zero moment widths become larger with the GM method. (In the case of the 100m building, you can see that the rotation is still 0.2 degrees at the first black line from the left and almost 0 degrees at the third black line). This is a logical consequence of a combination of minimal moment due to the wave and increasing stability due to a larger platform.

Looking at the results of the model in Figure 35, these minimums on the zero moment widths are less clear. There are local decreases in the rotation but not as extreme as in the GM method. The local minimums are not much lower than the maximums. Especially with larger platform widths, the difference is minimal. This difference can be explained by the flexibility of the elements. In the GM method, the platform and building rotate as a whole. If the building causes extra rotation, the whole platform rotates a bit. With more flexible elements as in the model, with larger values of the width of the platform, there will be larger differences in the local rotations. When the building causes a rotation, the middle of the platform rotates a lot and the ends almost not. This is illustrated in Figure 37. This causes a big difference between the two methods. This difference can also be seen when you look at the ratio between the rotation of the model and the rotation of the GM method in Figure 38. Especially at the zero moment widths, the model has a much higher rotation than the GM method. It can be concluded that using infinite stiff properties for the platform results in inaccurate rotations. Especially when using the seemingly promising zero moment widths. These zero moment width are still promising when flexible elements are used, just not as promising as with infinitely stiff elements. For the dynamic analysis a platform with accurate stiffness should be used.

The rotation increases between two minimums but for the GM method, the wider the platform the less this increase. This is as expected as wider platforms give more stability. This is different in the results of the model. The model behaves less predictably. For the building of 100m, the rotation even increases. For higher buildings, the rotation follows the same pattern as the GM method, only it gives higher values. Again this can be explained by the local deformation as seen in Figure 37. The deviation from the GM-method is unpredictable. For the calm equator location this deviation is less, for the extreme waves of the Atlantic ocean the deviation is extreme. The GM method is thus not accurately usable when designing floating high-rise.

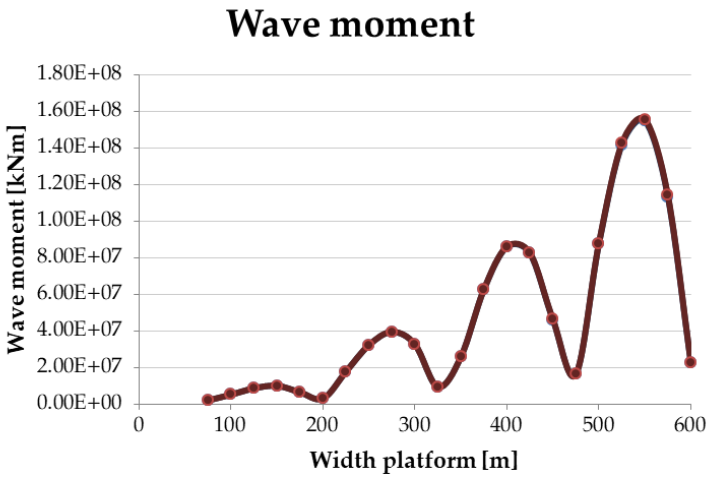

Figure 36 - Moment on the middle of the platform due to the force of the wave. The values are obtained from the model. The conditions of the North Sea are used for this graph.

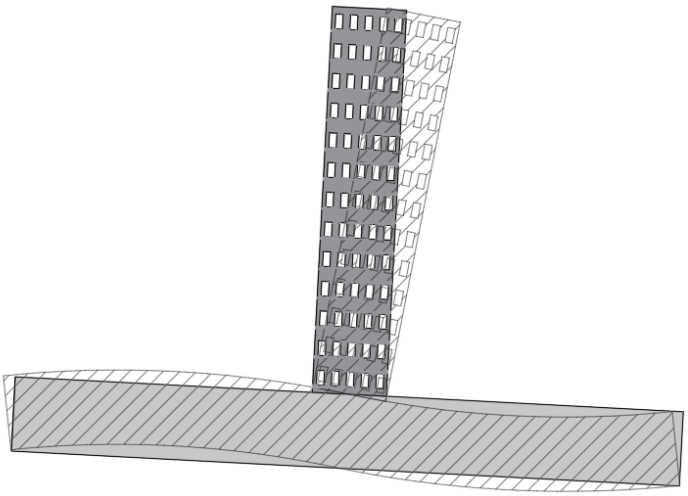

Figure 37 - Difference in rotation of a stiff platform and a flexible platform.

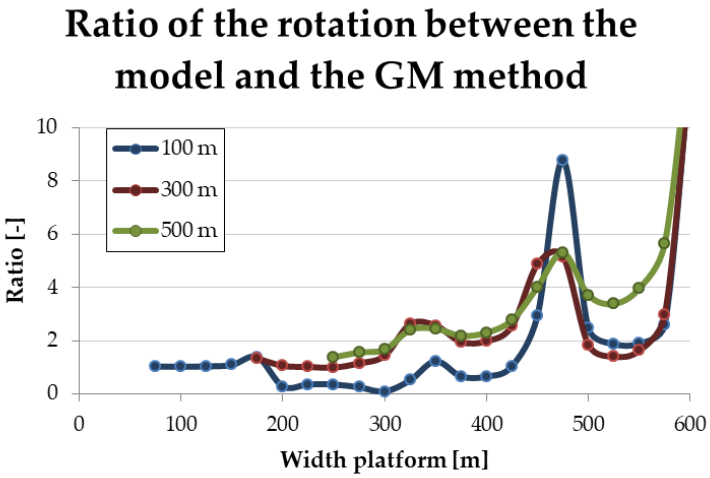

Figure 38 – Graph of the ratio between the results of the model and the GM method for the angle of rotation in the middle of the platform. These are shown for thee building heights: 100, 300 and 500 m. For this graph the conditions at the North Sea are used.

The graphs for the rotation already showed a difference in infinitely stiff elements (GM method) and flexible elements of the model. The rotation of the building causes a translation of the building. In addition, there is an extra translation in the building due to second order moments. The deflection can be determined with the model. It is compared in Figure 39 with the deflection of the building when all elements are infinitely stiff. The latter corresponds to the GM method where the rotation is multiplied by the height of the building.

Again, the local minimums can be seen. Since the displacement depends on the rotation, this is also in line with expectations. Furthermore, the same deviation from the GM method that was also seen in the rotation can be seen. The deviation from the GM method is also increasing. This is to be expected as the deformation of the platform will play an increasing role. In the dynamic analysis, this deflection is also determined. It may be that the displacement becomes more due to the dynamic aspect. This graph, together with the graph of the rotation, shows that using infinitely stiff elements gives different results than when the flexibility is taken into account. The GM method is often a too positive estimate. This is to be expected as the deformation of the building creates more second order moments. It also happens that the model gives more positive results. This can be due to the positive deformations as explained before.

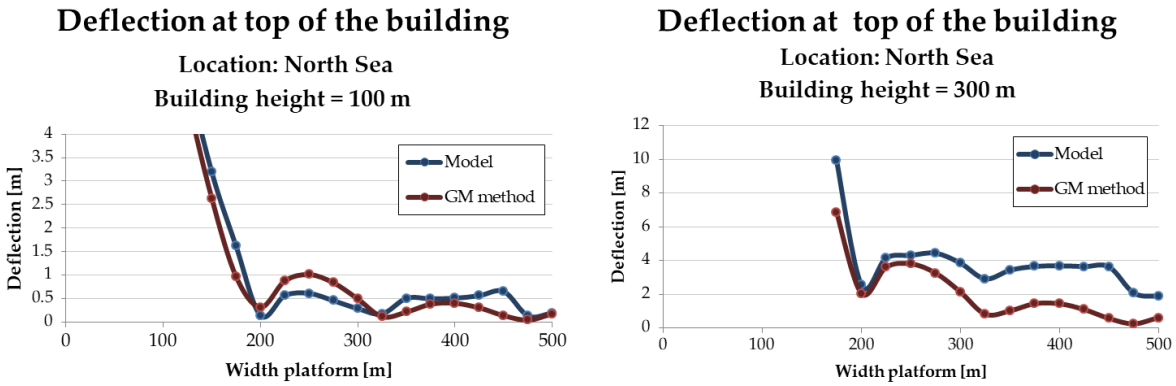

Figure 39 – Horizontal deflection at the top of the building for a building height of 100m and 300m. Calculated with flexible elements (model) and infinite stiff element (GM method).

5.5 CONCLUSION

A model was created to calculate the minimum platform width required for stability of the floating high-rise and to calculate the minimum depth and height of the platform using non-infinite rigid elements. Furthermore the model is used to investigate the influences of different parameters and to predict the static behaviour of floating high-rise.

For the minimum platform widths, the model cannot be used because it becomes less accurate with larger rotations. Using manual calculations in Excel based on the GM method, a linear relationship between the minimum width of the platform and the height of the building was found. $Height\ building = 2.3936 * Width\ platform - 44.817$. The fact that this relationship is linear is most likely because of the way the many parameters are defined. These are designed to depend only on the width of the platform and the height of the building. If other values are taken for these parameters, the relationship will deviate. However, it is a good estimate.

The minimum depth and height of the platform varies with the width of the platform. The required depth and height decrease for higher platform width in the lower platform width region,

up until a certain value (it is unknown why it is at this value and thus it cannot be determined beforehand. This value differs from locations and building heights.). Thereafter, the required depth and height increases and decreases several times until the platform is so big and thus stable that the required depth is equal to half the wave height and the height of the platform is equal to the height of the platform.

The rotation of the platform and the deflection of the top of the building calculated by the model is very different from the results from the GM method. It does follow the same pattern, there are minimum values for the rotation of the platform. These occur at the platform widths for which there is a minimum in the total moment on the platform due to the wave. These platform widths have been called the “zero moment widths”. For wider platform widths, the total rotation of the platform plays less of a role and the local rotation plays a bigger role. Therefore, the rotation does not decrease for larger platform widths as it does for the GM method. Increasing the height of the platform will result in less local rotation and thus a more stable building.

All in all, it can be concluded that the GM method is not adequate for the study of floating high-rise buildings and that an analysis should be done with flexible elements. Looking at the rotation, it is best to choose the width of the platform such that the moment due to the wave on it is minimal, called zero moment widths. These are certain values that depend on the wavelength of the wave. The height of the platform and the depth will also have to be determined with an analysis. No prediction can be made as to what the exact dimensions should be. Since the model with flexible elements differs so much from the GM method with infinitely stiff elements, for the dynamic stability elements with accurate stiffness should be used.

6. DYNAMIC STABILITY

This chapter deals with dynamic stability. The first paragraph discusses the different motions that exist for floating objects and for floating high-rise buildings. In the second to fourth paragraphs, the three motions vertical translation, horizontal translation and rotation are discussed. This will be done using a dynamic model consisting of one point mass, the so called single-mass model. The formulas and values are determined to determine the motion and acceleration of the motions. Next, the parameters that influence the motion are investigated. Finally, it is investigated whether a tsunami can cause problems for the motions of the floating high-rise.

In the fifth paragraph, the three motions are discussed in a single-mass model. This gives the same results as when they are considered separately but is an important stepping stone to paragraph six.

In paragraph six, multiple point masses are used to determine the dynamic behaviour. Called the multiple-mass model. In this paragraph, first the model is discussed together with the values and matrices that appear in the equation of motion. Then, using a model in Diana, it is examined whether the calculations for the eigenfrequency are correct and whether more than three point masses are necessary. Subparagraph 2 discusses the particular solution. Subparagraph 3 deals with the inclusion of the deformation of the platform in the model. Then the influence of a growing wave is examined in subparagraph 4. After this, again the influence of the parameters on the motions are examined and then the calculations are done with all assumptions available. This results in accelerations for different locations, building heights and platform widths. Finally, in this paragraph, limits are in the parameters are investigated to prevent resonance.

6.1 MOTIONS

One of the most important aspects of floating buildings is their dynamic behaviour. Although all buildings have motion, the displacement and acceleration of land-based buildings is many times lower than for buildings on water. This is due to the foundation being a liquid in motion instead of a (mostly static) solid. Both types of foundations can be modelled as a spring, in which water has a much lower spring stiffness than soil and can therefore be compressed much further with the same amount of force. In addition to wind loads, floating buildings are also subject to the variable force of waves, which causes motions.

Another big difference is the number of degrees of freedom. Buildings on land do not move in a vertical direction while buildings on water do. When the floating buildings are built on water with low depth, the degrees of freedom can be limited by using piles, for example. This is not possible on the open sea. The only possible support is a mooring line. However, this does not reduce the number of degrees of freedom, but rather reduces the amount of motion. So there is no restriction of motion and the building will have six degrees of freedom, three translations and three rotations. These six motion can be seen for a floating object in Figure 40. In maritime engineering, all six motions have their own name[5]:

- Surge (translation on the x-axis)

[5] Here the simplification is made to consider the boat as a rigid body, so without any internal deformation. For large vessels (high length to cross-sectional dimension proportion) internal deformation also needs to be taken into account. The same goes for floating platforms or tall buildings.

- Sway (translation on the y-axis)
- Heave (translation on the z-axis)
- Roll (rotation around the x-axis, denoted as ϕ)
- Pitch (rotation around the y-axis, denoted as θ)
- Yaw (rotation around the z-axis, denoted as Ψ)

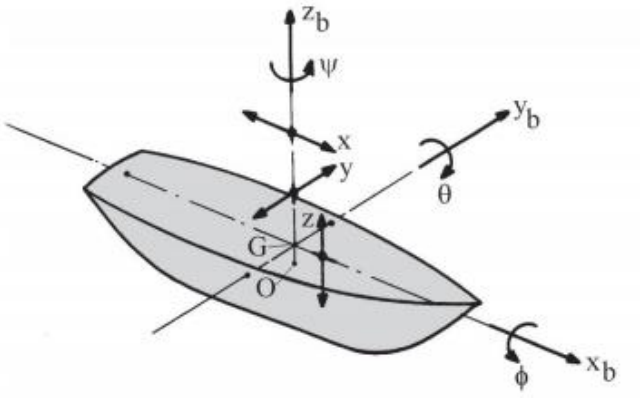

Figure 40 - Six different motions of a floating object. (Journee & Massie, 2015)

For boats, these six motions are different due to the non (rotationally) symmetrical shape. Buildings and platforms do not necessarily have this symmetry either. In this research, it is assumed that the building and the platform do have this symmetry. This will reduce the different motions from six to four. It ensures that the translations and rotations are the same in both the x and y direction. Leaving only four different motions.

Due to the simplifications used in this chapter, no research can be done on the Yaw motion. For this, a 3D model is required. This motion will be of less importance for comfort since the horizontal forces are less than the vertical forces and the uncomfortable feeling comes mainly from the vertical displacement in combination with horizontal displacement and roll and pitch rotation. The three motion left that are investigated in this study are thus:

- Vertical translation (heave) denoted as "w"
- Horizontal translation (surge and sway) denoted as "u"
- Vertical rotation (roll and pitch) denoted as θ

This chapter will discuss the behaviour of a floating building regarding the remaining three motions. The motions are described one by one and modelled with a mass-spring system with one mass and one degree of freedom. With this, the frequency and the motion in time of the whole structure is determined for the three different motions. The calculations and the values needed for this are described in this chapter as well. Then the motions are combined in a mass spring system with one mass. This helps in understanding the calculations of multiple motions in one mass. Finally, the model is extended with several masses over the height of the structure, each with three degrees of freedom.

6.2 VERTICAL TRANSLATION (HEAVE)

The vertical translation in a floating building occurs solely as a result of the wave force. The crest of a wave pushes the building upwards and a trough of the wave allows the building to

sink, see Figure 41. The latter can also be seen as the wave “pushing the floating building down” as the buoyancy force is reduced compared to the still water level buoyancy.

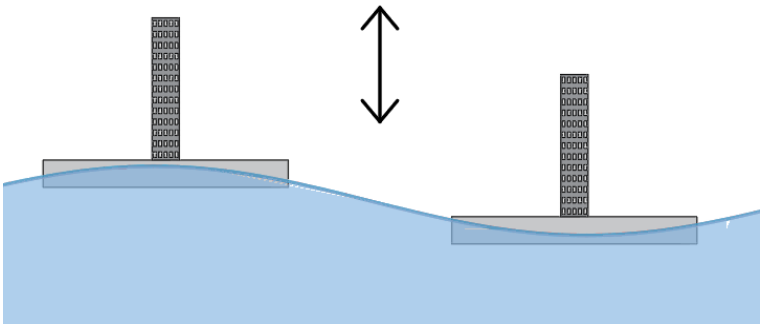

Figure 41 - Heave motion (vertical translation)

The vertical motion is determined with a mass-spring system. The mass-spring system can be seen in Figure 42. As with static stability, the structure is supported by springs to simulate water. With one mass, this also means one spring. In addition to providing spring support, the water also dampens the motion. Therefore, in addition to a spring, the mass is also supported by a damper. The mass is excited by an external force. This force is the wave that pushes the mass up and down. The spring, the damper and the force have a vertical direction, just like the motion.

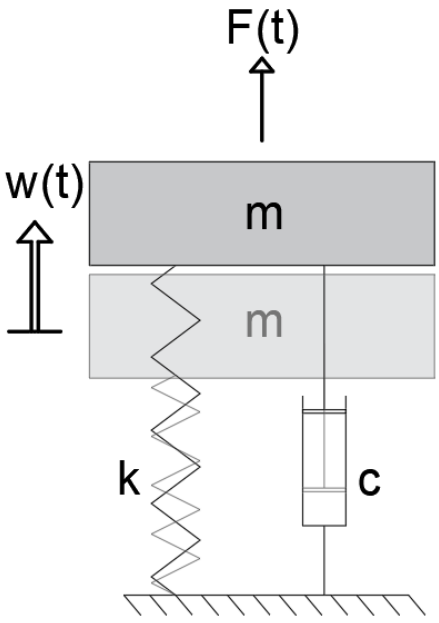

Figure 42 - Mass spring system for vertical translation.

6.2.1 EQUATION OF MOTION AND ITS VALUES

In chapter 2 the limits of the motion are determined. These are limitations in the acceleration. To determine the acceleration of the mass, the motion must first be found. The motion can be determined with the equation of motion. In the case of a floating structure, the equation is as follows:

$$(m + a)\ddot{w} + c\dot{w} + kw = F_v \tag{6.1}$$

Where

w is the vertical displacement [m]

m is the mass of the structure [kg]

a is the hydrodynamic mass coefficient (added mass) [kg]

c is the hydrodynamic damping coefficient [Ns/m]

k is the spring stiffness [N/m]

F_v is the exerted vertical force [N]

The mass depends on the sizes of the building and the platform. In chapter 4 a relation is shown between the mass and the buoyancy force. The mass can thus be expressed in terms of water density, gravity acceleration and the immersed volume of the platform as done in the chapter on buoyancy in formula (4.1):

$$m * g = \rho_{water} * g * V_{sub} \tag{6.2}$$

Where

g is the acceleration of gravity, 9.81 m/s^2

ρ_{water} is the density of salt water, 1025 kg/m^3

V_{sub} is the submerged volume [m^3]

The determination of the vertical spring stiffness has already been described in the chapter on static stability. This is equal to the density of water times the gravity acceleration. To model this as one spring, this value must be multiplied by the cross-sectional area of the platform at the height of the water. In the case of a square platform this is equal to the width of the platform squared. This results in the following formula for the spring stiffness:

$$k = \rho_{water} * g * w_p{}^2 \ [N/m] \tag{6.3}$$

Where:

w_p is the width of the platform [m]

The added mass (a) and damping (c) are caused by the hydrodynamic reaction of the water due to the displacement of the platform in relation to the water. Both are explained below.

Damping exist of two types; potential and viscous damping. Potential damping is the damping by creating waves. An oscillating object in water creates waves that cause the motion to dissipate energy and therefore dampen it. The amount of dissipation and thus damping is proportional to the speed of the motion (Journee & Massie, 2015). This damping can be evaluated numerically. This evaluation is however very time consuming as it involves many factors, difficult calculations and the damping will also be different for each motion as is showed by experiments.

For example for a hybrid floating platform for offshore wind turbines (Clement, Kosleck & Lie, 2021).

The viscous damping is damping due to friction between the platform and the viscous fluid that is water. According to Malta et al. (2010) the viscous damping can be evaluated through experiments. The common test for the viscous damping is a free oscillation test of a scale model in which the decay signal is analysed or an irregular wave test. According to Journee & Massie (2015) this damping is small for large floating structures. Although it can influence the damping and result in nonlinear damping coefficients especially in roll motions. Journee & Massie (2015) do show that the damping of vertical oscillation depends on the density of the water, the gravitational acceleration, the displacement of the platform itself, the frequency of the motion and the amplitude of the wave created.

As explained, determining the damping is very difficult and time-consuming. Although it is a very important parameter, the damping is not calculated or determined by experiments. A standard value of 0.1 is used for the damping ratio (not the damping constant) as this is the value usually used for ships. It is investigated what the change of this value means for the motions, but not how the conditions and the changes of the parameters influence the damping constant. For a more extensive determination of the motion of floating high-rise buildings, more research will have to be done into the damping.

The damping constant can be calculated using the formula:

$$c = 2\zeta(m + a)k \text{ [Ns/m]} \tag{6.4}$$

Where

ζ is the damping ratio.

The added mass coefficient (a) is the added mass or the effective mass of the fluid that surrounds the body which must accelerate along with the body. This is due to the effect of distortion of the flow pattern of the water created by a body floating in flowing water or an accelerating body in still water. Although the water particles surrounding the body will accelerate to varying degrees, depending on their position relative to the body, the added mass can be approximated by the weighted integration of the entire mass of accelerating fluid particles (Newman, 1977). Barltrop (1998) states that it is a complex effect which is dependent on the motion direction, oscillation frequency and the geometry of the submerged body but that it can be approximated by adding the mass coefficient to the total mass of the body in the equation of motion as can be seen in equation (6.1). In his book, Barltrop shows rough estimations for this added mass of a rectangular floating body for heave, sway and roll motions. These estimations can be seen in Figure 43.

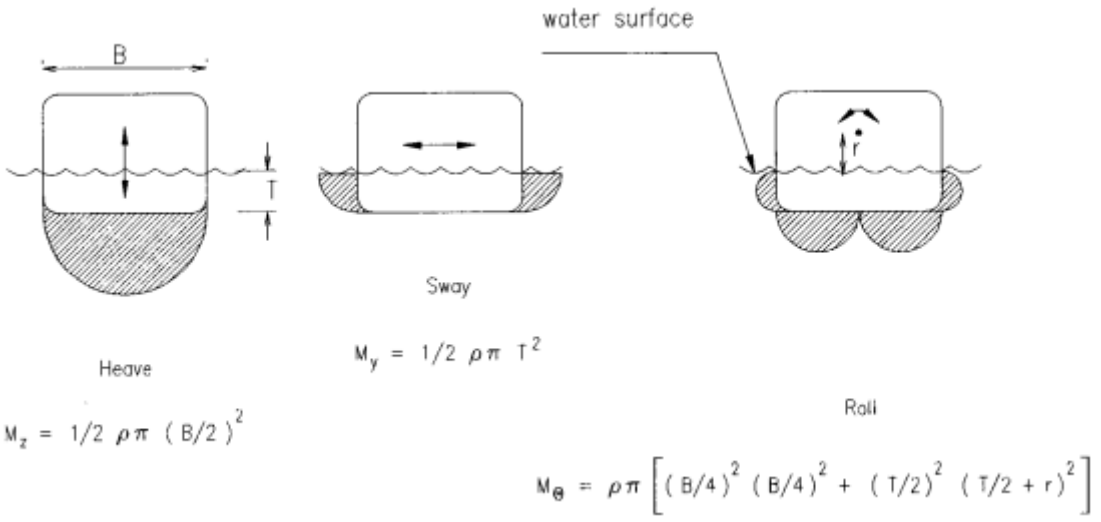

Figure 43 - Rough estimate of added mass (per unit length of hull). Source: Barltrop (1998).

As can be seen the added mass for the vertical translation is equal to:

$$a = \frac{1}{2} * \rho_{water} * \pi * \left(\frac{wp}{2}\right)^2 \tag{6.5}$$

6.2.2 HOMOGENEOUS SOLUTION

To solve the equation of motion, the eigenfrequency of both the damped and the undamped system must be found. For the undamped system this can be done by means of the homogeneous solution. To find this homogeneous solution the equation of motion (6.1) must be solved where the force (F_v) is equal to zero and the damping (c) is zero. This changes the equation of motion into:

$$(m + a)\ddot{w} + kw = 0 \tag{6.6}$$

To solve the equation, the following formula is used for the displacement:

$$w(t) = Acos(\omega_0 t + \varphi)\ [m] \tag{6.7}$$

Where

ω_0 is the eigenfrequency

φ is the phase shift

Using equation (6.7) in (6.6) and solve for ω_0 gives:

$$\omega_0 = \sqrt{\frac{k}{m + a}}\ [Hz] \tag{6.8}$$

As the damping value (ζ) is below 1, the system is of the under-damped type. The natural frequency of the damped system can then be calculated with:

$$\omega_e = \omega_0\sqrt{1-\zeta^2}\ \ [Hz]^6 \tag{6.9}$$

When using all the values and relationships from chapter 2, 3 and 4 for the parameters in the formula's in this paragraph, the eigenfrequency can be expressed into just two parameters; the height of the building and the width of the platform, for a specific depth of the platform. The result for a platform with as depth of 20m for a floating high-rise building at the North Sea is shown in the figure below as an example. Note that three parameters are used as variables in the calculation of the eigenfrequency: The height of the building, the width of the building and the depth of the platform. From the depth of the platform follows the necessary additional ballast to reach this depth as shown in chapter 4. The choice to take the depth as a variable and not as the minimum depth is because adjusting the mass gives a different eigenfrequency and the mass is adjustable freely.

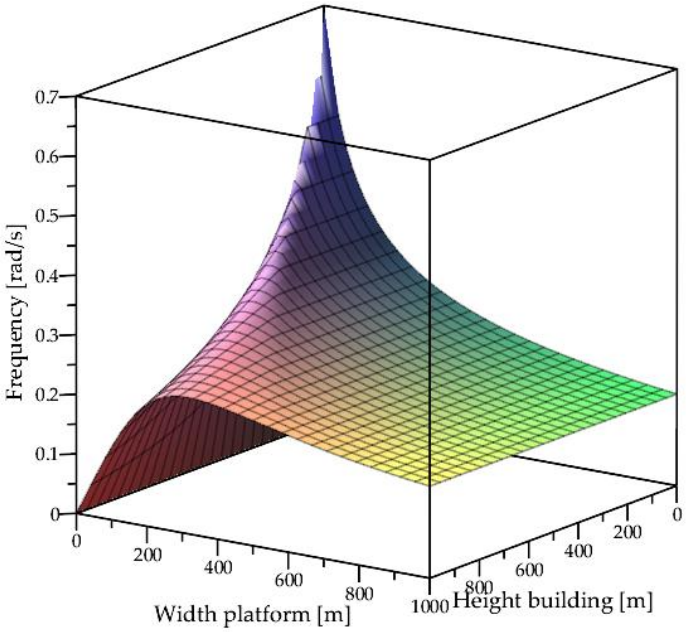

Figure 44 – 3D graph of the frequency of the vertical motion for different platform widths and building heights. For a platform with a depth of 20m at the North Sea.

6.2.3 VERTICAL WAVE FORCE

In chapter 2 the condition of the wave is described. For this research the waves are simplified to a sine function (2.1). In that same chapter is shown how to calculate the vertical wave force in equation (2.3). This force is a load distributed across the width of the platform. Because a point mass is used here, this must be converted to a point load. How this is done can be seen in Appendix II. It result in a extensive formula for the wave force which can be simplified into:

$$F_v(t) = \widehat{F}_w * \sin(\omega_w t + \ \varphi_w)\ [N] \tag{6.10}$$

With:

$$\widehat{F}_w = \frac{L * H * F_{water} * w_p * \sin(\frac{w_p * \pi}{L})}{2\pi}\ \ [N] \tag{6.11}$$

and

[6] Blaauwendraad. 2016

$$\omega_w = \frac{2\pi}{T}\ [Hz] \tag{6.12}$$

Since it does not matter for the result where and when the wave starts, in order to simplify (6.12), the phase shift (φ_w) is taken as zero. This results in:

$$F_v(t) = \widehat{F}_w * \sin(\omega_w t)\ [N] \tag{6.13}$$

6.2.4 PARTICULAR SOLUTION

For the particular solution the equation of motion in (6.1) needs to be solved where $F_v\ (t)$ is as show in (6.13). To solve the equation, the following formula is used for the displacement:

$$w(t) = C1 * sin(\omega_w t) + C2 * cos(\omega_w t)\ [m] \tag{6.14}$$

Substitution of (6.13) and (6.14) in (6.1) gives:

$$\begin{aligned} m * (-C1\omega_w^2 \sin(\omega_w t) - C2 * \omega_w^2 \cos(\omega_w t)) \\ + c\big(C1\omega_w \cos(\omega_w t) - C2\omega_w \sin(\omega_w t)) + k(C1 \sin(\omega_w t) + C2cos(\omega_w t)\big) \\ = \widehat{F}_{v,w} * \sin(\omega_w t) \end{aligned} \tag{6.15}$$

This can be solved by separating the sine and cosine parts:

$$m * -C1\omega_w^2 \sin(\omega_w t) + c * C2\omega_w \sin(\omega_w t) + k * C1 \sin(\omega_w t) = \widehat{F}_{v,w} * \sin(\omega_w t) \tag{6.16}$$

$$m * -C2\omega_w^2 \cos(\omega_w t) + c * C1\omega_w \cos(\omega_w t) + k * C2 \cos(\omega_w t) = 0 \tag{6.17}$$

Solving for C1 and C2 gives:

$$C1 = \frac{-(m\omega_w^2 + k)\widehat{F}_{v,w}}{m^2\omega_w^4 + c^2\omega_w^2 - 2km\omega_w^2 + k^2} \tag{6.18}$$

$$C1 = \frac{\widehat{F}_{v,w} c\omega_w}{m^2\omega_w^4 + c^2\omega_w^2 - 2km\omega_w^2 + k^2} \tag{6.19}$$

6.2.5 DISPLACEMENT AND ACCELERATION FOR HEAVE

For the total solution of the equation of motion, the homogeneous and particular solution needs to be combined and solved for the initial conditions:

$$w(0) = 0\ m \tag{6.20}$$

$$\dot{w}(0) = 0\ m/s \tag{6.21}$$

The displacement function (total solution) will have the following form:

$$w(t) = Ae^{-\zeta\omega_0 t} * \cos(\omega_e t + \varphi) + C1 * sin(\omega_w t) + C2 * cos(\omega_w t)\ [m]\ ^{7} \tag{6.22}$$

[7] Blaauwendraad (2016)

With A and φ unknown. Solving (6.22) for the initial conditions (6.20) and (6.21) gives the solved equation of displacement. The vertical acceleration in time can now be determined by taking the double derivative of the displacement. The maximum acceleration can then be determined from the acceleration function. This is the value that is most interesting because of its limits.

6.2.6 INFLUENCING PARAMETERS

In this subparagraph, the influence of various parameters on the vertical motion are examined. This is done by taking one of the parameters as variable and leaving the rest constant (They will have the values as shown in Table 4 in chapter 3). In this way, the influence of only that parameter can be investigated. There are several parameters and factors that influence the vertical motion of the platform. The factors are mainly location related such as wave height and wave period. These factors cannot be changed by choices in the design (but by choosing another location) and are kept constant in this subparagraph. In addition to the factors, there are parameters of the floating high-rise building that influence the motion. For the vertical motion these are as follows:

- Platform width (w_p)
- Height of the platform (h_p)
- Depth of the platform (d)
- Building height (h_b)
- Damping ratio (ζ, also referred to as “zeta”)

As explained in chapter 3, these are parameters for which the value can be freely chosen. (One can also choose to have the depth and height of the platform depend on the height of the building and the width of the platform. This has not been chosen here). The damping actually follows from the other parameters. Since the choice was made to assign a value to it and not to calculate it, the damping is examined as a free parameter.

The height of the building only influences the vertical motion because the mass changes with different heights. Because the mass can be changed by the extra ballast, the influence of the height is not discussed for the vertical motion. However, the influence of the mass is discussed.

The height of the platform has the only effect of changing the mass of the platform (it also provides more rigidity, but the flexibility of the platform is not included in the single-mass model). Since the mass is already being investigated and the change in mass is low, the height of the platform will not be investigated further.

For this investigation, we make use of the previous assumption, done in chapter 2, that the total solution of the equation of motion consists only of the particular solution at the most extreme wave height. (The case of a tsunami is discussed in the next subparagraph). For the total solution, the maximum acceleration is calculated and plotted against the variable parameter. The other parameters are constant (even though they would change. For example; if the platform widens the depth would decrease, but in these calculation the depth remains the same). This gives an indication of the influence of and sensitivity for each of these parameters in relation to the predicted acceleration. Of all the parameters above only the mass is not kept constant.

Platform width: In Figure 45, the maximum vertical acceleration is plotted against various values of the width of the platform for the condition of the North sea. The points in the graph are the calculated values. As can be seen the acceleration drops rapidly for the lower platform widths. It has a local minimum for a platform width of 133m. Then it goes up slightly until the next local minimum of 266m. (These two minimums are indicated with a triangle in the graph with its platform width value). These local minimums are where the width of the platform is equal to the wavelength (=133 m) or a multiple of the wavelength.

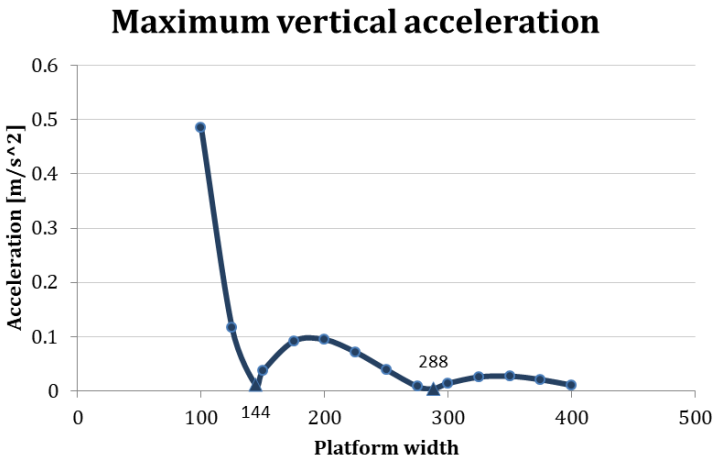

Figure 45 - Maximum vertical acceleration for different platform width for a building of 100m high at the North Sea. Single-mass model.

Damping ratio: Figure 46 shows the maximum acceleration for different values of zeta for a building of 100m for the conditions at the North sea. The value of the damping has a great influence on the maximum acceleration. The graph decreases approximately linearly, with a value of 0.5 having only half the maximum acceleration compared to no damping. Also, the homogeneous solution will be dampened faster with a higher damping value. However, it will not be easy to create a higher damping.

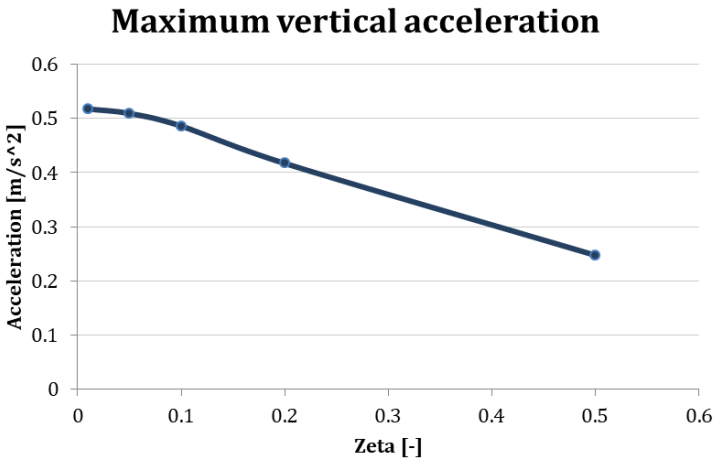

Figure 46 - Maximum vertical acceleration for different values of zeta for a building of 100m high for the conditions of the North sea. Single-mass model.

Platform depth: The depth of the platform does not affect the maximum acceleration for vertical motion in the single-mass model. This can also be seen from the formulas where the parameter "d" does not occur.

Mass: Figure 47 shows the maximum acceleration plotted against the total weight of the floating high-rise for a 100 m building at the North sea. The horizontal axis has a logarithmic scale. The graph makes an S-curve where the limit of the weight to infinity is equal to no acceleration. In other words, increasing the weight reduces the maximum vertical acceleration. The reduction in acceleration does differ for the different weight domains. In Figure 48 the graph is made without a logarithmic scale and only up to a total mass of $5 * 10^8$ kg. It can be seen that the decrease in acceleration decreases.

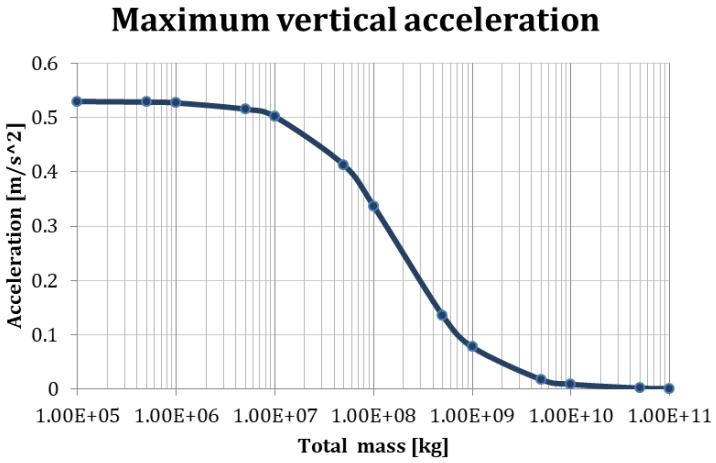

Figure 47 - Maximum vertical acceleration for different total mass for a building of 100m high. Single-mass model. The horizontal axis has a logarithmic scale

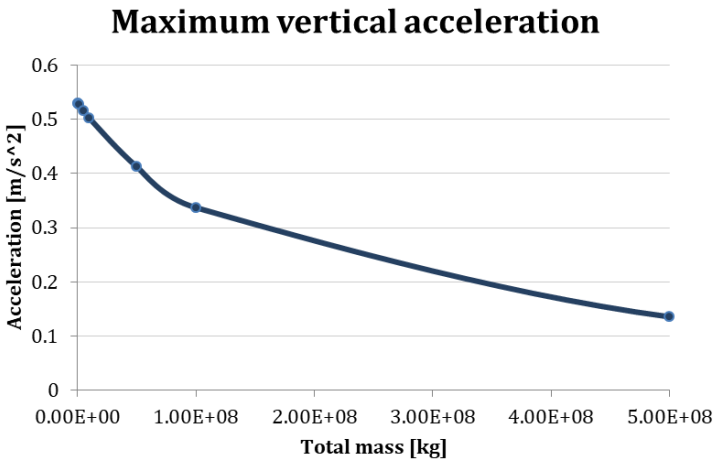

Figure 48 - Maximum vertical acceleration for different total mass for a building of 100m high with limited used values. Single-mass model.

Changing parameters: Until now, the different parameters determining the motion have been used as if they were independent of each other. Throughout this report it is explained how the different parameters depend on each other. This has been done in such a way that when all the relations are applied, there are only two parameters that remain variable; the height of the

building and the width of the platform. The others follow from these two parameters in combination with regulations (e.g. minimum 0.3 m height difference between the top of the platform and the crest of the highest wave).

Using all these relations, a more realistic graph of the maximum acceleration for different platform widths can be made. The resulting graph is shown in Figure 49. In addition to this graph with changing parameters, the previous graph is also included where the parameters were still independent.

The graphs hardly differ from each other. Only below 100m width there is a lower acceleration for the changing parameters. If the width of the platform is greater, the height and depth are constant because they have the minimum required values and thus this graph is as good as the same. When the same calculation, with changing parameters, is done for a building of 300m and 500m, it can be seen that for higher buildings the maximum acceleration decreases, see Figure 50. This is due to the increase of the weight at higher buildings, which causes less motion and less acceleration in the case of the vertical translation. The shape of the graphs are the same, however, there are minima at the platform width equal to the wavelength or a multiple thereof.

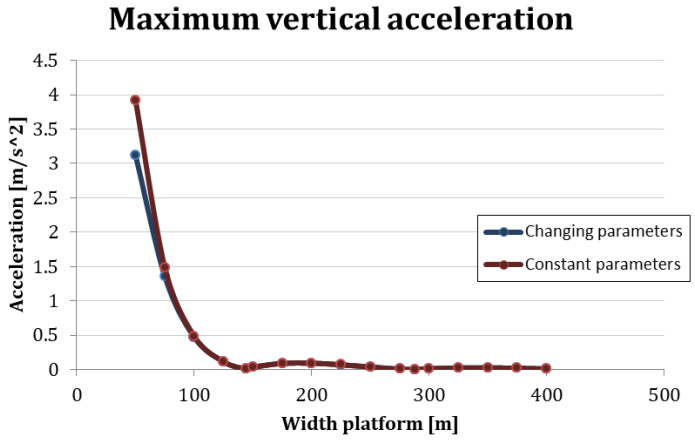

Figure 49 – Maximum vertical acceleration for different platform widths for a building of 100m high for both the constant parameter as the changing parameters. Single-mass model .

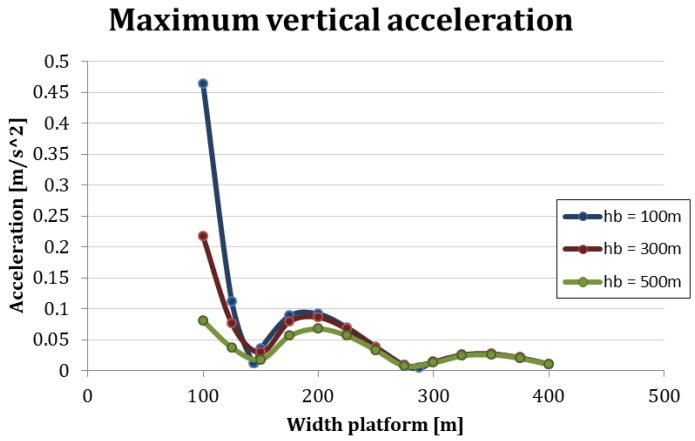

Figure 50 - Maximum vertical acceleration for different platform widths for a building of 100m, 300m and 500m high for changing parameters. Single-mass model .

6.2.7 TSUNAMI

The polynomial function (2.8) as described in the paragraph on location and conditions was used in the equation of motion to determine the motion of the floating high-rise building for the case of a tsunami. The result for the acceleration of only the homogenous part of the motion of the mass is shown in Figure 51. Only the homogeneous solution is interesting here. The particular solution will not be relevant because of the low wave height. This homogeneous solution is calculated by subtracting the acceleration of the particular solution from the acceleration of the total solution. The acceleration is negligible as can be seen in the figure. Since the maximum height of the tsunami is much lower than in a storm, it is concluded that a tsunami wave is not a problem for the vertical dynamic stability.

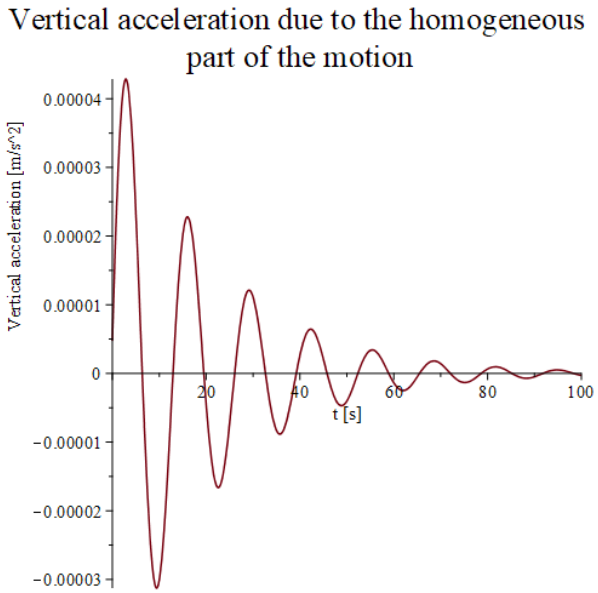

Figure 51 - Acceleration of the vertical motion for only the homogeneous part of the motion due to a tsunami.

6.3 HORIZONTAL TRANSLATION (SURGE AND SWAY)

The second motion discussed is horizontal displacement, see Figure 52. This displacement is caused by four things; The difference in water level at both ends of the platform, the impulse of the wave on the side of the platform, the wind on the structure and the flow of water. For the determination of the motion, not all four of these causes are taken into account. The current of the water will have a constant character and therefore the acceleration of the building due to the current will be negligible. Since acceleration is the cause of discomfort for people, this motion is not included. In addition to the flow, the impulse of the wave is not taken into account. The impulse of a wave can be significant if the wave breaks (Kortenhaus et al, 1999). This only happens in shallow waters. The floating high-rise will be built on open water where the depth of the bed is great enough not to cause breaking waves. This leaves the difference in water level and the wind force.

The mass-spring system again uses one mass with a displacement, spring, damper and force in the same direction; the horizontal direction, see Figure 53.

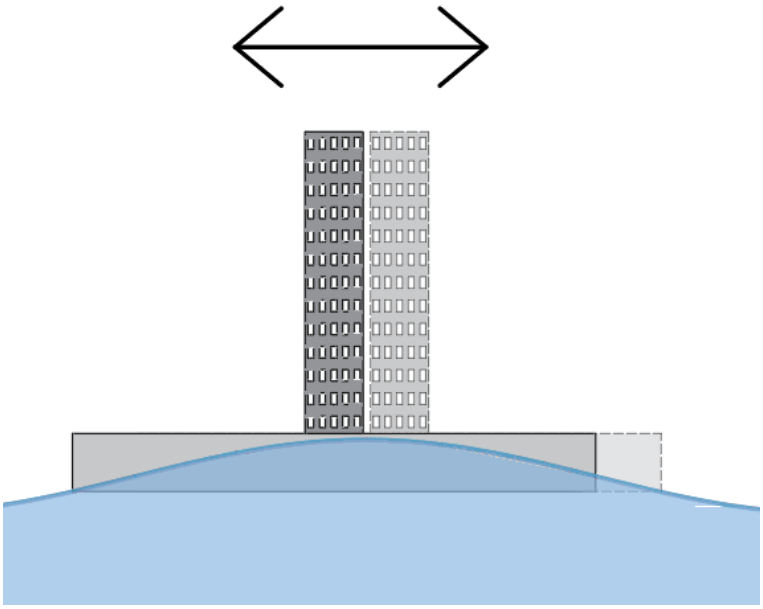

Figure 52. Horizontal translation (surge and sway).

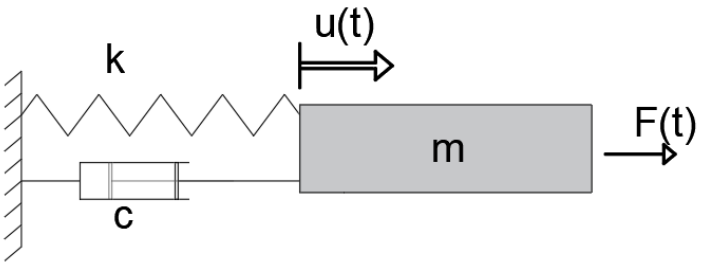

Figure 53 - Mass-spring system for the horizontal translation.

6.3.1 EQUATION OF MOTION AND ITS VALUES

For the motion the same equation of motion will be used as for the vertical translation only this time with the horizontal displacement u:

$$(m + a)\ddot{u} + c\dot{u} + ku = F_h \tag{6.23}$$

Where

u is the vertical displacement

According to Barltrop (1998), the added mass is as follows for the surge and sway (Figure 43):

$$a = \frac{1}{2}\rho_{water} * \pi * d^2 * w_p \, [kg] \tag{6.24}$$

The spring stiffness is again determined by the area where the water and the platform meet, multiplied by the density and the gravitational acceleration. For the horizontal motion, the surface area is the height of the water in relation to the bottom of the platform times the width of the platform. The height of the water constantly changes due to the waves, so the spring stiffness varies with time. This is not taken into account in this study as this makes it very difficult to find a solution to the equation of motion. This is because the height of the wave at the end of the plat-

form has a different phase shift than the resulting force acting on the platform. As a result, the formula of the solution to the equation of motion cannot be estimated properly. This is partly due to the presence of the spring stiffness in the root of the damping expression. To give the spring stiffness the desired constant value, the average of changing spring stiffness is taken. The average of a wave is its equilibrium position and thus the spring stiffness is multiplied by the depth of the platform. It has to be noted that this is a strong simplification and that for a more accurate model this change in spring stiffness should be taken into account. How much this simplification affects the results is unknown. The spring stiffness can then be calculated using:

$$k = \rho_{water} * g * w_p * d[N/m] \tag{6.25}$$

The same calculation for the damping is used:

$$c = 2\zeta(m + a)k \text{ [Ns/m]} \tag{6.26}$$

Again, the homogeneous solution can be used to find the eigenfrequency. The calculations are identical to those of the vertical motion, only the values used are different. The formula for the eigenfrequency of horizontal translating is as follows:

$$\omega_0 = \sqrt{\frac{k}{m + a}} \text{ [Hz]} \tag{6.27}$$

When using all the values and relationships from chapter 2, 3 and 4, the eigenfrequency can be expressed into the height of the building and the width of the platform for a specific depth of the platform. The result for a platform depth of 20m for a floating high-rise building at the North Sea is shown in the figure below as an example.

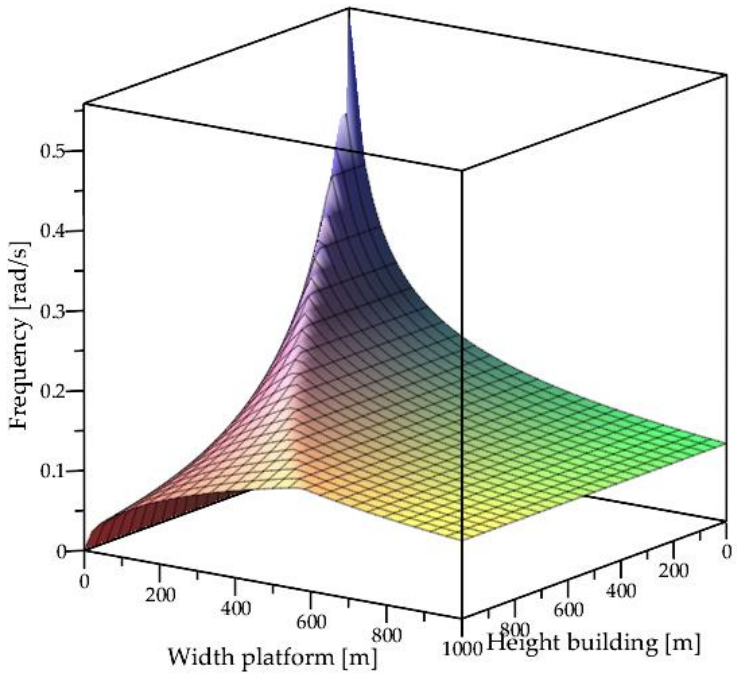

Figure 54- 3D graph of the frequency of the horizontal motion for different platform widths and building heights. For a platform with a depth of 20m at the North Sea.

6.3.2 HORIZONTAL WAVE AND WIND FORCES

Like the spring stiffness, the horizontal force depends on the water level. It is the difference in force between the two ends as shown in the figure below.

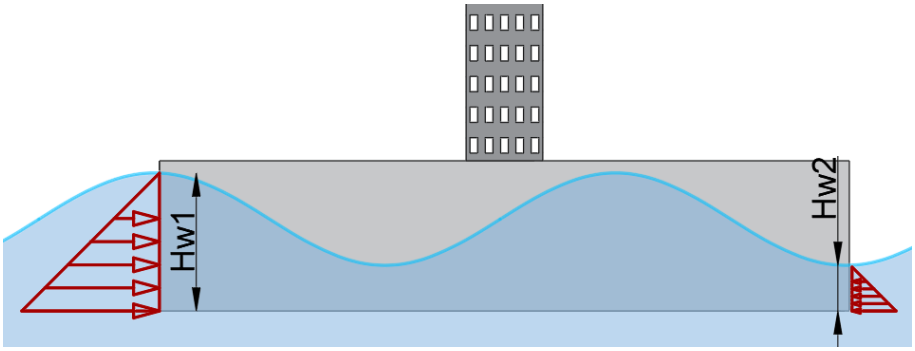

Figure 55 - Horizontal wave force on the platform.

If the wave is high at one end and low at the other, the force at one end is greater and the sum of forces is not zero. This resulting force can be calculated by:

$$F_{h,wave}(t) = \frac{1}{2} * \left(d + H_{w,1}(t)\right)^2 \rho_{water} * g - \frac{1}{2} * \left(d + H_{w,2}(t)\right)^2 \rho_{water} * g \tag{6.28}$$

Where $H_{w,1}$ and $H_{w,2}$ are the heights of the wave at the different ends of the platform. As said, these values are variable in time. The formulas are as follows:

$$H_{w,1}(t) = \frac{H_w}{2} \cos\left(\frac{2\pi t}{T_{wave}}\right) [m] \tag{6.29}$$

$$H_{w,2}(t) = \frac{H_w}{2} \cos\left(\frac{2\pi * w_p}{L_w} - \frac{2\pi t}{T_{wave}}\right) [m] \tag{6.30}$$

Where

H_w is the maximum height of the wave

L_w is the wave length

T_{wave} is the wave period

Since the time of the start of the motion does not matter for the calculations, the entire wave force can be written as one sinusoid.

$$F_{h,wave}(t) = \widehat{F}_{h,wave} * \sin(\omega_{wave} t)\ [N] \tag{6.31}$$

The expression for $\widehat{F}_{h,wave}$ is not shown as it is extensive. To include the wind in the dynamic analysis, the dynamic behaviour as described in chapter 2 is used. The function for the wind speed is shown in (2.5). The calculations for the wind forces is shown in Appendix II The only difference with the wind load in the static stability is that the reference speed is not constant but variable in time. And thus the wind force is variable in time. This results in a sine function:

$$F_{h,wind}(t) = \widehat{F}_{h,wind} * \sin(\omega_{wind} t)\ [N] \tag{6.32}$$

Where

$$\omega_{wind} = \frac{2\pi}{T_{wind}} \tag{6.33}$$

6.3.3 PARTICULAR SOLUTION

Again, a sine function is used for the displacement to find the particular solution. For the reaction to the wave force this is:

$$u(t) = C1 * sin(\omega_{wave} t) + C2 * cos(\omega_{wave} t)\ [m] \tag{6.34}$$

And for the reaction to the wind:

$$u(t) = C3 * sin(\omega_{wind} t) + C4 * cos(\omega_{wind} t)\ [m] \tag{6.35}$$

Different particular solutions have been used as the period of the wave and the wind can be different. This makes the total solution for horizontal displacement as follows:

$$\begin{aligned} u(t) = {} & Ae^{-\zeta\omega_0 t} * \cos(\omega_e t + \varphi) + C1 * sin(\omega_{wave} t) + C2 * cos(\omega_{wave} t) + C3 \\ & * sin(\omega_{wind} t) + C4 * cos(\omega_{wind} t)\ [m] \end{aligned} \tag{6.36}$$

6.3.4 INFLUENCING PARAMETERS

For the horizontal translation, the influence of various parameters was investigated, which is very similar to that for the vertical translation. Again, the important parameters were determined and investigated by fixing the other parameters. The difference lies in the parameters that have an influence. For the horizontal displacement, these are the following:

- Platform width
- Platform depth
- Total mass
- Damping ratio

Note: The parameters platform height, building height and building width again have an influence but were not investigated for the same reason as for the vertical translation.

The result of the examination of the parameters of the rotation is as follows:

Platform width: The result for the maximum horizontal acceleration for different platform widths is shown in Figure 56**.** The maximum horizontal acceleration for different platform widths is somewhat similar to that of the vertical translation, for small platform widths the maximum acceleration drops quickly to a local minimum. Then it goes up and down again until the next local minimum. Both minima are, as for the vertical translation, when the width of the platform is equal to the wavelength or a multitude of it. For the horizontal motion this is as expected as the height of the wave will be the same at both end at all times with these widths. The main difference is the much lower value of the maximum acceleration and the first local minimum is substantially higher than the second local minimum. That the maximum acceleration is less may be because the horizontal force is much less, but the spring constant is also less. Since the width

of the platform does not change its eigenfrequency, it could also be that with this set of parameters the eigenfrequency and the wave frequency are far apart and that this was less the case for the vertical translation.

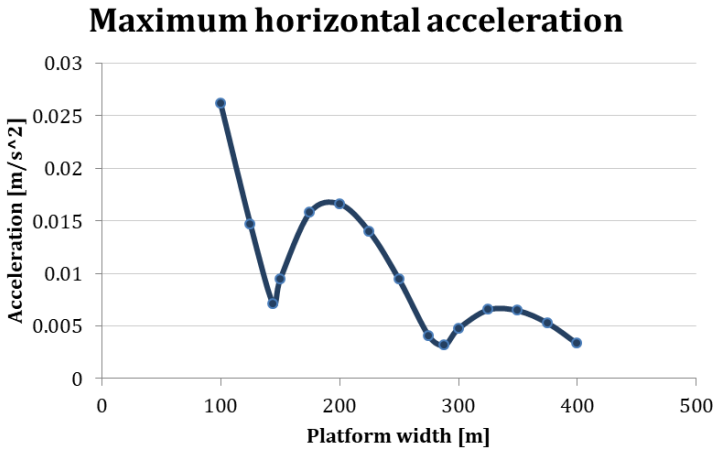

Figure 56 - Maximum horizontal acceleration for different platform width for a building of 100m high. Single-mass model.

Platform depth: The result for different depths of the platform can be seen in Figure 57. For shallower depths, an increase in depth also means an increase in maximum horizontal acceleration until a maximum is reached. Thereafter, the acceleration decreases exponentially at higher depth values. This result can be explained by the eigenfrequency. The formula for spring stiffness contains the term depth. If the depth changes, the spring stiffness changes too. As we have seen before with the equation of motion, the eigenfrequency is determined, among others things, by the value of the spring stiffness. So, changing the depth changes the eigenfrequency.

There is a certain value for which the eigenfrequency of the floating high-rise is equal to or close to the frequency of the excitation. When the response of the floating high-rise by the excitation is close to its eigenfrequency, resonance occurs. Resonance means that even small excitations can cause a large amplitude in the motion. This is illustrated in Figure 58, where the deflection is plotted against the ratio between the excitation frequency and the eigenfrequency. When this ratio approaches 1, the deflection increases dramatically. In a purely mathematical view of resonance, the deflection is even infinite when the ratio is equal to 1. In reality, this will not happen because there is always some form of damping, imperfection or other factor which causes it to have a limited deflection. It is always better to prevent resonance. The further away from this critical depth value, the less maximum acceleration. This type of influence of a parameter has not been seen for vertical acceleration.

The depth at which resonance occurs depends on several factors. For example, the mass plays a role in determining the eigenfrequency as can be seen from the formulas. Therefore, nothing can be said about what this critical value exactly is in different situations and Figure 57 serves only as an example.

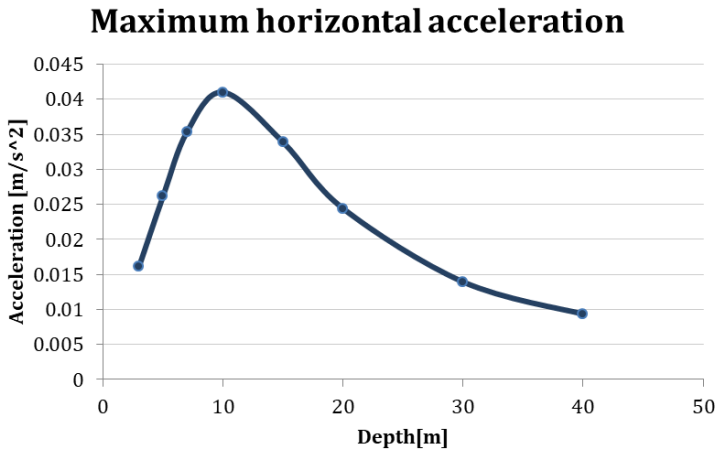

Figure 57 - Maximum horizontal acceleration for different platform depth for a building of 100m high. Single-mass model.

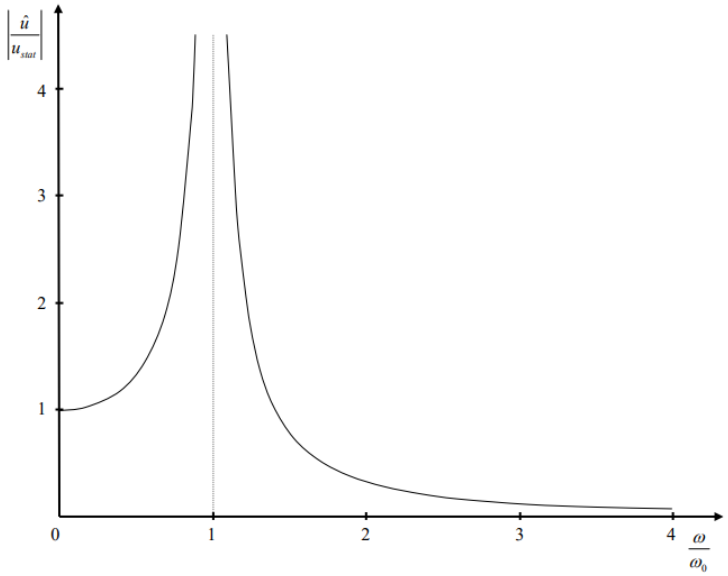

Figure 58 – Response of a system for different ratio's between the eigenfrequency and the excitation frequency. Source: J. Blaauwendraad. (2016) ***Dynamica van Systemen.***

Total mass: Figure 59 shows the graph with the results for different total mass of floating high-rise buildings, the horizontal axis has a logarithmic scale. The maximum horizontal acceleration decreases rapidly as the total mass increases until the acceleration is negligible. This is different from the vertical translation where the graph had a s curve.

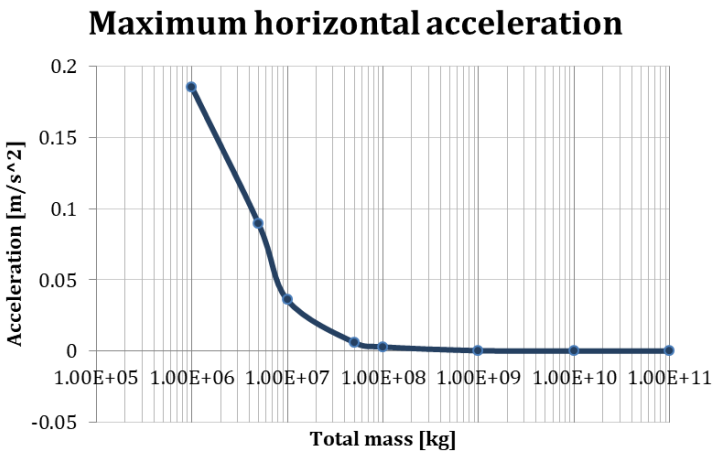

Figure 59 - Maximum horizontal acceleration for different total weight for a building of 100m high. Single-mass model.

Damping value: Figure 60 shows the maximum acceleration for different zeta values. This is approximately equal to the vertical acceleration, the acceleration decreases approximately linearly with increasing value of zeta.

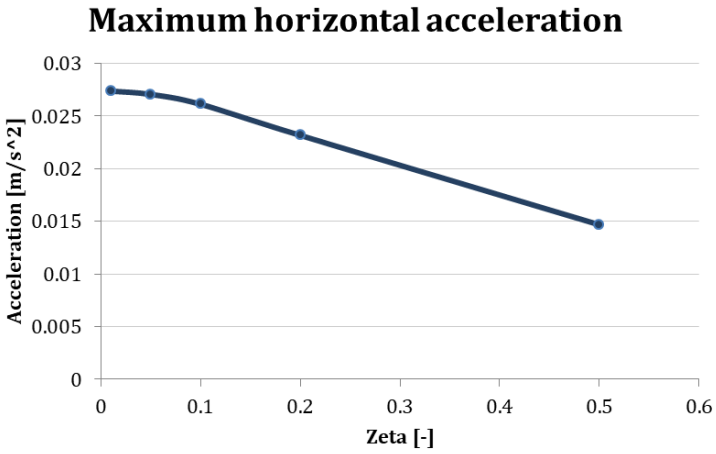

Figure 60 - Maximum horizontal acceleration for different damping values (zeta) for a building of 100m high. Single-mass model.

Changing parameters: Again, all relationships between the parameters were used to calculate the maximum acceleration to see what effect widening the platform has. The result is shown in Figure 61. With the changing parameters, a lower maximum acceleration is found. Furthermore, the graph resembles that of the constant parameters, only the local extreme values are less far apart. Still the minima are found at platform widths equal to the wavelength. When the same calculation, with changing parameters, is done for a 300m and 500m building, the results are quite different as can be seen in Figure 62. For the higher buildings, for small platform width, the maximum acceleration is less. This is due to the greater depth caused by the bigger weight. This causes more spring stiffness. The average decrease is less for higher buildings. Whereas the maximum acceleration between the first and second minima of a 100m building is still about 80%, it is only 23% for the 500m building. The graphs also do not go to zero acceleration for wider platforms, so for the larger platform widths, the acceleration is greater for taller buildings. This is because the effect of the deeper platform is no longer there as they all need extra ballast

to reach the minimum depth and because the taller buildings are wider so the wind load increases and so the maximum acceleration.

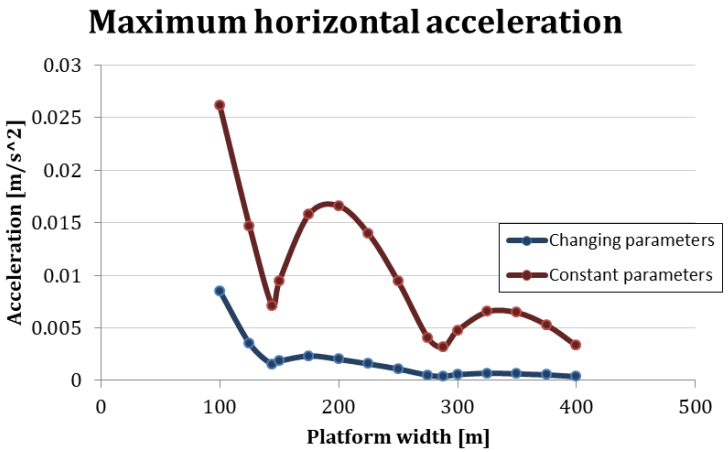

Figure 61 - Maximum horizontal acceleration for different platform weights with both the changing and the constant parameters for a building of 100m high. Single-mass model.

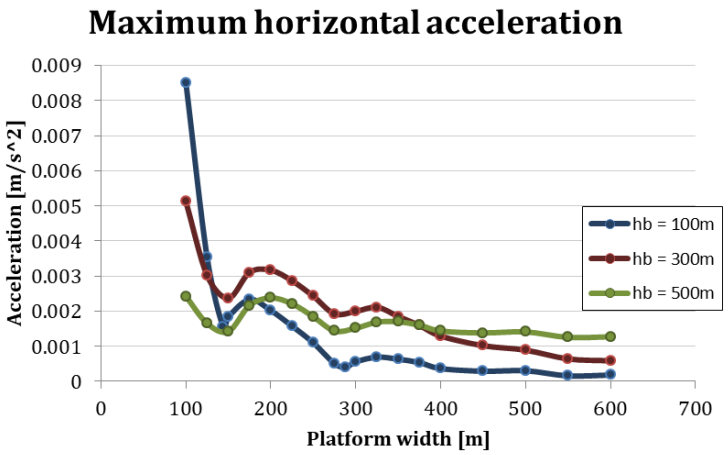

Figure 62 - Maximum horizontal acceleration for different platform widths for a building of 100m, 300m and 500m high for changing parameters. Single-mass model .

6.3.5 TSUNAMI

The calculations for the motion and acceleration of the mass were done for the situation of a tsunami. As with the vertical translation, the tsunami causes small accelerations which can be ignored, as can be seen in Figure 63.

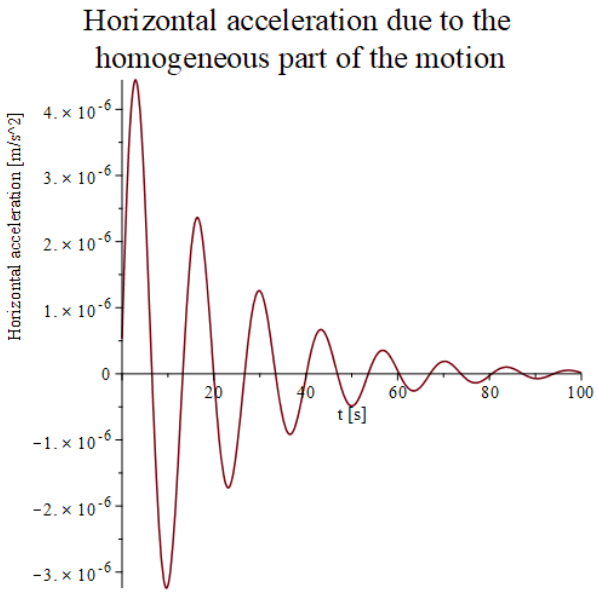

Figure 63 – Horizontal acceleration of the homogenous part of the solution due to a tsunami

6.4 VERTICAL ROTATION (ROLL AND PITCH)

In addition to the vertical and horizontal translation, the waves also cause a rotation. This is because the forces by the waves on the platform are not equally distributed. The wind causes a rotation as well. This is because the centre of gravity and the centre of rotation are lower than the centre of the distributed wind load. This creates a moment and thus a rotation. This is the same rotation as treated in the static stability. Figure 64 shows the motion in the waves.

Like the vertical and horizontal motion, the rotation is determined by means of a mass-spring system. With the difference that the motion, the spring and the damper are in the direction of the rotation. And instead of an external force there is an external moment which causes the excitation. This moment is the combination of the moment due to the waves and the moment due to the wind. Figure 65 shows the mass-spring system. The rotation is denoted with a θ. (θ is the standard letter for the pitch. The roll has ϕ as its default letter. To avoid confusion with the φ which stands for phase shift in a sine function, θ is chosen for all vertical rotations.)

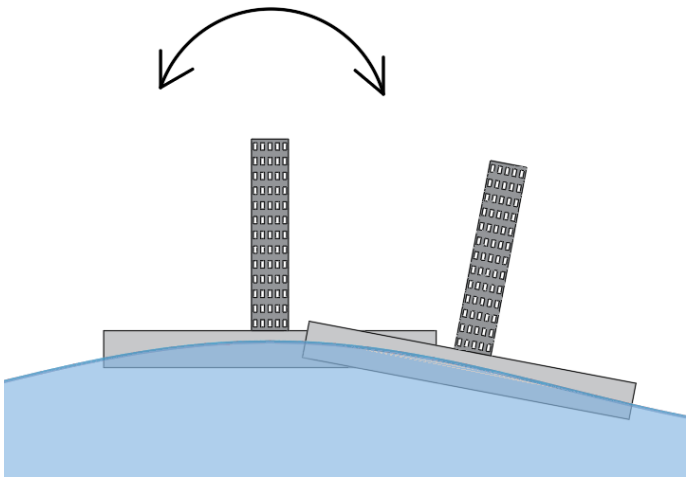

Figure 64 - Rotation due to the waves.

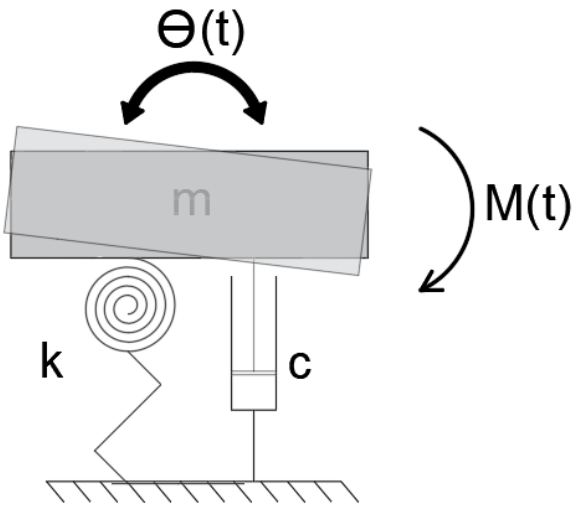

Figure 65 - Mass spring system with damping for the rotation.

6.4.1 EQUATION OF MOTION AND ITS VALUES

The equation of motion for the rotation of a one mass spring system is as follows:

$$(J + a)\ddot{\theta} + c\dot{\theta} + k\theta = M \tag{6.37}$$

Where:

θ is the rotation [rad]

J is the mass moment of inertia [kgm^2]

M is the external moment [N/m]

As can be seen, the equation of motion does not use the mass but the mass moment of inertia for rotation. This mass moment of inertia can be calculated by multiplying the mass and the radius of gyration:

$$J = m * K^2 \ [kg/m^2] \tag{6.38}$$

Where:

K is the radius of gyration also known as the polar inertia radius [m]

The radius of gyration can be calculated as follows:

$$K = \sqrt{\frac{I_{pol}}{A_w}} \ [m] \tag{6.39}$$

The polar moment of inertia can be calculated by summing the moments of inertia in x and y direction. (x is in direction of the wave and y is perpendicular to the water). For a floating structure, this is about the dimensions of the platform underwater.

$$I_{pol} = I_x + I_y = \frac{1}{12} * \left(d * {w_p}^3 + w_p * d^3\right) \ [m^4] \tag{6.40}$$

The area in (6.39) is the area of water (in x and y direction)

$$A_w = d * w_p \ [m^2] \tag{6.41}$$

Using (6.39),(6.40) and (6.41), (6.38) becomes:

$$J = \frac{\rho * {w_p}^2 * d({w_p}^2 + d^2)}{12} \ [kg/m^2] \tag{6.42}$$

The spring stiffness of the rotation can be determined with one formula using the GM value. The rotation spring stiffness is as follows:

$$k = \rho g V_{sub} * \overline{GM} \ [N/m]^8 \tag{6.43}$$

Where

$\overline{GM}$ is the metacentric height as described in chapter 5 on Static stability.

The added mass for the rotational motion can be obtained from Figure 43 as well:

$$a = \rho\pi\left(\left(\frac{w_p}{4}\right)^2 * \left(\frac{w_p}{4}\right)^2 + \left(\frac{d}{2}\right)^2 * \left(\frac{d}{2} + r\right)^2\right) \ [kg] \tag{6.44}$$

Where

r is the distance between the centre of gravity and the surface of the water [m]. This can be calculated with:

$$r = \text{COG} - \text{d [m]} \tag{6.45}$$

Where

COG is the height of the centre of gravity [m]

The same calculation for the damping is used as for the vertical translation:

$$c = 2\zeta(J + a)k \ [\text{Ns/m}] \tag{6.46}$$

Again, the homogeneous solution can be used to find the eigenfrequency. The calculations are identical to those of the vertical motion, only the values used are different. The formula for the eigenfrequency of rotation is as follows:

$$\omega_0 = \sqrt{\frac{k}{J + a}} \ [Hz] \tag{6.47}$$

[8] Journee & Massie. 2015

When using all the values and relationships from chapter 2, 3 and 4, the eigenfrequency can be expressed into the height of the building and the width of the platform for a specific depth of the platform. The result for a platform depth of 20m for a floating high-rise building at the North Sea is shown in the figure below as an example.

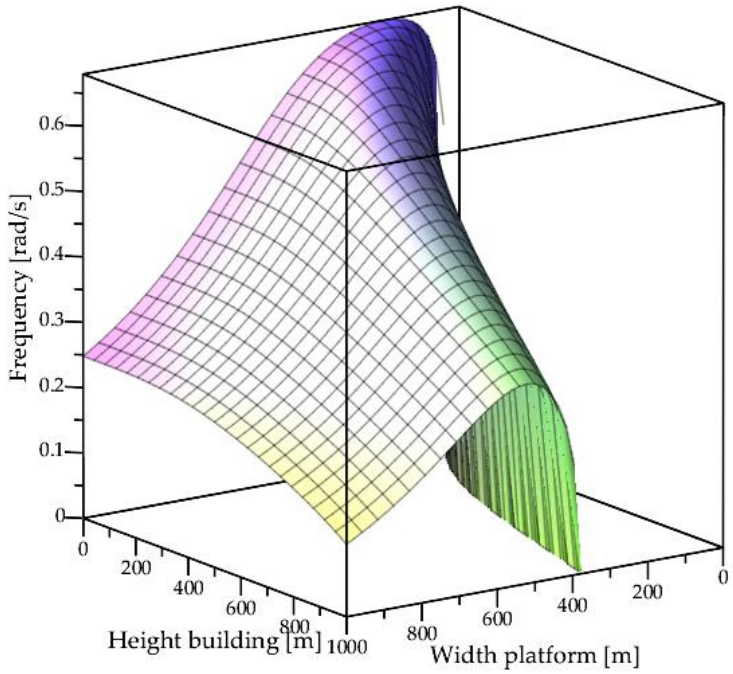

Figure 66 - 3D graph of the frequency of the rotational motion for different platform widths and building heights. For a platform with a depth of 20m at the North Sea.

6.4.2 WAVE AND WIND MOMENT

The calculation of the moment on the platform due to the waves is less straightforward than the calculation for the vertical or horizontal force. For the determination of the moment only the vertical force of the wave is taken into account. If the horizontal force of the wave was taken into account the calculation would have been substantially more difficult as the these forces do have the same period but a different phase shift. The horizontal force due to the wave is also substantially lower than the vertical force.

The distributed vertical force of the wave along the length of the platform is used. With some effort, the centre of the surface enclosed by this formula and the line y = 0 (symbolising the platform) can be determined. This point is where the resulting force of the wave passes through. With this point, the lever arm can be determined between the resulting force and the centre of the platform. The length of this arm is then multiplied by the enclosed surface itself (which is equal to the total vertical force). This gives the moment at the centre of the platform. The entire calculation can be found in Appendix II. The function, like that for the vertical force, can be simplified to a sine function with an amplitude and a frequency:

$$M_{wave}(t) = \widehat{M}_{wave} * \sin(\omega_{wave} t)\ [N] \tag{6.48}$$

As said, not only the wave causes a rotation but also the wind. The calculation for the moment due to the wind is also shown in Appendix II and can be simplified to a sine function:

$$M_{wind}(t) = \widehat{M}_{wind} * \sin(\omega_{wind} t)\ [N] \tag{6.49}$$

6.4.3 PARTICULAR AND TOTAL SOLUTION

The same steps were used as for the vertical translation, to find the particular solution. The resulting expressions are larger and will not be shown here. All that is shown here are the formulas used to find the solutions. To start with, the formula for the rotation. It consists of two parts, one to determine the reaction to the wave load (6.48) and one for the reaction to the wind load (6.49).

$$\theta(t) = C1 * sin(\omega_{wave} t) + C2 * cos(\omega_{wave} t)\ [rad] \tag{6.50}$$

$$\theta(t) = C3 * sin(\omega_{wind} t) + C4 * cos(\omega_{wind} t)\ [rad] \tag{6.51}$$

The formula for the rotation to find the reaction to the wind has an additional constant compared to that for the waves. This is because the waves have an equilibrium position at zero and the wind does not. Therefore an extra constant must be used to get the correct reaction.

For the total solution, the same term can be used for the homogeneous part as was used for the vertical translation, and the two different particular solutions can be added to this:

$$\begin{aligned}\theta(t) = \ & Ae^{-\zeta\omega_0 t} * \cos(\omega_e t + \varphi) + \ C1 * sin(\omega_{wave} t) + C2 * cos(\omega_{wave} t) + \ C3 \\ & * sin(\omega_{wind} t) + C4 * cos(\omega_{wind} t)\ [rad]\end{aligned} \tag{6.52}$$

6.4.4 INFLUENCING PARAMETERS

As for the translations, a parameter study was done for the influencing parameters. For the rotation, these are the following:

- Platform width
- Platform depth
- GM value
- Height of the centre of gravity
- Total mass
- Damping ratio

Platform width: For the maximum angular acceleration for different platform widths, see Figure 67. The rotational acceleration has the same pattern as the vertical and horizontal accelerations. With local minimums. Different from the translations is that the minimums occur at the zero moment widths. These are the platform widths for which the moment on the platform due to the wave is minimal regardless of time. These widths were also found in the rotation of the static stability model. These zero moment widths are further explained in Appendix V. The rotational acceleration decreases with increasing width. So the peaks between the zero moment widths become lower and lower.

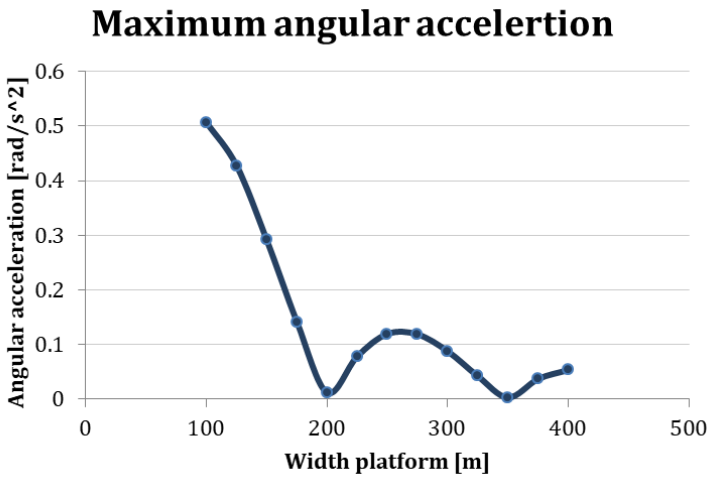

Figure 67 - Maximum angular acceleration for different platform width for a building of 100m high. Single-mass model.

Platform depth: Figure 68 shows the maximum angular acceleration for different depths of the platform. This has a similarity to the results of the horizontal acceleration. There is a certain value at which resonance occur and thus the acceleration is maximum and the further you are from this value, both lower and higher, the lower the maximum angular acceleration. So there is a value for depth such that the eigenfrequency is close to the excitation frequency. As with the horizontal displacement. The critical value for depth is not easy to determine for different situations as it depends on the other factors.

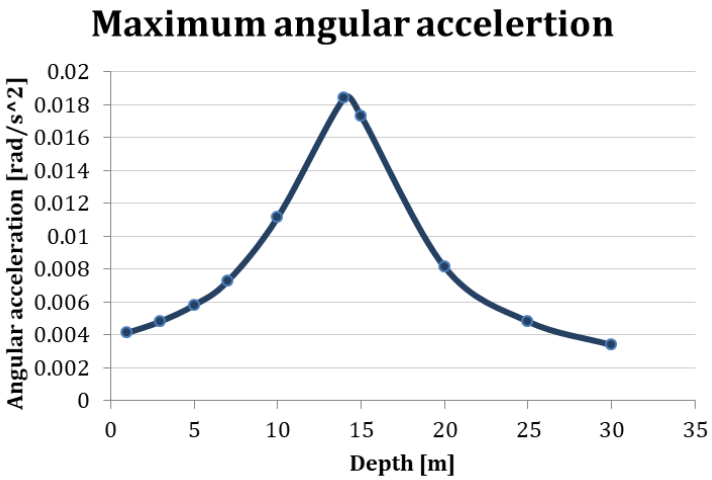

Figure 68 - Maximum angular acceleration for different platform depth for a building of 100m high. Single-mass model.

GM value: In the chapter on static stability it was shown that the value of GM was important for the rotation. The higher the value, the lesser the rotation. This value is also important for dynamics. Figure 69 shows the maximum angular acceleration for different values of GM. It can be seen that for the GM value, just as for the depth, resonance can occur at a certain critical value. This value therefore causes a peak in maximum acceleration. This is due to the presence of the GM value in the determination of the spring stiffness. If a value higher or lower than this critical value is chosen, the maximum acceleration will be less. In contrast to static stability, it is there-

fore not always more advantageous to increase the GM value for dynamic stability. As with the depth, the critical value for the GM value depends on other factors.

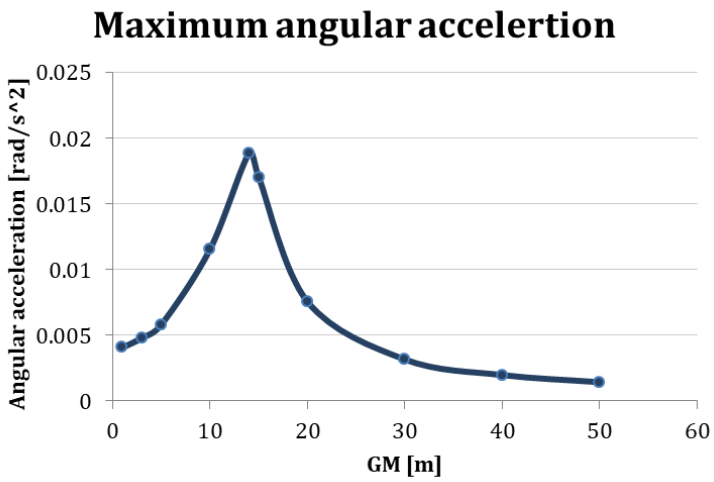

Figure 69 - Maximum angular acceleration for different GM values for a building of 100m high. Single-mass model.

Height of the centre of gravity: Another new parameter is the height of the centre of gravity (COG height). Since the GM value strongly depends on the height of the COG, they can hardly be seen separately. Nevertheless, the parameter is seen separately in order to draw certain conclusions. Figure 70 shows the result in maximum angular acceleration for different COG heights. The maximum angular acceleration decreases exponentially for higher values, however, the difference in maximum acceleration is very small for the first 100 m. Therefore, it can be concluded that the change of the COG does not have much influence on the acceleration. This also means that if it turns out that the building needs more mass at the bottom or top, this will not have a large negative effect due to the change in COG height. Of course, the change in COG height does cause a change in GM value that can have an huge influence.

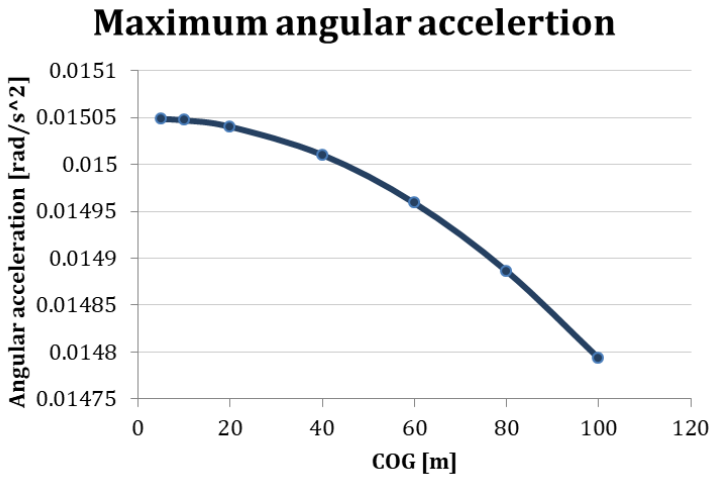

Figure 70 - Maximum angular acceleration for different Centre of gravity heights for a building of 100m high. Single-mass model.

Total mass: Figure 71 shows the maximum angular acceleration for the total mass of the floating high-rise building. This also contains resonance. This is not remarkable when looking at the

formulas, since the mass is included in the determination of the eigenfrequency, but this did not occur in the translations. The rotation is apparently more sensitive to the occurrence of resonance.

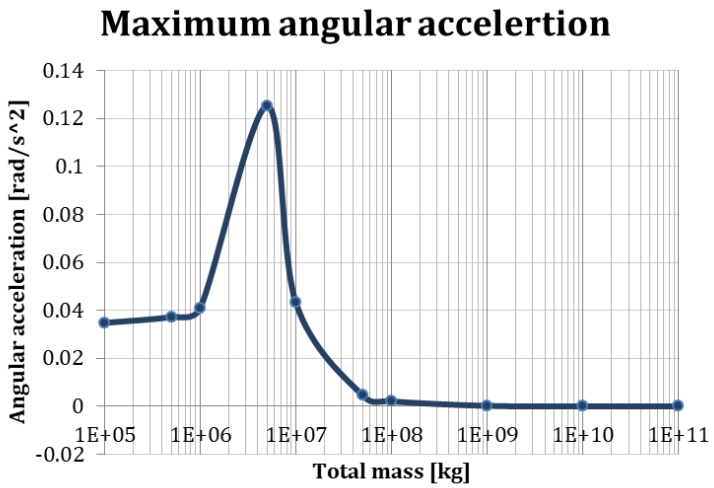

Figure 71 - Maximum angular acceleration for different total weights for a building of 100m high. Single-mass model.

Damping value (zeta): The damping graph, as shown in Figure 72, has the same pattern as for the translations. However, the difference in maximum acceleration is much less. Increasing the damping will therefore not be as positive on the maximum angular acceleration as it is for the maximum translational acceleration.

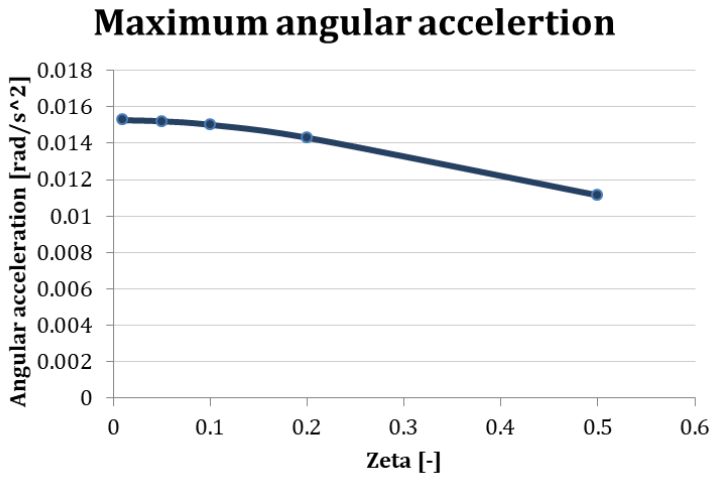

Figure 72 - Maximum angular acceleration for different damping values (zeta) for a building of 100m high. Single-mass model.

Changing parameters: Finally, the relation between the parameters was used to determine the maximum angular acceleration. The result is shown in Figure 73. At first glance, it looks identical to the results of the constant parameters. However, in Figure 74 it can be seen that the pattern is the same, but the value is much lower for the changing parameters.

The fact that the shape of the graphs do not differ much despite the resonance peaks in the graphs for depth, GM value and total mass may be due to the chosen height of 100 m for the

building. At this height the total mass is too little to achieve the necessary depth. An extra ballast is added to reach this depth and therefore the depth does not change with the different width of the platform (the wider the less depth the platform, so the depth will not increase) and the GM value is soon much higher than the resonance peak, for a platform of 100 m width and a building of 100m height, the GM value is already 287 m. To see if the resonance in these parameters still have an influence, the maximum angular acceleration is also calculated with changing parameters for a building of 200m, 300m, 400m and 500m. The results are shown in Figure 75. The absence of accelerations for certain widths is due to the fact that the GM value is negative, so there is no stability. With increasing height, a resonance peak appears in the graph. This is particularly noticeable in the case of the 500 m high building. Apparently, the influence of the three parameters with resonance (or at least one of the three) increases as the height of the building increases. It can be concluded from the graph that; The higher the building is, the more resonance occurs for the rotation.

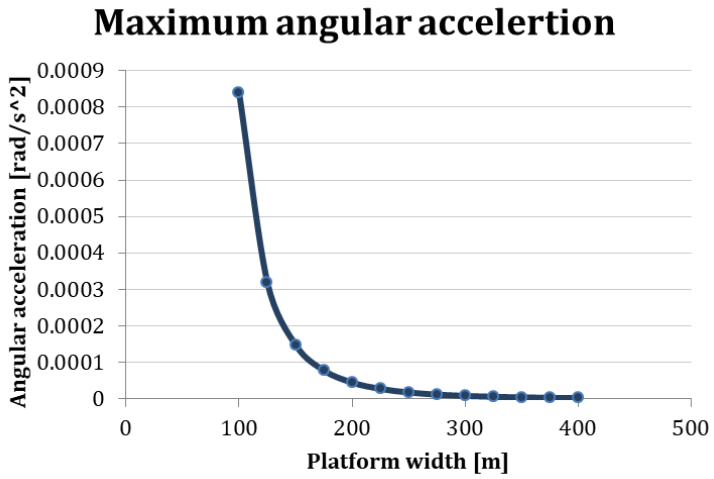

Figure 73 - Maximum angular acceleration for different platform width with all the other parameters depended on the width of the platform and the height of the building for a building of 100m high. Single-mass model.

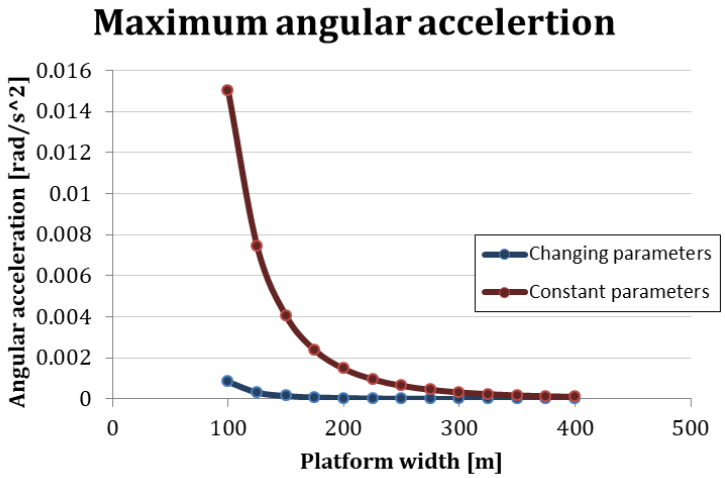

Figure 74 - Maximum angular acceleration for different platform width with both the constant as the changing parameters for a building of 100m high. Single-mass model.

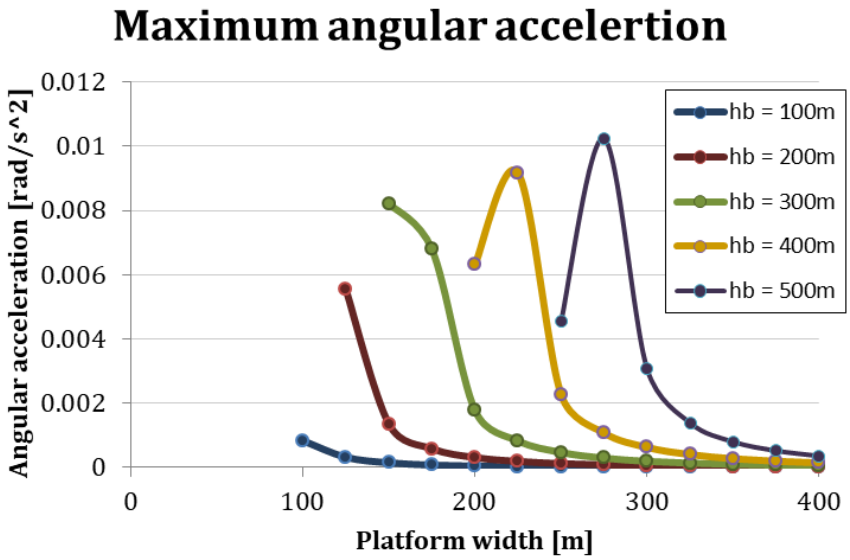

Figure 75 - Maximum angular acceleration for different platform width with all the other parameters depended on the width of the platform and the height of the building for a building of 100m, 200m, 300m, 400m and 500m high. Single-mass model.

6.4.5 TSUNAMI

The calculations for the motion and acceleration of the mass were done for the situation of a tsunami. As with the vertical and horizontal translation, the tsunami causes small accelerations which can be neglected as shown in Figure 76. Since for all three possible motions this reaction is negligible, no calculation will be done for the situation of a tsunami in the multi-mass model either.

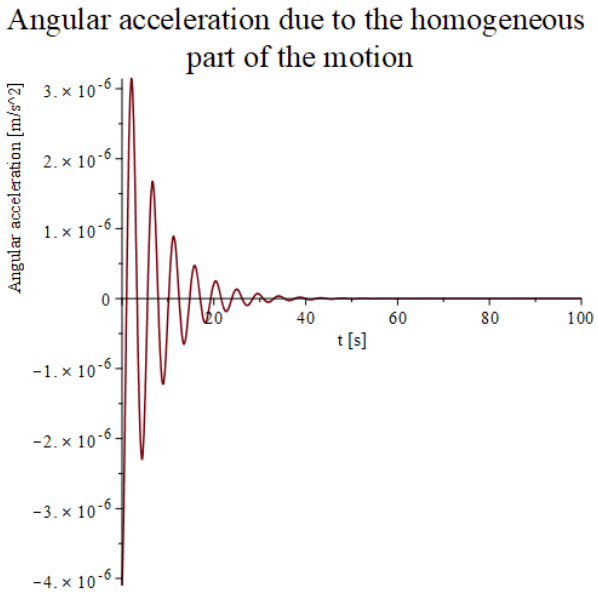

Figure 76 - Angular acceleration of the homogenous part of the solution due to a tsunami

6.5 MULTIPLE MOTIONS

The different motions are up until now all considered separately. In reality, all motions will occur simultaneously. This can cause the maximum acceleration to increase. Therefore, the differ-

ent motions are determined together. This means that the point mass has not one but several degrees of freedom (DOF's). Again the one mass spring system is used. This time with vertical and horizontal displacement and rotation, three DOFs, see Figure 77.

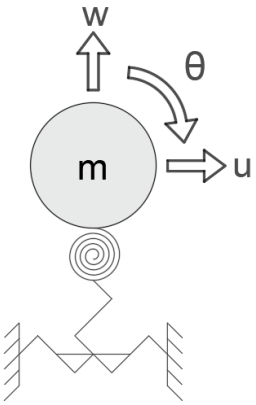

Figure 77 - Single-mass model with three DOF's.

Because these are three different motions, there are also three different equations of motion. The equation of motion of the vertical displacement (6.1) horizontal displacement (6.23) and the equation of motion of the rotation (6.32)) For this 3 mass spring system, the equation of motion changes from a single equation to a set of equations. This can be written as matrices.

$$(\boldsymbol{M} + \boldsymbol{A}) * \ddot{\boldsymbol{m}}\boldsymbol{v} + \boldsymbol{C} * \dot{\boldsymbol{m}}\boldsymbol{v} + \boldsymbol{K} * \boldsymbol{m}\boldsymbol{v} = \boldsymbol{F}_{ext} \tag{6.53}$$

Where:

$\boldsymbol{mv}$ is the motion vector

$\boldsymbol{M}$ is the mass matrix

$\boldsymbol{A}$ is the added mass matrix

$\boldsymbol{C}$ is the damping matrix

$\boldsymbol{K}$ is the spring stiffness matrix

$\boldsymbol{F}_{ext}$ is the external force matrix

The motion vector with the three degrees of freedom is as follows:

$$\boldsymbol{Motion\ vector} = \begin{bmatrix} w \\ u \\ \theta \end{bmatrix} \tag{6.54}$$

All matrices are, in a model with one mass, diagonal matrices. The mass matrix is as follows:

$$\mathbf{M} = \begin{bmatrix} m_1 & 0 & 0 \\ 0 & m_2 & 0 \\ 0 & 0 & I_3 \end{bmatrix} \tag{6.55}$$

The first and second mass are the masses that correspond to the vertical and horizontal motion. This is the same mass. The third "mass" is the mass moment of inertia corresponding to the rotation.

The added mass matrix contains the three different added masses of the three motions. These are the same as described for the individual motions. The same holds for the damping matrix and the spring stiffness matrix:

$$\mathbf{A} = \begin{bmatrix} a_1 & 0 & 0 \\ 0 & a_2 & 0 \\ 0 & 0 & a_3 \end{bmatrix} \tag{6.56}$$

$$\mathbf{C} = \begin{bmatrix} c_1 & 0 & 0 \\ 0 & c_2 & 0 \\ 0 & 0 & c_3 \end{bmatrix} \tag{6.57}$$

$$\mathbf{K} = \begin{bmatrix} k_1 & 0 & 0 \\ 0 & k_2 & 0 \\ 0 & 0 & k_3 \end{bmatrix} \tag{6.58}$$

The forces, like the motions, can be described by a vector:

$$\boldsymbol{F} = \begin{bmatrix} F_{vertical} \\ F_{horizontal} \\ M \end{bmatrix} \tag{6.59}$$

The equation of motion with matrices is as follows:

$$\left(\begin{bmatrix} m_1 & 0 & 0 \\ 0 & m_2 & 0 \\ 0 & 0 & I_3 \end{bmatrix} + \begin{bmatrix} a_1 & 0 & 0 \\ 0 & a_2 & 0 \\ 0 & 0 & a_3 \end{bmatrix}\right) * \begin{bmatrix} \ddot{u} \\ \ddot{w} \\ \ddot{\theta} \end{bmatrix} + \begin{bmatrix} c_1 & 0 & 0 \\ 0 & c_2 & 0 \\ 0 & 0 & c_3 \end{bmatrix} * \begin{bmatrix} \dot{w} \\ \dot{u} \\ \dot{\theta} \end{bmatrix} + \begin{bmatrix} k_1 & 0 & 0 \\ 0 & k_2 & 0 \\ 0 & 0 & k_3 \end{bmatrix} * \begin{bmatrix} w \\ u \\ \theta \end{bmatrix} = \begin{bmatrix} F_{vertical} \\ F_{horizontal} \\ M \end{bmatrix} \tag{6.60}$$

6.5.1 EIGENFREQUENCY AND HOMOGENEOUS SOLUTION

Just as in the calculation of the single-mass model, the eigenfrequency can be calculated. This is done with the equation of motion without the damping and the external force.

$$\boldsymbol{M} * \ddot{\boldsymbol{m}}\boldsymbol{v} + \boldsymbol{K} * \boldsymbol{m}\boldsymbol{v} = \boldsymbol{0} \tag{6.61}$$

For the displacement a cosine function is used:

$$mv_i = \hat{A}_i \cos(\omega t) \tag{6.62}$$

To find the eigenfrequency the determinant has to be found of $-\omega^2 * \boldsymbol{M} + \boldsymbol{K}$. The solution for the eigenfrequency is the solution for which the determinant is equal to zero. As there are multiple equations this will lead to multiple eigenfrequencies and eigenmodes. The number of eigenfrequencies and eigenmodes is equal to the number of degrees of freedom. In the example used, there is one mass with 3 degrees of freedom and thus 3 eigenfrequencies and 3 eigenmodes.

For a single-mass model the eigenmode is simple as it only has one frequency and one eigenmode. When there are several natural frequencies, the eigenmode can only be expressed as a ratio between the displacements. To do this, one of the motion is set equal to one (for example the vertical motion is 1). Then the remaining motion can be calculated with this set motion. With these results the ratio between the displacement for a certain eigenfrequency is known. This is

called the eigenmode. This eigenmode can be determined for all frequencies and can be described using a vector:

$$EM_{\omega i} = \begin{bmatrix} w_{\omega i} \\ u_{\omega i} \\ \theta_{\omega i} \end{bmatrix} \tag{6.63}$$

To find the homogeneous solution this eigenmode will be multiplied by the standard form of the homogeneous solution. For the first eigenfrequency this will look as follows:

$$u\ homogeneous_1\ (t) = \begin{bmatrix} w_{\omega 1} \\ u_{\omega 1} \\ \theta_{\omega 1} \end{bmatrix} A_1 * e^{-\zeta_{\omega_1} t} * \cos\left(\omega_{e,1} t + \varphi_1\right) \tag{6.64}$$

For the total homogeneous solution this is done for all eigenfrequencies. This gives the following formula for the motions:

$$Motion\ vector = \sum_{i=1}^{Degrees\ of\ freedom} EM_{\omega i}\ A_i e^{-\zeta \omega_i t} * \cos(\omega_{ei} t + \varphi_i) \tag{6.65}$$

Where

i is the index of the frequency.

The unknown A_i and φ_i values can be solved by using an initial displacement and rotation and an initial velocity of zero at t=0 for each motion, giving six equation to solve the six unknowns. When this all is done for the single-mass model it turns out that there is no relation between the three motions. This could already be seen in the equation of motion as all matrices are diagonal matrices. So the motions will not influence each other. This is called 'uncoupled'. In reality this is not the case and the different motions dependent on each other. To find a relationship between the motions, several masses must be used.

6.6 MULTIPLE-MASS MODEL

To model the entire structure as a single point mass is too simplistic. In reality, the rotation in the platform causes a translation in the building and platform. Furthermore both the platform and the building will deform and therefore influence the forces and motion of the structure. Therefore, it is more accurate to divide the structure into several masses in order to take this deformation into account. However, it is chosen to model the platform again as only one point mass. This is because each point mass has three degrees of freedom in a 2D plane. Because of this, each point mass creates three rows and columns in the matrices in the equation of motion (as seen in the previous paragraph). With more point masses the work to create the calculations exponentially grows. By keeping the platform as one point mass, the calculation work is limited. Besides the calculation work, it is also simpler to apply the values of the added mass, the mass moment of inertia and the rotational spring stiffness. These are difficult to divide correctly into different point masses over the platform width as these are not linear distributed. As one point mass for the platform does not include the flexibility of the platform, in this paragraph a subparagraph is dedicated to the inclusion of the deformation of the platform in the determination of the rotational stiffness of the spring.

Initially, the building is divided into three point masses with the mass of the platform in the lower point mass and the mass of the tower distributed over the three point masses, see Figure 78a. As mentioned, each point mass has three degrees of freedom (Figure 78b). The lower point mass is supported by springs in the directions of the three degrees of freedom, just like in the model with one point mass. In this model the point masses are connected to each other with a beam. The beam has the same properties as the tower.

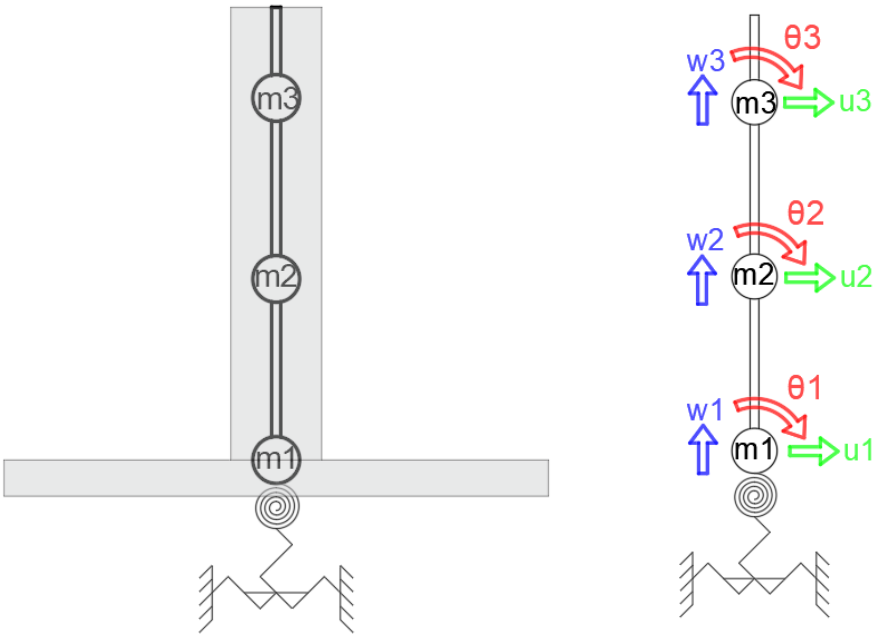

Figure 78 - Multiple mass model with 3 masses.

The three point masses together have nine different motions. These motions can be written in one motion vector:

$$motion\ vector = \begin{bmatrix} w_1 \\ w_2 \\ w_3 \\ u_1 \\ u_2 \\ u_3 \\ \theta_1 \\ \theta_2 \\ \theta_3 \end{bmatrix} \tag{6.66}$$

The formulas for the motions are again sinusoidal, in the form:

$$A * \cos(\omega t) \tag{6.67}$$

The motions can again be determined with the equation of motion. For the multiple mass model, this is as follows:

$$(\boldsymbol{M} + \boldsymbol{A}) * \boldsymbol{m\ddot{v}} + \boldsymbol{C} * \boldsymbol{m\dot{v}} + (\boldsymbol{K}_{spring} + \boldsymbol{K}_{beam}) * \boldsymbol{mv} = \boldsymbol{F} \tag{6.68}$$

Where:

$\boldsymbol{K_{spring}}$ is the spring stiffness matrix

$\boldsymbol{K_{beam}}$ is the beam matrix

The matrices of the mass, added mass and spring stiffness are nine by nine, diagonal matrices. In the added mass and spring stiffness matrices, there are only values for the motions of point mass one, since this point mass is the only one that is supported by springs and has extra mass due to the motion in water. The matrices are as follows:

$$\boldsymbol{M} = \begin{bmatrix} m_1 & 0 & 0 & 0 & 0 & 0 & 0 & 0 & 0 \\ 0 & m_2 & 0 & 0 & 0 & 0 & 0 & 0 & 0 \\ 0 & 0 & m_3 & 0 & 0 & 0 & 0 & 0 & 0 \\ 0 & 0 & 0 & m_4 & 0 & 0 & 0 & 0 & 0 \\ 0 & 0 & 0 & 0 & m_5 & 0 & 0 & 0 & 0 \\ 0 & 0 & 0 & 0 & 0 & m_6 & 0 & 0 & 0 \\ 0 & 0 & 0 & 0 & 0 & 0 & I_7 & 0 & 0 \\ 0 & 0 & 0 & 0 & 0 & 0 & 0 & I_8 & 0 \\ 0 & 0 & 0 & 0 & 0 & 0 & 0 & 0 & I_9 \end{bmatrix} \tag{6.69}$$

$$\boldsymbol{A} = \begin{bmatrix} a_1 & 0 & 0 & 0 & 0 & 0 & 0 & 0 & 0 \\ 0 & 0 & 0 & 0 & 0 & 0 & 0 & 0 & 0 \\ 0 & 0 & 0 & 0 & 0 & 0 & 0 & 0 & 0 \\ 0 & 0 & 0 & a_4 & 0 & 0 & 0 & 0 & 0 \\ 0 & 0 & 0 & 0 & 0 & 0 & 0 & 0 & 0 \\ 0 & 0 & 0 & 0 & 0 & 0 & 0 & 0 & 0 \\ 0 & 0 & 0 & 0 & 0 & 0 & a_7 & 0 & 0 \\ 0 & 0 & 0 & 0 & 0 & 0 & 0 & 0 & 0 \\ 0 & 0 & 0 & 0 & 0 & 0 & 0 & 0 & 0 \end{bmatrix} \tag{6.70}$$

$$\boldsymbol{K_{spring}} = \begin{bmatrix} k_1 & 0 & 0 & 0 & 0 & 0 & 0 & 0 & 0 \\ 0 & 0 & 0 & 0 & 0 & 0 & 0 & 0 & 0 \\ 0 & 0 & 0 & 0 & 0 & 0 & 0 & 0 & 0 \\ 0 & 0 & 0 & k_4 & 0 & 0 & 0 & 0 & 0 \\ 0 & 0 & 0 & 0 & 0 & 0 & 0 & 0 & 0 \\ 0 & 0 & 0 & 0 & 0 & 0 & 0 & 0 & 0 \\ 0 & 0 & 0 & 0 & 0 & 0 & k_7 & 0 & 0 \\ 0 & 0 & 0 & 0 & 0 & 0 & 0 & 0 & 0 \\ 0 & 0 & 0 & 0 & 0 & 0 & 0 & 0 & 0 \end{bmatrix} \tag{6.71}$$

The values for the added mass and the spring stiffness are the same as described earlier for the individual displacements. In the mass matrix, the masses m_4, m_5 and m_6 are equal to m_1, m_2 and m_3 respectively as these are the same masses. The first mass is equal to the mass of the platform plus one fifth of the mass of the building. The second and third masses are equal to two fifths of the mass of the building. The mass moment of inertia of mass 2 and 3 are substantially smaller than the mass moment of inertia of mass 1 due to the influence of the water on that mass.

The connection of the point masses creates another matrix in the equation of motion, the beam stiffness matrix. This is determined by the stiffness and lengths of the beams. The length between the masses is denoted by L. Appendix VI shows how this matrix was determined. The beam matrix is as follows for the model with three masses:

$$\boldsymbol{K}_{beam} = \begin{bmatrix} \frac{EA}{L} & -\frac{EA}{L} & 0 & 0 & 0 & 0 & 0 & 0 & 0 \\ -\frac{EA}{L} & \frac{2EA}{L} & -\frac{EA}{L} & 0 & 0 & 0 & 0 & 0 & 0 \\ 0 & -\frac{EA}{L} & \frac{EA}{L} & 0 & 0 & 0 & 0 & 0 & 0 \\ 0 & 0 & 0 & \frac{12EI}{L^3} & -\frac{12EI}{L^3} & 0 & \frac{6EI}{L^2} & \frac{6EI}{L^2} & 0 \\ 0 & 0 & 0 & -\frac{12EI}{L^3} & \frac{24EI}{L^3} & -\frac{12EI}{L^3} & -\frac{6EI}{L^2} & 0 & \frac{6EI}{L^2} \\ 0 & 0 & 0 & 0 & -\frac{12EI}{L^3} & \frac{12EI}{L^3} & 0 & -\frac{6EI}{L^2} & -\frac{6EI}{L^2} \\ 0 & 0 & 0 & \frac{6EI}{L^2} & -\frac{6EI}{L^2} & 0 & \frac{4EI}{L} & \frac{2EI}{L} & 0 \\ 0 & 0 & 0 & \frac{6EI}{L^2} & 0 & -\frac{6EI}{L^2} & \frac{2EI}{L} & \frac{8EI}{L} & \frac{2EI}{L} \\ 0 & 0 & 0 & 0 & \frac{6EI}{L^2} & -\frac{6EI}{L^2} & 0 & \frac{2EI}{L} & \frac{4EI}{L} \end{bmatrix} \tag{6.72}$$

Where

L is the length between the masses

E is the Young's-modules of the material used for the tower

I is the second moment of area of the tower

A is the cross-sectional area of the tower

This matrix can be used to calculate the force required to move the masses in the direction of the degrees of freedom. This can be done by multiplying the beam matrix by the motion vector. In formula form:

$$\boldsymbol{F} = \boldsymbol{K}_{beam} * \boldsymbol{motion\ vector} \tag{6.73}$$

Just like the forces of the springs, the forces in the beam are dependent on the motions. Therefore, the spring stiffness and beam matrixes are added together in the equation of motion.

Now that all the matrices are known, the eigenfrequency can be calculated as explained in the previous paragraph.

6.6.1 EIGENFREQUENCIES AND MODES

So far, the analytical approach has been used. To see if the calculations work and are correct, the eigenfrequencies and modes are calculated for the standard set of values for the parameters as an example. Then, these are compared with the results of a model in Diana. Diana is a Finite Element Analysis solver which can work well with schematic models with point masses. The results from this model are used to check whether the calculations are correct. This is done using one set of parameters. The model in Diana can then also be used to find out what the influence is of dividing the model into more point masses and how many masses are needed to model the structure accurately. This can then be used in the analytical approach. Finally a comparison is made between the frequencies from the single-mass model and the multiple-mass model.

Calculations of the eigenfrequencies of the standard set

For the calculation of one set of parameters to compare to the Diana model, the values given in Table 4 in chapter 3 are used. Since the Diana programme cannot assign a different value to the point masses in the horizontal and vertical directions, the same value is used in both the manual calculations and the Diana model. This is later on explained further. For the beam (core) element the following values are used:

Table 5 - Values for the beam used in the example.

L (length between masses)	E - modules	EI (building)	EA
40 m	$*1.3 * 10^{10}\ N/m^2$	$1.38 * 10^{13}\ Nm^2$	$1.68 * 10^{11}\ N$

* This is the reduced E-modules of a core.

Using these values result in the following values used in the matrixes:

Table 6 - Masses of the example.

m_1, m_4	m_2, m_3, m_5, m_6	J_7	J_8, J_9
$1.04 * 10^7$ kg	$7.58 * 10^6$ kg	$8.68 * 10^9$ kgm²/rad	$7.82 * 10^8$ kgm²/rad

Table 7 - Spring stiffness's of the example.

k_1	k_4	k_7
$1.01 * 10^8\ N/m$	$2.51 * 10^6\ N/m$	$6.71 * 10^{10}\ N/m$

Table 8 - Added mass values of the example.

a_1	a_4	a_7
$4.03 * 10^8$ kg	$1.00 * 10^6$ kg $4.03 * 10^8$ kg*	$1.27 * 10^9$ kgm²/rad

* For the added mass is horizontal direction the same value is used as for the vertical direction for this example. This is due to the limits in modelling in Diana which is explained later.

Now that all the values of the matrices are known, the eigenfrequencies can be calculated by setting the determinant of $-\omega^2 * \boldsymbol{M} + \boldsymbol{K}$ to zero and solving for ω. The eigenfrequencies are given in the table below.

Table 9 - Eigenfrequencies of the example.

Number	1	2	3	4	5	6	7	8	9
Frequency [rad/s]	0.0765	0.485	0.938	7.779	14.806	19.611	38.144	43.354	64.505
Frequency [Hz]	0.0121	0.0771	0.149	1.238	2.357	3.121	6.071	6.900	10.267

The calculation gives 18 eigenfrequencies for these matrices. This is the expected number, since the number of eigenfrequencies is normally twice the number of DOFs. The 10th to 18th frequencies give the same frequencies as the first nine, only negative. Therefore only the first nine eigenfrequencies are given.

Diana model

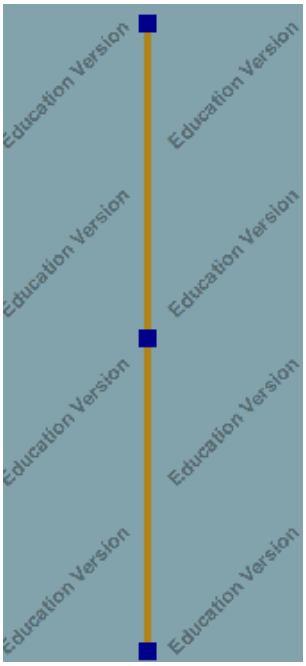

The same model, as used in the analytical model, was created in the programme Diana. There are three point masses connected with two line elements. In the program, a point can be either a translation mass or a rotation mass. Since the masses can both translate and rotate, two points are used at each position. These two points are attached to each other and to the end of the line element (also a point) by the 'unite' option. This ensures that the motions of the points are the same. There is no option in Diana to divide the translation mass into two different masses, one for the vertical motion and one for the horizontal motion. Often these are the same and thus there is no difference, however, due to the influence of the added mass, the bottom mass is different in the horizontal direction and vertical direction since the added mass of the vertical motion is greater than that of the horizontal motion. It was decided to give this point the added mass of the vertical motion for both motions. Therefore, the results of this Diana model are not completely accurate and hand calculations are better. For the comparison with the model, the same mass is used in the hand calculations as in the model. After this subparagraph, the correct mass is used. Therefore, some frequencies may deviate. The results of the Diana model are not used as results, but purely as a check on the calculation.

The values used in Diana are those given in Table 5, Table 6, Table 7 and Table 8. Where the mass and the added mass are added together and m4 has the same added mass as m1. Next, a structural eigenvalue analysis was done with the implicitly restarted Arnoldi method. The number of eigenfrequencies is set to 20 and a shift frequency of 0.01 Hz is used in order for the program to find the eigenvalues.

The resulting eigenfrequencies from the programme are shown in Table 10. The analysis in Diana gives the same nine eigenfrequencies as the hand calculations. Therefor it can be concluded that the hand calculations are correct when calculating the eigenfrequencies. Diana also gives eigenfrequencies higher than a million. These have not been included. The eigenmodes of this model are shown in Appendix VIII. These were used to determine the DOF at the frequencies and to check the results.

The building has so far been divided into three point masses. Now it is being investigated whether more point masses are needed to describe the motions. Diana is used for this purpose. The same values are used but they are now divided into 3, 5 and 9 point masses distributed over the height. The mass of the platform is still entirely in the bottom point mass. Also only the bottom point mass is supported by springs. Since the dimensions do not change, the spring constants and added masses do not change either. The mass and mass moment of inertia are changed accordingly.

The resulting eigenfrequencies of the Diana models are shown in Table 10. In addition, the table also shows the DOF of the frequency.

Table 10 - Eigenfrequencies of models with 3, 5, and 9 masses obtained from Diana. Including the DOF.

Number of masses	3		5		9	
Frequency Number:	Frequency [Hz]	DOF	Frequency [Hz]	DOF	Frequency [Hz]	DOF
1	0.0122	u_1	0.0122	u_1	0.0122	u_1
2	0.0771	w_1	0.0771	w_1	0.0771	w_1
3	0.149	θ_1	0.109	θ_1	0.0149	θ_1
4	1.238	u_3	1.288	u_5	1.291	u_9
5	2.357	w_3	2.385	w_5	2.395	w_9
6	3.121	u_2	2.989	u_3	2.964	u_5
7	6.071	w_2	6.501	w_3	6.429	w_5
8	6.9	θ_3	6.759	θ_5	6.991	θ_9
9	10.266	θ_2	10.169	θ_3	10.477	θ_5

The table shows that there is little difference between the eigenfrequencies of the models. There is some difference, but this can be caused by different rounding or by the fact that the masses are not at the same heights (see Appendix VIII). The only frequency that deviates somewhat is the 3rd (rotation of the lower mass) of the model with 5 point masses. The reason for this deviation is unknown. In the 9 point mass model this deviation is not there. It may be that it is a small modelling error. The larger deviations are in the eigenfrequencies higher than 2 Hz. These are far away from the eigenfrequencies limits and will therefore have no influence on the further calculations. It can be concluded that three point masses are enough to model the floating high-rise accurately and therefore, in the analytical method the use of three point masses can be continued and no more are used.

The table also shows that it is always the same DOF of the same mass that determine the eigenfrequency. These are always at the bottom, top or middle of the tower. (Appendix VIII shows that the frequencies corresponding to the extra point masses of the 5 and 9 point mass model are always higher than the three from the three point mass model.) In Table 11 the subscript indicates the DOF and location. Also the value in the matrix the motion is most depending on, excluding the mass, is show in the table. If this value changes, the eigenfrequency changes.

Table 11 – Eigenfrequencies and the location of the leading motion.

Frequency [Hz]	0.012	0.077	0.149	1.24	2.36	3.12	6.07	6.90	10.26
DOF	u_{bottem}	w_{bottem}	θ_{bottem}	u_{top}	w_{top}	u_{middle}	w_{middle}	θ_{top}	θ_{middle}
Most depending on (excluding the mass)	$k_{horizonta}$	$k_{vertical}$	$k_{rotationa}$	EI_{tower}	EA_{tower}	EI_{tower}	EA_{tower}	EI_{tower}	EI_{tower}

As already mentioned, the model has so far used the same added mass for the vertical and horizontal displacement of the lower mass. However, this is not correct. The calculations have been done again with the correct added mass. This, together with the results obtained earlier, can be seen in Table 12. The biggest change is in the first eigenfrequency. This is logical, because that is the eigenfrequency at the horizontal displacement of the bottom point mass. Also the eigenfre-

quency of the rotation of the bottom point mass changes reasonably. Furthermore, all eigenfrequencies of the horizontal and rotational motion change a little. It is clear that the Diana model is not accurate enough and cannot be used further for the calculations.

Table 12 - Eigenfrequencies with equal vertical and horizontal mass (Diana) and with correct added mass.

Number	1	2	3	4	5	6	7	8	9
Frequency (Diana) [rad/s]	0.0765	0.485	0.938	7.779	14.806	19.611	38.144	43.354	64.505
Frequency (correct added mass) [rad/s]	0.300	0.485	1.264	7.828	14.806	21.596	38.144	44.332	64.907

Limiting values have been set for the eigenfrequencies. These are between 0.3 and 1.44 rad/s. In order to determine which DOF must be examined to ensure that no resonance can occur, the eigenfrequencies are calculated for different values of the platform width and building height. This involves platform widths of 100, 300 and 500 m and building heights of 100, 300 and 500 m. The result and the analysis can be seen in Appendix VIII. From the results it is concluded that only the eigenfrequencies of the three motions of the bottom point mass are close to the limiting frequencies. These will therefore have to be investigated further in order to prevent resonance occurring in one of these motions. This is done in subparagraph 6.6.7.

Comparison single-mass model and the multiple mass model.

Now that it is known that the three mass model is sufficient and the frequencies of the different DOFs have been determined, the comparison can be made between the single-mass model and the multi-mass model. To do this, a 3D graph was made for the eigenfrequency of the vertical motion of the bottom point mass, as shown in Figure 80. The figure shows a blue and a red surface. The red surface is the result of the single-mass model and the blue surface the result of the multi-mass model. This graph is calculated differently from the previous one in paragraph 6.2. Before, the minimum platform depth was calculated and the additional ballast was adjusted accordingly. In the upcoming calculations and graphs a standard depth of 20 m is used. This makes the calculations less complicated and therefore possible to calculate analytically in Maple. Because of this method it deviates from the previously calculated eigenfrequencies as the depth and mass differs.

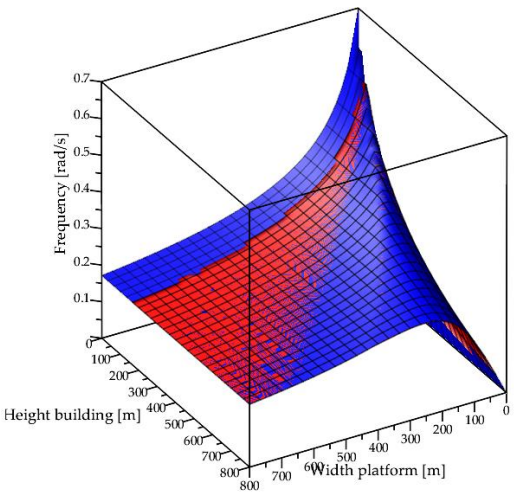

Figure 80 - 3D graph for the vertical frequencies single-mass model (red) and multi-mass model (blue).

For this vertical motion, there is almost no difference between the single-mass model and the multi-mass model. This is as expected since the three point masses act as one in the vertical direction (at this frequency, the frequency in which they move "apart" has an eigenfrequency which is much higher than the wave frequency and is thus not of interest). Therefore, it gives the same results as when only one point mass is used.

The frequency of vertical motion was relatively easy to express in the two variable parameters. This is more difficult for the horizontal motion and rotation. Therefore 2D graphs were made. For the horizontal motion, graphs have been made for a depth of 20 m with a building height of 100, 200 m and 500 m. These are shown in the following figures.

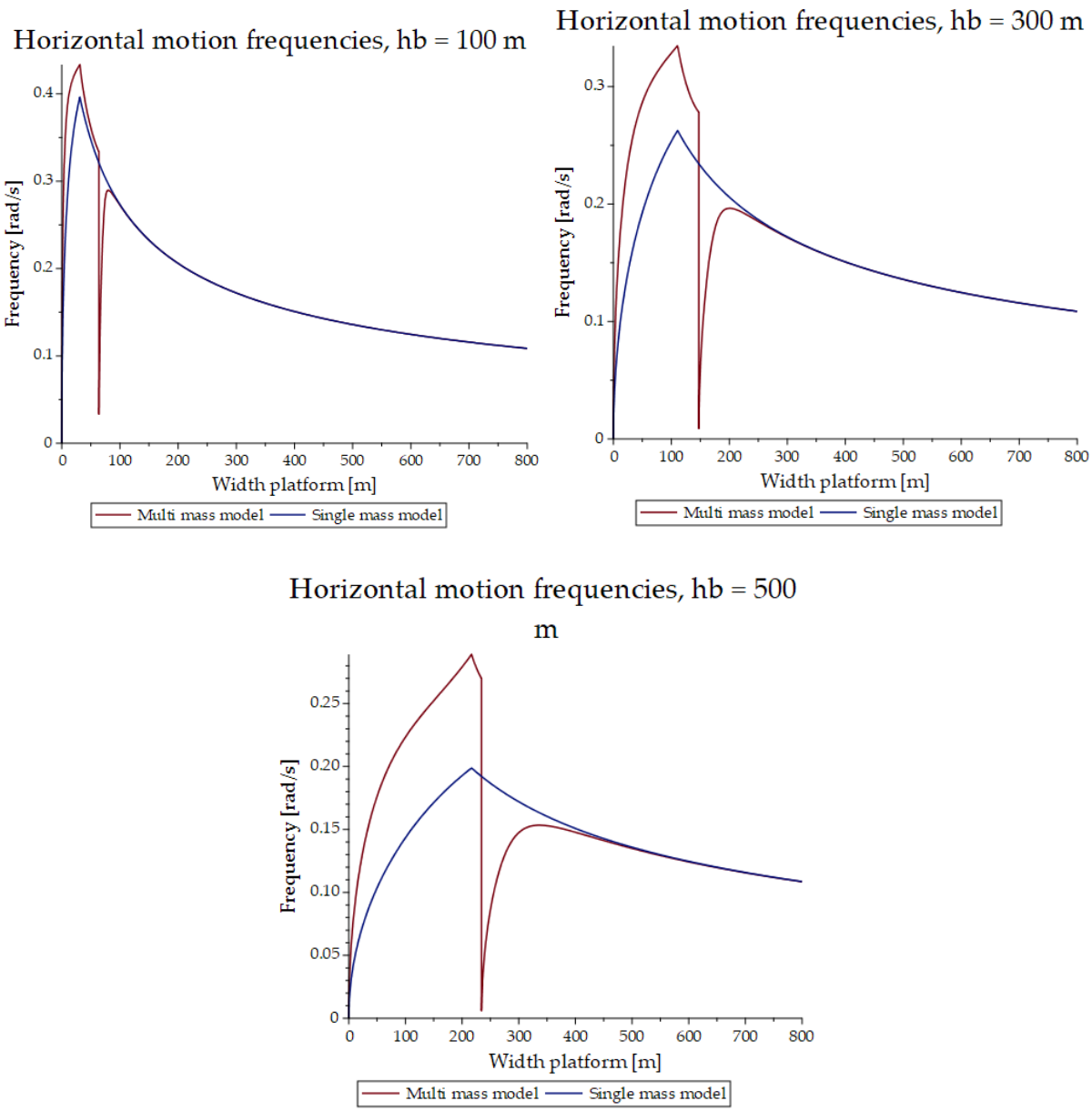

Figure 81 - Frequencies of the horizontal motion for the single and multi-mass model for a platform depth of 20m at the North Sea for a building height of a) 100 m, b) 300 m and c) 500 m

For the horizontal motion, the results of the multi-mass model are different from the single-mass model. Particularly for low platform widths and large building heights. Especially striking is the sudden drop in the graph of the multi-mass model. In order to investigate where this drop comes

from, graphs were made for all parameters used (e.g. spring stiffness, mass, building stiffness, etc.). None of the input parameters show the same valley, peak or other deviation. The drop is therefore a consequence of the expression of the frequency that follows from the matrix. Because it concerns a drop, the single-mass model estimates the frequency conservatively because the frequencies in question are below the limit frequencies drawn up in chapter 3. Before this drop, the estimation of the horizontal frequency of the single-mass model is lower than for the multi-mass model. Therefore, the single-mass model is not as accurate. This should be taken into account when using the single-mass model. After the drop, the two models are equal.

For the vertical and horizontal motion, the eigenfrequency was first expressed in the various parameters from the matrices (by solving the eigenfrequency analytically using the matrices). Then these parameters are expressed in the two parameters; height of the building and platform width. However, this analytical way of solving the problem gives only 8 results, where 18 were expected. These 8 results are from the three different vertical DOF and from the horizontal DOF of the bottom point mass. And the negative of these four. The other horizontal motion frequencies and those of the rotation do not result from this analytical calculation (for unknown reasons). They do arise from the numerical calculation. Because Maple cannot be used numerically in the right way, this programme is not an option to make the comparison between the single-mass model and the multi-mass model. And because the expression cannot be expressed in the parameters, no other programme can be used either. Therefore, it was not possible to make the comparison. Because the rotation and the horizontal displacement "work together", it is assumed that also for the rotation the single-mass model and the multi-mass model can strongly differ.

6.6.2 PARTICULAR SOLUTION AND TOTAL SOLUTION

As with individual motions, there are two components in the solution of the equation of motion. In a previous subparagraph, the requirements for the homogeneous solution were discussed. In this subparagraph, the particular solution will be dealt with. To start with the force matrix. This is a column matrix with, in the case of three point masses and three DOFs, 9 rows. three vertical forces (F_{ver}) , 3 horizontal forces (F_{hor}) and 3 rotational moments (M_{rot}).

$$\boldsymbol{F} = \begin{bmatrix} F_{ver,1} \\ F_{ver,2} \\ F_{ver,3} \\ F_{hor,1} \\ F_{hor,2} \\ F_{hor,3} \\ M_{rot,1} \\ M_{rot,2} \\ M_{rot,3} \end{bmatrix} \tag{6.74}$$

The forces on the platform (wave forces) have already been described earlier when dealing with the different motions. These forces all act on the lower mass (m_1) in this model. The other two masses ($m_2$and m_3) have no vertical harmonic forces and so these forces are zero. However, they do have horizontal forces acting on them, namely the wind force. All the formulas for the forces have been converted to a sine form. Using the previously defined formulas for the forces in the forces matrix, the matrix will be as follows:

$$\boldsymbol{F} = \begin{bmatrix} \widehat{F}_{ver,1,wave} * \sin(\omega_{wave} t) \\ 0 \\ 0 \\ \widehat{F}_{hor,1,wave} * \sin(\omega_{wave} t) + \widehat{F}_{hor,1,wind} * \sin(\omega_{wind} t) \\ \widehat{F}_{hor,2,wind} * \sin(\omega_{wind} t) \\ \widehat{F}_{hor,3,wind} * \sin(\omega_{wind} t) \\ \widehat{M}_{rot,1,wave} * \sin(\omega_{wave} t) + \widehat{M}_{rot,1,wind} * \sin(\omega_{wind} t) \\ \widehat{M}_{rot,2,wind} * \sin(\omega_{wind} t) \\ \widehat{M}_{rot,3,wind} * \sin(\omega_{wind} t) \end{bmatrix} \tag{6.75}$$

Note that the terms in front of the sine are factors in this matrix. This is indicated by the circumflex above the letter.

To solve the particular part of the equation of motion, a standard formula for the motion with unknown factors is used, as before. These look like the following:

$$w_i(t) = C_{i,1} * sin(\omega_{wave} t) + C_{i,2} * cos(\omega_{wave} t) + C_{i,3} * sin(\omega_{wind} t) + C_{i,4} * cos(\omega_{wind} t)\ [m] \tag{6.76}$$

The unknown factors $C_{i,j}$ can be solved by using the equation of motion with the formulas as seen above in the motion matrix.

The total solution is again the summation of the homogeneous solution and the particular solution. The form of the solution is as in (6.65) .This time with the eigenmodes as a column matrix with nine rows. This also means that each of the nine motions, has nine homogeneous terms plus a particular term. All the unknowns (nine factors and nine phase shifts) can be solved by setting the total motion and the total acceleration (derivative of the motion) equal to 0 at t = 0.

By doing this, you calculate the situation where there is an ocean without waves, and all at once the highest possible wave makes the platform move. This causes an enormous reaction. This reaction is in the homogenous part. The structure is displaced and rotated a lot in a small period of time. This causes a big acceleration. The structure has not yet “found its rhythm” in the waves. Finding the rhythm will be when the homogeneous solution is damped out and the total motion will be equal to the particular solution (only if the homogeneous solution is damped out). As explained in the paragraph on extreme cases in chapter 2, the biggest wave does not arise out of nowhere. Therefore, the two cases that have been described are used. For the growing wave an additional investigation is done into neglecting the homogeneous part of the solution.

With the single-mass models, it has already been concluded that the tsunami does not cause any problems. Therefore, this case is not further investigated in the multi-mass models. And so only the growing waves and the irregular waves remain. The growing wave is used as the most extreme situation as it uses the highest possible wave height. The irregular waves will later be used when analysing the possible eigenfrequencies. These irregular waves are fully described in chapter 2. The growing wave is missing a part about ignoring the homogeneous part of the solution. This is done in the next subparagraph.

6.6.3 DEFORMING PLATFORM

As explained earlier, the deformation of the platform is not included in the calculations due to using only one point mass to model the platform. To include the deformation, the formula of the rotational stiffness as described in the paragraph on rotation can no longer be used, as it does not include deformation. This method is based on the GM value. As described earlier, using the GM value simplifies the calculation of the moment balance of the support springs, the moment due to the weight and an external moment. To calculate the rotational stiffness, this balance is used. Appendix X contains the complete explanation and all the calculations for the determination of the rotational stiffness Here a summarized explanation is given.

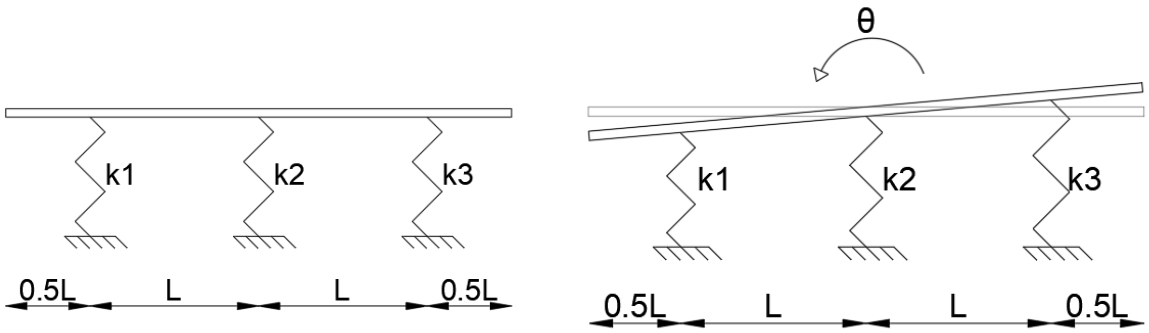

Figure 82 - Model of the platform supported by spring to calculate the rotational stiffness.

To find the rotational stiffness, the relationship between the rotation and the moment that causes the rotation must be found. Figure 82 shows the model of the rotation of the platform supported by three springs. The moment created by the forces in the springs is equal to:

$$M_{springs} = 2k_{vertical} * L^2 * \theta \ [Nm] \tag{6.77}$$

Where

$k_{vertical}$ is the vertical spring stiffness of each spring (all springs are equal) [N/m]

L is the distance between the springs [m]

θ is the rotation [rad]

The rotational stiffness is the factor that is multiplied with the rotation:

$$k_{rotation} = 2k * L^2 \ [N/m] \tag{6.78}$$

Instead of three springs, the water actually forms a line-spring-support. In order to achieve this support, an infinite number of springs must be used. To calculate this, the number of springs is set equal to n. Next, the lengths between the springs and the spring stiffness's can be determined in terms of n:

$$L = \frac{w_p}{n} \ [m] \tag{6.79}$$

$$k_{vertical} = \frac{\rho_{water} * g * w_p}{n} \ [N/m] \tag{6.80}$$

The rotational rigidity can also be described in terms of n using a summation:

$$k_{rotation,spring} = \ 2k * L^2 * \sum_{x=1}^{\frac{n-1}{2}} x^2 \ [N/m] \tag{6.81}$$

Combining (6.79), (6.80) and (6.81) and using unlimited springs $n \rightarrow \infty$. The formula for the rotational spring will be:

$$k_{rotation,spring} = \frac{1}{12} * \rho_{water} * g * {w_p}^4 \ [N/m] \tag{6.82}$$

In the GM method, the moment by weight is also included. This can also be written as a stiffness:

$$k_{weight} = d * {w_p}^2 * \rho_{water} * g * \left(\overline{COG} - \frac{1}{2}d\right) [N/m] \tag{6.83}$$

When these two stiffness's are added together, the formula is exactly the same as the formula with the GM value. This shows that with this spring moment method the correct stiffness can be calculated. To include the deformation, the same spring model will be used, but Ordinary Differential Equations (ODEs) will be used. With these ODEs the relation can be found between the rotation and the moment in the centre of the platform with a deforming platform. An investigation, shown in Appendix X, shows that supporting the platform with nine springs is accurate enough to approach a line-spring support. Using the ODEs, the following formula is determined for the rotational stiffness:

$$k_{rotation} = \frac{0.0329 * wp^4 * rho * g * \left(9.91 * 10^{-11} * g^3 * rho^3 * wp^{15} + 2.28 * 10^{-5} * EI * g^2 * rho^2 * wp^{10} + 0.889 * EI^2 * g * rho * wp^5 + 3240. * EI^3\right) * EI}{5.23 * 10^{-14} * g^4 * rho^4 * wp^{20} + 1.53 * 10^{-8} * EI * g^3 * rho^3 * wp^{15} + 8.91 * 10^{-4} * EI^2 * g^2 * rho^2 * wp^{10} + 6.58 * EI^3 * g * rho * wp^5 + 1300. * EI^4 - d * wp^2 * \rho_{water} * g * (\overline{COG} - \frac{1}{2}d)} \tag{6.84}$$

Where

EI is the stiffness of the platform

Using the standard values from the example, the new rotation stiffness can be calculated. Figure 83 shows the ratio between the spring stiffnesses of the rotating spring for a flexible platform (as determined by the formula above) and an infinitely stiff platform (as described in formula (6.43)) for different values of the stiffness of the platform. When the stiffness goes to infinity, the ratio goes to 1. This is in accordance with the expectation, since formula (6.43) assumed an infinite stiffness. The graph is made using the standard values. When these values change, the value for the stiffness at which the platform can be seen as infinite stiffness also changes. This value can therefore not be determined from this graph for other sets of parameters.

The reduction in rotational stiffness means an change of the eigenfrequency which depends on the rotation stiffness. The lower the bending stiffness of the platform, the lower the rotational stiffness and thus the higher the eigenfrequency.

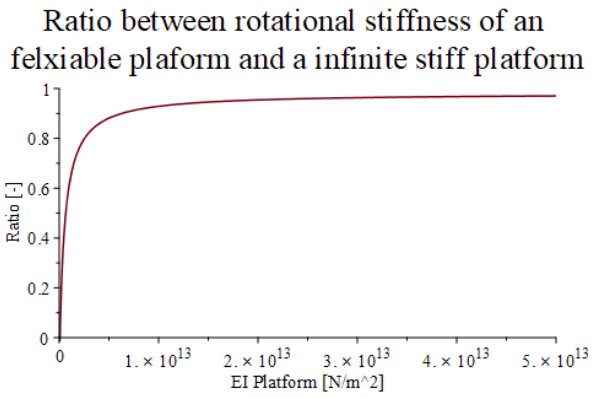

Figure 83 – Ration between the spring stiffnesses of the rotating spring for a flexible platform and an infinitely stiff platform for different values of the stiffness of the platform.

6.6.4 GROWING WAVES

For the response of the floating high-rise, only the particular solution was considered in the single-mass models because it was assumed that, even when the wave grows, the homogeneous solution is negligible. This is proved in this subparagraph.

A study was made into the total solution of the motion and thus the motion of the floating high-rise. To investigate this with a growing wave, a growth factor must be added to the formula of the wave. A normal exponential function was not used for this growth because this would mean that after reaching the full height (growth factor = 1), the wave would continue to grow. Instead, a formula for the growth factor was sought that starts "slowly" and does not exceed 1. In mathematical terms, the function must have a limit of $\lim_{t\to-\infty}(g(t)) = 0$ and $\lim_{t\to\infty}(g(t)) = 1$ This can be achieved with a so-called "S" curve. The standard formula for an S curve is as follows

$$\frac{1}{1+e^{-t}} \tag{6.85}$$

However, a typical S curve has a value of 0.5 at t = 0. The growth factor at t = 0 should actually be 0. In addition, the value 1 is approached very quickly. Therefore, a few adjustments have been made to the formula. The formula has been shifted and a factor has been added so that the formula has a value of 0.001 (=0.1%) at t = 0 and a value of 0.999 (=99.9%) at t = develop time. In this case, the develop time is equal to 40 hours * 60 * 60 = 144000 seconds. This is the develop time determined in chapter 2. The formula becomes:

$$growth\ factor\ (t) = \frac{1}{1+e^{-0.0000959271*(t-\frac{1}{2}*144000)}} \tag{6.86}$$

The growth factor in time looks as follows:

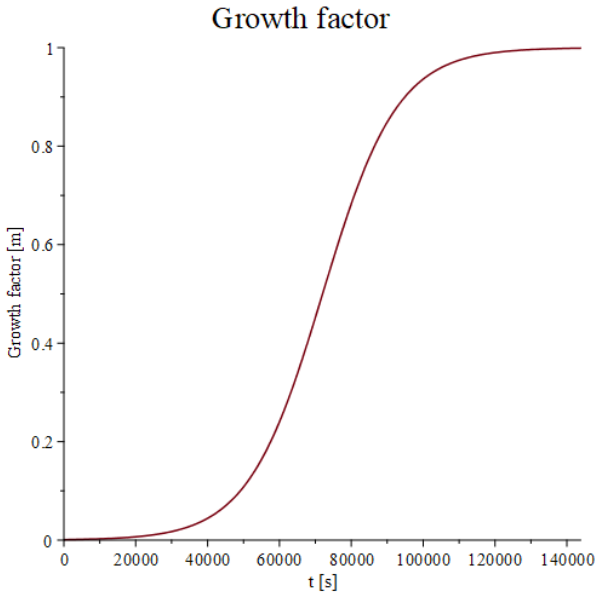

Figure 84 - Growth factor of the growing wave.

This growth factor is added to sine and cosine part of both the wave load (6.75) and to the standard formula used to solve the particular part of the equation of motion (6.76). Then the total solution can be determined. As an example, this is again done for an extreme situation: A building with a height of 500m and a platform with a width of 500 m at the Atlantic Ocean. Figure 85 shows the displacement of solely the vertical motion. There are two figures. The first figure is from t = 0 to t = develop time and thus concerns the growth of the reaction. The second figure is from t = develop time to t = develop time + 300 and is about the motion after the wave has reached its full height. The graphs of the horizontal motion and rotation are similar and can be seen in Appendix X.

In the graph from the develop time to the develop time +300, it can be seen that the peaks and troughs have the same period and that the deviation is the same. So there is no influence of the homogenous part anymore. No graphs are show here of only the homogenous parts as these are zero. These can also be found in Appendix X.

As the floating high-rise may not only be caught in a storm starting from a calm ocean, but may also sail into a storm, the same calculations were done with a develop time of 1 hour. Also for this develop time, the homogeneous part of the solution is negligible. The graphs for the motions with this develop time are shown in Appendix X.

From the graphs it is concluded that in a storm with maximum wave height, the homogeneous solution does not matter and the total solution is equal to the particular solution. Therefore, in the continuation of the study, the homogenous solution is no longer calculated for the situation with maximum wave height and the particular solution is considered to be the total solution. This saves a considerable amount of calculation time. (Please note that this was also done in the previous calculations of the single-mass models.)

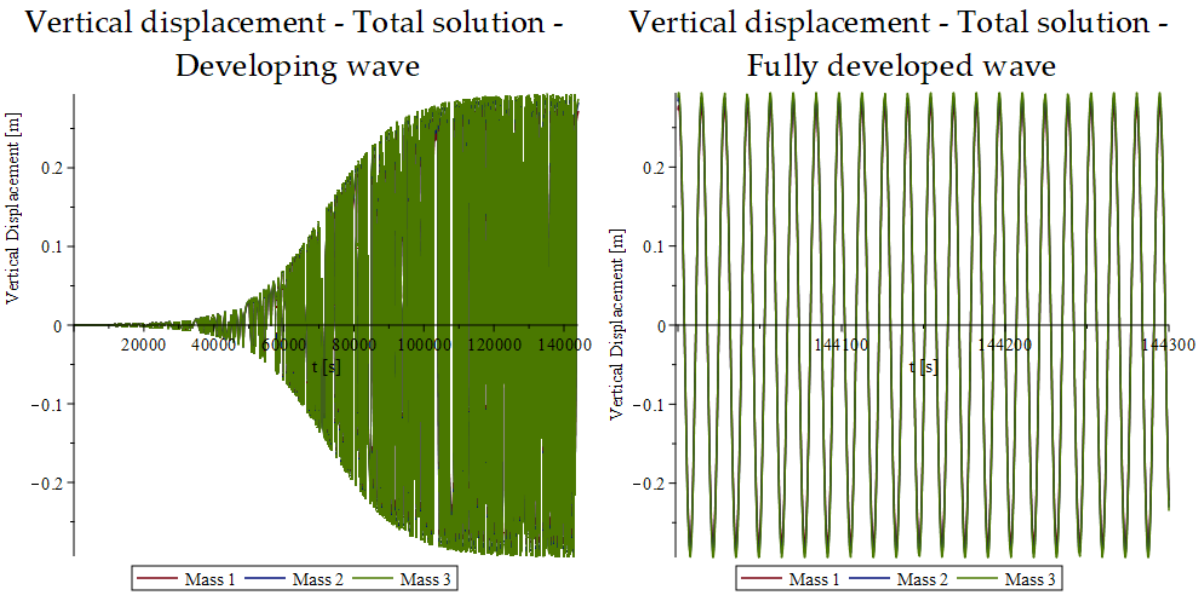

Figure 85 – Total vertical motion of the three point masses due to a growing wave.

6.6.5 INFLUENCING PARAMETERS

In subparagraph 6.6.4 it was shown that the total motion of the floating high-rise consists only of the particular solution of the equation of motion. In subparagraph 6.6.2 it was discussed how this particular solution can be found. However, it is not the motion, but the acceleration that is limited. Whereby the maximum possible acceleration is of interest. The maximum acceleration is influenced by several parameters as discussed earlier in the single-mass models. In this subparagraph, these parameters are examined in the multi-mass-model. This is done by calculating the maximum acceleration for different values of the parameters under investigation and plotting it in a graph. The parameters investigated are as follows:

- Width of the platform (w_p)
- Depth of the platform(d)
- GM value (GM)
- Width of the building (w_b)
- Stiffness of the building/core (EI_b)
- Mass (of the different point masses) (m)

These are the main parameters that can be changed. There are some other parameters which are not investigated such as the height of the building. This will be used as the "most important" and first parameter to be chosen, after which the rest will follow. Also the height of the platform will not be investigated, the height of the platform will follow from the required height above the waves and will mainly influence the depth of the platform, which will be investigated. The parameters "centre of gravity height" and "damping value" are not included in this chapter as they are not interesting. The height of the centre of gravity has a negligible influence when it does not change the GM value and the damping value has not been extensively investigated in this study. The influences of these are shown in Appendix XI.

Again, the relations between these parameters will not be used in this subchapter. This means that all values of the parameters remain the same, except for the parameter under investigation. For example, in the investigation of the influence of the width of the platform, the depth will re-

main constant. In reality, the depth will decrease with increasing width. This is done to study the influence of just the parameter. Later in the research, all relationships between the parameters will be used. The only parameter that does remain changing is the mass. For example, when the width of the building increases, the mass of the building also increases. The standard values used are as described in the chapter on assumptions.

For each parameter the results will be presented in graphs together with an explanation. In addition, a comparison will be made with the results from the single-mass models.

Please note that all graphs are created for the default value used, shown in chapter 3. Caution is taken in drawing conclusions about standard forms of the graphs and about values, as these can change greatly as the parameters change. The graphs are intended to extract the obvious features and see why the results are as they are. As the results do not give a realistic value for the acceleration and are only a form of ratios (for example, a platform of 100 m gives twice as much acceleration as one of 150 m). Therefore, for each graph, the vertical axis representing the acceleration is not provided with numbers.

Width of the platform

First, a difference in the width of the platform is considered. The width of the platform is perhaps the most important parameter as it appears in many parts of the calculations and also affects many other parameters. Therefore, it is difficult to determine in advance how changing the width would affect the accelerations. This has to be determined with the help of the model. The results of the model for the maximum accelerations for different widths of the platform are shown in Figure 87. These are the maximum vertical, horizontal and angular acceleration of all three masses.

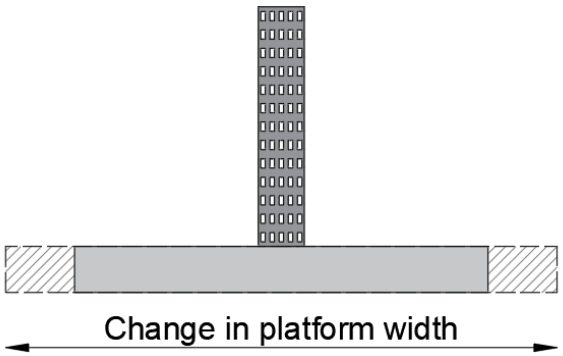

Figure 86 - Changing the platform width.

In Figure 87a the result for the vertical acceleration is shown. In this graph the results of all three masses are included but the three masses have (almost) the same results. At the left side the graph decreases sharply with increasing platform width until it reaches a local minimum. This is, as with the single-mass model, the value for which the width of the platform is equal to the wavelength. As the platform widens, the acceleration first increases and then decreases again until it reaches the second local minimum. This is when the platform has twice the width of the wavelength. When the results of the single-mass model with only vertical motion are compared with those of the multi-mass model, it can be seen that the vertical acceleration is the same.

The results for the horizontal acceleration are shown in Figure 87b. In contrast to the single-mass model, where the minimum was equal to the wavelength, just like the vertical motion, the minimum in the multi-mass model is equal to the zero moment width just like the rotation. This can be explained by the fact that there is a lot of horizontal displacement due to the rotation. In the single-mass models these motions were still independent of each other. Until the first minimum, the acceleration in the lower mass is normative, after the first minimum it does not increase so much anymore and the acceleration of the upper mass becomes normative. In these

platform widths, the rotation plays a greater role in the horizontal displacement of the upper point mass than the horizontal displacement of the lower point mass does. It is expected that the upper mass will be normative when the building is higher as the rotation arm will be longer. Point mass 2 has much less acceleration than the lowest and highest point mass. This will not be the case in all cases and has among other things to do with the height of the building and the value of the mass of the point masses. The latter will be investigated when different values for the masses are examined.

For the angular acceleration, shown in Figure 87c, the results show the same pattern as the single-mass models. The three point masses have the same results and, like the horizontal motion, have a minimum at the zero moment widths.

Changing the platform width changes the spring stiffness and mass of the floating high-rise. Therefore, it could also have a value for which resonance occurs. It may be that this resonance occurs at extremely low or high values for the width. Nevertheless, it must be taken into account that the choice of the platform width can cause resonance.

The conclusion of these results is that the most important thing that the width of the platform determines is how much force is acting on the platform. When the platform has the same width as the wavelength, the vertical acceleration will be minimal because the vertical force is minimal. When the platform has the width for which the wave moment is minimal, the horizontal acceleration and angular acceleration are minimal. For the best choice for the width of the platform it will have to be found out whether the value should be chosen so that either the vertical or horizontal acceleration is minimal, or whether a value in between is better to keep both accelerations low.

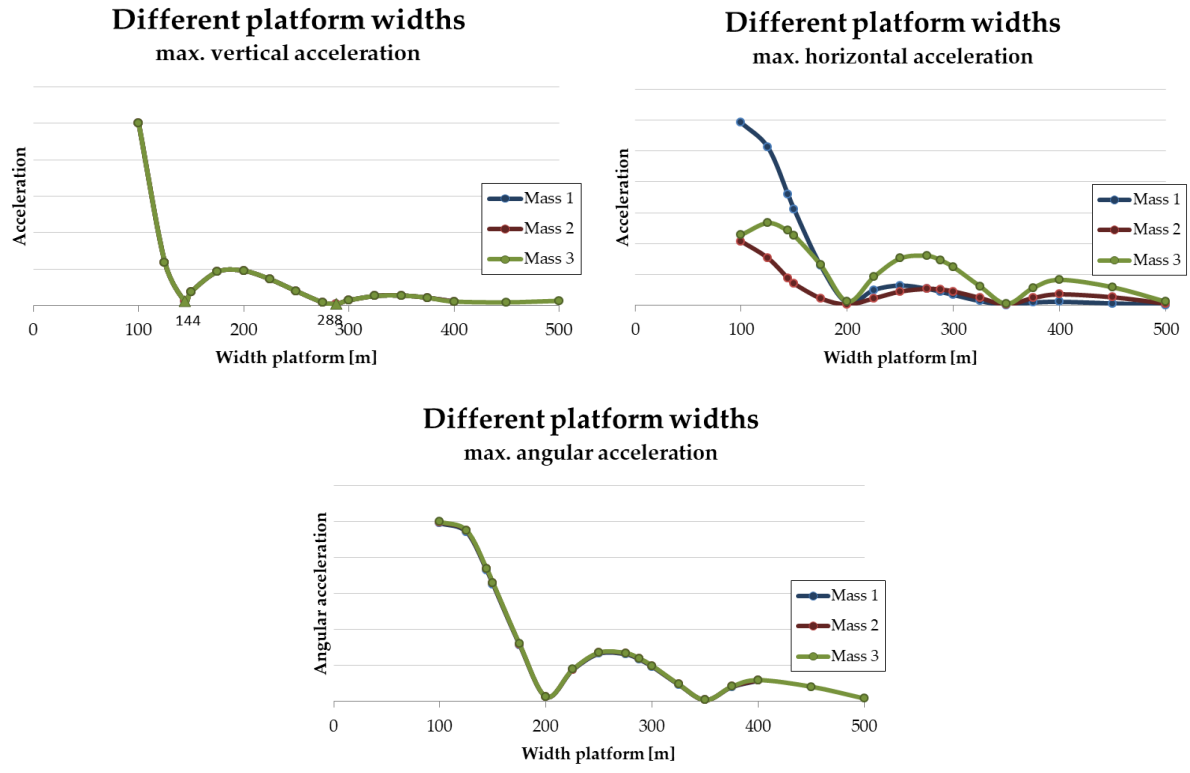

Figure 87 - Maximum accelerations for different platform widths. a) Vertical acceleration. b) Horizontal acceleration. c) Angular acceleration.

Depth of the platform:

The second parameter investigated is the depth of the platform. The depth of the platform will influence the horizontal acceleration because it changes the spring stiffness and the added mass in the horizontal direction. The excitation force depends only on the wave height, so it will remain constant. The change in depth will not affect the vertical acceleration as it does not appear in the calculations. It should be mentioned here that the change in depth is a consequence of changing the width of the platform or the mass. These changes are not included. So the mass remains constant. The influence of the mass will be examined later.

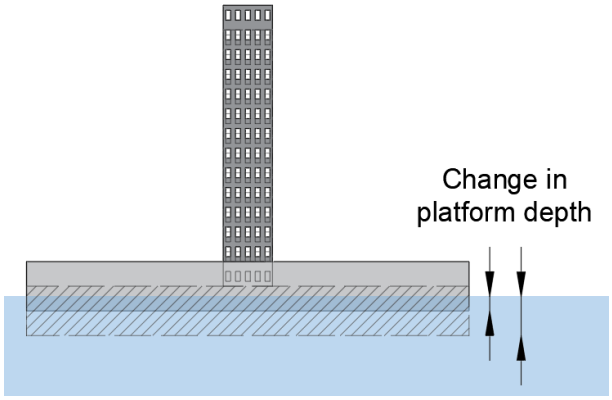

Figure 88 - Changing the depth of the platform.

The results for the maximum accelerations for different depths of the platform are shown in Figure 89. These are the horizontal and angular acceleration of all three masses. As expected the depth has no direct influence on the vertical acceleration and this graph is thus not included.

In Figure 89a the horizontal acceleration is shown. The acceleration of the lower and middle point mass initially increases up to a maximum, and then decreases again. This is similar to the result of the single-mass model where it was concluded that there is a certain value for the depth at which resonance occurs. However, the value of the depth at which the resonance peak occurs is slightly lower in the multi-mass model. The acceleration of the upper point mass continues to increase with increasing depth.

The results for the rotation of the three point masses, see Figure 89b, are again very similar. They also have a resonation peak. The resonance peak of the horizontal acceleration and the angular acceleration occur at the same value for depth.

These results show the influence of depth on spring stiffness and added mass. The frequency that belongs to the horizontal motion is also determined by these two factors. There is a certain value for depth for which these factors are such that the frequency is equal to the excitation frequency which causes resonance. As the frequency of the platform is also determined by its mass, the depth at which resonance occurs is not easy to determine in advance and will vary with different choices of parameters. This possible resonance should be taken into account when looking for the best parameters.

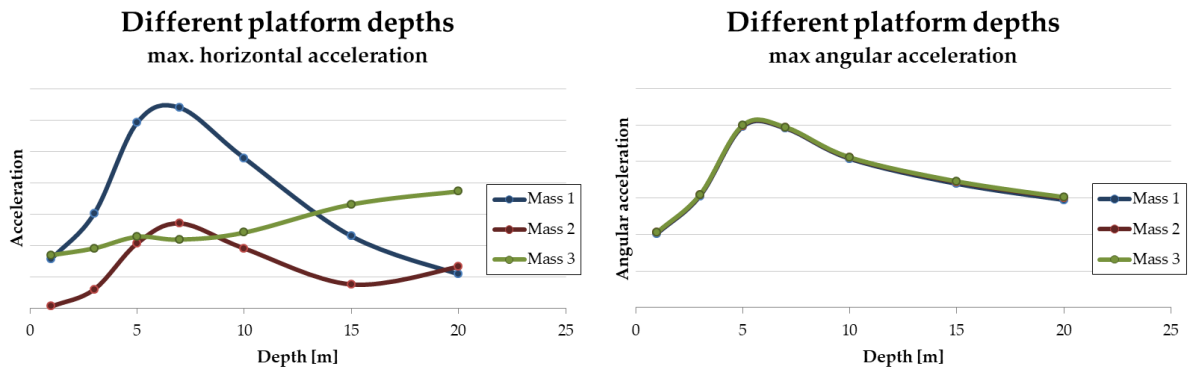

Figure 89 - Maximum accelerations for different depths of the platform. a) Horizontal acceleration. b) Angular acceleration.

GM value

The next parameter to be examined is the value of GM. To examine this parameter, the value is increased or decreased. In the chapter on static stability it is described that the GM value is the difference in vertical direction between the centre of gravity and the metacentre. Since the centre of gravity is kept constant, a change in the GM value can be seen as a shift of the meta centre as shown in Figure 90a. With formula (5.7) from the chapter on static stability it can be seen that a change in the GM value results in a change of the rotation under a certain moment. The higher the GM value, the less rotation, Figure 90b. The GM value thus determines the amount of the rotation. In this chapter, this is translated into a certain spring stiffness for the rotation. Changing the GM value will therefore influence the results of the rotation. And since the rotation and horizontal displacement are linked, the change will also influence the horizontal acceleration.

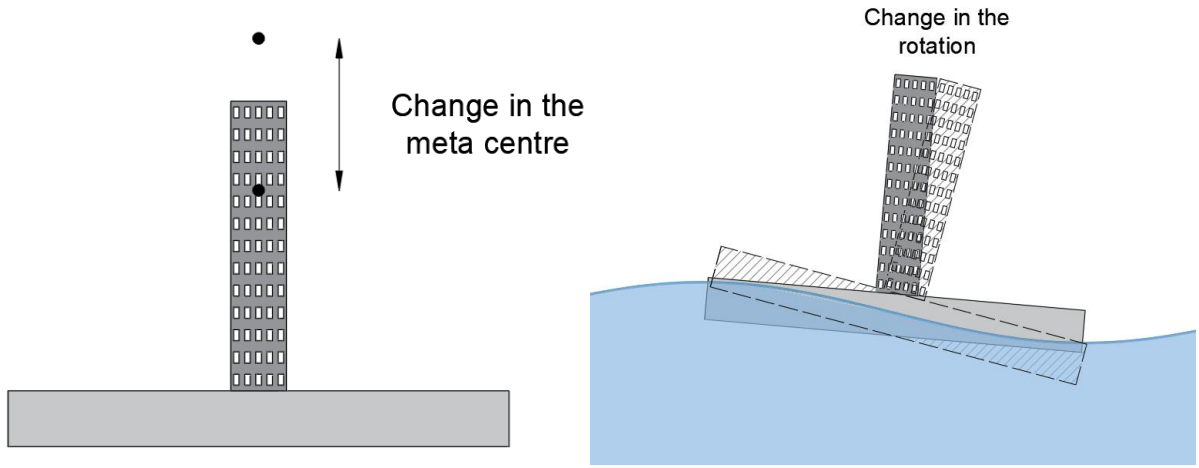

Figure 90 - Change in the meta centre and rotation due to a change in GM value.

The results for the maximum accelerations for different GM values of the floating high-rise are shown in Figure 91. These are the horizontal and angular acceleration of all three masses. The GM value has no direct influence on the vertical acceleration as expected and this graph is thus not included.

The graph shows that the GM value has a very large influence on the horizontal acceleration of all three point masses. The three point masses have a resonance peak at the same GM value, something that does not follow from the single-mass model as this motion was not linked to the

rotation yet. It can be seen that the resonance occurs in the rotation motion as the three masses have the resonance peak at the same GM value, in contrast to the "depth" parameter.

The angular acceleration of the three masses are equal and have the same shape as the horizontal acceleration.

There is a value for GM for which resonance occurs in all masses. As with the parameter "depth of the platform", there is a value for GM that provides a certain value of spring stiffness that makes the eigenfrequency of the platform equal to the wave frequency. Again it is not easy to determine in advance what GM value results in resonance. Increasing the GM value is thus not always positive from the dynamic aspect. This is an important result since for the static stability increasing the GM value is mostly positive.

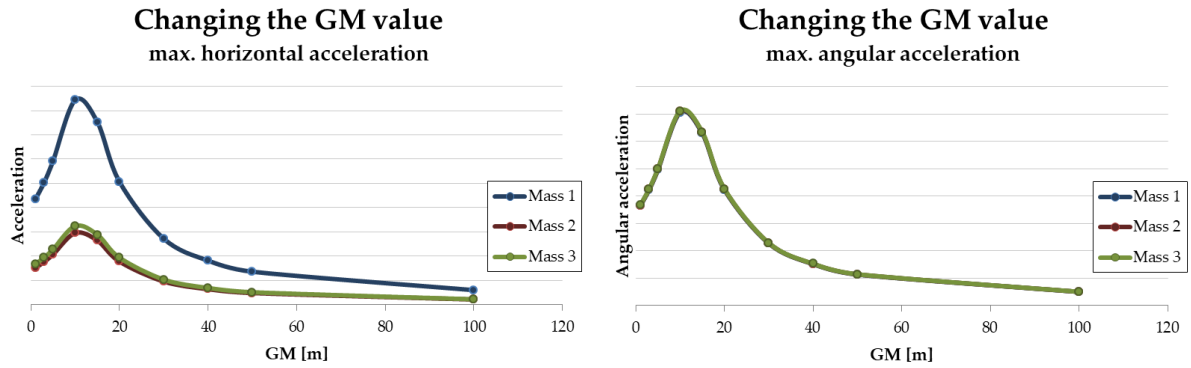

Figure 91 - Maximum accelerations for different GM values. a) Horizontal acceleration. b) Angular acceleration.

Width of the building

The parameters of the building were also considered. Starting with the width of the building. In the way this research has been done, the width has no influence on the stiffness of the building. The stiffness will be investigated next. What the width of the building does influence is the amount of wind force on the building, the mass of the building and the mass moment or inertia of the building.

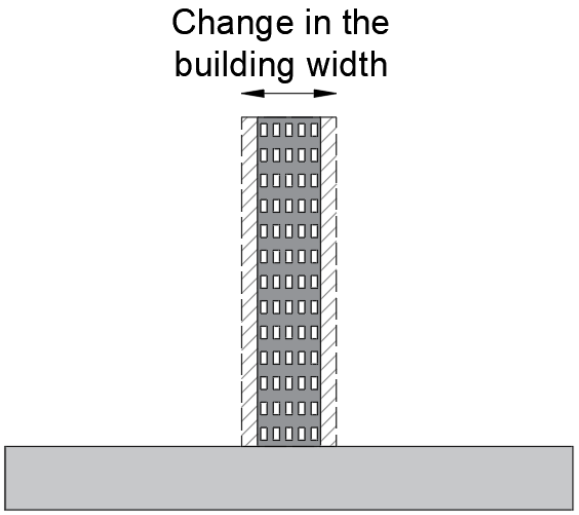

Figure 92 - Changing the building width.

The results for the maximum accelerations for different widths of the building of the floating high-rise are shown in Figure 93. These are the vertical, horizontal and angular acceleration of all three masses.

The vertical acceleration decreases with increasing building width for all point masses. This is because the weight of the building increases.

The horizontal acceleration also decreases with increasing building width for all masses, except for the lowest point mass which first peaks before decreasing. This is due to the influence on the mass moment of inertia. This will cause a change in the eigenfrequency of motion and can there-

fore lead to resonance. The acceleration decreases when for a larger building width. The increase in wind force does not outweigh the decrease in acceleration due to increasing mass.

The angular acceleration shows the same peak for all point masses at the same building width.

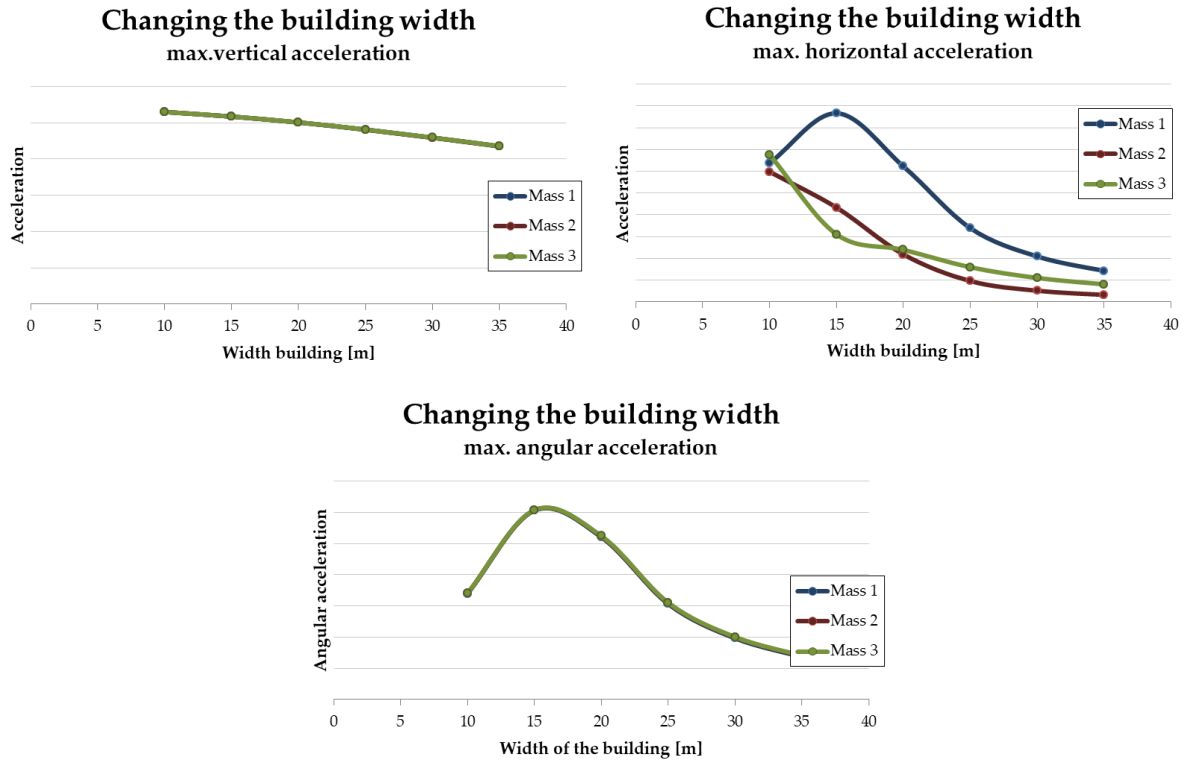

Figure 93 - Maximum accelerations for different widths of the building. a) Vertical acceleration. b) Horizontal acceleration. c) Angular acceleration.

Stiffness of the building

As mentioned, different stiffnesses of the building were also considered. These stiffnesses have a great influence on the values of the beam stiffness matrix regarding horizontal and rotational motion and thus on the spring stiffness of these two motion.

The results for the maximum accelerations for different stiffness's of the building (EI value) of the floating high-rise are shown in Figure 95. These are the horizontal and angular acceleration of all three masses. The building stiffness has no direct influence on the vertical acceleration and this acceleration is thus not included.

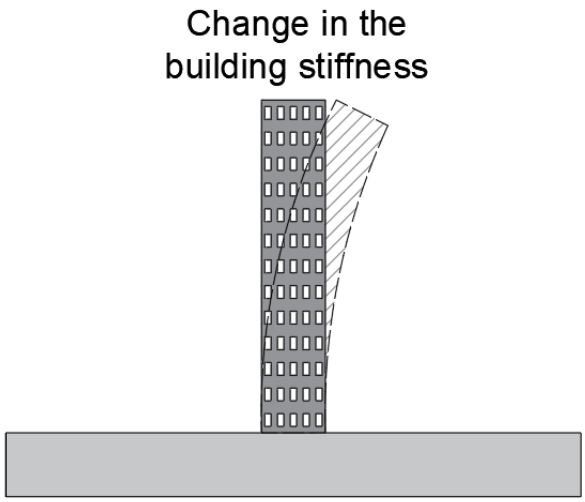

Figure 94 - Changing the stiffness of the building.

The graph for the horizontal acceleration gives a remarkable result. For very low stiffness, the acceleration of the lower point mass increases and the acceleration of point masses 2 and 3 decreases. Up to the stiffness of about 10^{12} N/m^2, from where the acceleration remains constant.

With a higher stiffness than 10^{15} N/m^2 the results start to oscillate where the acceleration of point mass 1 first increases and then falls to zero and finally increases again. Point mass 2 has the same shape only its top and bottom differs much less from its average. Point mass 3 has a maximum when the other two have a minimum. This makes it difficult to determine an ideal stiffness. It must be said that the value for the stiffness is most likely in the flat part of the graph (with the standard value the stiffness is $\sim 2 * 10^{13}$ N/m^2). Only for very high buildings the stiffness will be in the fluctuating part. The lower stiffness's are of interest because of the loss of stiffness of concrete when it cracks. This means that the maximum acceleration of the floating high-rise can change over time as more cracks are formed. It is important to take this into account when designing floating high-rise buildings.

The graph for the angular acceleration also shows a flat section with deviations at lower or much higher stiffness's.

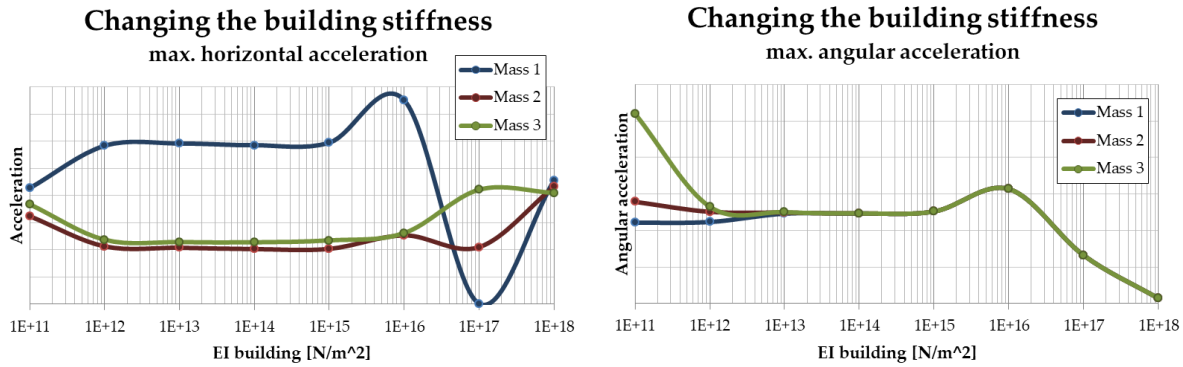

Figure 95 - Maximum accelerations for different stiffness's of the building. a) Horizontal acceleration. b) Angular acceleration.

Mass of the point masses

The last parameter to be examined, mass, is a more special case. The mass is normally a result of selected parameters. However, as explained before, ballast water can be used to make the platform heavier. This makes the mass a parameter which can be chosen. Since the mass of the building also has a large influence on the motion, other values for the parameters can be chosen with the final mass in mind. Other materials can be used to make the building lighter or heavier, or an additional mass can be used. An example of this is the Taipei 101 tower. This tower is located in an area where very violent typhoons and earthquakes occur and is thus vulnerable of high accelerations. As a measure to suppress induced vibrations a tuned mass damper is placed in Floors 87–91. This is a ball made of steel with a diameter of 6 m and weighing 660 ton. (Li et al, 2011). However, the mass is only a very small percentage of the total mass and the effect of the tuned mass damper comes mainly from moving in

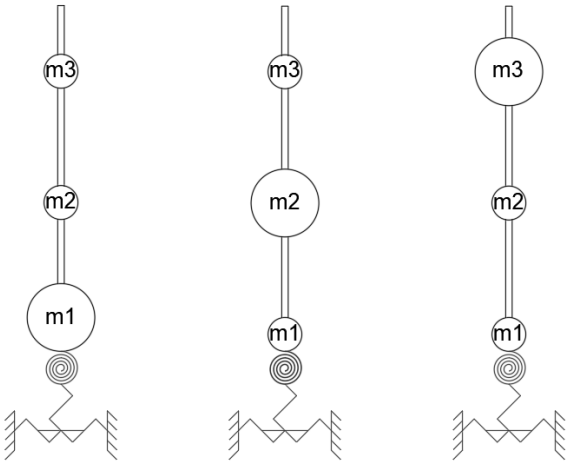

Figure 96 - Changing the masses of the point masses.

the resonance frequency of the building but in the opposite direction. This is a very interesting option for floating high-rise buildings, but was not investigated in this study.

The influence of the mass can be derived directly from the equation of motion. The mass therefore has a direct influence on the motion itself. When the mass becomes infinite, the acceleration becomes zero. Because of its presence in the equation of motion, the mass also affects the frequency of the motion of the point masses, so a change in the mass can cause resonance to occur. Modelling the whole structure as three point masses also ensures that the parameter mass is in three different forms. (The mass of point mass 1, 2 and of 3). Therefore, all three masses of the point masses are examined.

For each point mass, the three acceleration graphs are made for different masses of the point mass in question. The graphs are shown in Figure 98, Figure 99 and Figure 100. The graphs for the vertical acceleration are identical for the three different masses because the masses act as one in this direction. (This is because the masses can move little apart due to axial stiffness). This is why this graph is only shown in the first figure.

In all three cases, an increase in mass at one of the point masses causes a decrease in vertical acceleration of all point masses. Just like the result of the single-mass model. So increasing the mass will lead to a reduction in vertical acceleration regardless of the position of the additional mass. It must be said that mass is one of the parameters in the calculation of the eigenfrequency and can therefore cause resonance. Apparently the mass, calculated with the value from the graph, does not cause resonance but this can be the case in other cases.

The horizontal accelerations show that the acceleration does indeed go to zero when the mass becomes infinitely high. However, this is not true for the other two point masses (the point masses of which the mass does not change). In fact, the accelerations of these can even become larger. Figure 97 shows schematically how the other two point masses theoretically would move if one of the point masses has a lot of mass (displacement by vertical forces not included). This heavier mass will then move much less and the other two will move "around" it.

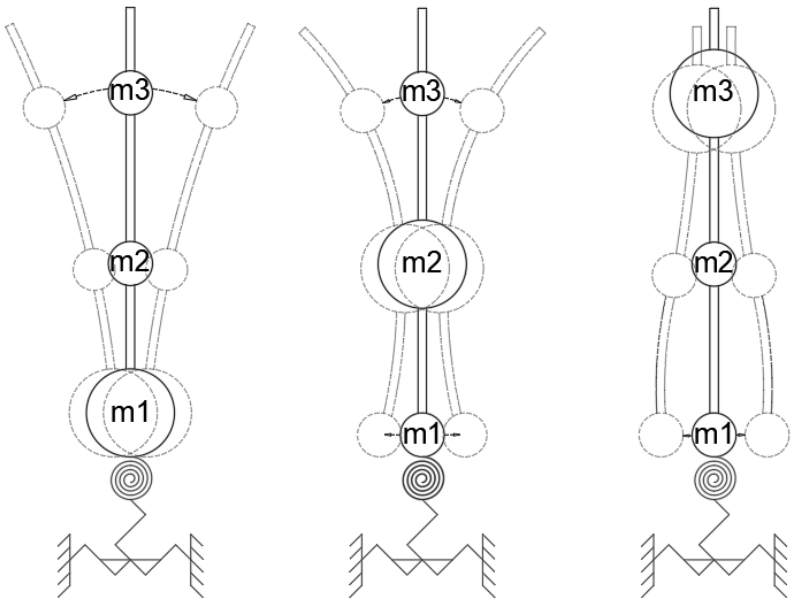

Figure 97 - Motion of the point masses if one point mass is very heavy.

When the mass of the lower point mass is increased, the horizontal acceleration of point masses 1 and 3 increases first to a maximum. This mass therefore causes resonance as was expected that could happen. With a mass greater than the mass causing resonance, the horizontal accelerations decrease as the mass increases. This is contrary to the theoretical scheme of Figure 97. This is because the forces due to the waves are many times greater than those due to the wind. When the mass of the lowest point mass is very large, it "absorbs" all these forces since these forces only act on this point mass. The other masses will therefore move much less.

When the mass of the middle point mass increases, the horizontal acceleration of the lower and middle point mass decreases similarly but the acceleration of the upper point mass increases. Up to a certain value after which the horizontal accelerations no longer changes. After this point, it makes no sense to increase the mass. The upper mass behaves differently because it is not restrained by a large mass like the middle mass or by springs like the lower mass.

If the mass of the upper point mass increases, the horizontal acceleration of the lower mass also decreases and the horizontal acceleration of the middle mass increases. Again, up to a certain mass, after which the horizontal accelerations remain constant.

For the angular acceleration, as with every parameter so far, the resulting acceleration of the three masses is the same. For the changing mass of the lowest point mass, a resonance peak takes place in the angular acceleration at the same value of the mass as for the horizontal acceleration. When the mass of the middle point mass changes, there also appears to be a kind of resonance peak in the graph, but it is less steep than with the changing mass of the bottom point mass. This resonation peak can also not be found in the horizontal acceleration results. When the mass of the highest point mass changes, all angular accelerations decrease until the previously found mass, after which the results remain the same.

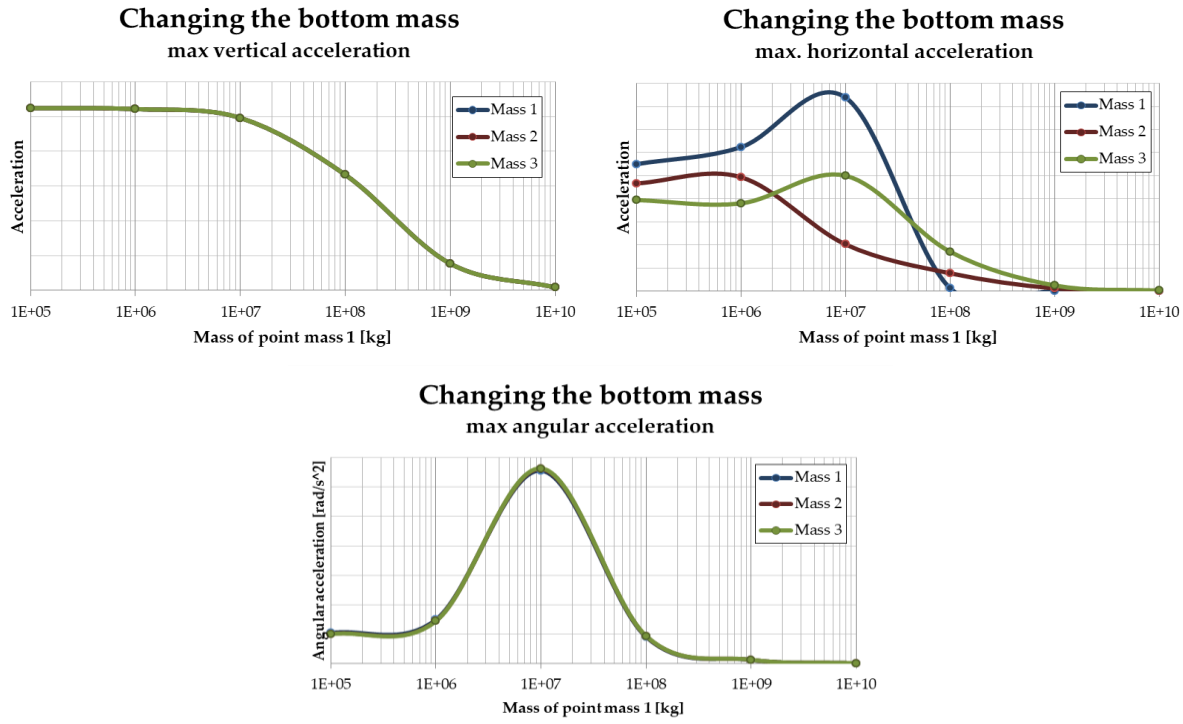

Figure 98 - Maximum accelerations for different masses of the bottom mass (point mass 1). a) Vertical acceleration. b) Horizontal acceleration. c) Angular acceleration.

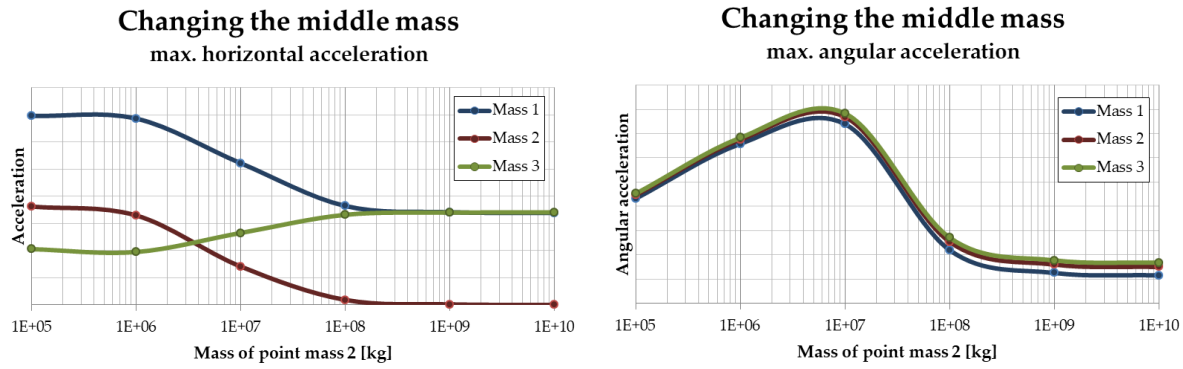

Figure 99 - Maximum accelerations for different masses of the middle point mass (mass 2). a) Vertical acceleration. b) Horizontal acceleration. c) Angular acceleration.

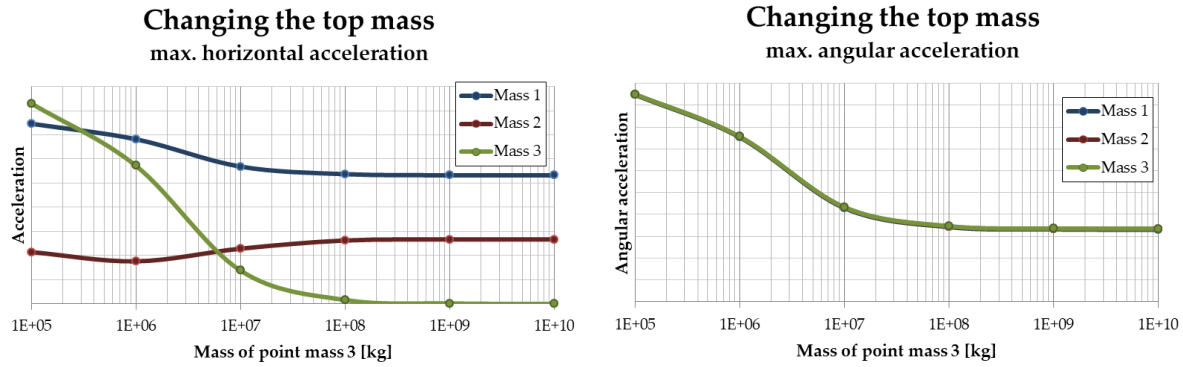

Figure 100 - Maximum accelerations for different masses of the upper mass (point mass 3). a) Vertical acceleration. b) Horizontal acceleration. c) Angular acceleration.

Now that the different parameters have been investigated for the standard parameters as described in chapter 2, it is clear that due to many different choices for the parameters, resonance can occur in one of the three motions. For the width of the platform, no resonance can be seen in the results but it is certainly possible when other input values are used. For example, a higher building. The depth of the platform, the GM value and the width of the building can cause resonance in the horizontal and rotational motion. The greater the depth, after the resonance value, the less acceleration in the lower point mass, this is not the case for the other two point masses. The greater the GM value and the width of the building, after the resonance value, the lower the acceleration. It does not seem that the stiffness of the building leads to resonance. However, it does change how the masses interact and so it can greatly change the acceleration in the masses. The position of the weight can also cause resonance. The differences in acceleration are various for the increase of the different masses.

It can be concluded that it is important to further investigate the possibility of resonance. In this subparagraph the parameters without dependence on each other and only one wave frequency have been considered. For a more realistic approach and to reduce the amount of parameters, the relations as described in chapter 3 can be used to reduce the parameters to the two most important ones; height of the building and width of the platform. This is done in subparagraph 6.6.6. for the most extreme wave. In addition, the limiting frequencies described in chapter 2 should be used to investigate the resonance. This is done in subparagraph 6.6.7.

6.6.6 TOTAL CALCULATIONS

In the previous paragraph, the various parameters were examined as independent. This is to determine what influence these parameters have on the results. In this paragraph, the relations determined between the parameters are used to base the total calculation, and the calculation of the maximum acceleration, on only two or three parameters. These are again the parameters; height of the building and width of the platform. The third is the extra ballast. At first the minimum required depth will be calculated, and with that the extra ballast to reach this depth will be calculated. In this way it is no longer an input parameter. Later in this paragraph the depth will also be an input parameter, from which the independent parameter, extra ballast, will follow directly. With the depth as input, the building can be intentionally made heavier than necessary for the regulations, because this can change the eigenfrequency and thus the results for the maximum acceleration. The three parameters are called the independent parameters. The other parameters follow from these two/three parameters in combination with regulations (e.g. minimum 0.3 m height difference between the top of the platform and the crest of the highest wave), these are called the dependent parameters.

For the waves, it has already been determined that both the tsunami and the growing waves do not cause any problems. Therefore, the most extreme waves are used. In chapter 2 it was determined that an acceleration of 0.55 m/s^2 is the limit. The limit will be shown in the results.

Since the height of the building is often chosen and the width of the platform is adjusted accordingly, a parameter study of the width of the platform for a constant height will follow. For this purpose, a height of 100 m, 300 m and 500 m will be taken for the building. For all heights the other parameters will be calculated together with the maximum acceleration for the three possible motions. All with the width of the platform as a variable. Initially, the calculations were done for the North Sea. Conclusions are drawn on this. Later in the paragraph, the results from the other locations will be used to determine whether these conclusions are correct and/or also apply to the other locations. Not all figures are included in this subparagraph. The other graph together with larger version of the graphs shown here can be seen in Appendix XIII.

Results for a 100 m high building

Using all the relations for the dependent parameters, the maximum accelerations of the three masses for different widths of the platform can now be calculated. The results are shown in Figure 101. Due to the modelling method, the top mass is not the top of the building. However, this top side is often normative and so the motion and acceleration at the top side must be determined. This is done using the results of the three masses and is only done for the horizontal displacement. The horizontal displacement of the three masses and the rotation of the top mass are used to determine the horizontal displacement at the top of the building. This can be described by a third degree polyhedral. The entire calculation is shown in Appendix XII.

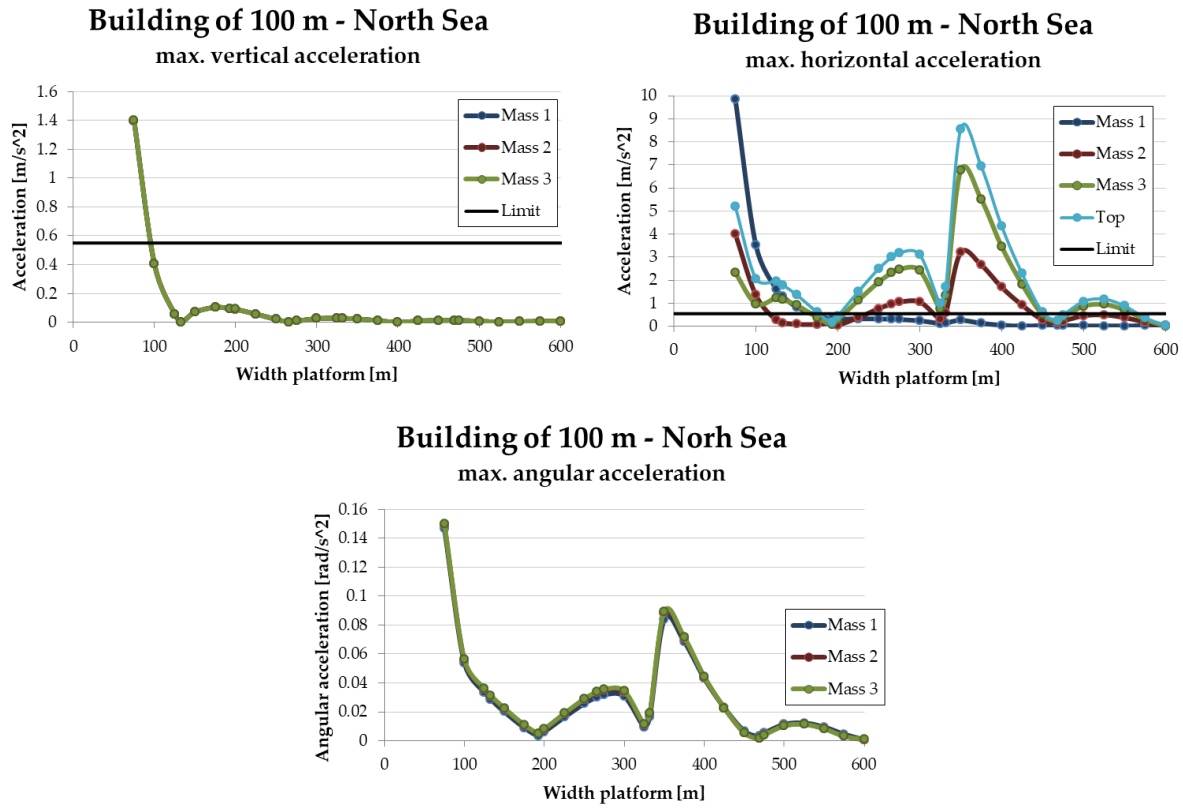

Figure 101 - Maximum vertical, horizontal and angular acceleration of all three masses with different platform widths for a building height of 100m.

For the vertical acceleration, the graph resembles Figure 87a where the influence of the platform was examined without using the relationships. The graph has local minimums at a platform width equal to the wavelength. The peaks between the local minimums decrease as the platform widens. The resonance takes place below 100 m width. The limit line in the graph shows that all platform widths that give a positive GM value have a lower maximum acceleration than is acceptable, apart from the 75 m which causes resonance.

The graph for the horizontal acceleration is somewhat less consistent compared to the vertical motion. However, it is clear that this motion also has local minimums. These minimums are equal to the zero moment widths as previously found. The graph seems to have three resonance peaks, but in fact there are two. One for low platform widths (<100m) and one between 300 and 400 m. The zero moment width at ~332 m, however, causes a huge dip in this resonance peak. It will therefore be very beneficial to use these zero moment widths to limit the horizontal acceleration. Especially since, looking at the acceleration limit, the horizontal acceleration is much more problematic than the vertical acceleration, even with a 100 m high building. This will only get worse with taller buildings. The two resonance peaks can be explained by the fact that both the horizontal and the rotation "work together" and thus the resonance in one of the two causes high acceleration in the horizontal motion. After the resonance peak, the maximum acceleration seems to decrease for larger platform widths. This will be because the eigenfrequencies will be further and further away from the resonant frequency and the rotation will decrease due to a higher GM value. It can be seen in the graph that the bottom mass is normative for very low platform widths and the top of the building for all other widths. This is due to the resonance in de horizontal motion of the bottom mass at low platform widths. Therefore it is necessary to look at

all the horizontal motions and not only the, seeming most problematic, horizontal motion of the top of the building.

The horizontal motion is thus normative for this building height. The maximum acceleration can be reduced by changing the spring stiffness of the rotation (this was a conclusion from the eigen-frequency analysis). This spring stiffness is determined by the width of the platform, the depth, the GM value and the stiffness of the platform. The latter can be changed, for instance by choosing a higher platform. The mass can also be adjusted. This will be examined later in this paragraph. The results of the rotation are very similar to the results of the horizontal motion as expected.

It can be concluded that the horizontal acceleration is normative for a building of 100 m. And since the vertical acceleration under any choice is lower than the limit, a value close to one of the minimum of the horizontal acceleration can be sought for the optimal platform width. From these results, the expectation can be drawn that the vertical acceleration for taller buildings will not be normative either, except if resonance can occur. The largest change for the vertical acceleration with a taller building will be the mass and from the graph in Figure 98a it can be seen that an increase in the mass only causes a reduction in the acceleration. The horizontal acceleration is expected to worsen with a taller building due to the greater arm.

Maximum accelerations for a 300 m high building

The same calculations were done for a 300 m high building. The results for the three motions are shown in Figure 102. Just like for a 100 m building, the vertical acceleration is much lower than the limit. Because the platform has to be wider for stability, the initial peak is also no longer there. For the horizontal motion, the graph seems even more problematic than for a 100 m building. This was partly expected but is mainly due to the resonance that occurs between 200 and 300 m width. In this case, the local minimums are also not below the limit. However, it can be seen again that with larger platform widths, the horizontal acceleration decreases. An increase in mass in this case would be necessary to shift the resonance peak.

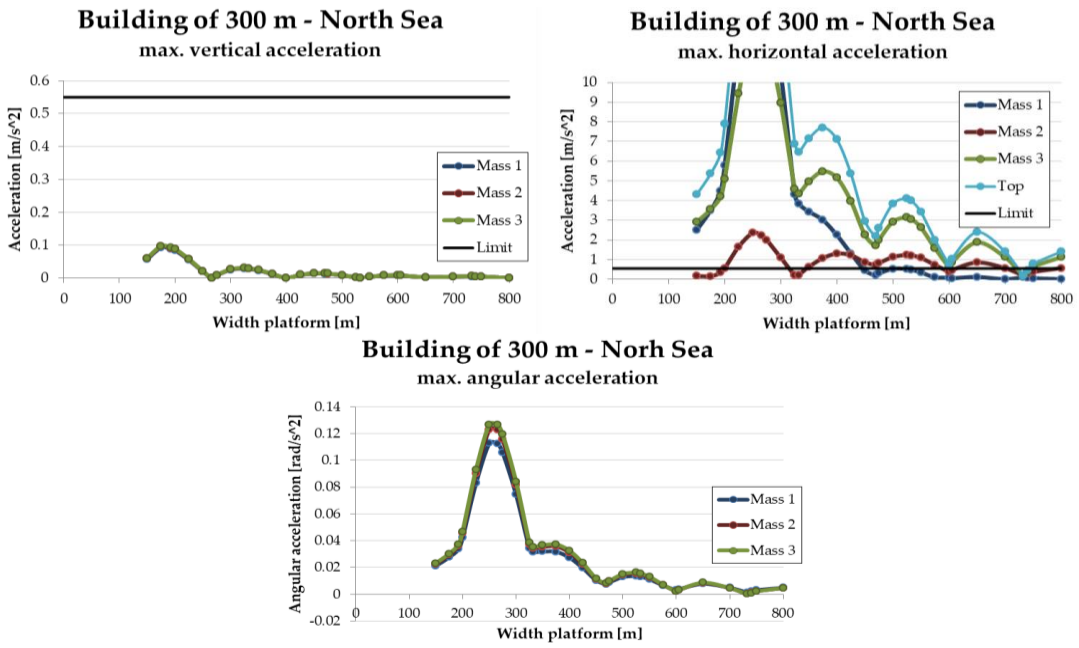

Figure 102 - Maximum vertical, horizontal and angular acceleration of all three masses with different platform widths for a building height of 300m.

Maximum accelerations for a 500 m high building

Finally, the calculation was also done for a building of 500 m. The results are shown in Figure 103. The result for the vertical motion is as expected, but for the horizontal motion it is surprising. There is no extreme peak. This will be because the weight has increased so much that resonance no longer takes place. More problematic is the fact that the horizontal acceleration does not seem to decrease with a larger platform width and the local minimums are nowhere below the limit. Therefore, going for the minimum depth with this height is not an option.

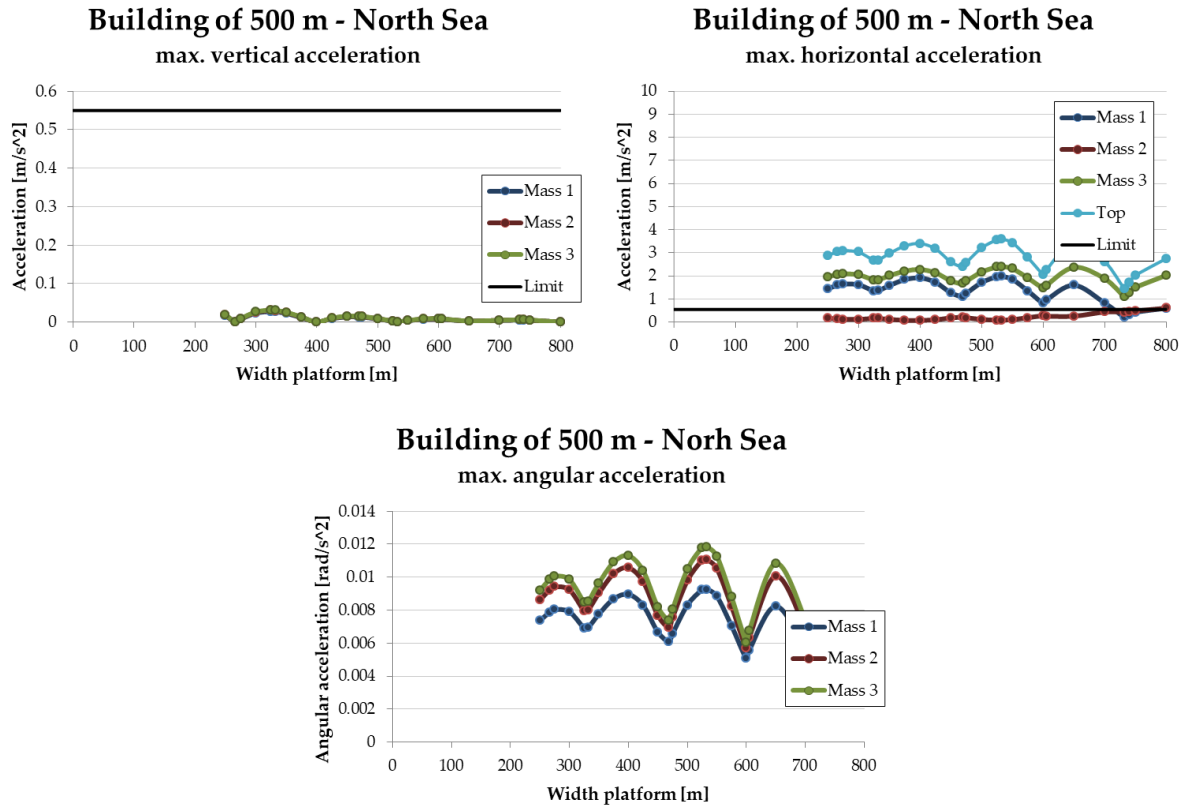

Figure 103 - Maximum vertical and horizontal acceleration and angular acceleration of all three masses with different platform widths for a building height of 500m. Note: The three graphs can be on top of each other.

Extra mass

As mentioned, additional mass can be added in the form of extra ballast. This is done by taking the depth as input. Then the extra ballast needed to reach this depth is calculated and used. The results for a building of 100 m on the North Sea with a depth of 20 m are shown in Figure 104. For comparison, the previous calculations with depth as a dependent parameter result in a depth of about 2.5 m.

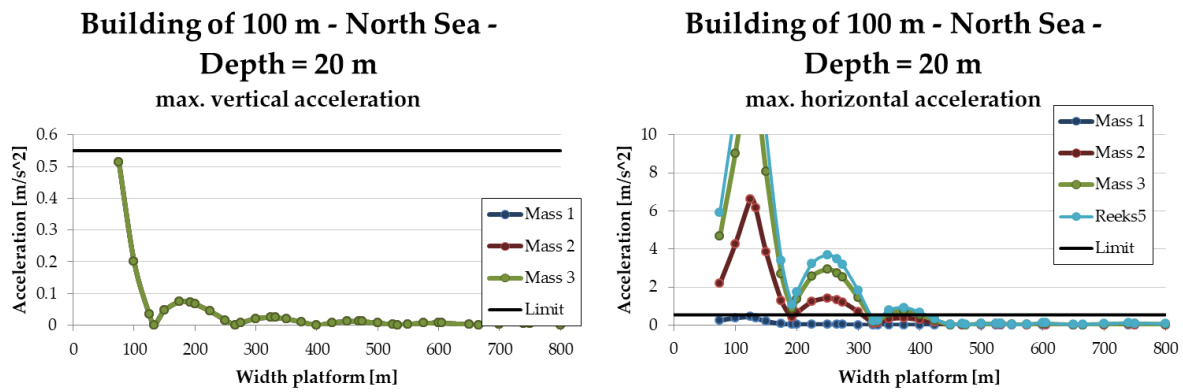

Figure 104 - Maximum vertical and horizontal acceleration of all three masses with different platform widths for a building height of 100m and a depth of 20m.

For the vertical motion, the accelerations are much lower than in Figure 101. For the horizontal motion, the resonance peak has shifted to a smaller platform width. Also, the maximum acceleration decreases strongly for larger platform widths. For the maximum horizontal acceleration, there is mainly a shift in the platform width that causes resonance. Whereas in Figure 101 this was around 350 m, for this option it is around 125 m. This causes the acceleration for wider platforms to drop below the limit more quickly. Therefore, this seems to be a very promising solution.

Different locations

In addition to the different heights, there are also the different locations that provide different results. To illustrate this, a building height of 100 m is taken and the acceleration is calculated for the vertical and horizontal motions (as the rotation results are similar to the horizontal results these are omitted) for the three different locations. The results are shown in two sets of three graphs in Figure 105 and Figure 106. The first three graphs deal with vertical acceleration, the second three with horizontal acceleration. Each time, the first graph is about the North Sea, the second about the Atlantic Ocean and the third about the Equator.

For the vertical motion, the graphs are similar. As expected, the more extreme conditions of the Atlantic Ocean give larger maximum accelerations and the moderate condition of the equator gives lower maximum accelerations. All with local minimums equal to the wavelengths of the locations.

For the maximum horizontal acceleration, the resonance peaks can be seen at other platform widths. This is because the wave frequency is different at the location. For this set of parameters, the acceleration is most extreme at the equator, despite less high waves and less wind. So it can happen that there is a set of parameters which causes the eigenfrequency to be exactly equal to the wave frequency. In that case the height of the waves does not matter anymore. The graphs also show the zero moment width for each location. In general, the Atlantic Ocean gives the highest accelerations, as is to be expected, and it is also the location that needs the highest zero moment width to ensure that the accelerations are below the limit. (around 750 m compared to the 200 m of the North Sea and the 225 m of the equator).

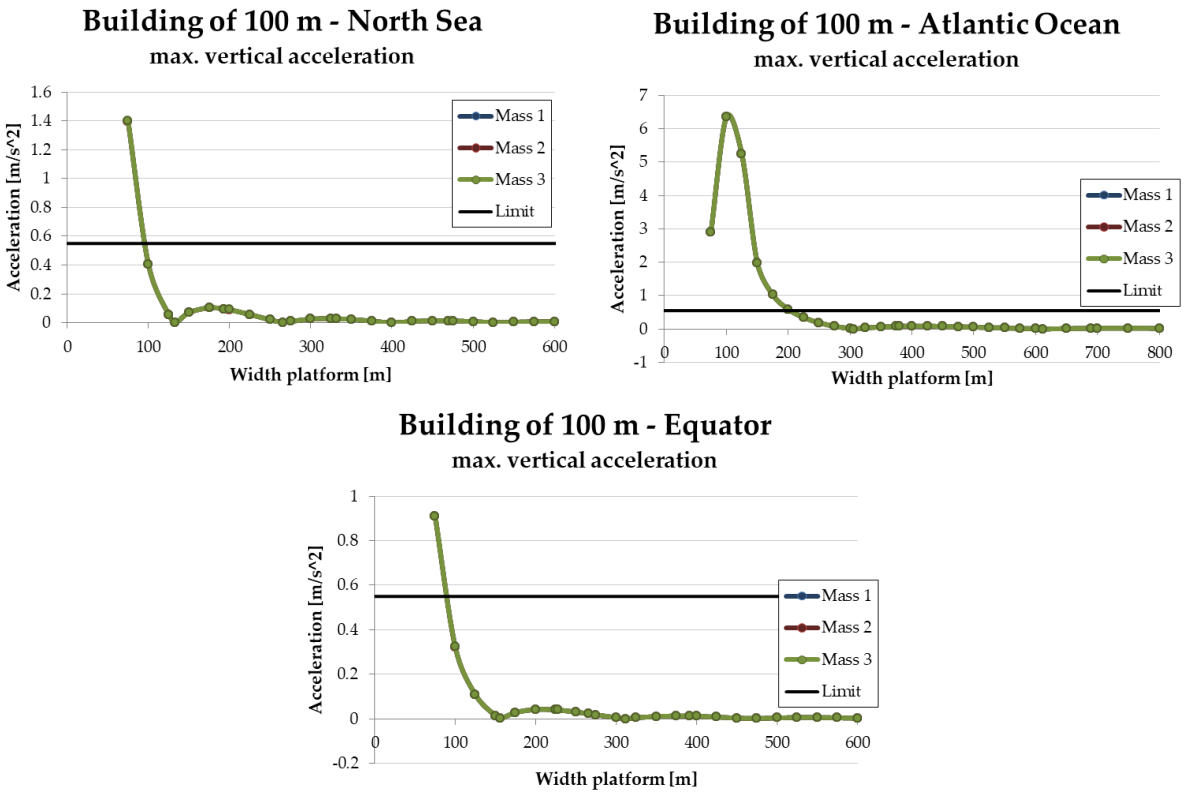

Figure 105 - Maximum vertical acceleration for all three masses for the location: a) North Sea, b) Atlantic ocean and c) Equator.

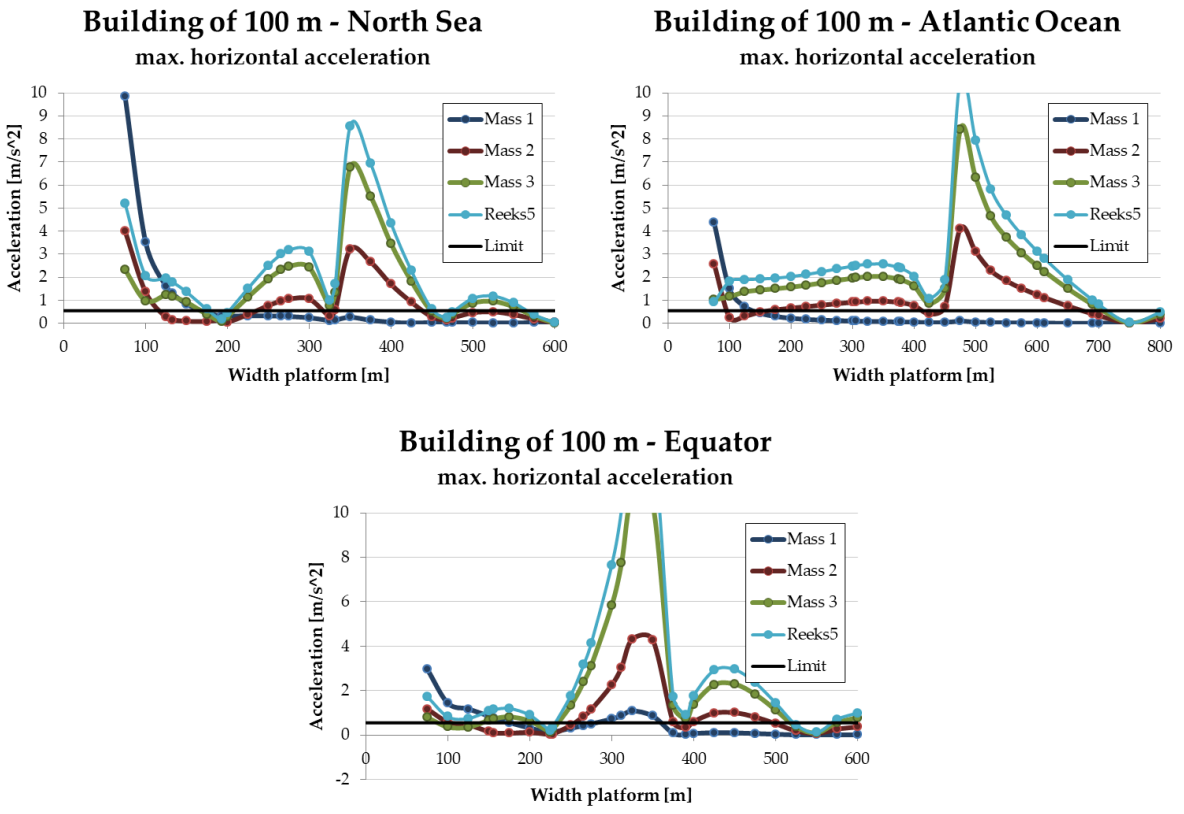

Figure 106 - Maximum horizontal acceleration for all three masses for the location: a) North Sea, b) Atlantic ocean and c) Equator.

From both the results of the previous subparagraph on the different parameters, and this subparagraph using the relationships, it follows that the best value for the platform width is either equal to the wavelength for a minimum vertical acceleration or equal to the zero moment width for a minimum horizontal acceleration and angular acceleration. Because the horizontal motion gives larger accelerations and is more often above the limit, the best option seems to be to limit this acceleration as much as possible. It follows from both subparagraphs that the resonance can be caused by various parameters and is difficult to predict. To ensure that resonance does not occur at the chosen zero moment width chosen, additional ballast can be added to change the total mass. This shifts the resonance peak and reduces the acceleration.

6.6.7 FREQUENCY LIMITS

So far, one period, and thus frequency, has been used for the waves. As explained in chapter 2, the wave field contains several frequencies, all with different wave heights. In the same chapter, with the help of the distribution of the frequency of the wave field, a frequency interval is determined in which no eigenfrequency of the motion may fall. Because these can lead to resonance. Now that all the motions have been determined and described, these eigenfrequency limits can be translated into limits in parameters.

To calculate this limit relation, it has again been attempted to use all the relationships described in chapter 3. This includes a relationship between the wave height, platform depth, platform height and the additional ballast. What the script does is calculate the minimum extra ballast for which the depth and height of the platform meet the requirements. This is the minimum extra ballast that is required. In this part of the research, however, it is desirable to increase the extra ballast. This changes the total mass and thus the eigenfrequency. Therefore, the same calculation cannot be used. For this reason, the depth of the platform is also taken as an independent variable (just like the height of the building and the width of the platform). From this depth, the extra ballast, which is actually the parameter to be chosen, will follow automatically. For the height of the platform it is assumed to be half a wave height higher than the depth of the platform. Not all depths are possible for the different sets of parameters. When the platform is small and the building high, the minimum depth (depth without additional ballast) will already be greater than the depth used as input. (For example: a building of 300 m high with a platform of 150 m wide already has a depth of 20 m without additional ballast.) These incorrect values should not be included. Therefore there is an additional limit; the depth limit

Starting with the vertical motion. This is the simplest one since the three masses move as one in the vertical direction, as seen in this chapter, and therefore there is only one eigenfrequency of this motion that matters (the eigenfrequency of the motion in which the point masses “move apart” are much higher than the limiting frequencies). For the vertical motion the single-mass model expression can be used as this is accurate enough. That eigenfrequency can thus be determined with the mass, added mass and the spring stiffness as explained in the single-mass model paragraph. When all relations are used for the different parameters, the eigenfrequency can be expressed in the width of the platform and the height of the building. With the limits of the frequency, it can now be determined which width of the platform has to be avoided for certain heights.

.

As for the vertical motion, the eigenfrequencies of the horizontal and rotational motion also give a limit in parameters. However, here the three masses, into which the whole building is divided, provide three different eigenfrequencies for each motion. These are determined with the 9x9 matrix. In the paragraph about the frequencies in this chapter it was concluded that the frequencies of the horizontal motion and the rotation of the multi-mass model cannot be expressed in the two parameters. Therefore, the single-mass model calculations are used. This is dangerous territory because in the same paragraph it was concluded that this is actually not accurate enough for these motions. Nevertheless, it is used here to try to determine a result. Afterwards, a conclusion will be drawn about the reliability of these results.

In the program Maple, the eigenfrequency is thus expressed in the two independent parameters; height of the building and width of the platform for a predetermined depth and height of the platform. With this expression, a 3D graph can be made. This is used to visualise what is done and to check whether the following steps taken are correct. These figures were already shown in the paragraphs of the single-mass models. Figure 107 shows the frequencies of the vertical motion and the rotational motion with a depth of 20 m for the North Sea. The red surface is the limiting frequency of 0.43 rad/s. The horizontal motion is omitted as it is similar to the vertical motion. The graph for the horizontal motion can be seen in Appendix XIV together with the 3D graphs and results of the other two locations. The eigenfrequency is set equal to the two outermost frequencies of the frequency interval. Then these equations are solved to obtain the limit in which the height of the building is expressed in the width of the platform. In Figure 108 the result is shown for the vertical and rotational motions lower limit with a depth of 20 m for the North Sea. The upper limit is omitted because the eigenfrequencies will always remain lower than this limit (This can be seen in the 3D graph, they do not go as high as 1.43 rad/s). This is most often the case and so the upper limit is not always visible.

For the rotation, the expression for the eigenfrequency is too large/complex for Maple to solve the equation. Therefore, it is chosen to solve it in a numerical way. Since Maple is not useful for numerical solution, the expression of eigenfrequency is copied to a Python script. In this script, for each platform width (with steps of 5) it is determined for which height of the building the eigenfrequency is closest to the limit. When for all platform widths a matching height has been determined, a formula is determined with the help of curve fitting. This is a polynomial formula of degree 10. This formula is then transferred to Maple to create the graphs.

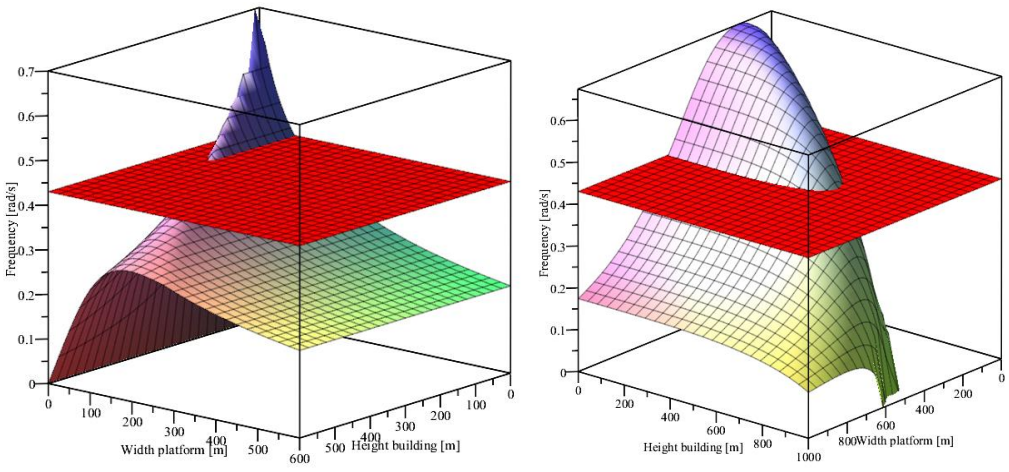

Figure 107 - 3D graph of the eigenfrequency of a) the vertical motion and b) rotational motion with a depth of 20 m for the conditions at the North Sea.

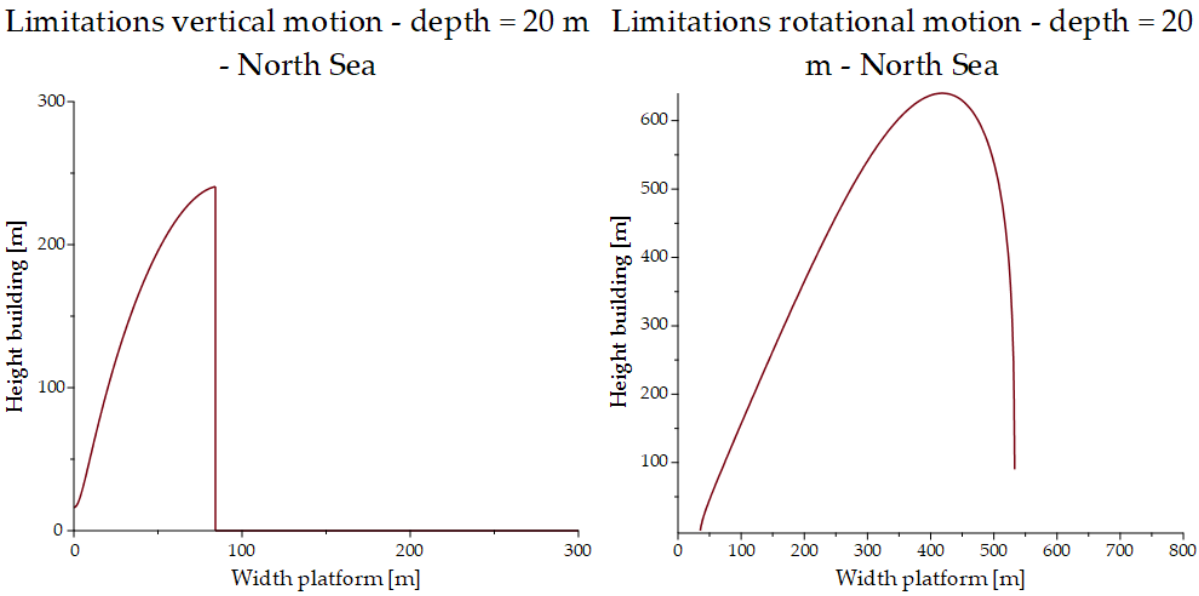

Figure 108 - Limitation for a) the vertical motion and b) rotational motion with a depth of 20 m for the North Sea.

The two graphs look quite different. For the vertical motion, the limit goes up to a certain platform width, in this case to 84 m. After that, the graph goes straight to zero. This can be explained by the parameters in the eigenfrequency formula. Both the spring stiffness and the added mass depend only on the width of the platform and not on the height of the building. This is also the case for the mass. Theoretically this would not be the case, a higher building gives a higher mass, however, by assuming a certain depth, the extra ballast is determined in such a way that together with the mass of the building and the platform, it results in that certain depth. If a higher, and therefore heavier, building is chosen, the extra ballast will be less but the total mass will be the same to reach the same depth. This continues until the building has a mass for which the extra ballast should be equal to zero to reach the depth. This is the line up until it drops to zero which can be seen in the graph. Since the three parameters which determine the eigenfrequency (spring stiffness, mass and added mass) all depend only on the width of the platform, the height of the building no longer has any influence on the eigenfrequency. So there is one platform width which, for every height of the building, gives an eigenfrequency equal to the limit frequency. This is in all cases the case for the vertical and also for the horizontal motion. This is not the case for the rotation motion. The height of the building does have an influence on this eigenfrequency.

The graphs for the vertical and rotational motion show that the eigenfrequency of rotation causes the biggest problems. The eigenfrequency limit of the horizontal motion is lower than that of the vertical one.

Now that the limits of the three motions are known, they can be combined in one graph. This is shown in Figure 109. This figure shows the graph of only the limits and a graph with shaded area. The sets of parameters in this shaded area cannot be used. In addition to these limits, the limit of the depth is determined. This curve are the set of parameters for which the depth is possible without any ballast water. The sets below the curve need extra ballast water to achieve the wanted depth. The sets above the curve are not possible as the mass of the building and platform are such that the depth is more than 20 m. Finally the limit of the static stability (from chapter 5)

is added. In the graph with shaded areas the area with the sets that are not possible due to instability or not enough depth are also shaded. The same calculations are one for the Atlantic ocean and the equator. For the Atlantic ocean the result can be seen In Figure 110. As the limiting frequencies is about the same for the North Sea and the equator these graphs are the same and thus the graph of the North Sea can be used for the equator.

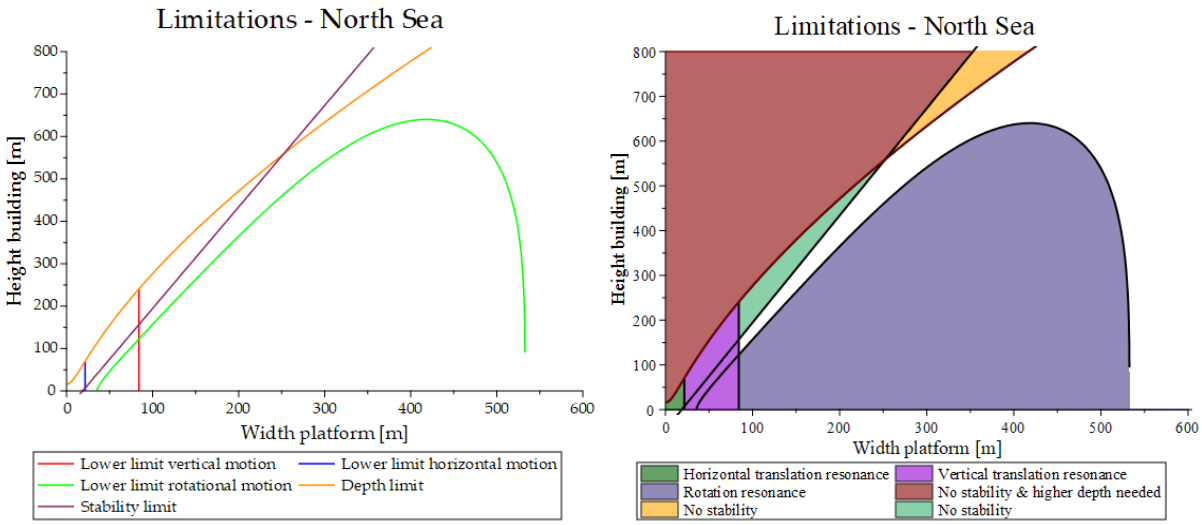

Figure 109 – A graph of different limitations for the building height and the platform width. This graph is applicable for the North Sea location, for a platform with a depth of 20m. a) Shows only the limit lines. b) The shaded areas are not usable. Note: The shaded areas can overlap, this is not visible.

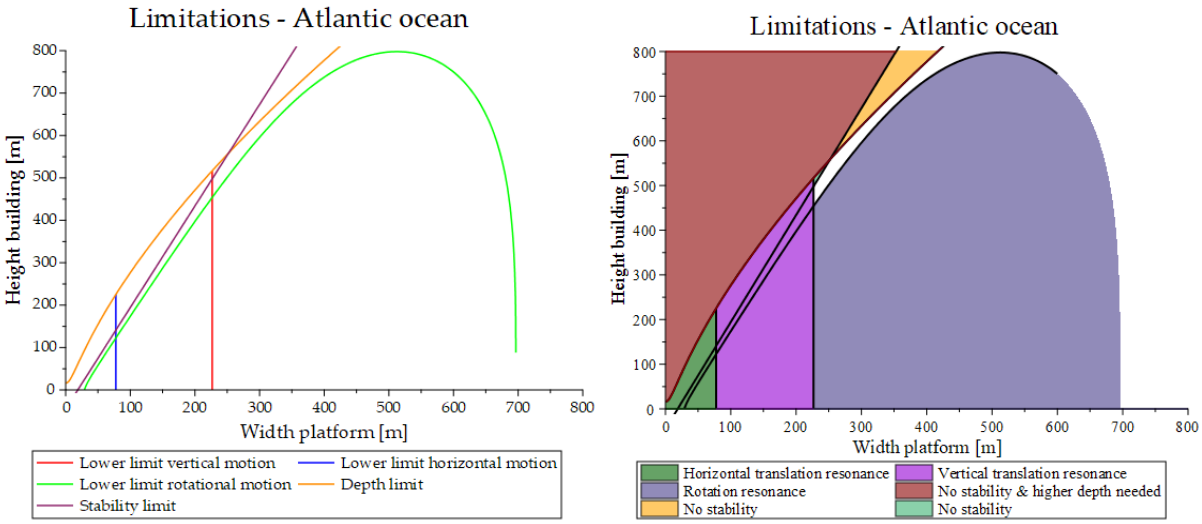

Figure 110 - A graph of different limitations for the building height and the platform width. This graph is applicable for the Atlantic ocean location, for a platform with a depth of 20m. a) Shows only the limit lines. b) The shaded areas are not usable. Note: The shaded areas can overlap, this is not visible.

As can be seen, many combinations of the two parameters cause resonance in at least one of the motions. This is very problematic. The only combinations that seem promising lie in the area above the limit of rotation, below the limit of depth and stability and to the right of the vertical motion. When the combination of the two parameters have to be determined, the formula for the depth limit and the stability limit can be used. The one that gives the biggest platform width is governing. The limit of the vertical motion can be used as a minimum value for the platform. To illustrate: for a building of 500m high with a depth of 20m on the North Sea, the stability limit is

equal to 228 m and the depth limit gives 217 m. As 228 m is bigger this is the governing size. This is also bigger than the limit of 84 m of the vertical limit therefore this would therefore be the platform width to choose.

However, these are the results for one particular depth. This depth can be selected differently. This changes the depth limit. A different depth means actually a different mass which causes a change in the eigenfrequencies. The graphs therefor change when changing the depth. Since the rotation seems to be the normative motion, a graph has been made for the rotation frequency limit for different depths. This is shown in Figure 111. The graph of the limit seems to increase and shift to the right for greater depths. In this graph, it might seem that a shallower depth is a better option, however the depth limits are also different. In **Fout! Verwijzingsbron niet gevonden.**, both the rotation limit and the depth limit are plotted for three depths. It can be seen that for a depth of 5 m there is no option "left or above" the rotation limit. And so this is not an advantageous option. Only at a depth of 15 m (for the North Sea) is there this space between the two limits. The more depth the more space there is between these two limits. Note that the other eigenfrequencies and the stability limit are excluded but do restrict more possibilities.

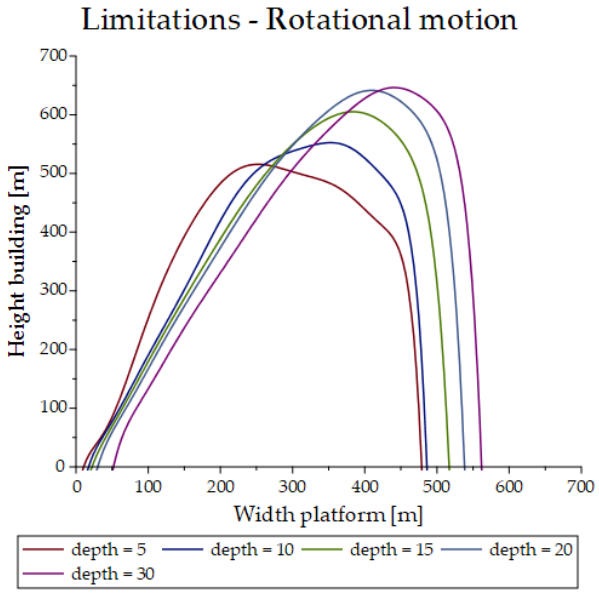

Figure 111 – Graph of the Rotation limit for different depth. This graph applies to the North Sea.

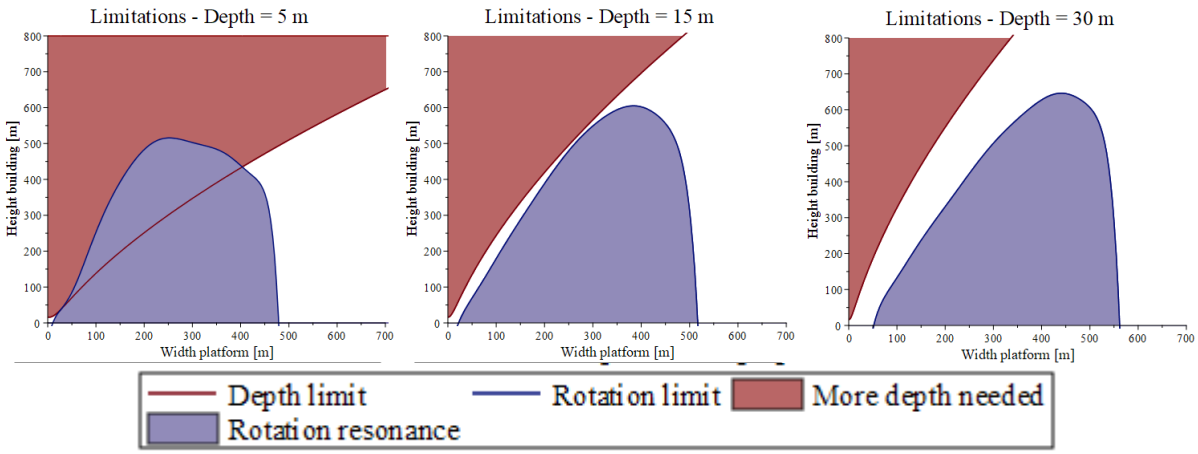

Figure 112 - Graphs for the limitation in parameters due to the depth limit and the rotation resonance for a) a platform depth of 5m. b) a platform depth of 15m and c) a platform depth of 30m. All graphs apply to the North Sea location.

In the previous paragraph the acceleration was calculated for the different motions for different building heights and platform widths. In these calculations the eigenfrequencies are calculated as well with the single-mass model formulas and the multi-mass model method. The results can be seen in Appendix XIV. In those graphs it can be seen that the eigenfrequency of the horizontal motion and the rotation of the single-mass model is different from the multi-mass model. The higher the building the more these differ. For the lower building the multi-mass model gives lower eigenfrequencies. For higher building heights it can be either higher or lower. The deviation is bigger in the eigenfrequencies of the rotation than for the horizontal motion. It can be concluded that the eigenfrequency limits for the rotation and de horizontal motion, determined in this subparagraph, are not accurate enough.

In this frequency limit analysis it can be seen that many combinations of the parameters, building height and platform width, lead to resonance because one of the frequencies of the different motions is equal to one of the possible frequencies of the wave. The best option is to choose a minimum depth of 15 m for the North Sea and the Equator and a depth of 20 m for the Atlantic. In those cases, there is a small range of options for the platform widths for different heights that do not lead to resonance. To determine these widths, the limit of possible depth and the limit of stability can be used. The limit that gives the largest platform width is leading and should be chosen. These limits can be used until the vertical motion limit is reached. The limit of stability is the same for all options, the limit of depth differs per chosen depth and the limit of vertical motion depends on depth and location.

When these minimum advised depths are compared with the minimum depths in the static stability analysis, it can be seen that the depth of the frequency limit is by far the most normative. For the platform width, the stability relation of the static stability can be used, as long as the desired depth can be reached.

7. CASE STUDY

Now that the analyses of static stability and dynamic stability have been done, they can be used for practical purposes. In this chapter, a few case studies are used to apply the results and to see what the results really mean. These have three different starting situations. For the first case, a building height of 500 m is used as input. For this height, with all the results found, the other parameters are determined and it is determined whether it can meet the regulations. For the second case, a value for the width of the platform is used. This will be taken equal to the zero moment widths because these result in the least amount of rotation. For the last situation, the height of 50 m for the building is used. This gives a different situation than 500 m because it turned out that with this height, resonance cannot be avoided. However, the height is much less and so the top has less horizontal displacement and acceleration.

To determine whether the acceleration is acceptable, it is considered whether the accelerations of the vertical and horizontal motions are below the 0.55 m/s^2 determined in chapter 2.

7.1 BUILDING OF 500 M

For the first case study, the building height is taken as 500 m. This is the only input. For the three different locations, it is determined what the other parameters (can) be and how much acceleration this provides.

7.1.1 NORTH SEA

For the 500 m building, a platform depth of 15 m is used because the frequency limit prescribes this as the minimum depth for this location (subparagraph 6.6.7). The figure for this depth can be seen in Figure 113.

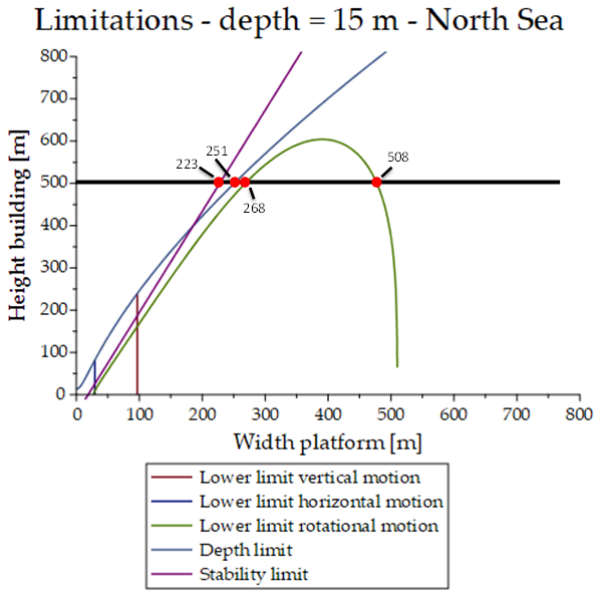

Figure 113 - Limits for a building of 500 m, a depth of 15 m at the North Sea.

From Figure 113 it can be determined that the height of 500 m and 15 m depth gives the following limits expressed in the platform width:

- Stability limit: platform width = 227.6 m (min.) (chapter 5)

- Depth limit: platform width = 250.7 m(min.) (chapter 6)
- Rotation frequency limit: platform width = 268.2 m (max.) (chapter 6)

The depth limit is normative in comparison to the static stability as the lower limit of the width. The width of the platform may therefore be between 250.7 m and 268.2m. To make things easier, these have been rounded off to 251 m and 268 m. From the graph for the minimum depth at the North Sea for a 500 m building (from the results of the static stability, see Appendix IV), it follows that the depth of the platform for a platform width of 251 m should be about 15 m and for a width of 268 m about 13 m. The chosen depth of 15 m is therefore above this. The static stability model was used to check that the 251 m width with 15 m depth can indeed meet the requirements. (The graph cannot be read very accurately.) In addition, the model was used to determine that the height of the platform for a width of 251 m should be 20.8 m and for a width of 268 m the platform should have a height of 20.3 m. In Table 13 below an overview is given together with other results obtained with the static stability model. The sizes can also be seen in Figure 114.

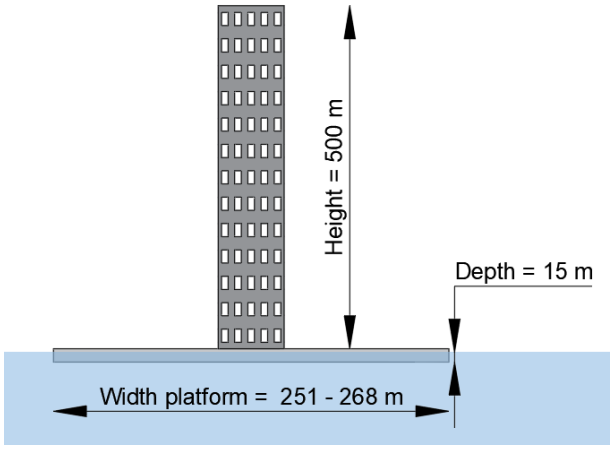

Figure 114 - Dimensions of the building and platform in case study 1.

Table 13 – Results of the static stability analysis for a building of 500 m and a depth of 15 m at the North Sea.

Parameter/ result	Width platform = 251 m	Width platform = 268 m
Min. Depth platform [m]	~15	~13
Depth platform [m]	15	15
Height platform [m]	20.8	20.3
GM value [m]	110.0	188.6
Angle of rotation [deg]	3.75	2.66
Deflection at the top [m]	35.5	25.6

Now that the parameters have been determined, the dynamic calculation can be carried out. The platform width of 268 m is the rotation frequency limit. This frequency limit was equal to 0.43 rad/s (in subparagraph 6.6.7). So the rotation of the single-mass model will have to have this value if this platform width is used. As this was determined with the formulas of the single-mass model, it can deviate in the multiple mass model. The eigenfrequencies are calculated for all degrees of freedom (DOF's) with both the single-mass model and the multiple mass model. The results are shown in Table 14 below. For the horizontal and rotational DOF of the middle and top

mass it is not determined which eigenfrequency corresponds to which mass as this is difficult and not needed.

Table 14 - Eigenfrequencies with a building height of 500m.

Eigenfrequencies [rad/s]	Width platform = 251 m		Width platform = 268 m	
DOF	Single-mass model	Multiple mass model	Single-mass model	Multiple mass model
u_{bottem}	0.189	0.081	0.183	0.112
w_{bottem}	0.294	0.294	0.286	0.285
θ_{bottem}	0.329	0.318	0.433	0.304
w_{top}	-	2.114	-	2.095
w_{middle}	-	3.891	-	3.519
$u_?$	-	5.281	-	5.278
$u_?$	-	10.891	-	9.069
$\theta_?$	-	93.320	-	93.304
$\theta_?$	-	155.465	-	155.444

The eigenfrequency of the rotation in the single-mass model for a platform width of 268 m is indeed around 0.44 rad/s. It is slightly lower. This is due to the rounding off. So there is a small margin of error in it. The same eigenfrequency is in the multi-mass model a lot lower, 0.304 rad/s. The limit therefore overestimates the limit by using the single-mass model and is therefore too conservative. The eigenfrequency of the horizontal motion of the bottom mass is lower than the single-mass model. Both are not close to the frequency width of the wave (all the possible frequency the wave can have). This deviation is expected as it was concluded in the frequency analysis of chapter 6 that the single-mass model is not as accurate as the multi-mass models. As expected, the eigenfrequencies of the vertical motion are equal in the single-mass model and the multiple mass model. Also this is not in the frequency width of the wave.

Now that it is known that the eigenfrequencies are not within the range of the wave frequencies, we can look at the actual accelerations. The fact that no resonance occurs does not necessarily mean that the accelerations are low enough. The accelerations have been calculated for the two specific platform widths. These are shown in Table 15.

Table 15 - Maximum accelerations of the vertical and horizontal motion for the three point masses for a building of 500 m and a depth of 15 m at the North Sea.

Motion	Point mass	Max. acceleration [m/s²]	
		Width platform = 251 m	Width platform = 268 m
Vertical	1	0.016	0.001
	2	0.017	0.002
	3	0.018	0.002
Horizontal	1	1.422	1.061
	2	0.184	0.351
	3	1.976	1.953
	Top of the building	2.890	2.771

The maximum accelerations of the horizontal motion are way too high. Despite the fact that no resonance occurs. In Chapter 6, where the calculations for the maximum acceleration were shown, it can be seen that there are local minimum values for specific widths of the platform (See Figure 102 for an example). Only these specific values for the width have accelerations below the limit. These were called the “zero moment widths”. These are the platform width for which the moment due to the waves is minimum. The parameters chosen here are not close to these zero moment widths and are therefore not optimal. Also when a depth of 20 m or 30 m is used, the accelerations are too high, see Table 16 below. (it was concluded in subparagraph 6.6.6 that changing the depth changes the extra ballast needed and thus the mass. This change in mass causes a change in eigenfrequency.) The acceleration do not even necessarily decrease with increasing depth. So it seems to be a fruitless attempt to simply choose a height of a building and then determine the platform width.

Table 16 - Maximum accelerations of the vertical and horizontal motion for the three point masses for a building of 500 m and different widths and depth of the platform at the North Sea.

		Max. acceleration [m/s²]			
Motion	**Point mass**	**Width platform = 251 m Depth = 20 m**	**Width platform = 251 m Depth = 30 m**	**Width platform = 268 m Depth = 20 m**	**Width platform = 268 m Depth = 30 m**
Vertical	**1**	0.015	0.014	0.001	0.001
	2	0.016	0.015	0.001	0.001
	3	0.017	0.015	0.002	0.001
Horizontal	**1**	0.642	0.277	0.530	0.238
	2	0.486	0.610	0.549	0.634
	3	1.777	1.640	1.795	1.652
	Top of the building	2.436	2.167	2.433	2.173

To see what happens to the displacement, the maximum horizontal displacement of the top of the building and the maximum rotation of the lower mass were calculated for both platform widths. The results are shown in table 1 below.

Table 17 - Displacement and rotation from the dynamic model,

Motion	Width platform = 251 m	Width platform = 268 m
Horizontal displacement [m]	7.03	1.25
Rotation [deg]	1.02	0.034

The results are much smaller than in the static stability model. Therefore, the floating high-rise is not able to achieve the most extreme rotation in these waves. The code for floating buildings has a limit of 4 degrees. This is not exceeded in this case

The platform widths that have been determined do not meet the acceleration requirements. However, more platform widths are possible. Namely the widths larger than the rotation limit. (For illustration, the "right side" of the rotation limit in Figure 109.) These are much larger widths. In Chapter 6, the conclusion was drawn that with larger platform widths the accelerations would be less. This was partly due to the fact that the eigenfrequencies was further away from the excitation frequency. For a building of 500 m, the rotation limit gives a width of 508 m

at the "right side" border. For this width the same calculations were done as for the previous platform widths. Since the depth was already possible for a platform width of 251 m, it is certainly possible for this platform width. The static stability model gives a necessary platform height of 20.5 m at a depth of 15 m. From the zero moment width analysis (see Appendix V) it is concluded that the best platform width to choose, higher than 508 m is the zero moment width of 597 m. The calculations are therefore also done for this width. This width also needs a platform height of 20.5 m. The resulting accelerations are shown in Table 18.

Table 18 - Maximum accelerations of the vertical and horizontal motion for the three point masses for a building of 500 m, a platform width of 508 m and 597 m and a depth of 15 m at the North Sea.

Motion	Point mass	Max. acceleration [m/s²] Width platform = 508 m	Max. acceleration [m/s²] Width platform = 597 m
Vertical	**1**	0.006	0.007
	2	0.006	0.008
	3	0.007	0.008
Horizontal	**1**	0.112	0.027
	2	0.648	0.306
	3	1.531	0.515
	Top of the building	1.984	0.621

Even these widths do not result in accelerations below the maximum permissible acceleration. However, the accelerations are less than before. The platform width of 597 m does result in a minimum acceleration caused by the wave. However, at this location the wind speed is very high and this wind is normative. Therefore there is still too much acceleration. In this study, the focus was mainly on the waves, and the frequency of the wind was taken to be equal to that of the waves. For lower buildings and smaller platform widths the waves are also normative. With this large platform width, the platform is so stable that the building behaves roughly in the same way as a building on land. Buildings of these heights already have great problems with motion and acceleration due to the wind. It is therefore logical that they also have this problem on these platforms. Even if the waves are not included in the calculations, the wind still causes an acceleration just above the permissible limit. It is obvious that a building of 500 metres on land will already experience too many problems under the wind load without additional measures. This research focuses on platforms with a limited width. These are widths for which floating has (great) influence on the design of the whole. With these results, and the results of subparagraph 6.6.6 it can be concluded that when the widths are larger than 600, the motion will be closer to the condition for a building on land and wind will be governing. The same measures can then be taken as for buildings on land to reduce the acceleration.

Since the wind is a big problem, The same determination and calculations are done for the location around the equator. There the wind speed is more than twice as low. The determination Is not done for the Atlantic ocean as this will be even worse than the North Sea.

7.1.2 EQUATOR

As for the North Sea location, the parameters are determined using the static stability calculations. And then the maximum accelerations are determined. The stability limit, depth limit and frequency limits are almost the same for the equator as for the North Sea. Therefore, the same

platform widths are used as found for the North Sea. Except for the zero moment width. This is 552 m instead of 597 m. The results can be seen in Table 19 and Table 20

Table 19 - Results of the static stability analysis for a building of 500 m and a depth of 15 m at the Equator.

Equator	Width platform			
Parameter/ result	**251 m**	**268 m**	**508 m**	**552 m**
Depth platform [m]	15	15	15	15
Height platform [m]	18.6	19.5	19.3	19.3
GM value [m]	112	189	1374	1642

Table 20 - Maximum accelerations of the vertical and horizontal motion for the three point masses for a building of 500 m and a depth of 15 m at the Equator.

		Width platform			
Motion	**Point mass**	**251 m**	**268 m**	**508 m**	**552 m**
Max. vertical acceleration [m/s²]	**1**	0.025	0.018	0.004	0.005
	2	0.027	0.019	0.005	0.006
	3	0.028	0.020	0.005	0.006
Max. horizontal acceleration [m/s²]	**1**	0.227	0.197	0.172	0.005
	2	0.043	0.031	0.202	0.075
	3	0.385	0.427	1.596	0.072
	Top of the building	0.622	0.681	2.607	0.074

Again, the accelerations for the platform widths 251 m and 268 m are too high. And again, they do not come close to the zero moment width. For the width of 508 m the horizontal acceleration is even worse. This is either because it is close to the value in the middle between two zero moment widths, where there is a local maximum in the acceleration or because the eigenfrequency is close to the wave frequency. For the widths 552 m, the accelerations are low enough. So it is possible to reach this height at this location with less wind. It can be concluded that when the "right side" of the rotation frequency limit is chosen, resonance is no longer a problem and the platform is so wide that the waves have little influence anymore and the wind is the main problem. In order to determine whether a certain height can be achieved for the building, one can check whether it can be achieved on land with the same wind speeds. If so, it may well be possible on a large platform.

With these results, it seems better to use the zero moment width as a starting point, and then see which building heights are possible. This will be done in the next paragraph.

7.2 ZERO MOMENT WIDTH

7.2.1 NORTH SEA

In this paragraph, not the height of the building but the width of the platform is taken as the starting point. And specifically the zero moment widths. These ensure the least moment due to the waves and thus less rotation and horizontal displacement. The motion that is almost always normative. Again, the North Sea is taken. The zero moment widths for this location are 191 m, 328 m, 462 m, 597 m and 730 m. The depth of the platform is again 15 m. With the results of the

eigenfrequency limits and other restrictions, the possible heights are determined for these widths.

Table 21 shows the minimum and maximum possible heights for the various widths. The stability and depth limits are maximum and the rotation limit is minimum. The depth limit is always normative in comparison to the stability. Thus, more depth can be chosen. For the time being, the depth remains 15 m. For both the minimum and maximum heights of the different platform widths, the maximum accelerations of vertical and horizontal motions have been calculated. These are shown in Table 22. For these calculations, the minimum heights have been taken as at least 100 m and the maximum heights as up to 800 m.

Table 21 - Limits in possible height with a platform depth of 15 m at the North Sea. The stability limit and depth limits are maximums and the rotational frequency limit is a minimum.

Platform width [m]	191	328	462	597	730
Stability limit height [m]	412	740	1061	1384	1703
Depth limit height [m]	408	608	776	929	1067
Rotational frequency height [m]	361	574	542	0	0

Table 22 - Maximum accelerations of the vertical and horizontal motion for the three point masses for a depth of 15 m at the North Sea.

Accelerations [m/s²]		Width platform [m]									
		191		328		462		597		730	
		Building height [m]									
Motion	Point mass	361	408	574	608	542	776	100	800	100	800
Max. vertical acceleration [m/s²]	1	0.078	0.077	0.025	0.025	0.013	0.012	0.008	0.007	0.005	0.005
	2	0.081	0.082	0.028	0.028	0.014	0.015	0.008	0.009	0.005	0.006
	3	0.083	0.084	0.029	0.030	0.014	0.016	0.008	0.010	0.005	0.007
Max. horizontal acceleration [m/s²]	1	0.671	1.219	0.689	0.985	0.127	0.748	0.004	0.244	0.003	0.085
	2	0.618	0.290	0.334	0.176	0.520	0.130	0.028	0.308	0.030	0.332
	3	2.001	1.905	1.519	1.517	1.260	1.227	0.095	1.031	0.099	0.845
	Top of the building	2.702	2.725	2.128	2.206	1.640	1.798	0.130	1.410	0.134	1.115

Even with the use of the most optimal platform widths and other parameters so that the eigenfrequencies are not equal to those of the wave, the acceleration in the top of the building is too high for most heights in the situation of the highest waves. Only for a width of 462 m and a height of 542 m is the acceleration below the limit. Also for the buildings of 100 m height at the platform widths 597 and 730 the accelerations are low enough. There will be a limit somewhere between 100m and 800m building height for which there is too much acceleration even for these platform widths.

Chapter 6 has shown that changing the depth of the platform can reduce the maximum acceleration. Therefore, for a depth of 30 m, the same determinations and calculations were made. The zero moment widths remain the same. The depth limit and the rotation limit are different. The results of the limits are shown in Table 23. The resulting accelerations are shown in Table 24.

Table 23 - Limits in possible height with a platform depth of 30 m at the North Sea for the zero moment widths. The stability limit and depth limits are maximums and the rotational frequency limit is a minimum.

Platform width [m]	191	328	462	597	730
Stability limit height [m]	412	740	1061	1384	1703
Depth limit height [m]	530	781	992	1182	1354
Rotational frequency height [m]	314	547	641	0	0

Table 24 - Maximum accelerations of the vertical and horizontal motion for the three point masses for a depth of 30 m at the North Sea for the zero moment widths.

Accelerations [m/s²]		Width platform [m]									
		191		328		462		597		730	
		Building height [m]									
Motion	Point mass	314	412	547	740	641	800	100	800	100	800
Max. vertical acceleration [m/s²]	1	0.064	0.063	0.023	0.022	0.012	0.011	0.007	0.007	0.005	0.005
	2	0.066	0.067	0.025	0.026	0.013	0.014	0.007	0.008	0.005	0.006
	3	0.067	0.069	0.026	0.028	0.014	0.015	0.007	0.009	0.005	0.006
Max. horizontal acceleration [m/s²]	1	0.097	0.236	0.138	0.448	0.079	0.186	0.002	0.072	0.001	0.008
	2	0.813	0.650	0.545	0.277	0.463	0.347	0.031	0.363	0.032	0.300
	3	1.773	1.618	1.341	1.190	1.117	1.069	0.099	0.930	0.101	0.600
	Top of the building	2.258	2.110	1.751	1.666	1.455	1.448	0.134	1.229	0.137	0.757

The results do not differ much for a depth of 30m compared to 15m. So this is not an option for the North Sea either.

The conclusion can be drawn that, with the design choices as they have been made in this study, the horizontal accelerations for this type of extremely tall building are almost always too high in the North Sea. But there can be a perfect combination, were the zero moment width can be used together with other parameters without causing a form of resonance.

No example calculation is made for the Atlantic Ocean. Chapter 6 has already shown that this location is more problematic than the North Sea, so it too is not suitable for high-rise buildings on platforms with limited dimensions.

Because of the milder conditions, the equator is a better location than the North Sea. This is also reflected in the results of the previous paragraph. Since the North Sea is not an option, we will look into the possibility of floating high-rise buildings around the equator with the zero moment widths.

7.2.2 EQUATOR

The zero moment widths for the equator are shown in Table 25. Together with the results of the limits. Table 26 gives the results of the static stability analysis and Table 27 the accelerations for the minimum and maximum heights of the different zero moment widths.

Table 25 - Limits in possible height with a platform depth of 15 m at the Equator for the zero moment widths. The stability limit and depth limits are maximums and the rotational frequency limit is a minimum.

Platform width [m]	223	384	542	699
Stability limit height [m]	489	874	1252	1628
Depth limit height [m]	458	681	868	1036
Rotational frequency height [m]	423	604	0	0

Table 26 - Results of the static stability analysis for a depth of 15 m at the Equator for the zero moment widths.

	Width platform [m]							
	223		384		542		699	
	Building height [m]							
Parameter/ result	423	458	604	681	100	800	100	800
Depth platform [m]	15	15	15	15	15	15	15	15
Height platform [m]	17.5	17.7	20.3	21.4	16.6	24.2	16.6	24.1

Table 27 - Maximum accelerations of the vertical and horizontal motion for the three point masses for a depth of 15 m at the equator for the zero moment widths.

Accelerations [m/s²]		Width platform [m]							
		223		384		542		699	
		Building height [m]							
Motion	Point mass	423	458	604	681	100	800	100	800
Max. vertical acceleration [m/s²]	1	0.033	0.033	0.011	0.011	0.005	0.005	0.003	0.003
	2	0.035	0.035	0.012	0.012	0.005	0.006	0.003	0.004
	3	0.036	0.037	0.013	0.013	0.005	0.007	0.003	0.004
Max. horizontal acceleration [m/s²]	1	0.108	0.167	0.055	0.097	0.001	0.043	0.001	0.007
	2	0.042	0.004	0.008	0.039	0.040	0.062	0.041	0.120
	3	0.312	0.311	0.253	0.254	0.127	0.253	0.128	0.020
	Top of the building	0.459	0.480	0.394	0.425	0.172	0.446	0.173	0.096

These results are much more promising. All accelerations are below the limit and so all these combinations (and most probably the building heights between the minimum and maximum heights) are possible. The location around the equator is thus the only location where high-rise buildings are possible on limited platforms.

There is however a but, these zero moment widths are optimal for a wave with the frequency equal to the peak frequency mentioned in chapter 2. This is the frequency at which the highest wave occurs. It is therefore a logical choice to match the platform widths to the zero moment widths of this frequency. It is now necessary to look at another frequency to see whether the accelerations at these frequency are also low enough. As an example the frequency of 11 rad/s is used (10 rad/s is the peak frequency). The wave height for this frequency is less than for the peak frequency. The calculation of the wave height for different frequencies is explained in chap-

ter 2 . The result for the horizontal acceleration at the top of the building (the normative acceleration) is shown in Table 28 below.

Table 28 - Maximum acceleration at the top of the building for a depth of 15 m and a wave frequency of 11 rad/s. At the equator for the zero moment widths.

	Width platform [m]							
	223		384		542		699	
	Building height [m]							
Motion	**423**	**458**	**604**	**681**	**100**	**800**	**100**	**800**
Max. horizontal acceleration at the top of the building [m/s²]	2.84	2.86	2.20	2.24	0.17	1.68	0.06	1.32

This wave frequency is causing problems. The limit of 0.55 m/s2 is already exceeded by the lower platform widths. Therefore, the parameters used do not necessarily have low enough horizontal acceleration for all frequencies.

The equator is the only location that has not yet been completely written off for high-rise buildings on limited platforms in this study. However, a problem has already been discovered that has not yet been further investigated in this study. In order to determine whether floating high-rise is possible on the equator, with the design choices used, this will require further research.

7.3 Building of 50m

Starting with an height of 500 m also seems to be an excessive height. This height was chosen because the graphs from subparagraph 6.6.7 indicated that for this height there are possibilities. For more logical heights, between 50 m and 100 m, there are none because of resonance in the rotation or vertical motion. However, there is one major difference between the two options, at a height of 500 m the rotation has much more influence on the horizontal displacement at the top of the building than at a height of 50 m. It is clear that at 500 m there should be absolutely no resonance. But perhaps this is less of a problem with a low building. To test this, the calculations are done with a building height of 50 m and a depth of 15 m.

7.3.1 North Sea

This building height gives the following limits for the North Sea location:

- Stability limit: platform width = 39.6 m
- Depth limit: platform width = 18.19 m
- Vertical motion frequency limit: platform width = 96.9 m
- Horizontal motion frequency limit: platform width = 29.4 m
- Rotation frequency limit: platform width = 41.1 m and 514.9 m

As mentioned, this option always gives resonance (for platforms smaller than 515 m). To avoid the resonance in the vertical motion, the platform must be at least 96.9 m and to avoid the resonance in the rotation, the platform must not exceed 41.1 m, so there is always resonance in one motion. After calculations it also appears that below 97 m there is too much vertical acceleration. Therefore, a platform width higher than this needs to be chosen. That width will cause resonance in the rotation. To limit the rotation a platform width of 190 m is considered, which is a

zero moment width for the North Sea. In subparagraph 6.6.6 it was already shown that this is a value that gives low enough accelerations. However, there is again the one drawback to these zero moment widths. They are only optimal for a specific wavelength and thus for a specific frequency of the wave. Therefore for this width of the platform the calculations were done with different wave frequencies and corresponding wave heights to see how good this zero moment width is for other frequencies. The calculated acceleration of the top of the building is shown in Figure 115 for different wave frequencies. In addition to the acceleration, the vertical lines indicate the frequency at which the zero moment width has been "tuned" (and thus the minimum acceleration) and the eigenfrequency of the rotation. The eigenfrequencies of the horizontal and vertical motions are below 0.4 rad/s.

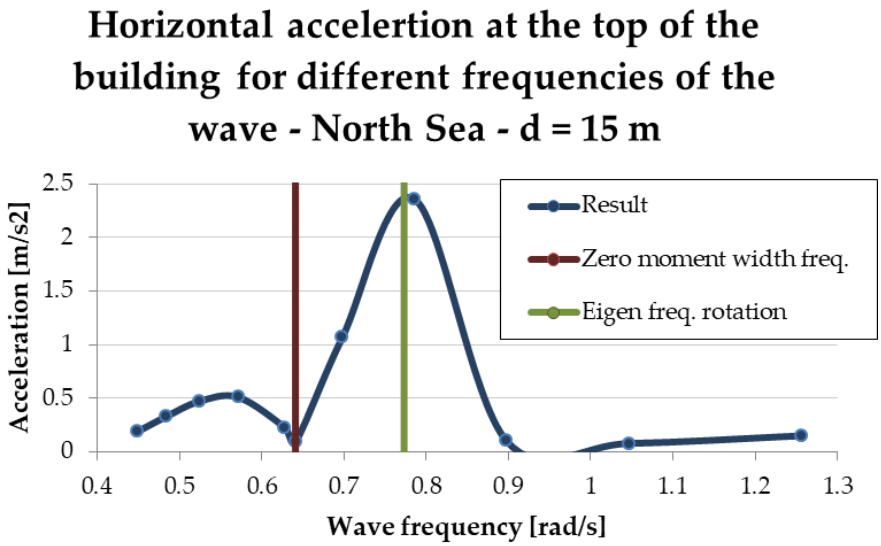

Figure 115 - Horizontal acceleration at the top of the building for different frequencies of the wave for a building of 50m and a platform depth of 15 m at the North Sea.

It can be seen that the zero moment width does indeed give very low acceleration but that this advantage only applies to that one frequency. The rest of the frequencies show the resonance peak and thus much too high accelerations. So the zero moment width only makes a “dent” in the resonance peak and is not a solution for the resonance and can therefore not be used to always make the floating high-rise possible. If it is precisely tuned to the eigenfrequency, it can be very advantageous. However, this is very difficult to match.

7.3.2 EQUATOR

Even for 50m buildings, the North Sea is not an option. Again, it is assumed that this also applies to the Atlantic Ocean.

The final question is then, is it possible on the equator? Again the calculations are done with the height of 50 m and a depth of 15 m. The result is shown in Figure 116. Still the acceleration for the wave frequencies close to the eigenfrequency is much higher than the acceptable 0.55 m/s2 and so it does not seem possible for the equator either. After many different, unsuccessful, attempts to make floating high-rise possible on platforms with a limited width, one last attempt has been made. A depth of the platform was determined for which, together with the platform width equal to the zero moment width of 223m, the eigenfrequency is equal to the peak frequency and thus the frequency for which the zero moment width is ideal. The "dent" in the graph is

therefore exactly at the maximum of the graph. The platform depth in that case equals 22.7 m. The result is shown in Figure 117. And miraculously, the accelerations fall below the limit for every frequency. So the floating high-rise is possible on a limited sized platform, for the minimum height of high-rise buildings, 50 m, for one specific platform width and one specific depth. After all the fruitless attempts, one small success.

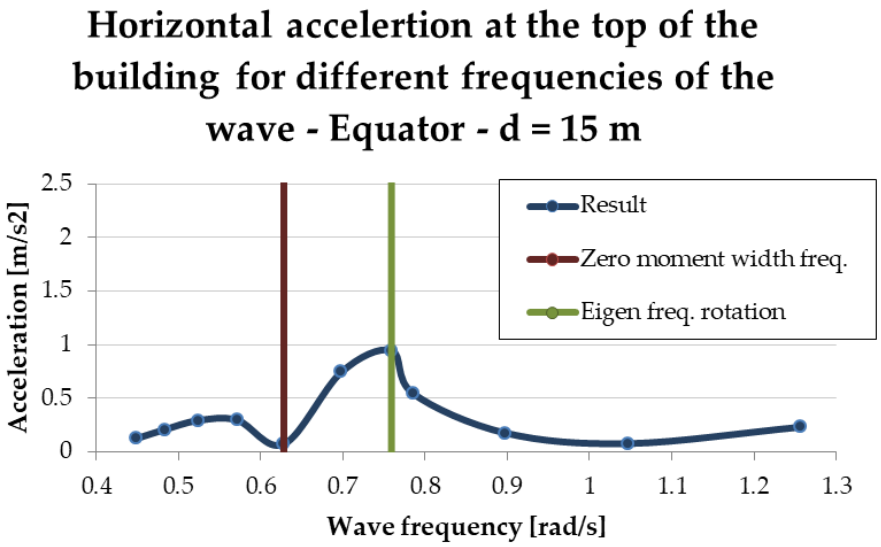

Figure 116 - Horizontal acceleration at the top of the building for different frequencies of the wave for a building of 50m and a platform depth of 15 m at the Equator.

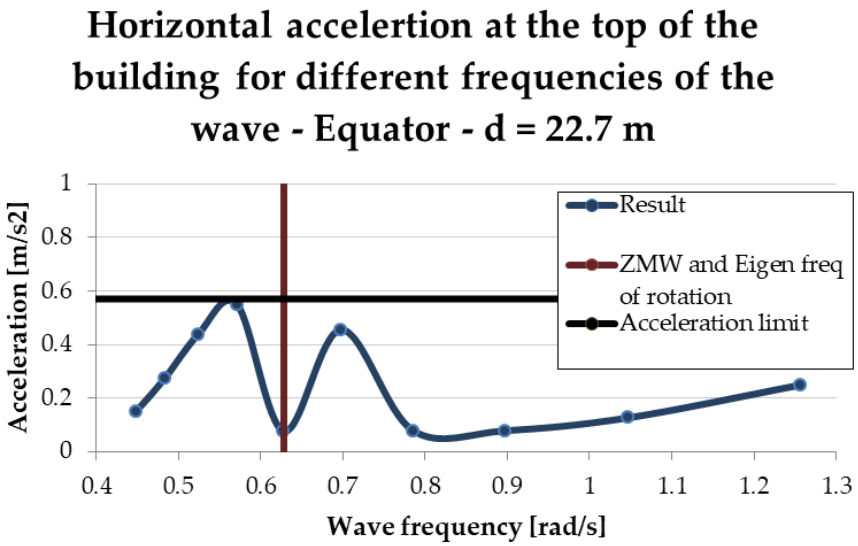

Figure 117 - Horizontal acceleration at the top of the building for different frequencies of the wave for a building of 50m and a platform depth of 22.7 m at the Equator. (ZMW is zero moment width)

7.4 Conclusion

With the results from chapters 6 and 7, it can (again) be concluded that the major problem is the horizontal acceleration at the top of the building due to the rotation of the platform. The four main problems of this rotation found are as follows:

1. The higher the building, the more the rotation of the platform affects the acceleration of the top of the building.
2. If the platform is close to the stability limit, the GM value is low and thus the rotation is high.
3. When the platform is not equal to the zero moment width values, much higher forces act on it, leading to much more rotation.
4. The eigenfrequency of the rotation lies, for most cases, in the wave-frequency width and thus resonance can occur.

The first problem is easy to solve, don't build too high. However, the aim of the research is to find out whether it is possible to build high. In addition, the case study with a low building height also shows enough problems with the horizontal acceleration.

The second problem can be solved by taking wider platforms than this stability limit. The disadvantage of this is that these widths can cause resonance.

The third problem seems easy to solve. Take platform widths equal to the zero moment width. However, this has four disadvantages:

- The zero moment widths are large, and there are large steps between them.
- They only work for one specific wavelength and thus wave frequency, the advantage diminishes quickly for different wavelengths.
- They can be close to the stability limit, which in turn leads to large rotations.
- The zero moment width can also cause an eigenfrequency that results in resonance.

The last disadvantage of the zero moment width and the problem of increasing the platform width are connected to the fourth problem: Resonance. To prevent resonance, there are two options: The eigenfrequency must either be lowered or raised. To do this, the formula of the eigenfrequency of the rotation must be examined. It contains the spring stiffness, the mass moment of inertia and the added mass.

Lowering the eigenfrequency can be done by:

- Increasing the mass moment of inertia. This in turn can be done by increasing the mass of the platform, making the platform wider or increasing the depth.
- The added mass can be increased. This can also be done by increasing the width of the platform.
- Finally, the spring stiffness can be reduced. This can be done , among other things , by making the platform smaller.

For the first two options, the platform width must be increased, for the third option it must be reduced. This makes it very complicated. It is not clear which of the three is the normative one, because the degrees of increase and decrease are not constant. In addition, it can be seen from the figures in subparagraph 6.6.7 that many combinations lead to resonance. The eigenfrequency must therefore also change significantly for many combinations before it no longer causes resonance. The other option, increasing the eigenfrequency, is exactly the same but then reversed. So this also gives the same problems.

The combination of the second to fourth problems means that in (almost) all cases there is only one solution: The width of the platform must be made so large that the rotation is minimal and there is no resonance in the rotation. This only happens at platform widths of more than 600 m (depending on the location). By also partly solving the first problem, not building too high, a less extreme width might be needed. The only option that gave good results in this research was the location around the equator with a building of 50 m high, a platform width equal to the zero moment width of 223 m and a depth of 22.7 m so that the eigenfrequency of the rotation is equal to the frequency for which the wave is highest, which is also the frequency the zero moment widths are tuned to.

8. DISCUSSION

This research investigated something that is still in its infancy; the building of floating platforms and building on top of floating platforms, floating on the sea or the ocean. This research serves as a first step towards one aspect: High-rise buildings on floating platforms. This aspect involves two large, complex structures. The high-rise building and a floating platform. To investigate both, and more importantly, to investigate the cooperation of these two, simplifications and assumptions have been made. These are necessary to make the problem manageable, but they also lead to less detailed, less accurate and therefore less reliable results. This chapter discusses the simplifications and assumptions. These are subdivided into: Locations and conditions; building and platform, methodology and finally software, models and calculations.

8.1 DISCUSSION ON LOCATIONS AND CONDITIONS ASSUMPTIONS

The locations and conditions are described in Chapter 2 and are the result of the literature study and research. The first subject are the locations. For this research:

- Three locations are used.
- This research therefore concludes something about the conditions of these three locations and not about all possible locations.
- For other locations a comparison can be made with the conditions of the three used locations to investigate whether it is possible to realise the floating high-rise at that location.

In addition to the limited number of locations, not all the different possible conditions for the three locations have been taken into account. The following statements are about the conditions used at the sites:

- One set of conditions has been used for each locations. This means one maximum wave height with the corresponding peak frequency. These values can differ, even at the same location.
- Different wave frequencies have been taken into account. These are based on the peak frequencies. No accelerations have been calculated with these frequencies.
- No further research has been done into the wave heights at other frequencies.
- And thus also no research into how these waves combine to form a wave field.

This study is focused on the waves. The wind load is included but not separately investigated. Therefore, it is not possible to draw conclusions on the exact difference between the effect of the wave load and the wind load and when which load is normative. This study focused on platforms with limited widths. For these, the waves are normative. However, the platform widths, for which floating high-rise is possible, have proven to be very large and can hardly be called limited in size. It was noted that heights of the buildings and widths of the platforms for which the floating high-rise is possible, the wind load is equal to or greater than the wave load. Therefore, more research is needed into the wind load separately from the wave load. The following simplifications are used for the wind:

- The wind is not governing. This is not something that can be chosen, but it is from this perspective that the calculations and results have been looked at.
- The wind has one frequency.

- The wind has no separate frequency in this research. The frequency of the wind is equal to that of the wave. This is reasonable to investigate because especially the combination of wind and waves in the same frequency is dangerous. However, it is possible that the wave frequency is not close to the frequency of the wave but that the wind has a frequency that can cause resonance. This has not been investigated in this study.
- The method of calculating wind loads is only valid for buildings up to a height of 200 m. As many buildings that have been calculated with are higher than this, the wind calculation is no longer accurate.

8.2 DISCUSSION ON BUILDING AND PLATFORM ASSUMPTIONS

In this study, a simplification of the building and platform into 1D elements was used. To do this, the “behaviour” of the building is simplified and many values are based on other existing buildings and studies and not on the model itself. The following simplifications and assumptions were made for the building:

- For the building only the core is used as an element, for stability. This is more often done in the preliminary research of the stability. In the preliminary research also a model/calculation is made for the core together with the frame of columns and beams or any other stability system. This is then a simple 2D model. This has not been done in this study. This does result in an simplification that leads to less accurate results.
- No lateral load resisting stability systems such as outriggers, tube systems or mega frames were used. These can only be examined properly if the building is modelled as 2D or 3D. These systems are often used in high-rise buildings on land and are therefore necessary for stability and can be extremely useful for high-rise buildings on floating platforms.
- It is assumed that the building can deform "infinitely" without causing problems.
- Since this study focuses on the stability, no research has been done into the strength of the building.
- A square cross-section was used. In reality, buildings have all sorts of different shapes. These can be disadvantageous, but also advantageous. For example, a building with a round cross-section would have to withstand far fewer wind forces
- A prismatic shape was used. A non-prismatic shape could also be advantageous. The lower the centre of gravity, the better the (floating) stability and the more rigidity at different heights in the building.

Modelling the platform as a one-dimensional element also needed simplifications and assumptions. These are the following:

- The platform is modelled as a beam. In reality, a three-dimensional platform could deform in all kinds of ways, other than a simple beam. The platform needs to be investigated as a slab or a similar sort of structure.
- This 3D deformation can also cause cracks to appear in the concrete in different places, which will result in differences in stiffness.
- It is assumed that the platform can deform "infinitely" without causing problems.
- Since this study focuses on the stability, no research has been done into the strength of the platform.

- One shape was examined for the platform: a box-shaped shape. In which the horizontal cross-section is a square. This form was chosen for its simplicity in determining, for example, the spring stiffness and added mass. However, it is not the best shape for the platform. Previous studies have shown that polygonal shapes are better, especially when it comes to attaching multiple platforms together.
- A prismatic shape is used in the horizontal direction. In ships, the centre is often deeper than the sides, creating a (fishing rod) float shape. This is much more stable than a flat platform. Also, a greater platform height below the building would be better. The platform deforms much more here than in other places due to the great weight of the building. A bigger height can increase the rigidity at this spot.

The simplifications mentioned above were necessary for parametric research where many different situations and sizes could be tested. This gives a more quantitative result than a qualitative one. The results of this research can be used as a limit from which more targeted research can be done on specific dimensions and locations. The parametric investigation not only made it necessary to simplify the modelling of the building, but also to make assumptions about the various parameters. The more parameters that remain variable, the greater the calculations. To keep these calculations limited, assumptions were made for many parameters based on existing projects or small studies. These assumptions are mostly based on expressing the parameters in the two parameters; height of the building and width of the platform. This results in a calculation with far fewer variables, but also simplifications, inaccuracies and fewer design choices. These assumptions are briefly described here, together with the consequences of these assumptions for the parameters relating to the building and the parameters relating to the platform.

For the building these are:

- **Width of the building**. The width of the building is based on three example buildings with different widths and heights. In reality, the width can be chosen freely and depends on the height of the building, but is not directly related to it. The width can be adjusted and may lead to different results. For example, a wider building would lead to more stiffness but also to more wind load. The influence of changing the width of the building is investigated in the chapter on dynamic stability.
- **Stiffness of the building**. The stiffness of the building is perhaps the most important parameter for the building in this study. It is determined in such a way that the same building on land (i.e. without rotation at the bottom) exactly meets the requirements of horizontal displacement as described in the Eurocode. When this stiffness is applied to the floating high-rise, it will not be enough. Therefore the estimate is also very conservative. This may have led to the negative results. In Chapter 6, however, the effects of increasing the stiffness on the accelerations have been investigated. This can be positive but also negative. Therefore, more research will have to be done on the stiffness.
- **Mass of the building.** The mass of the building is the most difficult parameter to estimate. This is because it is very much influenced by different choice. For this study, one standard weight per floor area has been used. This is taken from another study. This mass is therefore dependent on the width of the building and on the height. This mass could very well be different, which would lead to different results. However, a lot of research has been done in this study into changing the mass and the influences of this.
- **Mass moment of inertia of the building**. The mass moment of inertia is also based on one example because this is also a very difficult parameter to determine. Especially when

working with a one-dimensional element. The mass moment of inertia of the building could vary greatly. However, the research showed that this value mainly influenced the eigenfrequency of the rotation of the upper two masses. These eigenfrequencies were far away from the frequencies of the wave and therefore this assumption will not have much influence on the results.

For the platform, different assumptions have been made for the parameters. These are:

- **Stiffness of the platform**. The stiffness of the platform was investigated separately in this study. A parametric model was made in which the stiffness was calculated for different lengths and heights by modelling a three point bending test. From this a calculation was made of the stiffness of the platform expressed in width and height. In these calculations the platform was assumed to be a beam, so it was a 2D calculation. In reality 3D platform will behave differently. This mainly causes other deformations where the building and the platform are connected. Still, it is a pretty good approximation.
- **Mass of the platform**. The mass of the platform is calculated in the same model as the stiffness. The mass is thus expressed in the height and width of the platform using the model. The mass of the platform is only based on the dead weight. Live loads were not taken into account. However, this is not a problem. In most calculations, extra ballast was used to increase the mass of the platform. The mass of the platform therefore has more of a chosen value than a value that follows from the dimensions.
- **Damping**. The damping value of the floating platform is assumed constant. This is because it is an almost impossible parameter to determine. It is often determined by testing scale models. The value that is often used for ships was used. It may well be that the damping is different for the platform. This will also lead to different results. However, it is concluded that the wave excitation changes so slowly that the homogeneous part of the solution of the equation of motion (the part that strongly depends on the damping) is negligible.

Finally, a parameter that affects both the building and the platform is the E-modules. Only one value for the E-modules was used in the entire study. In addition, only the reduced E-modules for cracked concrete were used in the calculations. Initially, the concrete would not have been cracked yet. This would lead to different results. This has not been taken into account in this study. For the building, a different choice would not lead to different results. As mentioned before, the stiffness follows from the Eurocode requirements. The stiffness will therefore remain the same if the E-modulus changes. For the platform it has consequences. The stiffness of the platform does depend on the choice for the E modulus.

8.3 Discussion on Methodology

In this study, static and dynamic stability were treated separately. This is possible because the two stabilities are very different. However, it would have been better to have the two parts (partially) overlap. The following parts would have been easier or better if the two models could be used together:

- To determine whether water could get onto the platform. This is now investigated in the static stability part at two moments. The moment of no rotation and the moment of maximum rotation. It could well be that somewhere between these moments the water could

be on the platform. This could have been more easily investigated with the dynamic behaviour. This has not been investigated further.

- The dynamic stability shows that the skew and horizontal displacement of the top of the building from the static stability are not reached. This will be due to the building already moving into reverse before it has undergone the maximum rotation/displacement. This will not lead to a difference in minimum values for the parameters (if it is stable, it does not matter anymore how much it rotates, it is stable anyway) but it will lead to a difference in results.
- Parts of the static stability were investigated that ultimately did not matter at all because the dynamic stability is normative, which was unknown at the time. Especially some optimisation for the static stability were useless. When the two parts are used together they can be optimised together.

The choice to keep static stability and dynamic stability separate is mainly due to the way of modelling and the programmes that are useful for it. In this research, the parametric program Grasshopper was very useful. However, no dynamic analysis can (yet) be done with this program. Therefore, other programs were chosen for the dynamic stability. If in the future a dynamic analysis can be done in Grasshopper, this programme would be very useful to combine the two forms of stability.

The last phase of the research in which the case study was done is on the short side. A case study was also not the main objective but the results from the case study reveal many problems and some inaccuracies. In addition, a case study is a form of anecdotal evidence. The few values that have been studied are not representative. By using the results of the other phases, parameters were chosen to investigate whether floating high-rise is possible, not whether it is impossible. In other words, if an example is found that works, it is proven that it is possible. But with a few examples it is not possible to conclude that it is never possible. The conclusion of the case study chapter does draw such conclusions. These are not only based on the case study, but especially on the case study together with the other chapters, from which a better conclusion can be drawn whether it is possible or not.

8.4 Discussion on software, models and calculations

In the paragraph on assumptions for the building and the platform, there has already been a discussion about modelling the elements as 1D. It subsequently follows that the models and the calculation are 2D. This is fine for a preliminary study on floating high-rise buildings. But because of this, there are parts which have not been investigated or which have been taken little or no account of. These are the following:

- Three of the six possible motions are omitted. For two of these this is not a problem. These are the horizontal displacement and the rotation in the direction perpendicular to the 2D model. Due to the symmetry of the platform and building, these are equal to the two examined horizontal motion and rotation. What has not been investigated is the sixth motion; the Yaw (rotation in the horizontal plane). For this, a 3D model is needed.
- In the model, the combination of the three motions are investigated. In reality, this will be a combination of all six motions. This will lead to differences. Especially when working with a square platform.

- It has not been investigated what the motions are when the wave is not perpendicular to the platform. This is a major simplification, especially for a square platform. The spring stiffness and added mass will be different if the platform rotates diagonally (e.g. if the corner of the square platform becomes the lowest point after rotation instead of the side of the square). This gives other accelerations that can be higher than the accelerations of the wave loads investigated in this research.
- The wave is assumed to be prismatic in the direction that is not modelled. In reality there will be a complex 3D wave field that can make the platform move in all kinds of ways. This has not been taken into account in this investigation.

In addition to modelling in 2D, there are several components in the static stability model that are inaccurate:

- No horizontal springs are used. This is because it would not be accurate when using a 1D element for the platform. It also causes horizontal displacement due to the compression of the spring by the horizontal forces. It is then no longer possible to determine whether the displacement is due to the horizontal displacement of the platform or due to the rotation and/or deformation of the building. The latter was the main purpose of the model. The only downside is that these springs produce a small moment. This moment is not taken into account. In the dynamic model the horizontal springs are used.
- Secondly, a support was added to the height of the centre of gravity in the static stability model. Because of the lack of horizontal springs, this was necessary to keep the model "in place" so that the model could find an equilibrium. This support did not cause a difference between the GM method and the model, and the rotation of the platform was calculated accurate. However, it does lead to incorrect results in the deformation of the building. These did not influence the results used for the conclusions.
- Thirdly. The model is inaccurate for those platform widths where the stability is low but still sufficient. This inaccuracy is due to the platform and building rotating too much to achieve a final rotation. In other words, the rotation changed so much per iteration that it could not be determined whether there was stability, and thus an end rotation could be found, or whether there was no stability and the model would rotate infinitely.
- Finally, a modelling assumption used for both static and dynamic stability that has an impact is the assumption that the building is modelled as a clamped beam. This means that the rotation in the middle of the platform is equal to the rotation of the bottom of the building. This simplification is more often used in preliminary models of high-rise buildings. However, in reality there will be a difference in rotation and the connection will not be a moment fixed connection but will have the behaviour of a very stiff rotational spring.

This paragraph concludes with a discussion of the dynamic model. Modelling the entire building as one point mass or as three point masses gives the following simplifications/inaccuracies:

- The platform is included in one point mass. If the platform is the focus of the study, it too will have to be divided into several point masses. For this research, one point mass with an adjusted stiffness for the rotational spring, to take into account the deformation of the platform, was enough.
- In the program Diana it was showed that for the eigenfrequencies close to the values of the wave frequencies three point masses is enough. This model is also used to check if

the matrices, which are used for the calculations of the multi-mass model, and the eigenfrequencies that follow from them are correct. However, it has not been checked whether the resulting solutions of the equations of motion are correct.

- In the calculations of the limits of the frequency paragraph, the single-mass model formulas were used. This is not accurate for the horizontal and rotational motions. Therefore, these results should be used with care. Since the use of the multiple mass model leads to other eigenfrequencies. The single-mass model does give higher eigenfrequencies than the multiple mass model. In this research, this resulted in a conservative estimate.

9. CONCLUSION

In this chapter, the research questions, as formulated in Chapter 1, are presented again. Subsequently, the various research objectives are addressed and the conclusions are discussed. This is done by answering sub-questions using the results from Chapters 4, 5, 6 and 7 of the study, taking into account the assumptions and different situations investigated as described in Chapters 2 and 3 and the discussion of these assumptions and situations and the subsequent results in Chapter 8 . These answers and conclusions are then used to answer the main research questions in the final paragraph.

The main research questions of this study are as follows:

Research question 1:

Is it structurally feasible to construct high-rise buildings on floating platforms which are limited in size regarding stability?

Research question 2:

What are the requirements for both the platform and the building regarding the stability of a floating high-rise building for different building heights?

To answer these questions, the three phases, which were divided into five objectives, in this research are discussed.

9.1 PHASE 1

The first phase consists of the first objective; Examining the various topics that form a basis for this research. For this objective, the existing literature on floating cities and floating homes was examined. From this literature, a beginning of the research has been made and various assumptions have been based on it. In addition to the research done on floating construction, there is research done on the various information that should be used as input and limitation of the research as well. The following properties are used for the building and the platform.

- The cross-section of the building is square and the building is prismatic, see Figure 118.
- The cross-section of the platform is square and the platform is prismatic, see Figure 118.
- The core of the building and the platform are made of concrete class C60/75.

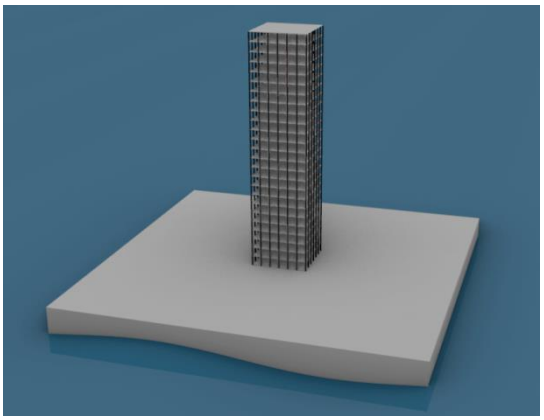

Figure 118 - Render of the platform and building.

It was determined which locations needed to be examined in order to answer the research question for a wide range of locations. This resulted in three locations:

- The North Sea. With high wind speed, high waves and limited depth.
- The North of the Atlantic Ocean. With extreme wave heights.
- The Atlantic Ocean around the equator. With calm wave and wind conditions

These form three locations with differences in depth, wave length, wave height and wind conditions from extreme to minimal. In addition to the locations, various extreme cases were investigated for which the floating high-rise had to be tested. These are:

- A tsunami. A sudden wave with a very long wave length.
- A growing storm. A transition from a calm sea to the most extreme wave heights.
- The most extreme wave height. A regular wave of the most extreme wave the floating high-rise need to resist.
- Irregular waves. The combination of multiple waves with different frequencies.

Finally, the limits and regulations that the floating building had to meet in terms of stability were investigated. These regulations consist of the following serviceability limit state limits:

- The minimum distance between the top of the platform and the water must be at least 0.3 m. This is to prevent water from getting onto the platform.
- The depth of the platform must be large enough so that the trough of the wave is not lower than the platform
- The GM value* must be at least 0.25 m.
- Both the vertical and horizontal acceleration at any position in the building needs to be below 0.55 m/s^2.

* The GM value is the distance between the centre of gravity and the meta centre. The meta centre is where the direction of the buoyancy force intersects the central axis. If the GM value is positive, there is stability. The higher the GM value, the less rotation under a certain heeling moment.

9.2 PHASE 2

The second phase consists of three objectives. Examining; buoyancy, static stability and dynamic stability. All three are discussed.

9.2.1 BUOYANCY

For the buoyancy, mainly the relation between the mass and the depth of the platform is determined. This is a relationship that has been used extensively in static and dynamic stability. The mass of the building and platform pose few problems for staying afloat. In fact, extra ballast water can easily be used to make the platform heavier in order to achieve the desired mass or depth.

9.2.2 STATIC STABILITY

For the static stability a combination of hand calculations based on the GM-method, in which the GM value is calculated on the basis of certain values of the platform and building, and a model that can include deformations in the calculations as well is used. The GM method was used to check if the model was correct. The comparison showed that the results are the same when infinite rigid elements are used in the model. When realistic stiffnesses are used, the results of the rotation and deformations are very different. Thus, the GM method is not enough when investigating the different requirements for a floating high-rise building. For the limit of stability, the GM method was used because the model was not accurate due to the high rotations. For the stability, a linear relationship was found between the height of the building and the width of the platform for which the floating high-rise is stable.

- The floating high-rise is stable if the following inequality formula is fulfilled:

$$Height\ building \leq 2.3936 * Width\ platform - 44.817 \tag{9.1}$$

The relationship is the result of a complicated calculation despite the seemingly simple linear formula found. The relationship does result from basing the other parameters (e.g. width of the building) on the two parameters in question. When these can be chosen freely, it may deviate somewhat.

Changing the various parameters of the building and platform can have several positive and negative effects on the stability of the platform. These are as follows:

- Making the platform wider provides a higher GM value and thus less rotation. This is positive for the displacement of the building. However, it can be negative because more forces act on the platform. This can be detrimental and thus cause more rotation.
- Making the building higher causes the weight in the middle of the platform to increase. This will cause the platform to sink deeper in the middle and create a banana shape. This can be disadvantageous, because the middle is now lower, but it can be positive because the ends, where the water can reach the platform, bend upwards and are therefore higher. The increasing weight can lead to more rotation, which in turn leads to much more horizontal translation in the building. Finally, a taller building has a wider width and thus catches more wind, which leads to an increase in moment and thus rotation.
- Making the platform higher provides more stiffness. This can be positive or negative for the same reason as explained above.

The calculations gave various results with local minimums. For example, the required depth of platform was minimal around the values for the platform width equal to that of the wavelength, or a multiple of it. Investigation of the forces showed that the vertical forces on the platform were minimal at these platform widths. Minimum values were found for the results depending on the moments due to the wave force. However, these were for other platform widths than for the vertical force. These values are called "zero moment widths" because for these widths the wave moment, regardless of position or time, is approximately equal to 0 kNm. Therefore the rotation is minimal when these zero moment widths are used for the platform width. It is not easy to determine in advance which value of the platform width this is, but it is the width for which the moment due to the wave force is minimal. Between two zero moment width values there is approximately the value of a wavelength. The zero moment widths are therefore dependent on the wavelength, different wavelengths give different zero moment widths. The following therefore applies to the various locations:

- The vertical forces on the platform are minimal if the platform has the same length as the wavelength of the wave, or a multiple of it.
- The moment on the platform, and thus the rotation, by the wave is minimal at the so-called zero moment width. These are different from the wavelength.

9.2.3 DYNAMIC STABILITY

For the last objective of the second phase; the dynamic stability, the floating high-rise was first modelled as a single mass (single-mass model). Then, for three different motions; Vertical motion (heave), horizontal motion (surge and sway) and rotation (roll and pitch), it was investigated how these should be calculated and which parameters influence these motions. Next, the floating high-rise building was modelled as three point masses (multi-mass model) with three degrees of freedom (DOF's) for all three point masses, the platform being included in the lowest point mass. These eigenfrequencies obtained by the models differ for the horizontal motion and rotation. The single-mass model gave higher eigenfrequencies than the multiple mass model. The eigenfrequency of the vertical motion is the same for both models. In addition, the multiple mass model gave more eigenfrequencies. However, these were far from the frequency of the waves. With a model in Diana, it was concluded that three point masses is accurate enough for determining the eigenfrequencies and no more are needed.

With both the single-mass models and the multi-mass model the following was concluded:

- The vertical acceleration is minimal when the width of the platform is equal to the wavelength or a multiple of it.
- The vertical acceleration is only normative for small building heights and platform widths, whereas it is the biggest cause of seasickness.
- If the zero moment widths are used for the width of the platform, the rotation and thus the horizontal acceleration is minimal. This does not mean that the accelerations are below the limit.
- The horizontal acceleration at the top of the building due to both the horizontal motion and the rotation is almost always normative.
- A tsunami, which has little height and a very large wavelength on the open ocean, does not cause an extreme reaction. As the wave is not high, this situation is not normative.
- The growth of the waves from a calm ocean to a storm does not cause extreme reactions as this happens over a longer period of time.

- The most extreme wave height is the normative of the three. In addition to the extreme wave height, irregular waves can be normative.

For the three motions, the most influential parameters have been investigated. They are listed here with the explanation of their influence. For the vertical motion, these are:

- **Platform width**. A larger platform provides more spring stiffness and more added mass. This changes the eigenfrequency. With increasing width a reduction in maximum acceleration was found. As in static stability, there are minimums in the results for platform widths equal to the wavelength or a multiple thereof.
- **Mass.** A change in the mass of the floating high-rise causes a change in the eigenfrequency. The higher the mass the lower the eigenfrequency and the higher the mass the lower the maximum vertical acceleration. The eigenfrequency of the vertical motion is only close to the wave frequency for low buildings (below 100 m) and can consequently lead to resonance.

For the horizontal motion:

- **Platform width.** As with the vertical motion, an increasing platform width results in a lower maximum acceleration. There are minimum as found in the static stability for this motion. For the horizontal motion, these are equal to the zero moment widths.
- **Platform depth.** An increasing depth causes a reduction in horizontal acceleration. However, the depth can change the eigenfrequency in such a way that the eigenfrequency approaches that of the waves and thus resonance can occur. So increasing the depth is not always beneficial for limiting the maximum horizontal acceleration.
- **Mass**. The influence of mass on the horizontal motion is the same as for the vertical motion.

For the rotational motion:

- **Platform width**. A larger platform width provides a larger GM value. This will be discussed later. The results showed a decrease in maximum rotational acceleration with increasing width together with the minimums when the platform width equals the zero moment widths.
- **Platform depth**. The analysis of the depth of the platform shows, as with the horizontal motion, that there is the possibility of resonance if you change it.
- **GM value**. A higher GM value means less rotation of the platform. This is positive for static stability but not necessarily for dynamic stability. Just as for the depth of the platform, a certain value for GM can cause resonance and thus extreme accelerations. Increasing the GM value can therefore have a negative effect on the dynamic stability.
- **Total mass**. The same applies to the mass for rotation as for vertical and horizontal motion. More mass means lower maximum acceleration. However, the eigenfrequency of this motion is higher and much closer to the frequency of the waves. Therefore, a resonance peak was seen in the analysis of the mass. This motion is the problem in the analyses of the irregular waves.

In the results of the calculations with all parameters depending on the height of the building, the width of the platform and the weight of the additional ballast, it can be seen that the vertical acceleration is only above the limit for low buildings and small platform widths. Otherwise, the

vertical acceleration is not a problem. However, the horizontal acceleration is a much bigger problem. For a 100m building, these accelerations are only below the limit for platform widths equal to zero moment widths. For heights of 300m and 500m, the accelerations only came below the limit for platforms larger than 700m. The results showed that this is even more problematic for the Atlantic Ocean. For the equator, the results are better, but here too resonance can be very problematic.

In addition to calculating the accelerations due to the largest possible regular waves, research has been carried out into the different frequencies of the wave that occur in an irregular wave field. Each of these frequencies could occur and thus cause resonance. Therefore, the eigenfrequencies of the floating high-rise must not be equal to these frequencies. Using the formulas for the eigenfrequency of the single-mass model, it was not possible to do this with the multiple mass model, the combination of height of the building, width of the platform and depth of the platform (and therefore mass) that can lead to resonance were determined. The graphs are shown below for a depth of 20m.

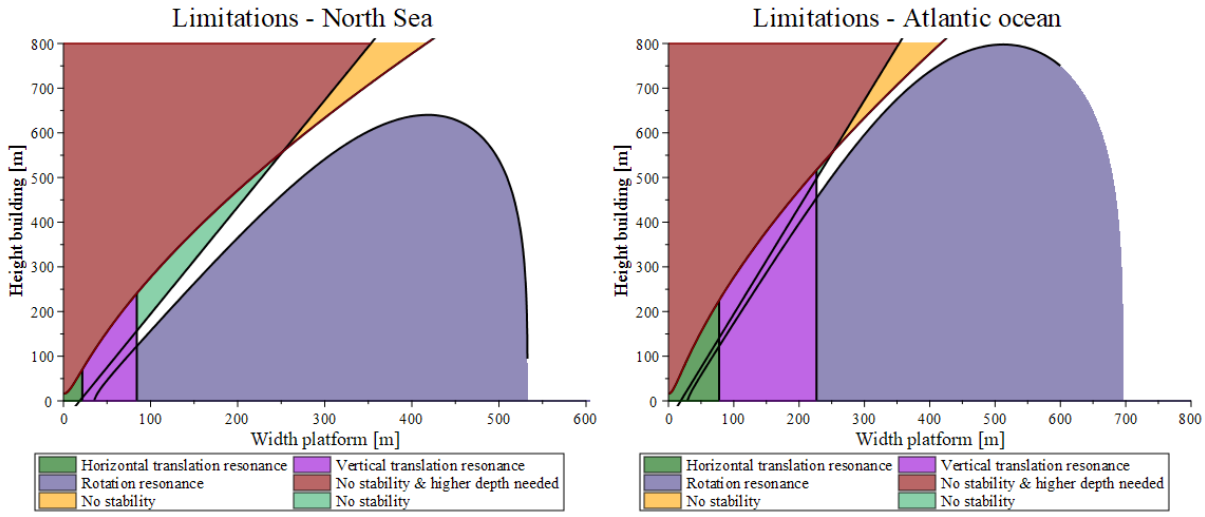

Figure 119 - A graph of different limitations for the building height and the platform width. This graph is applicable for a) the North Sea location and b) the Atlantic ocean, for a platform with a depth of 20m.

The graphs for the North Sea and the equator are almost identical because the wave frequencies are almost identical. In addition to the eigenfrequency limits, the static stability limit and the depth limit have been added. The depth limit is an upper limit for which the chosen depth is still possible. In the graph, there is a "gap" between the rotational motion limit and the stability limit/ depth limit. This "gap" is there for platform depths from 15 m for the North Sea and the equator and from 20 m for the Atlantic. With lower platform depth the depth limit will be lower than the rotational frequency limit and thus there are no options in between these areas.

9.3 PHASE 3

The third phase is the test phase, in which the results of phase two are used in a case study for the purpose of testing, assessing and drawing conclusions. Three different inputs were used in the case study. One building of 500 m, one building of 50 m and platform widths equal to zero moment widths. The following problems were determined using the results of phase 3 together with phase 2:

- The higher the building, the more the rotation of the platform affects the acceleration of the top of the building.
- If the platform is close to the stability limit, the GM value is low and thus the rotation is high.
- When the platform is not equal to the zero moment width values, much higher forces act on it, leading to much more rotation.
- The eigenfrequency of the rotation lies, for most cases, in the wave-frequency width and thus resonance can occur.

These problems lead to the following recommendations/necessary choices:

- Don't build to high.
- Choose platform widths that are far from the stability limit to limit rotation.
- Choose platform widths equal to the zero moment width which is tuned to the wave-length of the peak frequency of the wave.
- Avoid resonance.

To fulfil the last three conditions, only one option remains in almost all cases. The platforms must be so extremely large that the conditions for the building on the platform are similar to those of a building on land. In this case, the conditions of the waves are almost irrelevant and the wind becomes the governing factor. Then the same measures and design choices can be made to resist the wind as on land.

The following conclusions were drawn for the various locations:

- For the North Sea, the waves are too high for limited platform widths. The widths should be greater than 600 m to avoid resonance and keep the rotation low enough. Next, the extreme wind load is the big problem for high buildings. Even on huge platforms. Therefore, it is not possible to build high-rise buildings on platforms with limited dimensions in the North Sea.
- For the North Atlantic Ocean, the conditions are even more extreme than the North Sea, so the same conclusions apply.
- For the equator it is possible, albeit limited. When a building height of 50 m is used, a platform width equal to 223 m (a zero moment width) and a depth equal to 22.7 m, the eigenfrequency and the frequency at which the zero moment width is tuned coincide. This ensures that, despite resonance, the acceleration limit can be met at all wave frequencies. From the case study it follows that other heights are possible when the platform widths are equal to the zero moment width. However, this has only been tested with the highest possible wave and its frequency. For other frequencies these lead to too high acceleration as well. Therefore, it is concluded that floating high-rise buildings are limited in their possibilities at the equator.

9.4 Answering the research questions

All this leads to answering the two research questions. First, the question whether it is structurally feasible to build high-rise buildings on floating platforms with limited dimensions. The answer is that, with the design choices and simplifications used, it is not possible on limited plat-

forms in the North Sea and Atlantic Ocean. To get the horizontal acceleration low enough and to ensure that no resonance occurs, the platforms have to be larger than 600m, which is no longer covered by limited dimensions. So it is possible for these locations with these enormous platforms, but the approach to the whole design will be different. Not just a building, but a whole city will have to be built on it in order to be useful. For the equator it may be possible, although the case study still shows many problems, it does shows that there are combinations that are promising and that there is one possibility, with a building height of 50 m was found.

The second research question is about the requirements of the building and the platform. For the North Sea and the North Atlantic Ocean, a platform is needed that is so large and robust that the conditions are the same as on land. Then, with all the measures in place, it would be possible to build as high as on land. For the equator, the zero moment widths will have to be taken into account. These are the only possibilities that are promising. The depth of the platform will then have to be at least 15 m and the height of the platform 20 m. In that case, buildings between 100 m and 600 m might be possible on platforms smaller than 400 m. For the height of 50 m, a platform width of 223 m and a depth of 22.7 m must be chosen.

10. RECOMMENDATIONS

The conclusion of this study is that it is not possible to realise floating high-rise buildings with the assumptions and design choices used. This leaves a final question open; is it possible with other assumptions and design choices? From this study and previous and other research, the expectation is that floating high-rise is still possible, even on platforms with limited dimensions. In this study, parametric design was used to investigate the various possibilities as broadly as possible. So this research says a little about a lot. The next step will have to focus on the positive aspects that have emerged from this research. In this way, the research can be used as a basis for taking the steps towards more specific research in which improvements and optimisations are examined to make the floating high-rise possible. This chapter looks at the possibilities for further research.

This study is an investigation into a subpart of a topic that is still in its infancy: Floating housing on platforms. Since this topic is still being researched and has not yet been applied anywhere in the world (on a large scale), researching an extreme version, high-rise buildings on the floating platforms, is a study that is not supported by a great deal of research and practical knowledge. It is therefore important that good research is first carried out into the platforms and the habitability of the platforms. Much can then be learned from these studies to further investigate floating high-rise buildings. Nevertheless, after this research, there are recommendations to continue researching the floating high-rise structures. In this chapter, these recommendations are presented. They will be focused on the aspect of high-rise buildings and not on other forms of floating housing. In addition, the recommendations deal with the aspect of building engineering. Apart from this aspect, there are many other aspects that can be investigated, such as costs, assembly, sustainability, politics, etc. For these subjects, It is recommend to look at the projects of, for example, Blue21.

10.1 PLATFORM

The next step to be taken is to explore different forms for the platform. In this study, one shape was used for the platform. A box shape with a square cross-section. However, other platform shapes have already been researched and better options are available. In addition to the cross-section, the prismatic shape in the height is not ideal. There are so many possible shapes that are better than a box shape. Just think of ships or (fishing) floats. The improved stability that can be obtained with these shapes can greatly increase the possibility of floating high-rise buildings on platforms with limited sizes.

Changing the shape means that new research is required into the spring stiffness, added mass, damping, etc. Also the distribution of these values over the platform has to be investigated. With non-prismatic shapes, the values will vary over the width or height of the platform. In order to apply these other shapes, the platform will also have to be divided into several point masses for the dynamic analysis. It is not possible to predict in advance how many of these masses there will be.

Besides the form, many assumptions and simplifications have been made for the platform. It would greatly benefit the research if fewer assumptions needed to be made and less simplification needed to be done. Again, this could follow from a research focused on the platform only.

10.2 BUILDING

Just as for the platform, it is advisable to look at other forms for the building. Round cross-sections in particular can be very advantageous because of their streamlined shape. As a result, it catches much less wind. In addition, the prismatic shape is not necessarily ideal. For example, you can look at shapes like the Eiffel Tower.

Perhaps even more important than the shape of the building is the investigation of stability systems. On land, these are always used for high-rise buildings and they could be an enormous improvement for floating high-rise buildings. One can think of outrigger systems, tube systems and mega frames. It must be said, however, that this research shows that the rotation of the platform is normative for smaller platform widths and that restricting this rotation is therefore more important than the stability of the building or its flexibility.

Finally, many assumptions and simplifications were made for the building. It would benefit the study as well if fewer assumptions needed to be made and less simplification needed to be done.

10.3 MODELS

Most assumptions and simplifications of the building and platform come from using 1D elements for these two. This gives a good first indication but a lot can be gained by modelling the elements in 2D or even 3D. By doing so, most of the assumptions (e.g. weight of the building) can be calculated instead of doing an estimation. It will give more accurate results. It is easier to apply the recommendations for the platform and the building, for example the stability systems. However, this makes the models more difficult to adapt and the research less parametric. It is therefore recommended to take suitable/ideal dimensions in advance in order to make a more sophisticated and detailed model with that set of dimensions.

Modelling the elements in 3D ensures that the whole model has to be 3D. Here, too, there is much to be gained. Firstly, because all motions can then be taken into account, but because the irregular wave field can be applied properly as well. It is then possible to investigate how floating high-rise reacts to waves that are not perpendicular to the platform and to a combination of waves with different frequencies, heights, lengths and directions.

If the decision is made to keep the model in 2D, which certainly has its advantages, the next step is to divide the platform into different point masses and not just the building. This is necessary if there will be more buildings on the platform than one building in the middle.

In the discussion, it was discussed that there are many advantages to combining static and dynamic stability in one model. This would be best done in Grasshopper, to keep it parametric as well, but the possibility of a dynamic analysis is not there in this program. These scripts will have to be created by the user. Something that in itself can be quite a research or job. Perhaps there are other programmes that can combine these two components better.

10.4 OTHER RECOMMENDATIONS

So far, the recommendation has been to improve the design or models. There are many more recommendations that cannot be directly linked to these. These are discussed here and are as follows:

- A study is needed into the strength of the building and the platform. In this study, the focus was on the stability and stiffness, but the strength is just as important.
- A more comprehensive study of the various possible conditions at a location and the use of a much more accurate wave field.
- Finding the optimal location.
- The study of the effect of motion on people. This research used a combination of studies on motion in buildings and motion on ships. However, floating high-rise buildings are different from both and studies focused on floating high-rise buildings are needed to determine the limits. For example, the combination of vertical displacement and rotation that causes seasickness or feeling unwell from seeing motion in relation to the surroundings.
- Research into the use of tuned mass dampers and other forms of motion damping. These have not been addressed at all in this research but can be very beneficial. For extremely tall buildings, these dampers are already needed on land. For example in the Taipei 101 tower.
- Finally, the examination of several (tall) buildings on a platform. This research shows that it is almost always necessary to use an extremely large platform and it would be a shame to leave all the empty space unused. When multiple tall buildings are used, they can be connected in a way that reduces the displacement of the top and thus the accelerations. One can look at connecting multiple platforms into a larger whole and the effect this has on the high-rise.

REFERENCES

Altus, A. (2022). *Where houses are designed to float*. https://www.bbc.com/travel/article/20150915-where-houses-are-designed-to-float. Accessed 2 March 2022.

Balaji, R., Sannasiraj, S. A., & Sundar, V. (2007). *Physical model studies on discus buoy in regular, random and double peak spectral waves*.

Barltrop, N. (1998). *Floating Structures: a guide for design and analysis*.

Bezuyen, K. G., Stive, M. J. F., Vaes, G. J. C., Vrijling, J. K., & Zitman, T. J. (2011). *Inleiding waterbouwkunde*. Collegedictaat CT2320. Delft University of Technology.

Blaauwendraad, J. (2016). *Dynamica van Systemen*. Course reader of the Faculty of Civil Engineering and Geosciences TU Delft.

Blecha, P. (2010). *Seattle's Historic Houseboats*. https://www.historylink.org/File/9507. Accessed 2 March 2022.

Boyce, W. E., & DiPrima, R. C. (2010). *Elementary differential equations* (Tenth edition, international student version).

Caires, S., Groeneweg, J., & Sterl, A. (2006). Changes in the North Sea extreme waves. In *Preprints of 9th international workshop on wave hindcasting and forecasting.*

Centraal bureau voor de statistiek (2020). *Hoe wordt de Nederlandse bodem gebruikt?* https://longreads.cbs.nl/nederland-in-cijfers-2020/hoe-wordt-de-nederlandse-bodem-gebruikt/. Accessed 20 September 2021.

Ching, F. D. (2014). *Building construction illustrated*. John Wiley & Son

Clement, C., Kosleck, S., & Lie, T. (2021). Investigation of viscous damping effect on the coupled dynamic response of a hybrid floating platform concept for offshore wind turbines. *Ocean Engineering*, *225*, 108836.

Curriculum Research & Development Group (CRDG) (2015). Exploring Our Fluid Earth. *University of Hawai'i.*

Czapiewska, K. (2021). *Space@Sea*. Blue21. https://www.blue21.nl/portfolio/spaceatsea/. Accessed 8 November, 2021.

de Graaf, R. (2021). *Blue revolution*. Blue21. https://www.blue21.nl/portfolio/blue-revolution-4/. Accessed 8 November, 2021.

De Vries, P.A., Fennis, S.A.A.M. & Pasterkamp, S. (2013). Veiligheid. *Book of the course CTB2220/CTB2320 Veiligheid van constructies en Belastingen op constructies at the TU Delft, Delft.*

Fen-Yu Lin, Otto Spijkers and Pernille van der Plank. (2020). Legal framework for sustainable floating city development: A case study of the Netherlands. *Conference book: Paving the waves; WCFS2020, 2nd world conference on floating solutions 2020.*

Flikkema, M., Breuls, M., Jak, R., de Ruijter, R., Drummen, I., Jordaens, A., ... & Otto, W. (2021). *Floating Island Development and Deployment Roadmap*.

Holthuijsen, L. H., De Ronde, J. G., Eldeberky, Y., Tolman, H. L., Booij, N., Bouws, E., ... & Gal, J. A. (1995). The maximum significant wave height in the southern North Sea. In *Coastal Engineering 1994* (pp. 261-271).

Howe, B. M., Arbic, B. K., Aucan, J., Barnes, C. R., Bayliff, N., Becker, N., ... & Weinstein, S. (2019). SMART cables for observing the global ocean: Science and implementation. *Frontiers in Marine Science*, *6*, 424.

International Tsunami Information Center (2021). *How does tsunami energy travel across the ocean and how far can tsunamis waves reach?* http://itic.ioc-unesco.org/index.php?option=com_content&view=article&id=1164&Itemid=2031. Accessed 10 December, 2021.

ISO code 2631-1 (1997). *Mechanical vibration and shock - Evaluation of human exposure to whole-body vibration - Part 1: General requirements*.

ISO code 2631-2 (1997).. *Mechanical vibration and shock - Evaluation of human exposure to whole-body vibration - Part 2: Vibrations in buildings (1 Hz to 80 Hz)*.

ISO code 2631-4 (1997). *Mechanical vibration and shock — Evaluation of human exposure to whole-body vibration — Part 4: Guidelines for the evaluation of the effects of vibration and rotational motion on passenger and crew comfort in fixed guideway transport systems.*

Jonkers, H. (2019). *Materials and Ecological Engineering*. Reader of the TU Delft for the subject material and ecological engineering.

Journee, J., & Massie, W. (2015). *Offshore hydromechanics. Third edition*. Delft University of Technology.

Ko, K. K. M. (2015). *Realising a floating city*. (Master thesis). TU Delft, Delft

Kortenhaus, A., Oumeraci, H., Allsop, N. W. H., McConnell, K. J., Van Gelder, P. H. A. J. M., Hewson, P. J., ... & Vicinanza, D. (1999). Wave impact loads-pressures and forces. *Final Proceedings, MAST III, PROVERBS-Project: Vol. IIa: Hydrodynamic Aspects*.

Lau-Bignon, A. W. (2015). The Tonle Sap Lake, a birthplace of civilizations. *LEspace geographique*, *44*(1), 81-88.

Lawther, A., & Griffin, M. J. (1987). Prediction of the incidence of motion sickness from the magnitude, frequency, and duration of vertical oscillation. *The Journal of the Acoustical Society of America*, *82*(3), 957-966.

Li, Q. S., Zhi, L. H., Tuan, A. Y., Kao, C. S., Su, S. C., & Wu, C. F. (2011). Dynamic behavior of Taipei 101 tower: field measurement and numerical analysis. *Journal of Structural Engineering*, *137*(1), 143-155.

Lin, F. Y., Czapiewska, K., Iorga, G., Totolici, D & Koning, J. (2019). *Space@Sea: A catalogue of technical requirements and best practices for the design of Living@Sea*.

Liu, M. Y., Chiang, W. L., Hwang, J. H., & Chu, C. R. (2008). Wind-induced vibration of high-rise building with tuned mass damper including soil–structure interaction. *Journal of Wind Engineering and Industrial Aerodynamics*, *96*(6-7), 1092-1102.

Malta, E. B., Gonc¸alves, R. T., Matsumoto, F. T., Pereira, F. R., Fujarra, A. L., & Nishimoto, K. (2010). Damping coefficient analyses for floating offshore structures. In *International Conference on Offshore Mechanics and Arctic Engineering* (Vol. 49095, pp. 83-89).

March, R & Palo, P. (1998). Lighterage Seasickness Parametric Study. *Technical Memorandum TM-2306-OCN*

Myers, I. (2021). *The world's first floating city gets the green light*. Designboom. Architecture & design magazine. https://www.designboom.com/architecture/bigs-floating-city-to-be-built-in-south-korea-11-29-2021/. Accessed 10 January, 2022.

Naeem, S. et al. (2009). *Biodiversity, Ecosystem Functioning, and Human Wellbeing: An Ecological and Economic Perspective*. Oxford, UK: Oxford University Press.

Nakajima. T, Saito. Y & Umeyama. M. (2020). A Study on Stability of Floating Architecture and its Design Methodology. *Conference book: Paving the waves; WCFS2020, 2nd world conference on floating solutions 2020.*

National Oceanic and Atmospheric Administration (NOAA) Center for Tsunami Research. (2004) *Tsunami Event - The Indian Ocean Tsunami*. https://nctr.pmel.noaa.gov/indo_1204.html. Accessed 9 September, 2021.

National Oceanic and Atmospheric Administration (NOAA) Center for Tsunami Research. (2011) *Tohoku (East Coast of Honshu) Tsunami.* NOAA Center for Tsunami Research. https://nctr.pmel.noaa.gov/honshu20110311/. Accessed 9 September, 2021.

NEN-EN 1990. (2021) - *Basis of structural design*

NEN-EN 1991-1-4 (2011). *Eurocode 1: Actions on structures - Part 1-4: General actions - Wind actions*

Newman, J.N. (1977). *Marine Hydrodynamics*. MIT Press, Cambridge, UK.

Nijsse, R. (2019). *High rise building: Structural aspects*. [Powerpoint slides], Tu Delft, Delft, The Netherlands.
https://brightspace.tudelft.nl/d2l/le/content/193353/viewContent/1586979/View

NTA 8111. (2011). *NTA 8111:2011nl: Floating constructions.*

Oceanix Ltd. (2021). *Oceanix | Leading the next frontier for human habitation*. https://oceanixcity.com/ Accessed 14 December, 2021.

O'Hanlon, J. F., & McCauley, M. E. (1973). *Motion sickness incidence as a function of the frequency and acceleration of vertical sinusoidal motion*. CANYON RESEARCH GROUP INC GOLETA CA HUMAN FACTORS RESEARCH DIV.

Oppenheimer, M., Glavovic, B., Hinkel, J., van de Wal, R., Magnan, A. K., Abd-Elgawad, A., ... & Sebesvari, Z. (2019). *Sea level rise and implications for low lying islands, coasts and communities.*

Rui L. P. de Lima, Floris C. Boogaard and Vladislav Sazonov. (2020). Assessing the influence of floating constructions on water quality and ecology. *Conference book: Paving the waves; WCFS2020, 2nd world conference on floating solutions 2020.*

Shimizu corporation (2020). Brochure: *A Future of Harmonious Living. A Botanical Future City Concept.*

Shukla, P. R., Skea, J., Calvo Buendia, E., Masson-Delmotte, V., Pörtner, H. O., Roberts, D. C., ... & Malley, J. (2019). *IPCC, 2019: Climate Change and Land: an IPCC special report on climate change, desertification, land degradation, sustainable land management, food security, and greenhouse gas fluxes in terrestrial ecosystems*.

Solari, G., Carassale, L., & Tubino, F. (2007). Proper orthogonal decomposition in wind engineering-Part 1: A state-of-the-art and some prospects. *Wind and Structures*, *10*(2), 153-176.

Song, M. J., & Cho, Y. S. (2020). Modeling Maximum Tsunami Heights Using Bayesian Neural Networks. *Atmosphere*, *11*(11), 1266.

Starink, P. (2019). *Parametrisch ontwerpen*. Architectuur.nl. https://www.architectuur.nl/nieuws/evenementen/parametrisch-ontwerpen/ Accessed 23 February 2022.

Takeuchi, M., Yoshida, I. (2020). Mega floating city "Green Float" concept and technology innovations. *Conference book: Paving the waves; WCFS2020, 2nd world conference on floating solutions 2020.*

Thornhill, T. (2022). *The amazing floating cities of China: Entire bays covered by homes*. Mail Online. https://www.dailymail.co.uk/news/article-2773835/The-incredible-floating-cities-China-Entire-bays-covered-wooden-homes-provide-two-thirds-world-s-seafood.html. Accessed 2 March 2022.

Van Winkelen, M. (2007). *How high can we float?* (Master thesis). TU Delft, Delft

Wang, C. M., Han, M. M., Lyu, J., Duan, W. H., Jung, K. H., & An, S. K. (2020). Floating forest: a novel concept of floating breakwater-windbreak structure. In *WCFS2019* (pp. 219-234). Springer, Singapore.

Wertheim, A. H., Bos, J. E., & Bles, W. (1998). Contributions of roll and pitch to sea sickness. *Brain Research Bulletin*, *47*(5), 517-524.

Young, I. R. (1999). Seasonal variability of the global ocean wind and wave climate. *International Journal of Climatology: A Journal of the Royal Meteorological Society*, *19*(9), 931-950.

Young, I. R., Vinoth, J., Zieger, S., & Babanin, A. V. (2012). Investigation of trends in extreme value wave height and wind speed. *Journal of Geophysical Research: Oceans*, *117*(C11).

Zanon, B.D.B., Czapiewska, K., Kirkwood, D., Olthuis, K., Stan, A., de Korte, N., Subramani, S., Totolici, D. Chiriac, C., Murea, A.V. & Spiridon, C. (2017). *Space@Sea: Demonstrator Design*

APPENDIX I – LOCATION AND CONDITIONS

This appendix deals with the locations, the conditions at the locations and the calculation of the conditions. First the map of the different locations is shown and the standard conditions are given. Then the waves are discussed and the calculations for different wave values are shown. This paragraph ends with a table with all the values used in the study. Finally, the wind load calculations are shown.

LOCATION

The following figure shows the three locations used on the map. These are the North Sea (top right), north of the Atlantic Ocean (middle) and between the North and South Atlantic around the equator (bottom centre). The location in the north of the Atlantic Ocean is also just called "Atlantic Ocean" and the location around the equator as "Equator".

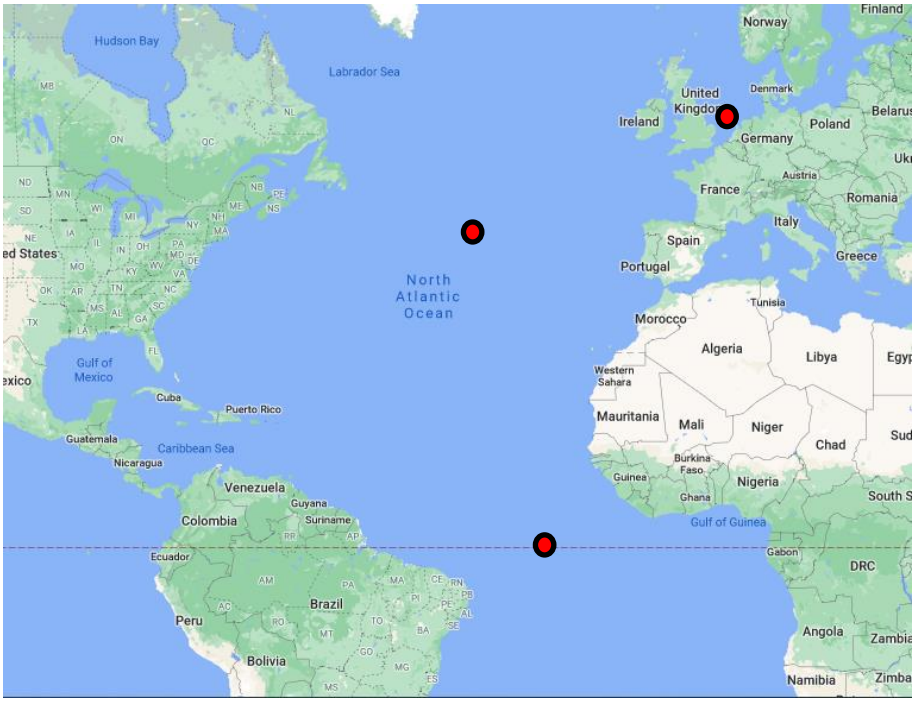

Figure 120 - Locations for the conditions used in the calculations.

The conditions for all three locations have been determined[9] . These locations give the following values for the conditions:

[9] Caires, Groeneweg, & Sterl, (2006). Holthuijsen et al., (1995). Young. (1999). Young, Vinoth, Zieger & Babanin. (2012).

Table 29 - Conditions at the different locations.

Location	Significant wave height [m]	Peak period [s]	Wind speed at reference height [m/s]	Depth [m]
North Sea	7.95	9.8	50	30
North Atlantic	16	14	40	-*
Equator	4	10	20	-*

* These depths are so large they have no influence

The peak period is the period for which the highest wave height occurs.

WAVES

REGULAR WAVE

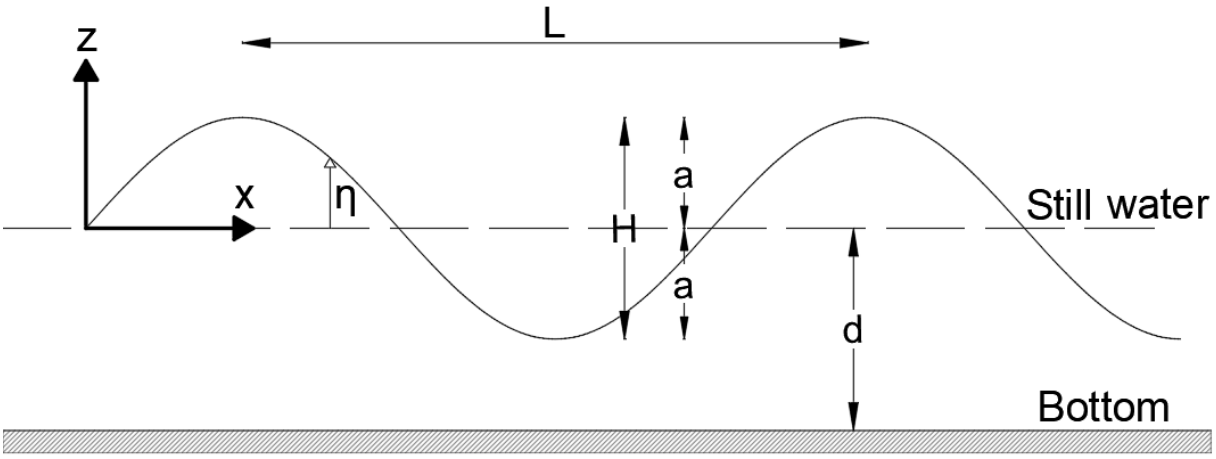

Figure 121 - Sinusoidal wave. (Based on figure 3-28, Bezuyen, Stive, Vaes, Vrijling & Zitman (2011)

A standard, most simple wave can be described as a sinusoid in which the height of the wave is calculated. Figure 121 shows such a wave with the parameters used in the formula. The height of the wave varies in both place and time. So the formula is expressed in these two variables. The formula is as follows:

$$\eta(x,t) = \frac{H_w}{2}\sin\left(\frac{2\pi x}{L_{wave}} - \frac{2\pi t}{T_{wave}}\right)^{10} \quad (0.1)$$

Where:

η is the vertical displacement of the water level [m]

H_w is the wave height [m]

x is the distance in the direction of the wave propagation [m]

L_{wave} is the wave length [m]

t is the time

T_{wave} is the wave period [s]

[10] Bezuyen et al (2011)

For the different locations the wave height and wave period are known. The wave length can then be calculated by the formula:

$$L_{wave} = \frac{g * T_{wave}^{2}}{2\pi} \tanh(\frac{2\pi z}{L})^{11} \quad (0.2)$$

Where:

g is the gravitational constant (9.81 m/s²)

z is the depth of the water [m]

For the Atlantic ocean locations the depth is so large that the wave length can be calculated with only the first part:

$$L_{wave} = \frac{g * T_{wave}^{2}}{2\pi} \quad (0.3)$$

For the North Sea the expression of (0.2) should be used. The wave length can then be calculated by an iterative process. For the period of 9.8 s this gives the following table:

Table 30 - Wave length of a wave with a period of 9.8 *s* for the North Sea.

Iteration	Wave length [m]
1	127.49
2	135.13
3	132.59
4	133.44
5	133.16
6	133.24
7	133.22
8	133.23
9	133.23
10	133.23

The wavelength of all three location for the peak period are shown in the table below

Table 31 - Wave lengths for the peak period of the three locations.

Location	North Sea	Atlantic ocean	Equator
Wave length [m]	133.23	306.02	156.13

SIGNIFICANT WAVE HEIGHT TO MAXIMUM WAVE HEIGHT

From the literature, the significant height of the waves is obtained from the different locations. This is the wave height with 13.5% change of exceeding. With this significant wave height the probability of exceedance can be calculated for different wave height with the formula from Bezuyen et al (2011):

$$P(\underline{H} > H) = e^{-2(\frac{H}{H_s})^2}$$

Where:

[11] Bezuyen et al (2011)

$P(\underline{H} > H)$ is the chance that the wave height H will be exceeded

H_s is the significant wave height

For the safety of the construction the Eurocode uses a 5% chance of exceeding (characteristic value of the loads) together with safety factors. By using this 5% and rewriting the formula, the wave height with 5% chance of exceedance can be calculated as follows:

$$H = \sqrt{\frac{\ln(0.05)}{-2}} * H_s$$

In the following table the different wave height with 5% chance of exceedance can be seen together with the halved wave height due to the breakwaters.

Table 32 - Wave height with a breakwater with transmission of 0.5. H_w is the wave height with breakwaters

Location	H_s [m]	$H_{5\%}$ [m]	H_w [m]
North Sea	7.95	9.73	4.87
North Atlantic	16	19.58	9.79
Equator	4	4.90	2.45

IRREGULAR WAVES

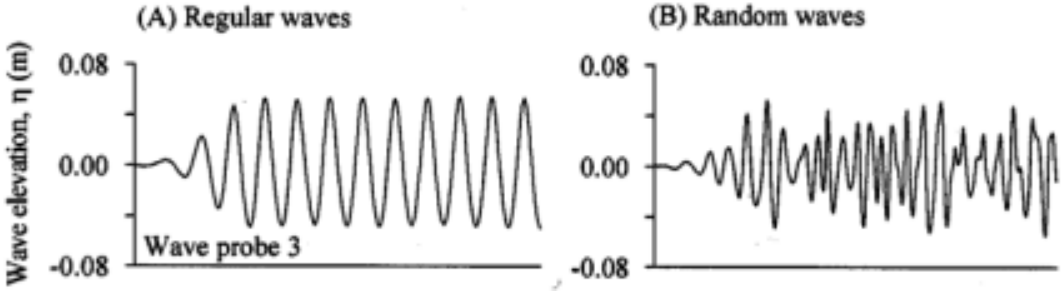

Figure 122 - Typical regular and random wave time histories, (Based on figure 4, Balaji, Sannasiraj, & Sundar. (2007))

The waves can be seen as regular waves, these waves have a certain period and wave height. For these the found values in this appendix can be used. In reality there will be more of a random wave pattern as shown in the figure above. This random wave or irregular wave cannot be described by a single sine wave function. One must use the so-called Fourier analysis of waves to describe the waves in multiple sine functions. Every possible frequency that can occur in the wave Fourier series can cause resonance. Therefore all the frequencies the wave field can have, have to be determined. This can be done by using the Pierson-Moskovitz spectrum (Bezuyen et al, 2011). This spectrum gives the energy density as a function of frequencies:

$$S(\omega) = \frac{\alpha g^2}{2\pi\omega^5} e^{-\frac{5}{4}*(\frac{\omega}{\omega_p})^{-4}} \quad (0.4)$$

Where

α equals 0.081 for storms

ω is the frequency

ω_p is the peak frequency

The peak frequency can be calculated with the previously determined peak wave periods. The wave with the peak frequency has the largest share in the total wave field. The other frequencies will have a lesser share.

Since this function is infinite, the limits of the wave frequency are chosen so that 5% of the frequencies lie above or below this width. These values are chosen because they are often used for the exceeding probability of a load (De Vries, Fennis & Pasterkamp, 2013). The frequencies that do need to be included must therefore contain 95% of the function. To determine this percentage, the graph must first be scaled to a distribution function with area equal to 1 (=100%). This can be done by adding the term "S peak" in the denominator of the energy density function and then setting the integral equal to 1:

$$\int_0^{\infty} \frac{\alpha g^2}{2\pi\omega^5 S_{peak}} e^{-\frac{5}{4}*(\frac{\omega}{\omega_p})^{-4}} d\omega = 1 \tag{0.5}$$

This results in the desired function. To calculate the limits of the middle 95%, the integral of constant "a" to constant "b" is set to 0.95:

$$\int_a^{b} \frac{\alpha g^2}{2\pi\omega^5 S_{peak}} e^{-\frac{5}{4}*(\frac{\omega}{\omega_p})^{-4}} d\omega = 0.95 \tag{0.6}$$

In addition, the results from the function must be equal at both constants:

$$S(a) = S(b) \tag{0.7}$$

These two equations can be solved to determine the limit values a and b. In the figure below the graph is shown with the lines at the boundary values for the North Sea conditions as an example.

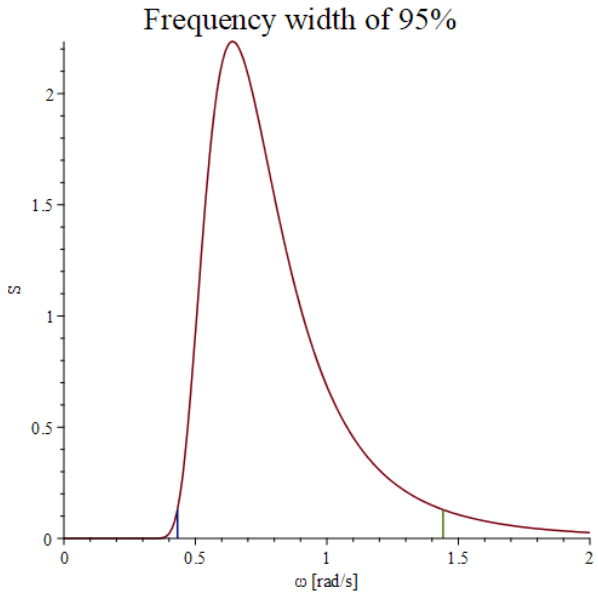

Figure 123 - Frequency width limits of 95% for the North Sea.

These give the following possible wave frequencies at the different locations:

Table 33 - Frequency width of the wave for the three locations.

Location	Frequency width [rad/s]
North Sea	0.43 – 1.44
North Atlantic	0.30 – 1.01
Equator	0.42 – 1.42

To translate the energy density into a wave height, the relation between the energy and the height of the wave is used. This relation is $E = a * H^2$ (where a is a unknown constant). With this relation the height of the wave is determined for the different frequencies. Instead of S_{peak}, to make the integral over the density function equal to 1, a factor is used to make sure the maximum wave height occurs at the peak frequency. In addition, the root is drawn from the total density function to translate it into the height of the wave. The result is the following formula:

$$Height\ wave = \sqrt{\frac{\alpha g^2}{2\pi\omega^5 factor} * e^{-\frac{5}{4}*\left(\frac{\omega}{\omega_p}\right)^{-4}}} \tag{0.8}$$

As an example, in Figure 124 the wave height is plotted for the conditions of the North Sea.

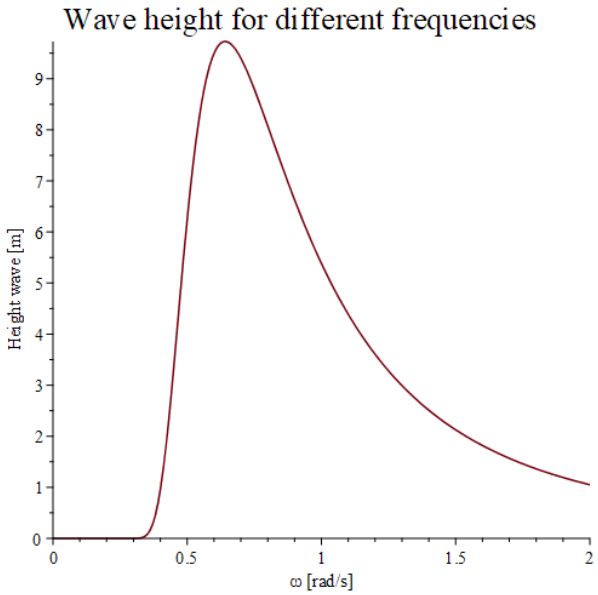

Figure 124 - Wave height for different frequencies for the conditions of the North Sea.

TABLE OF ALL CONDITIONS

Table 34 - All condition values of the three locations.

Location	$H_{5\%}$ [m]	H_w [m]	T_w [s]	ω_w [rad/s]	L_{wave} [m]	u_{10} [m/s]	Depth [m]	Frequency width [rad/s]
North Sea	9.73	4.87	9.8	0.64	133	50	30	0.43 – 1.44
North Atlantic	19.58	9.79	14	0.63	306	40	-*	0.30 – 1.01
Equator	4.90	2.45	10	0.45	156	20	-*	0.42 – 1.42

WIND

For the calculation of the wind force on the building the NEN-EN 1991-1-4 (2011) code is used together with assumptions and simplifications. In this appendix the formulas used are show and the assumptions are explained. The input for the wind force calculation, the wind speed at a reference height of 10 meters is used with a return period of 100 years.

In the calculation the recommended values for external pressure coefficients for vertical facades of buildings with a rectangular floor plan are used for every height. In practise these calculations can only be used for buildings with a height up to 200m. For the profile of the extreme thrust, the guidelines of a building with a height twice of its width is used. For the wind speed the speed at a reference height of 10 m (u_{10}) is used.

The following calculation formula is used for the wind speed at reference height:

$$v_m(z) = c_r(z) * c_o(z) * v_b \ [m/s] \quad \text{(A-III.9)}$$

Where:

z is the height [m]

$c_r(z)$ is the roughness factor [-]

$c_o(z)$ is the orography factor, taken as 1,0 for a terrain without mountains [-]

v_b is the wind speed at reference height [m/s]

For the roughness factor the following formula is used:

$$c_r(z) = k_r * \ln(\frac{z}{z_0}) \quad \text{(A-III.10)}$$

With:

$$k_r = 0.19 * \left(\frac{z_0}{z_{0II}}\right)^{0.07} \quad \text{(A-III.11)}$$

Where:

z_0 is the roughness lengt, taken as 0.003 m for a sea or coastal area;

z_{0II} is 0.05 m (terrain category II)

The formula for $c_r(z)$ only applies for buildings up to 200 m but for simplification it is also used for taller buildings in this research.

For the external thrust of the wind on the building the wind turbulence intensity is taken into account. This intensity can be calculated as follows:

$$I_v(z) = \frac{\sigma_v}{v_m(z)} \quad \text{(A-III.12)}$$

With:

$$\sigma_v = k_r * v_b * k_l \quad \text{(A-III.13)}$$

Where:

k_l is the turbulence factor, taken as 1 [-] (recommended value)

With the obtained values, the external thrust can be calculated with the following formula:

$$q_p(z) = \left(1 + 7I_v(z)\right) * \frac{1}{2} * \rho * v_m^2(z) \quad \text{(A-III.14)}$$

Where

$q_p(z)$ is the external thrust at reference height [kN/m^2]

ρ is the density of the air taken as 1.25 kg/m^3

For the wind pressure the external thrust needs to be multiplied with the pressure coefficient. For these coefficients the $c_{pe,10}$ is used for zone D and E (NEN-EN 1991-1-4, art 7.6 – 7.8) together this gives a factor of 1.5. For the wind pressure the following distribution from the code is used:

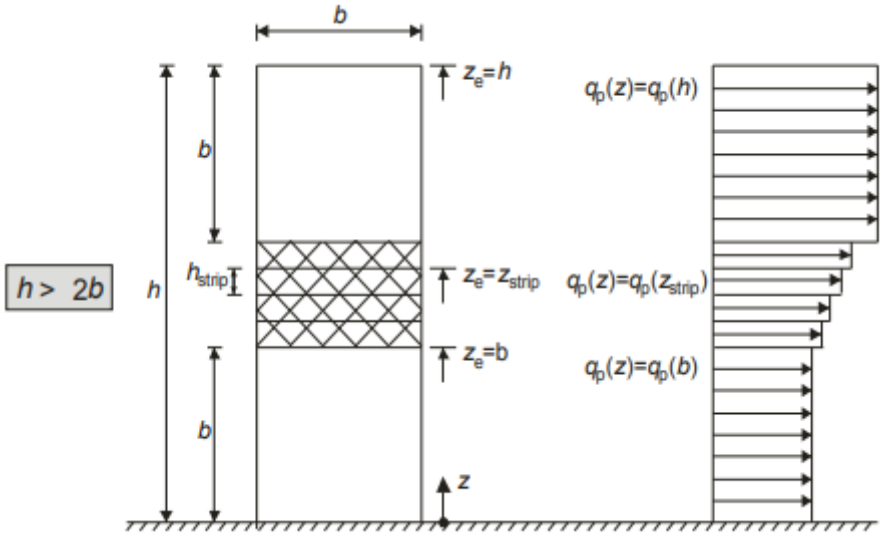

Figure 125 - Distribution of the wind force.

REFERENCES

Bezuyen, K. G., Stive, M. J. F., Vaes, G. J. C., Vrijling, J. K., & Zitman, T. J. (2011). *Inleiding waterbouwkunde*. Collegedictaat CT2320. Delft University of Technology.

Caires, S., Groeneweg, J., & Sterl, A. (2006). Changes in the North Sea extreme waves. In *Preprints of 9th international workshop on wave hindcasting and forecasting.*

De Vries, P.A., Fennis, S.A.A.M. & Pasterkamp, S. (2013). Veiligheid. *Book of the course CTB2220/CTB2320 Veiligheid van constructies en Belastingen op constructies at the TU Delft, Delft.*

Holthuijsen, L. H., De Ronde, J. G., Eldeberky, Y., Tolman, H. L., Booij, N., Bouws, E., ... & Gal, J. A. (1995). The maximum significant wave height in the southern North Sea. In *Coastal Engineering 1994* (pp. 261-271).

NEN-EN 1991-1-4 (2011). *Eurocode 1: Actions on structures - Part 1-4: General actions - Wind actions*

Young, I. R. (1999). Seasonal variability of the global ocean wind and wave climate. *International Journal of Climatology: A Journal of the Royal Meteorological Society*, *19*(9), 931-950.

Young, I. R., Vinoth, J., Zieger, S., & Babanin, A. V. (2012). Investigation of trends in extreme value wave height and wind speed. *Journal of Geophysical Research: Oceans*, *117*(C11).

APPENDIX II – WAVE AND WIND FORCES

VERTICAL WAVE FORCE

The function for the force due to the wave is the sinusoidal function for the wave height multiplied by the "force of the water", which is the density (1025 kg/m^3) multiplied by the acceleration of gravity (9.81 m/s^2). The wave is assumed constant perpendicular to the direction of wave propagation. Thus the 3D wave can be converted to 2D by multiplying the formula with the width of the platform. This is used for the static stability calculations.

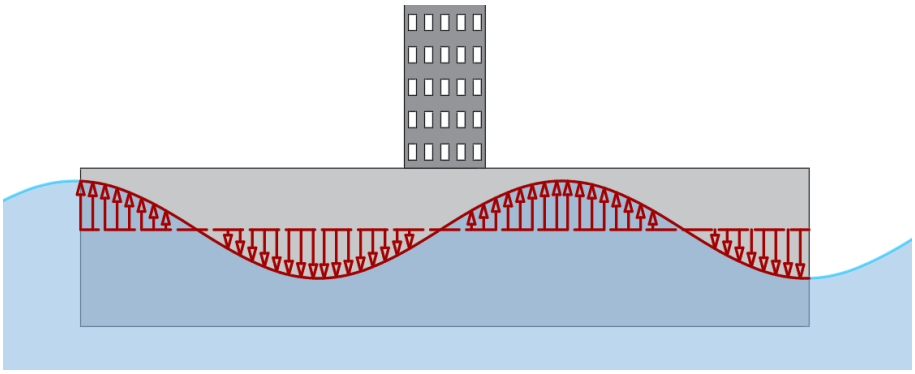

Figure 126 - Vertical wave force.

This gives the following function for the distributed vertical force:

$$q_{v,wave}(x,t) = \rho_{water} * g * w_p * \frac{H_w}{2} * \sin(\frac{2\pi * t}{Tw} + \frac{2\pi * x}{Lw}) \; [N/m] \tag{A-II.1}$$

Where

ρ_{water} is the density of salt water. Equal to 1025 kg/m^3

w_p is the width of the platform [m]

H_w is the maximum height if the wave [m]

Tw is the wave period [s]

Lw is the wave length [m]

In the chapter on dynamic stability, this distributed load must be translated into a representative point load. This can be done by taking the integral of 0 to the width of the platform:

$$F_{v,w}(t) = \int_0^{wp} q_{v,wave}(x,t)\, dx \;\; [N] \tag{A-II.2}$$

Which is equal to:

$$F_{v,w}(t) = \int_0^{wp} \rho_{water} * g * w_p * \frac{H_w}{2} * \sin(\frac{2\pi * t}{Tw} + \frac{2\pi * x}{Lw})\, dx \;\; [N] \tag{A-II.3}$$

This results in:

$$F_{v,w}(t) = \frac{L * H * F_{water} * (2 * \cos\left(\frac{\pi t}{T}\right)^2 * \cos\left(\frac{w_p \pi}{L}\right)^2 - 2\sin\left(\frac{\pi t}{T}\right)\cos\left(\frac{\pi t}{T}\right)\sin\left(\frac{w_p \pi}{L}\right)\cos\left(\frac{w_p \pi}{L}\right) - \cos\left(\frac{w_p \pi}{L}\right)^2 - 2\cos(\frac{\pi t^2}{T} + 1)}{2\pi} [N] \quad \text{(A-II.1)}$$

Since all values except t are known, the function is simplified to:

$$F_{v,w}(t) = \hat{F}_w * \sin(\omega_w t + \varphi_w) [N] \quad \text{(A-II.2)}$$

With:

$$\hat{F}_{v,w} = \frac{L * H * F_{water} * w_p * \sin(\frac{w_p * \pi}{L})}{2\pi} [N] \quad \text{(A-II.3)}$$

and

$$\omega_w = \frac{2\pi}{T_w} [Hz] \quad \text{(A-II.4)}$$

Since it does not matter for the result where and when the wave starts, in order to simplify it, the phase shift (φ_w) is taken as zero. This results in:

$$F_{v,w}(t) = \hat{F}_{v,w} * \sin(\omega_w t) [N] \quad \text{(A-II.5)}$$

HORIZONTAL WAVE FORCE

The horizontal force depends on the water level. It is the difference in force between the two ends. If the wave is high at one end and low at the other, the force at one end is greater and the sum of forces is not zero. This force is only in the dynamic stability calculations and not the static stability calculation. Therefore the distributed force is reduced to a point load.

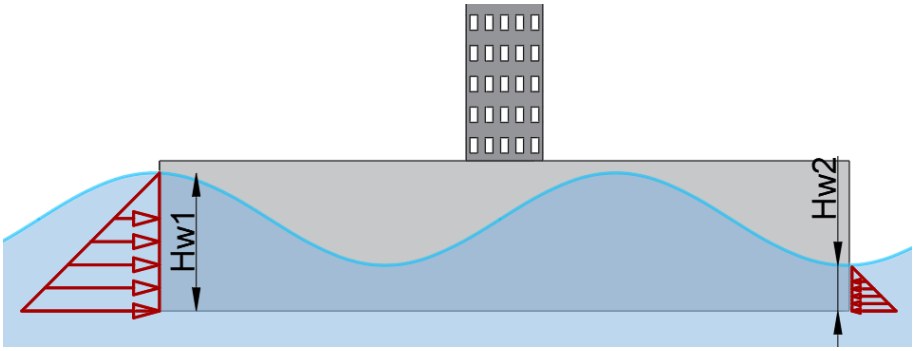

Figure 127 - Horizontal wave force

The resulting force of the distributed force can be calculated by:

$$F_{h,wave}(t) = \frac{1}{2} * \left(d + H_{w,1}(t)\right)^2 \rho_{water} * g - \frac{1}{2} * \left(d + H_{w,2}(t)\right)^2 \rho_{water} * g \quad \text{(A-II.4)}$$

Where $H_{w,1}$ and $H_{w,2}$ are the heights of the wave at the different ends of the platform. As said, these values are variable in time. The formulas are as follows:

$$H_{w,1}(t) = \frac{H_w}{2}\cos\left(\frac{2\pi t}{T_{wave}}\right)[m] \tag{A-II.5}$$

$$H_{w,2}(t) = \frac{H_w}{2}\cos\left(\frac{2\pi * w_p}{L_w} - \frac{2\pi t}{T_{wave}}\right)[m] \tag{A-II.6}$$

Where

H_w is the maximum height of the wave

L_w is the wave length

T_{wave} is the wave period

Since the time of the start of the motion does not matter for the calculations, the entire wave force can be written as one sinusoid.

$$F_{h,wave}(t) = \widehat{F}_{h,wwave} * \sin(\omega_w t)\ [N] \tag{A-II.7}$$

WAVE MOMENT

For the calculation of the moment only the vertical force of the wave is taken into account. To calculate the moment due to a distributed load of any function, the area under the function need to be multiplied by the difference between the centre of that area and the point of rotation (force * arm). The area under the function can be calculated with the integral:

$$A = \int_a^b f(x)dx \tag{A-II.8}$$

To calculate the horizontal centre of an area under a function the following formula can be used:

$$Centre\ (horizontal) = \frac{1}{A} * \int_a^b x * f(x)dx \tag{A-II.9}$$

The point of rotation is the middle of the platform. Therefor the arm can be calculated as follows:

$$arm = \frac{1}{2} * w_p - \frac{1}{A} * \int_a^b x * f(x)dx \tag{A-II.10}$$

The arm need to be multiplied by the total force to get the bending moment:

$$Moment = \left(\frac{1}{2} * w_p - \frac{1}{A} * \int_a^b x * f(x)dx\right) * A \tag{A-II.11}$$

This gives the formula for the moment through the wave where $q_{v,wave}(x,t)$ is the distributed wave force.

$$Moment_{wave}(t) = \frac{1}{2} * \int_a^b q_{v,wave}(x,t)\ dx * w_p - \int_a^b x * q_{v,wave}(x,t)\ dx \tag{A-II.12}$$

For the total moment on the platform, the constants a and b can be taken as 0 and w_p.

The formula for the moment is dependent on the time. For the dynamic analysis the formula for the moment can be simplified to a sine function:

$$M_{wave}(t) = \widehat{M}_{wave} * \sin(\omega_{wave} t)\ [N] \tag{A-II.13}$$

To calculate the most negative time for the static stability, the derivative of the moment formula equal to 0 has to be solved. As the time were the derivative is zero, the moment is maximum. This results in the following expression for the maximum moment:

$$Maximum\ Moment_{wave} = \left| \frac{\left(-w_p * \pi * \cos\left(\frac{w_p * \pi}{L_{wave}}\right) + L_{wave} * \sin\left(\frac{w_p * \pi}{L_{wave}}\right)\right) * L_{wave} * \rho_{water} * g * w_p * H_{wace}}{4\pi^2} \right| [Nm] \tag{A-II.14}$$

WIND FORCE

For the calculation of the wind force on the building the NEN-EN 1991-1-4 code is used together with assumptions and simplifications. In this appendix the formulas used are show and the assumptions are explained. The input for the wind force calculation, the wind speed at a reference height of 10 meters is used with a return period of 100 years.

The following calculation formula is used for the wind speed at reference height:

$$v_m(z) = c_r(z) * c_o(z) * v_b [m/s] \tag{A-II.15}$$

Where:

z is the height [m]

$c_r(z)$ is the roughness factor [-]

$c_o(z)$ is the orography factor, taken as 1,0 for a terrain without mountains [-]

v_b is the wind speed at reference height [m/s]

For the roughness factor the following formula is used:

$$c_r(z) = k_r * \ln\left(\frac{z}{z_0}\right) [-] \tag{A-II.16}$$

With:

$$k_r = 0.19 * \left(\frac{z_0}{z_{0II}}\right)^{0.07} [-] \tag{A-II.17}$$

Where:

z_0 is the roughness lengt, taken as 0.003 for a sea or coastal area [-]

z_{0II} 0.05 m (terrain category II)

The formula for $c_r(z)$ only applies for buildings up to 200 m but for simplification it is also used for taller buildings in this research.

For the external thrust of the wind on the building the wind turbulence intensity is taken into account. This intensity can be calculated as follows:

$$I_v(z) = \frac{\sigma_v}{v_m(z)} \; [-] \tag{A-II.18}$$

With:

$$\sigma_v = \; k_r * v_b * k_l \; [m/s] \tag{A-II.19}$$

Where:

k_l is the turbulence factor, taken as 1 (recommended value)

With the obtained values, the external thrust can be calculated with the following formula:

$$q_p(z) = \left(1 + 7I_v(z)\right) * \frac{1}{2} * \rho * v_m^2(z) \tag{A-II.20}$$

Where

$q_p(z)$ is the external thrust at reference height

ρ is the density of the air taken as 1.25 kg/m^3

For the wind pressure the external thrust needs to be multiplied with the pressure coefficient. For these coefficients the $c_{pe,10}$ is used for zone D and E (NEN-EN 1991-1-4, art 7.6 – 7.8) together this gives a factor of 1.5. For the wind pressure the following distribution from the code is used:

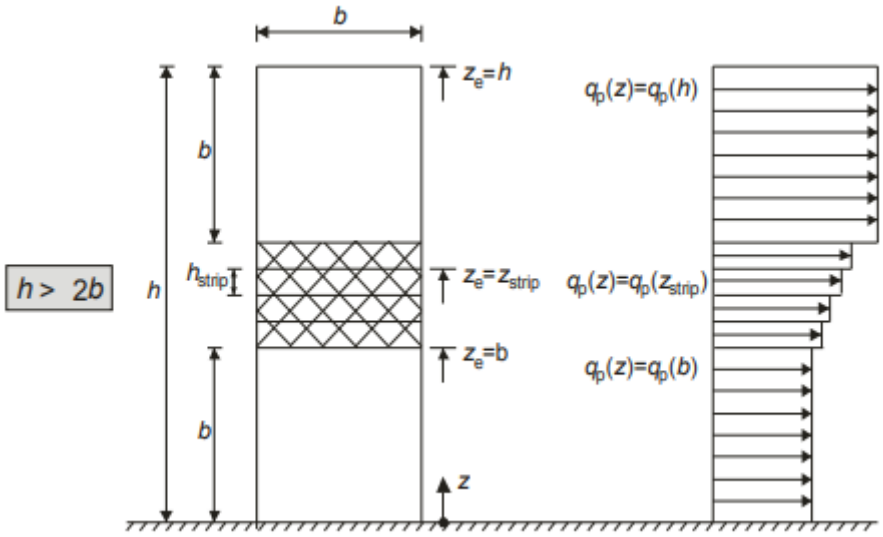

Figure 128 - Distribution of the wind force.

As shown in the figure above, two external thrusts must be calculated. One with the reference height equal to the width of the building $q_p(w_b)$ (In the figure $q_p(b)$), and one with the reference height equal to the height of the building $q_p(h_b)$ (In the figure $q_p(h)$). The calculation of the distributed forces can be divided into three parts. The two parts with constant distribution and the middle part with increasing distribution. These can be converted to line loads as follows:

$$q_1 = q_p(w_b) * w_b \tag{A-II.21}$$

$$q_2(h0 = q_p(w_b) + \frac{h - w_b}{h_b - 2 * w_b} * \left(q_p(h_b) - q_p(w_b)\right) * w_b \tag{A-II.22}$$

$$q_3 = q_p(h_b) * w_b \tag{A-II.23}$$

To converte these three representative forces the integral can be used:

$$F_1 = \int_0^{w_b} q_1 \, dh \tag{A-II.24}$$

$$F_2 = \int_{w_b}^{h_{b-}w_b} q_2 \, dh \tag{A-II.25}$$

$$F_3 = \int_{h_{b-}w_b}^{h_b} q_3 \, dh \tag{A-II.26}$$

The total wind force is the summation of these three representative forces:

$$F_{h,wind} = F_1 + F_2 + F_3 \tag{A-II.27}$$

For the horizontal windforce in the dynamic calculation, the windload is made into one function (q_{wind}) with the piecewise option. Then the forces on the point masses can ba calculated by taking the proper integral of this one function:

$$F_{point\ mass\ 1} = \int_{0}^{\frac{1}{2}L} q_{wind}\, dh \tag{A-II.28}$$

$$F_{point\ mass\ 2} = \int_{\frac{1}{2}L}^{\frac{3}{2}L} q_{wind}\, dh \tag{A-II.29}$$

$$F_{point\ mass\ 3} = \int_{\frac{3}{2}L}^{\frac{5}{2}L} q_{wind}\, dh \tag{A-II.30}$$

Where

L is the distance between the point masses.

WIND MOMENT

For the static stability calculation the moment can be calculated by multiplying the forces with the arm. Which is the centre of the force to the centre of gravity (COG). Note that the distance COG is used throughout this research as the distance from the bottom of the platform to the centre of gravity and thus the height of the platform needs to be added.

$$arm_1 = \frac{1}{2} * w_b + h_p - COG \tag{A-II.31}$$

$$arm_2 = w_b + \frac{2}{3} * (h_b - 2 * w_b) - COG \tag{A-II.32}$$

$$arm_3 = h_b - \frac{1}{2} * w_b + h_p - COG \tag{A-II.33}$$

The moment due to the wind can now be calculated with

$$M_{wind} = F_1 * arm_1 + F_2 * arm_2 + F_3 * arm_3 \tag{A-II.34}$$

For the dynamic stability this again a bit different. The function were the three functions for the wind are combined into one ($q_{wind}(t)$) is again used. Again the arm, which is the distance centre of the force and the bottom om the building, has to be multiplied with the area under de function. For the bottom mass the entire wind load has to be taken into account. For the middle mass only the upper 4/5 th and for the top point mass the upper 2/5 th. This results in the following formula's:

$$M_{wind,point\ mass\ 1} = \int_{0}^{hb} q_{wind}(t) * h\, dh \tag{A-II.35}$$

$$M_{wind,point\ mass\ 2} = \int_{L}^{hb} q_{wind}(t) * h\, dh \tag{A-II.36}$$

$$M_{wind,point\ mass\ 3} = \int_{2L}^{hb} q_{wind}(t) * h\ dh \tag{A-II.37}$$

These functions for the moment can then be simplified to:

$$M_{wind}(t) = \widehat{M}_{wind} * \sin(\omega_{wind} t)\ [N] \tag{A-II.38}$$

The expression for $\widehat{M}_{wind}$ is to extensive to be shown.

APPENDIX III - ASSUMPTIONS

BUILDING WIDTH

Because the building is modelled as a 1D element with only the "height" as dimension, either a constant value must be used for the dropped parameter "width of the building" or a relationship must be found between the height and the width of the building. Since in general the width of the building increases with height, a relationship is sought. To determine the width for a given height, three reference buildings were used; The Twin Towers of the World Trade Centre (New York), Zalmhaventoren (Rotterdam) and the New Orleans (Rotterdam). These are chosen as they have different heights and widths and a square cross-section. The dimensions of these buildings are given in the table below.

Table 35 - Building width and core sizes for three representative buildings. Sources: New World Encyclopedia. (2020). Smeets. (2012). Schaap & Hesselink. (2019).

Building	Height [m]	Building width [m]
World Trade Centre	416	63 x 63
Zalmhaventoren	215	38 x 38
New Orleans	150	30 x 30

Using curve fitting, a formula was created that expresses the width of the building in terms of its height. The formula is as follows:

$$Width_{building} = \frac{17}{3475290} * h_b^2 + \frac{421523}{3475290} * h_b + \frac{104225}{8911} \; [m] \qquad \text{(AIII.1)}$$

The following figure shows the relationship in a graph, together with the data points used.

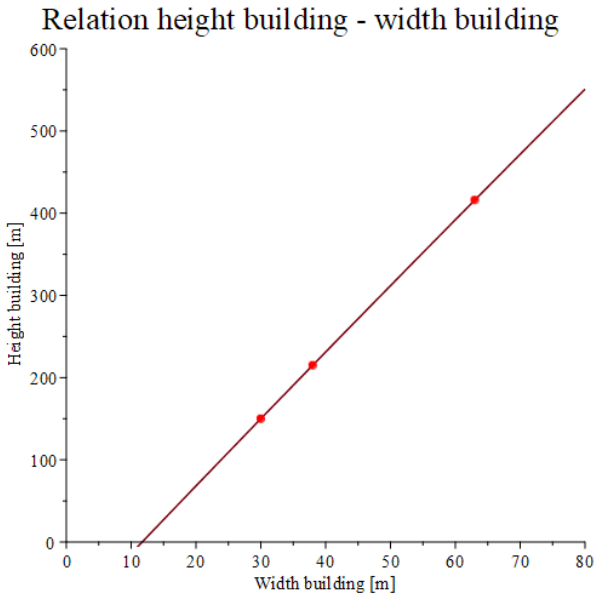

Figure 129 - Relation between the height of the building and the width of the building.

PLATFORM WIDTH AND MASS

In the model the platform is a 1D element. Different cross-sections can be used but none of these are close to how the platform will be in reality. Therefore the platform is modelled in 3D in a separate model in grasshopper. From this model the stiffness and the weight of the platform will be expressed in the parameters; width of the platform and height of the platform. These are than used in the main model. The platform will be made out of concrete with class C60/75 and consist of cubes of 5 x 5 x 5 m in a waffle shape. See figure Figure 131. The platform is than simply supported at both ends and loaded with a load of 100 kN/m^2. In Figure 130 a 2D representation is shown of the 3D loading.

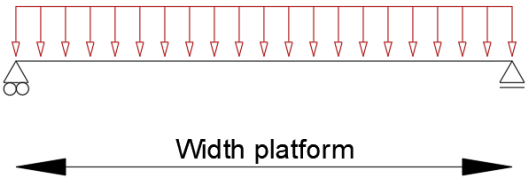

Figure 130 - 2D representation of the 3D model.

With the deformation of the platform, the second moment of inertia of the 3D model can be translated into a 1D element by using the forgetmenot of a simply supported beam: $u = \frac{5}{384} * \frac{q*L^2}{EI}$. The second moment of inertia is calculated for multiple platform heights and width. With these result, see Table 36, a relation is made between the sizes and the second moment of inertia. This is done by curve fitting. This gives the following relation:

$$I_{platform} = \left(0.01198 * h_p^3 - 0.05448 * h_p^2 + 1.1877 * h_p - 1.099\right) * w_p \; [m^4] \qquad \text{(AIII.2)}$$

Where

h_p is the height of the platform [m]

w_p is the width of the platform [m]

The same is done for the weight of the platform. This gives the following relation:

$$Weight_{platform} = \frac{h_p}{5} * \left(\frac{w_p^3}{6000} + 2.45 * w_p^2 + 43\frac{1}{3} * w_p - 2000\right) \; [kN] \qquad \text{(AIII.3)}$$

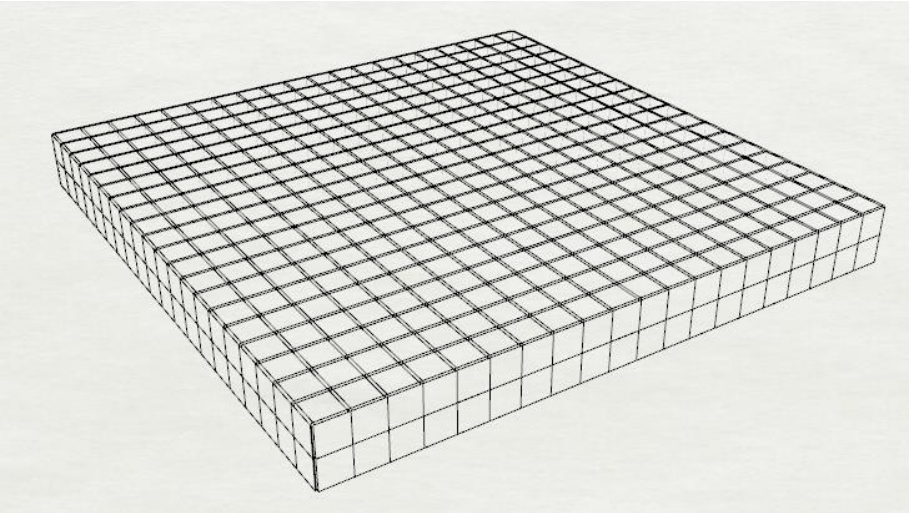

Figure 131 – 3D presentation of the platform.

Table 36 - Results from the grasshopper model for the second moment of inertia and weight of the platform for different platform widths and height.

Width platform [m]	Height platform [m]	Second moment of inertia [m⁴]	Weight [kN]
100	5	497.20	27035
200	5	994.82	105640
300	5	1487.32	235820
400	5	1972.33	417560
100	10	1688.16	54070
200	10	3420.08	211280
100	15	4164.44	81105
200	15	8656.62	316920
100	20	8301.23	108140
200	20	17978.9	422560

REFERENCES

New World Encyclopedia. (2020). *World Trade Center.* Retrieved 10:04, April 2, 2021 from https://www.newworldencyclopedia.org/p/index.php?title=World_Trade_Center&oldid=1043685.

Smeets, H. (2012). *De hoogste woontoren van Nederland: Wonen in pure elegantie*. Retrieved April 02, 2021, from https://www.rotterdamarchitectuurprijs.nl/prijs-2021

Schaap, F., & Hesselink, J. (2019). *Zalmhaven: Hoogste woontoren Van de Benelux.* Retrieved April 02, 2021, from https://www.cementonline.nl/zalmhaven-hoogste-woontoren-van-de-benelux

APPENDIX IV – RESULTS OF THE STATIC STABILITY

MINIMUM PLATFORM WIDTH

Excel was used to determine the minimum width of the platform. In Excel, the GM values and all values needed to calculate GM are calculated for platform widths between 50m and 500m for a building of a certain height. The required platform width is the platform width for which the GM is positive and the lowest. This platform width is the output of the calculation. As input the height can be chosen. For the total relationship, heights between 100 m and 800 m with steps of 25 m are chosen.

Below are the results for a building 100 m high and platform widths from 50 m to 67 m. This is only a small part of the whole and serves as an example. The red row is the row of the minimum platform width, in this case 59 m.

Height building [m]	Width buildng [m]	Mass building [kg]	Weight building [kN]	Width platform [m]	Heigt platform [m]	Mass platform [kg]	Weight platform [kN]
100	23.87	1.89E+07	1.86E+05	50	5	6.43E+05	6.31E+03
100	23.87	1.89E+07	1.86E+05	51	5	6.90E+05	6.77E+03
100	23.87	1.89E+07	1.86E+05	52	5	7.38E+05	7.24E+03
100	23.87	1.89E+07	1.86E+05	53	5	7.88E+05	7.73E+03
100	23.87	1.89E+07	1.86E+05	54	5	8.40E+05	8.24E+03
100	23.87	1.89E+07	1.86E+05	55	6	8.95E+05	8.78E+03
100	23.87	1.89E+07	1.86E+05	56	6	9.51E+05	9.33E+03
100	23.87	1.89E+07	1.86E+05	57	6	1.01E+06	9.91E+03
100	23.87	1.89E+07	1.86E+05	58	6	1.07E+06	1.05E+04
100	23.87	1.89E+07	1.86E+05	59	6	1.13E+06	1.11E+04
100	23.87	1.89E+07	1.86E+05	60	6	1.20E+06	1.18E+04
100	23.87	1.89E+07	1.86E+05	61	6	1.27E+06	1.24E+04
100	23.87	1.89E+07	1.86E+05	62	6	1.34E+06	1.31E+04
100	23.87	1.89E+07	1.86E+05	63	7	1.41E+06	1.38E+04
100	23.87	1.89E+07	1.86E+05	64	7	1.48E+06	1.46E+04
100	23.87	1.89E+07	1.86E+05	65	7	1.56E+06	1.53E+04
100	23.87	1.89E+07	1.86E+05	66	7	1.64E+06	1.61E+04
100	23.87	1.89E+07	1.86E+05	67	7	1.72E+06	1.69E+04

Depth platform [m]	Extra ballast	Total mass [kg]	Total weight [kN]	COG	BM	GM
7.64	0.00E+00	1.96E+07	1.92E+05	53.28	27.26	-22.2
7.36	0.00E+00	1.96E+07	1.93E+05	53.28	29.44	-20.2
7.10	0.00E+00	1.97E+07	1.93E+05	53.27	31.74	-18.0
6.85	0.00E+00	1.97E+07	1.94E+05	53.26	34.16	-15.7
6.62	0.00E+00	1.98E+07	1.94E+05	53.25	36.72	-13.2
6.40	0.00E+00	1.98E+07	1.95E+05	53.23	39.40	-10.6
6.19	0.00E+00	1.99E+07	1.95E+05	53.20	42.23	-7.9
5.99	0.00E+00	2.00E+07	1.96E+05	53.18	45.19	-5.0
5.80	0.00E+00	2.00E+07	1.96E+05	53.14	48.30	-1.9
5.63	0.00E+00	2.01E+07	1.97E+05	53.10	51.56	1.3
5.46	0.00E+00	2.01E+07	1.98E+05	53.06	54.96	4.6
5.30	0.00E+00	2.02E+07	1.98E+05	53.01	58.52	8.2
5.15	0.00E+00	2.03E+07	1.99E+05	52.96	62.24	11.9
5.00	0.00E+00	2.04E+07	2.00E+05	52.90	66.12	15.7
4.87	0.00E+00	2.04E+07	2.00E+05	52.83	70.16	19.8
4.73	0.00E+00	2.05E+07	2.01E+05	52.76	74.36	24.0
4.61	0.00E+00	2.06E+07	2.02E+05	52.69	78.74	28.4
4.49	0.00E+00	2.07E+07	2.03E+05	52.61	83.29	32.9

Figure 132 - Minimum platform width calculations for a building of 100m and platform width from 50m to 67 m.

The result of the minimum platform calculation is shown in the following figure:

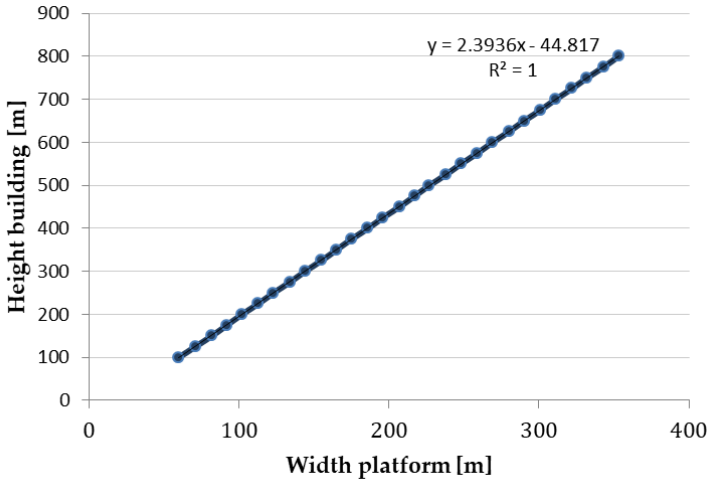

Figure 133 - Width of the platform need with the height of the building for stability.

Since it is very remarkable that a linear function comes out of it, the same calculations were done using the program Maple. Maple was not used before because calculating one equation (GM = 0) with two unknowns (height building and platform width) was not possible. What is possible with Maple is to make the formula in which the GM value depends entirely on the height of the building and the width of the platform:

$$GM = 1025 * \frac{wp^4}{12 * \left(20.38735984 * \left(\frac{11 * wp}{90} - \frac{10}{9}\right) * \left(\frac{1}{6000} * wp^3 + 2.45 * wp^2 + 43.33 * wp - 2000\right) + 1329.255861 * ceil\left(\frac{hb}{4}\right) * (4.891678105 * 10^{-6} * hb^2 + 0.1212914606 * hb + 11.69621816)^2\right)} + 0.0004878048780 * \frac{20.38735984 * \left(\frac{11 * wp}{90} - \frac{10}{9}\right) * \left(\frac{1}{6000} * wp^3 + 2.45 * wp^2 + 43.33 * wp - 2000\right) + 1329.255861 * ceil\left(\frac{hb}{4}\right) * (4.891678105 * 10^{-6} * hb^2 + 0.1212914606 * hb + 11.69621816)^2}{wp^2} - \frac{10.19367992 * \left(\frac{11 * wp}{90} - \frac{10}{9}\right)^2 * \left(\frac{1}{6000} * wp^3 + 2.45 * wp^2 + 43.33 * wp - 2000\right) + 1329.255861 * ceil\left(\frac{hb}{4}\right) * (4.891678105 * 10^{-6} * hb^2 + 0.1212914606 * hb + 11.69621816)^2 * \left(\frac{11 * wp}{90} - \frac{10}{9} + \frac{hb}{2}\right)}{20.38735984 * \left(\frac{11 * wp}{90} - \frac{10}{9}\right) * \left(\frac{1}{6000} * wp^3 + 2.45 * wp^2 + 43.33 * wp - 2000\right) + 1329.255861 * ceil\left(\frac{hb}{4}\right) * (4.891678105 * 10^{-6} * hb^2 + 0.1212914606 * hb + 11.69621816)^2} \quad \text{(AIV.1)}$$

As can be seen, there seems to be no linear relationship between the height of the building and the width of the platform. A 3D plot of this function is made, which is shown in the figure below. In the plot a clear linear intersection line can be seen between the GM value plane [coloured] and the zero plane (black).

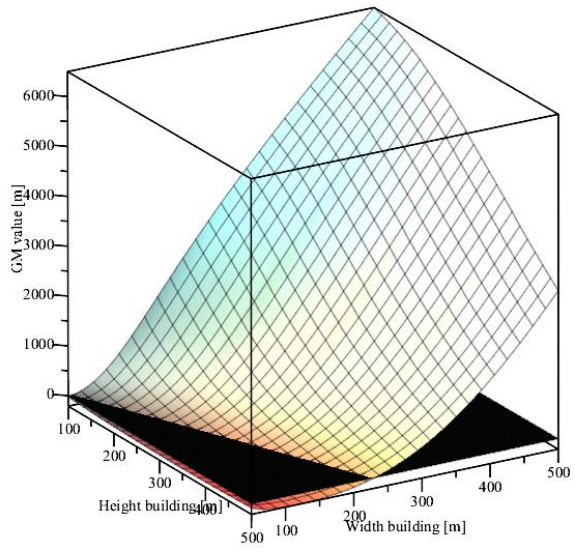

Figure 134 - 3D plot of the GM value with the height of the building and the width of the platform as variables.

MINIMUM PLATFORM HEIGHT AND DEPTH AND OTHER RESULTING VALUES

The research into the minimum height and depth of the platform has yielded the most results. It also gives a broad result and not only a result for optimal dimensions. These results can therefore be used well together with the results of the dynamic calculations. In this appendix, the results of the minimum platform height and depth are shown in the form of graphs. Because these depths and heights of the platform are the minimum values, results of a number of other parameters from the model were also obtained for these values. These are also shown. These are:

- Angle of rotation
- 2nd order moment
- Wind moment
- Deflection at the top of the building
- Ration between the model and the GM method
- Change in the angle at the fifth iteration of the model

The angle of rotation is determined with the model for the centre of the platform and is determined after the last iteration. It is possible that the angle of rotation is different on other parts of the platform. The second order moment is also taken from the model. The displacement of the top of the building is also taken from the model. This cannot be determined simply by the rotation of the platform, because the building is also flexible. The ratio between the model and the GM method is the ratio between the calculated angular rotation of the two methods. This ratio can indicate when the GM method is useful or when it underestimates or overestimates the rotation. Finally, the change in the angle after the 5th iteration. This is the percentage of the difference in the angle of the 4th and 5th iteration. This expresses how big the change still is and shows whether the model has reached an equilibrium or whether more iterations are actually needed.

All graphs have the same layout, they depend on both the platform width and the building height. The results different building height are plotted together. The horizontal axis shows the platform width and the vertical axis the parameter under investigation. The title of the graph indicates the parameter and the location. The graphs are subdivided by location and can be seen on the next page.

NORTH SEA

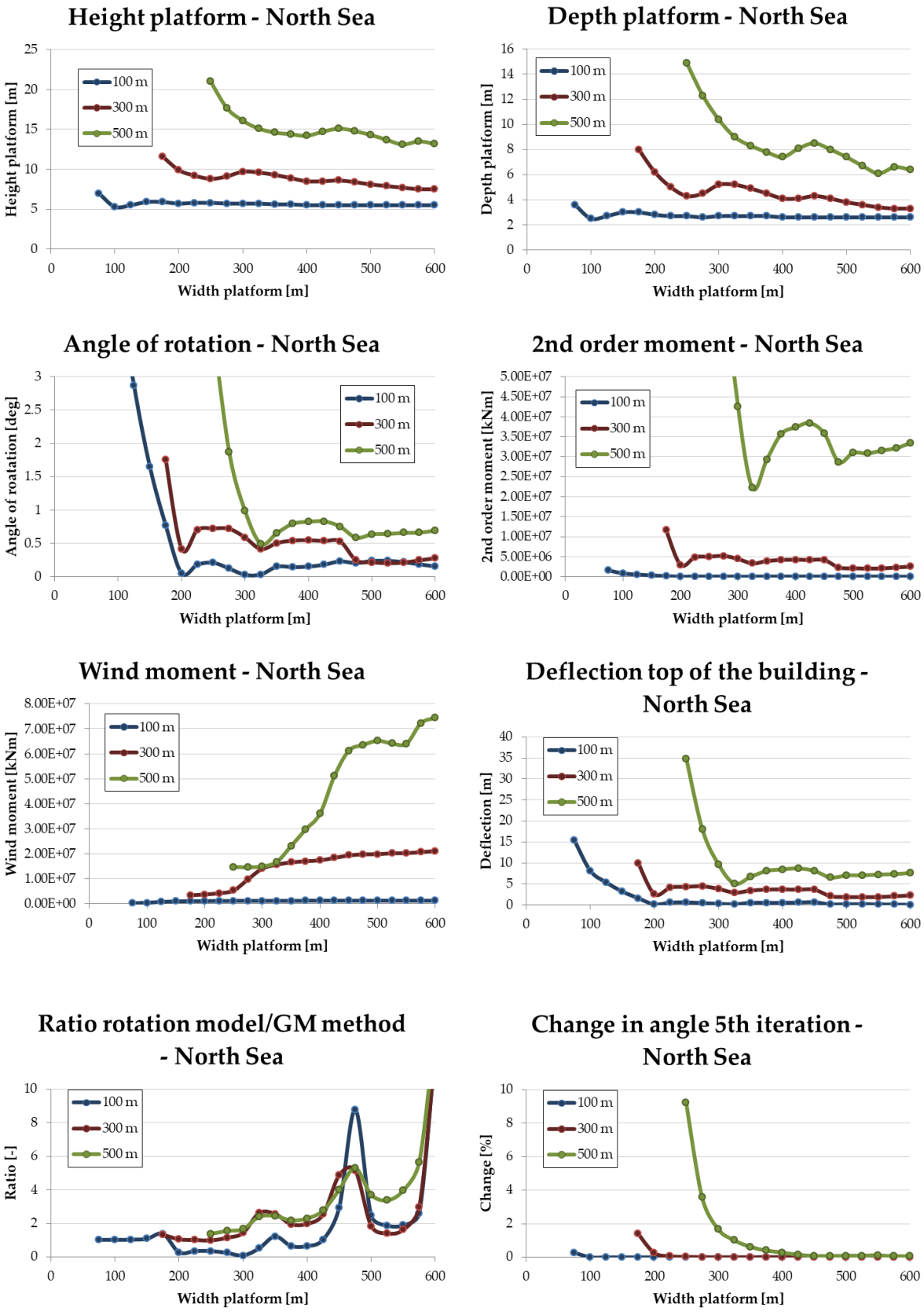

Figure 135 - Results of the analysis of the static stability for the North Sea.

ATLANTIC OCEAN

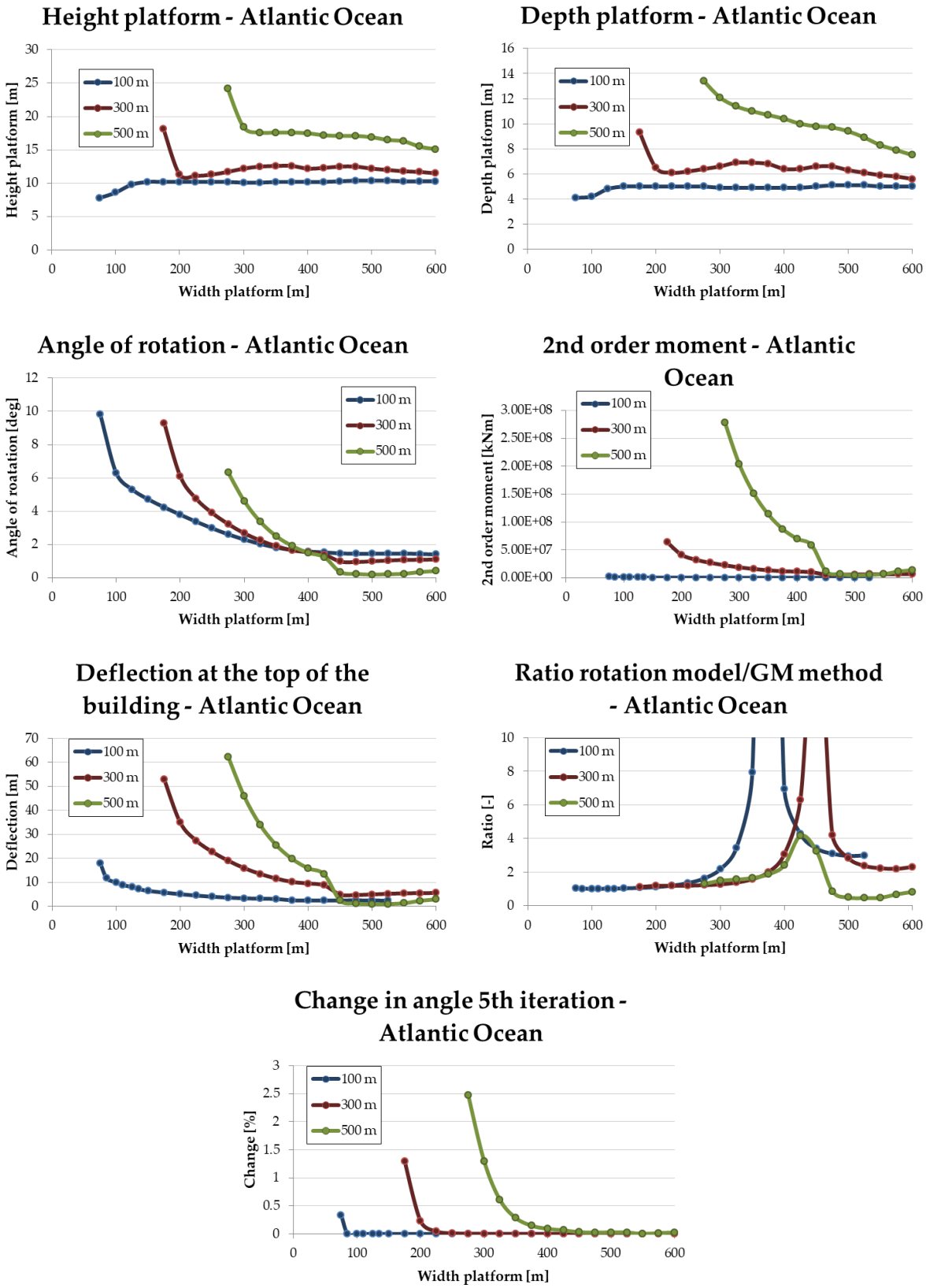

Figure 136 - Results of the analysis of the static stability for the Atlantic Ocean.

EQUATOR

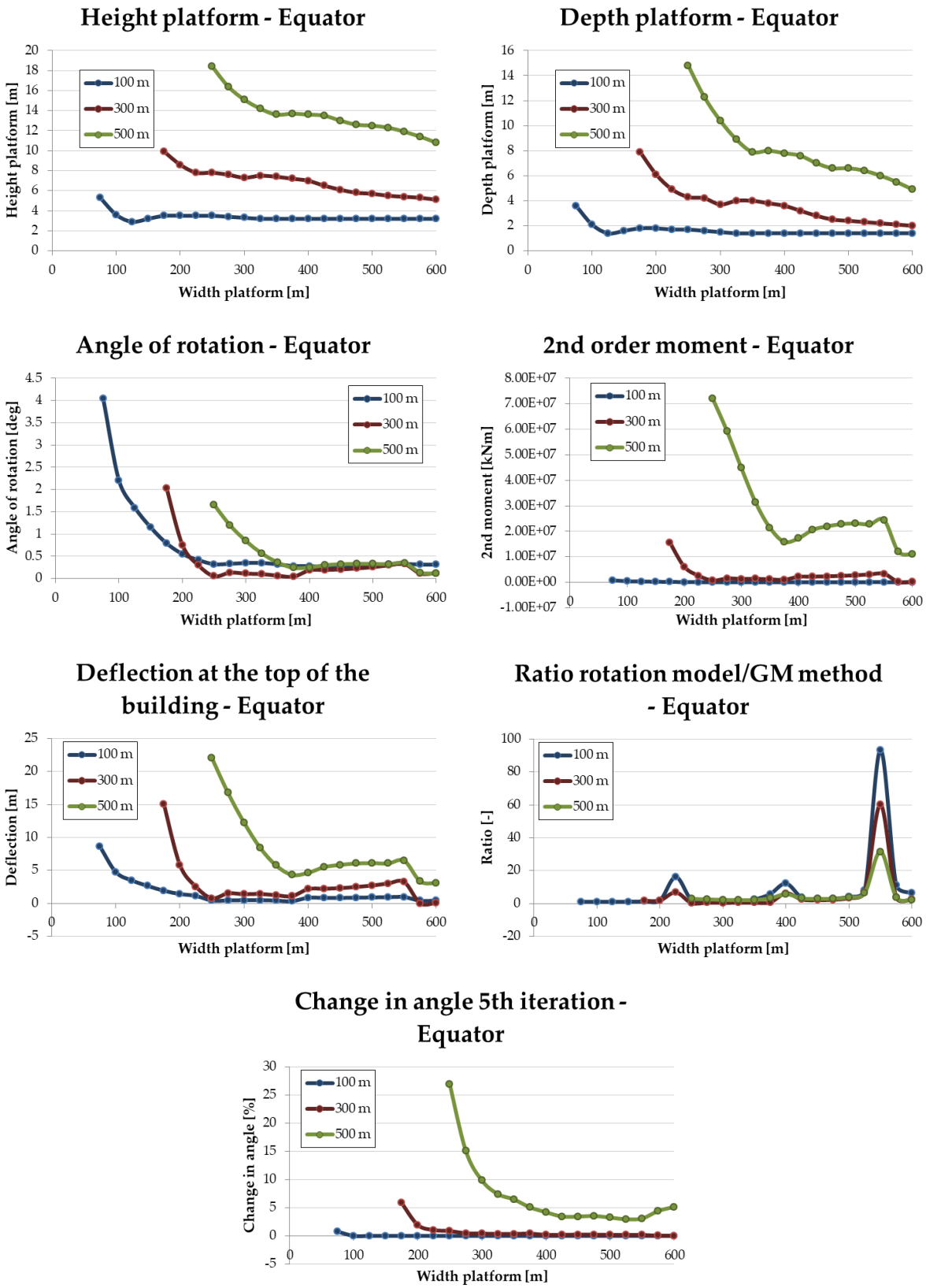

Figure 137 - Results of the analysis of the static stability for the Equator.

APPENDIX V – ZERO MOMENT WIDTHS

In many results, the optimum platform width is the one that has the least amount of moment due to the wave, in this research called the "zero moment widths". This is because the moment due to the wave does not increase with increasing platform width but it has a diverging sine shape, see Figure 138. The formula for the moment, (determined in Appendix II) depends on two variables, the time and the width of the platform. The graph shows that at time t = 2s there are several platform widths for which the total moment due to the waves is equal to 0 kNm. For the static stability, however, t = 2s is not used but a calculation is made for the most "negative" time. This is the time for which the wave moment is maximum.

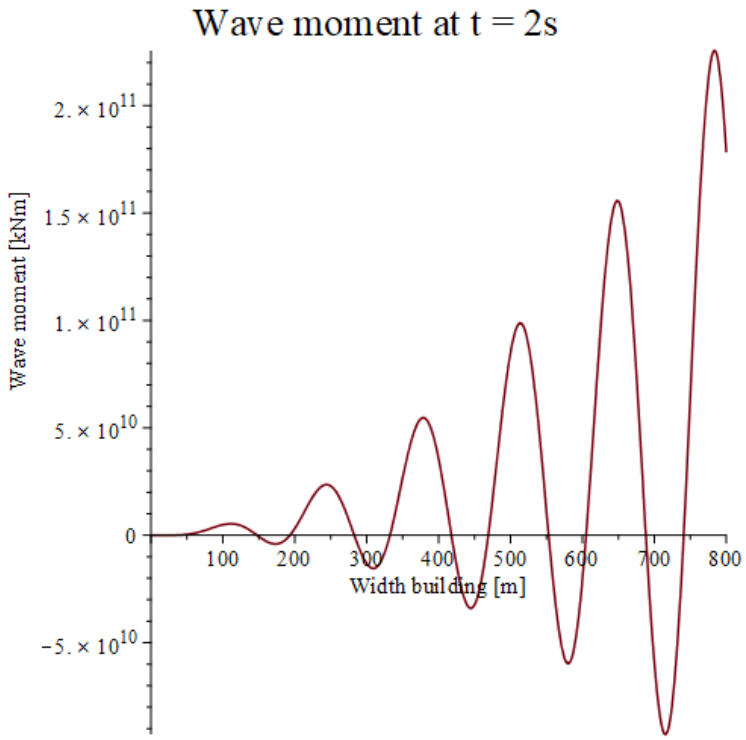

Figure 138 - Wave moment at t = 2s for different platform widths for the location North Sea.

To investigate whether there is a platform width that, regardless of time, always results in a wave moment of 0 kNm, a 3D graph was made of the moment due to the wave with time and platform width as variables. This is shown in Figure 139. The figure also shows the plane where the moment is equal to 0 (the black plane). The graph shows that there are certain widths of platform for which the maximum moment is zero. This can be seen better in Figure 140. These are the red and blue lines. Looking at t=2s in this 3D graph, the graph of Figure 138 can be recognised. However, there is a difference between the red and blue lines.

On the blue lines, the moment is equal to zero but, as mentioned, the time with the highest moment is used for a specific platform width. That moment is not on the blue lines. (for example a platform width of 150 m has zero moment at t = 2 s but it has a substantial moment at t = 0 s. Which will be normtive) When determining the zero moment widths, the results from the blue lines should not be used.

The red lines in the 3D graph, unlike the blue lines, are constant over time. For these platform widths, the moment due to the wave is, for all possible times, equal to zero. And so the moment

at the most negative time is also equal to zero. So these widths are the zero moment widths. To find these zero moment widths, a combination of Figure 138 and Figure 140 is used. The 3D graph shows that when in Figure 138 the moment goes from positive to negative, it is a blue line. And when the moment goes from negative to positive, it is the wanted red line. This is how the zero moment widths can be determined. These are determined for the three locations and can be seen in Table 37.

Please note that the zero moment widths are dependent on the wavelength. The wavelength in turn depends on the wave period/wave frequency. When working at a location with a different wave period than the peak period, the zero moment widths will be different.

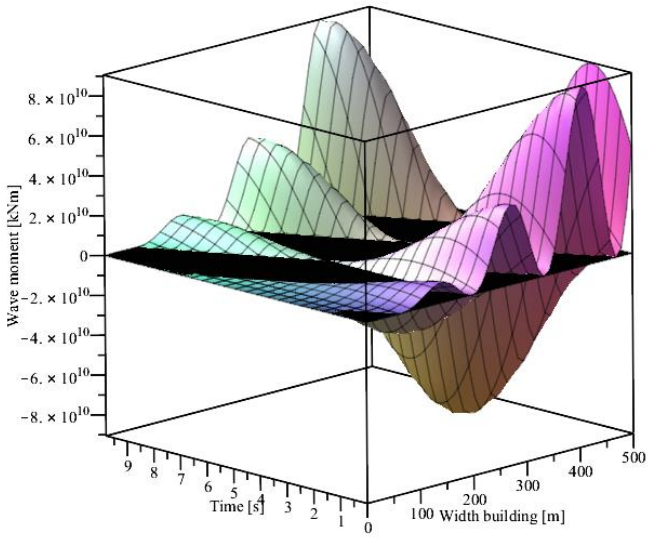

Figure 139 - 3D plot of the wave moment for different platform widths and times for the location of the North Sea. The black surface is equal to zero moment

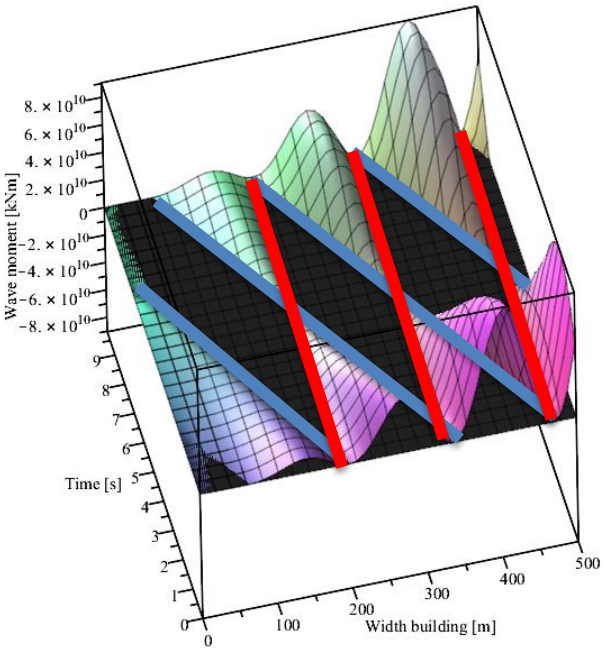

Figure 140 - 3D plot of the wave moment for different platform widths and times for the location of the North Sea. The black surface is equal to zero moment. The red lines are the zero moment width lines and the blue lines indicate the other set of values for which the moment is zero.

Table 37 - Zero moment widths up to 800 m for the three locations.

Location	Zero moment widths [m]				
North Sea	190.6	327.6	462.4	596.5	730.3
Atlantic Ocean	371.6	677.6			
Equator	223.3	383.9	541.9	699.1	

APPENDIX VI - BEAM STIFFNESS MATRIX

This appendix shows how the beam stiffness matrix was determined. Each row consists of stiffness's that link the motions to a force. To determine this, one degree of freedom (DOF) is given a displacement or rotation of 1. It is determined what is needed to achieve this displacement or rotation and what is needed to keep the remaining DOF at zero. This is done for each DOF. This results in the following matrix for the model with three masses and nine DOFs

$$K\_beam := \begin{bmatrix} \frac{EA}{L} & -\frac{EA}{L} & 0 & 0 & 0 & 0 & 0 & 0 & 0 \\ -\frac{EA}{L} & \frac{2 \cdot EA}{L} & -\frac{EA}{L} & 0 & 0 & 0 & 0 & 0 & 0 \\ 0 & -\frac{EA}{L} & \frac{EA}{L} & 0 & 0 & 0 & 0 & 0 & 0 \\ 0 & 0 & 0 & \frac{12\,EI}{L^3} & -\frac{12\,EI}{L^3} & 0 & \frac{6\,EI}{L^2} & \frac{6\,EI}{L^2} & 0 \\ 0 & 0 & 0 & -\frac{12\,EI}{L^3} & \frac{24\,EI}{L^3} & -\frac{12\,EI}{L^3} & -\frac{6\,EI}{L^2} & 0 & \frac{6\,EI}{L^2} \\ 0 & 0 & 0 & 0 & -\frac{12\,EI}{L^3} & \frac{12\,EI}{L^3} & 0 & -\frac{6\,EI}{L^2} & -\frac{6\,EI}{L^2} \\ 0 & 0 & 0 & \frac{6\,EI}{L^2} & -\frac{6\,EI}{L^2} & 0 & \frac{4\,EI}{L} & \frac{2\,EI}{L} & 0 \\ 0 & 0 & 0 & \frac{6\,EI}{L^2} & 0 & -\frac{6\,EI}{L^2} & \frac{2\,EI}{L} & \frac{2 \cdot 4 \cdot EI}{L} & \frac{2\,EI}{L} \\ 0 & 0 & 0 & 0 & \frac{6\,EI}{L^2} & -\frac{6\,EI}{L^2} & 0 & \frac{2\,EI}{L} & \frac{4\,EI}{L} \end{bmatrix} :$$

The determination can be seen in the drawings below:

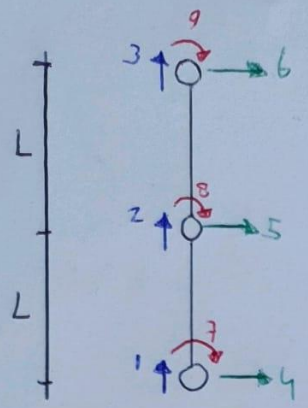

W_1 - 1
W_2 - 2
W_3 - 3
u_1 - 4
u_2 - 5
u_3 - 6
θ_1 - 7
θ_2 - 8
θ_3 - 9

1

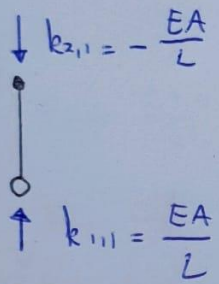

2

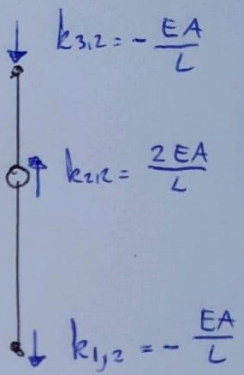

3

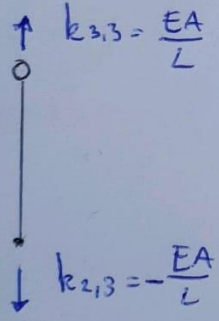

4

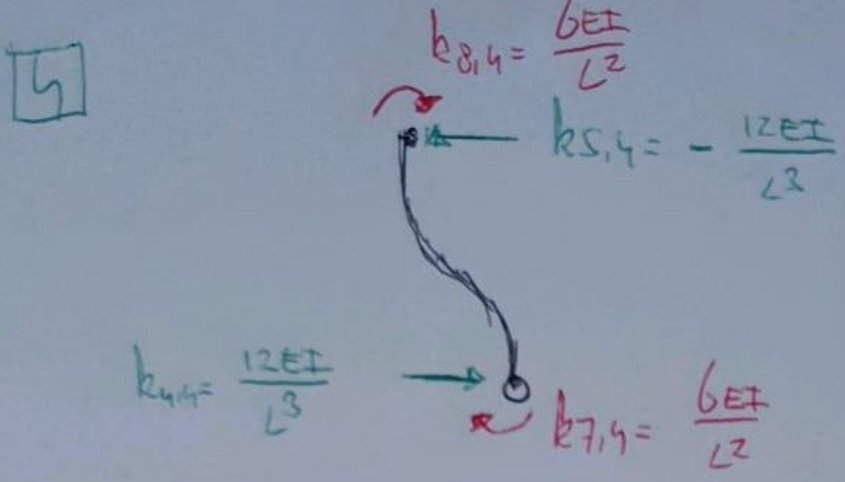
$k_{8,4} = \frac{6EI}{L^2}$
$k_{5,4} = -\frac{12EI}{L^3}$
$k_{4,4} = \frac{12EI}{L^3}$
$k_{7,4} = \frac{6EI}{L^2}$

5

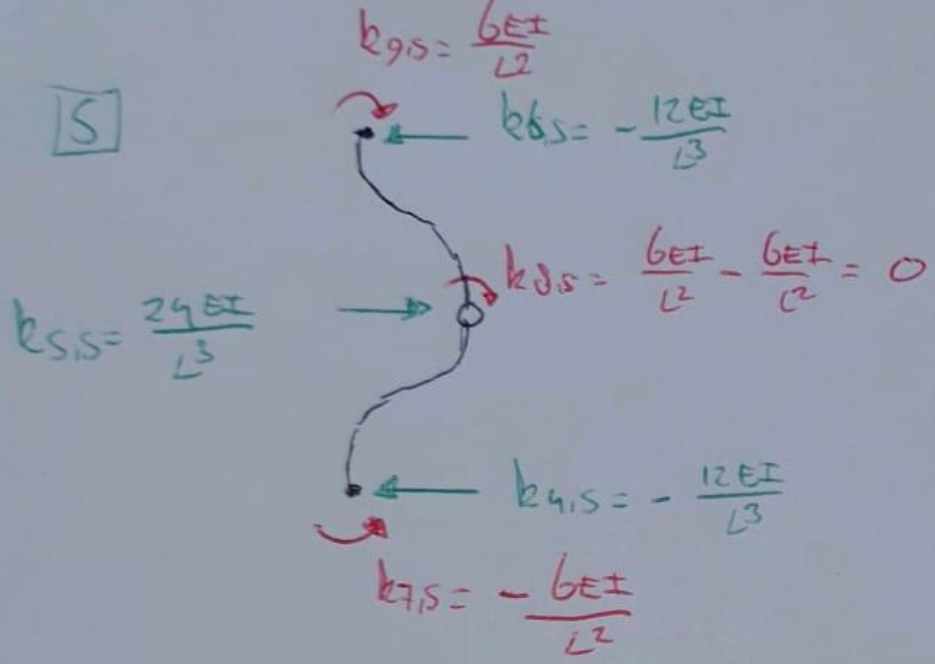
$k_{9,5} = \frac{6EI}{L^2}$
$k_{6,5} = -\frac{12EI}{L^3}$
$k_{3,5} = \frac{6EI}{L^2} - \frac{6EI}{L^2} = 0$
$k_{5,5} = \frac{24EI}{L^3}$
$k_{4,5} = -\frac{12EI}{L^3}$
$k_{7,5} = -\frac{6EI}{L^2}$

6

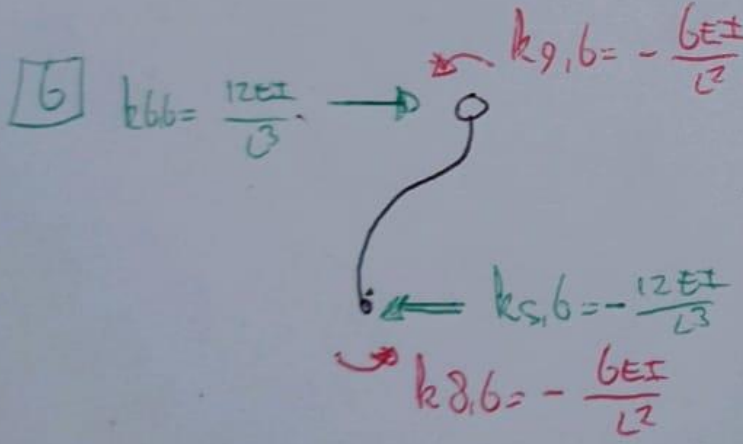
$k_{9,6} = -\frac{6EI}{L^2}$
$k_{6,6} = \frac{12EI}{L^3}$
$k_{5,6} = -\frac{12EI}{L^3}$
$k_{8,6} = -\frac{6EI}{L^2}$

7

$k_{8,7} = \frac{2EI}{L}$

$k_{5,7} = -\frac{6EI}{L^2}$

$k_{4,7} = \frac{6EI}{L^2}$

$k_{7,7} = \frac{4EI}{L}$

8

$k_{9,8} = \frac{2EI}{L}$

$k_{6,8} = -\frac{6EI}{L^2}$

$k_{8,8} = \frac{8EI}{L^2}$

$k_{5,8} = \frac{6EI}{L^2} - \frac{6EI}{L^2} = 0$

$k_{5,8} = \frac{6EI}{L^2}$

$k_{7,8} = \frac{2EI}{L^2}$

9

$k_{9,9} = \frac{4EI}{L^2}$

$k_{7,9} = \frac{-6EI}{L^2}$

$k_{6,9} = \frac{6EI}{L^2}$

$k_{8,9} = \frac{2EI}{L^2}$

APPENDIX VII – MULTIPLE MASS MODEL HAND CALCULATIONS

This appendix shows the calculations made in the program maple. These calculations are used in different parts of chapter 6. The first paragraph shows how the input values were named and shows the calculations of the dependent parameters as determined in chapter 3. The second paragraph shows how the matrices are defined together with the values of these as is determined in chapter 6. Paragraph 3 shown the calculation of the eigenfrequencies. Then paragraph 4 shows the calculation of the forces as explained in chapter 2 and Appendix II. Then in paragraph 5 the calculation for the particular solution is shown together with the calculations of the maximum accelerations. This Appendix ends with the calculation of the acceleration at the top of the building.

INPUT VALUES

This paragraph shows how the input values are named and shows the calculations of the dependent parameters as determined in chapter 3. There are two options: one option where the depth and height of the platform follows from the regulations and one option where the depth and height of the platform are used as input parameters.

> restart :

Complete dependend parameters

Input values

This first part gives the undependend parameters a value. The name is writen after the value. The red values are changed during the study to investigate different options.

Input values

> $n := 3$: #number of masses

> $g := 9.81$:

Changing parameters

> $wp := 100$: #Width platform [m]

> $hb := 100$: #Height building [m]

> $E := \frac{1}{3} \cdot 3.9 \cdot 10^{10}$:#$\left[\frac{N}{m^2}\right]$ Youngs modules concrete

> $tc := 0.6$:#Thikness core [m]

Wave properties

> $Hw := 9.975 \cdot 0.5$:#Height wave [m]

> rho $:= 1025$: #Density water [kg\m3]

> $Twave := 9.8$:# Wave period [s]

> $\omega wave := \frac{2 \cdot \pi}{Twave}$;# wave frequency [rad\s]

$$\omega wave := 0.6411413578 \quad (1)$$

> $depth := 30$: #depth of the water (distance from sea bottom to the surface of the water} [m]

The calculation of the wave length is an itterative process.

> $Lwave[0] := evalf\left(\frac{g \cdot Twave^2}{2 \cdot \pi}\right)$:**for** i **from** 1 **to** 10 **do** $Lwave[i] := evalf\left(\frac{g \cdot Twave^2}{2 \cdot \pi}\right) \cdot \tanh\left(\frac{2 \cdot \pi \cdot depth}{Lwave[i-1]}\right)$; **end do**: $Lwave := Lwave[10]$# wave length [m]

$$Lwave := 133.2308782 \quad (2)$$

Wind properties

> $Twind := Twave$:# Wind period [s]

> $\omega wind := \frac{2 \cdot \pi}{Twind + 0.0001}$;# Wind frequency [rad\s]

$$\omega wind := 0.6411348158 \quad (3)$$

> $vb := 50$:# Wind speed at refference height [m\s]

Damping properties

> zeta := 0.1 : #Damping ratio

>

The calculation of other used values

In this section the dependend parameters are expressed in either the building height or the platform width, other input values and/or eachother.

>

Building

> $n\_stories := \mathrm{ceil}\left(\frac{hb}{4}\right)$:#Number of stories

> $wb := evalf\left(\frac{17}{3475290}\cdot hb^2 + \frac{421523}{3475290}\cdot hb + \frac{104225}{8911}\right)$;# Width of the building [m]

$$wb := 23.87428100 \quad (4)$$

> $wc := 0.2690207148\cdot 10^{-3}\cdot hb^2 - 0.06626948398\cdot hb + 15.01245651$;# Width of the core [m]

$$wc := 11.07571526 \quad (5)$$

> $L := \frac{hb}{n - 0.5}$;#Length between the masses [m]

$$L := 40.00000000 \quad (6)$$

> $A\_core := wc^2 - (wc - tc)^2$; #Cross sectional area core [m2]

$$A\_core := 12.9308583 \quad (7)$$

> $EA := E\cdot A\_core$:
#Values for the tower, Note that the EI and EA of the building do not have a subscript

> $EI := evalf\left(0.7132958138\ vb^2\ wb\ hb^3\ \left(148.8202864 + 18.61828598\ \ln(hb) + \ln(hb)^2 + 18.61828598\ \ln(wb) + \ln(wb)^2\right)\right)$:

> $mass\_building := \frac{n\_stories\cdot wb^2\cdot 13.04\cdot 10^3}{9.81}$ #mass of the building [kg]

$$mass\_building := 1.894127437\ 10^7 \quad (8)$$

>

Platform

> $EI\_platform := E\cdot\left(0.01198\cdot hp^3 - 0.05448\cdot hp^2 + 1.1877\cdot hp - 1.099\right)\cdot wp$
#Stiffness of the platform

$$EI\_platform := 1.557400000\ 10^{10}\ hp^3 - 7.082400000\ 10^{10}\ hp^2 + 1.544010000\ 10^{12}\ hp - 1.428700000\ 10^{12} \quad (9)$$

This section is about the height and depth of the platform. The depth of the platform must be large enough so that the trough of the wave is not lower than the platform. When this happens there is a "chasm" next to the platform and the platform will rotate much more. The height of the platform should be such that the top of the platform should be 0.3 m higher than the height of the crest of the wave (regulation)

An additional ballast can be used to comply with the regulations. Equations 1 and 2 show the requirements and equation 3 ensures that only ballast can be added. Next, the relations between the height of the platform and the depth are used. Then the 3 values are solved. If there is no answer, no ballast is needed to reach the minimum depth. In that case only equation two needs to be used.

> $eq1 := d = \frac{1}{2}\cdot Hw$:

> $eq2 := hp = d + \frac{1}{2}\cdot Hw + 0.3$:

> $eq3 := extra\_ballast > 0$:

> $mass\_platform := \frac{hp}{5}\cdot\frac{\left(\frac{wp^3}{6000} + 2.45\cdot wp^2 + 43.33\cdot wp - 2000\right)\cdot 10^3}{9.81}$: # Mass platform [m]

> $d := \frac{mass\_platform + mass\_building + extra\_ballast}{wp^2\cdot \mathrm{rho}}$:# Depth platform

>

> $sol := solve(\{eq1, eq2, eq3\}, \{hp, extra\_ballast\}); assign(sol)$

$$sol := \{hp = 5.287500000,\ extra\_ballast = 3.709148601\ 10^6\} \quad (10)$$

> **if** $hp = 'hp'$ **then** $extra\_ballast := 0$ **end if**:

> **if** $hp = 'hp'$ **then** $d := \frac{mass\_platform + mass\_building}{wp^2\cdot \mathrm{rho}}$ **end if**:

> **if** $hp = 'hp'$ **then** $sol := solve(\{eq2\}, \{hp\}); assign(sol)$ **end if**

> d;# Depth platform

$$2.493750000 \quad (11)$$

> $total\_mass := mass\_building + mass\_platform + extra\_ballast$: #Total mass [kg]

>

> $COG := \frac{(mass\_platform + extra\_ballast)\cdot\frac{1}{2}\cdot hp + mass\_building\cdot\left(hp + \frac{1}{2}\cdot hb\right)}{mass\_platform + extra\_ballast + mass\_building}$;
Centre of gravity from the bottom of the platform [m]

$$COG := 41.65404501 \quad (12)$$

> $GM := \frac{\left(\frac{1}{12}\cdot wp^4\right)}{wp^2\cdot d} + \frac{1}{2}\cdot d - COG$ # GM value [m]

$$GM := 293.7615852 \quad (13)$$

> $r := COG - d$:#COG from the bottom

>

>

>

>

> restart :

Not complete dependend parameters (depth and height platform are independend)

>

Input values

This first part gives the undependend parameters a value. The name is writen after the value. The red values are changed during the study to investigate different options.

>

Input values

> $n := 3$: #number of masses

> $g := 9.81$:

Changing parameters

> $wp := 100$: #Width platform

> $hb := 100$: #Height building

> $d := 10$: #Depth platform

> $hp := 15$: #Height platform

>

> $E := \frac{1}{3} \cdot 3.9 \cdot 10^{10}$:#$\left[\frac{N}{m^2}\right]$ Youngs modules concrete

> $tc := 0.6$:#Thikness core

>

Wave properties

> $Hw := 9.975 \cdot 0.5$:#Height wave

> rho $:= 1025$: #Density water

> $Twave := 9.8$:# Wave period

> $\omega wave := \frac{2 \cdot \pi}{Twave}$;

$$\omega wave := 0.6411413578 \quad \textbf{(14)}$$

> $depth := 30$: #depth of the water (distance from sea bottom to the surface of the water)

>

The calculation of the wave length is an itterative process.

> $Lwave[0] := evalf\left(\frac{g \cdot Twave^2}{2 \cdot \pi}\right)$:**for** i **from** 1 **to** 10 **do** $Lwave[i] := evalf\left(\frac{g \cdot Twave^2}{2 \cdot \pi}\right)$

$\cdot \tanh\left(\frac{2 \cdot \pi \cdot depth}{Lwave[i-1]}\right)$; **end do**: $Lwave := Lwave[10]$# wave length [m]

$$Lwave := 133.2308782 \quad \textbf{(15)}$$

Wind properties

> $Twind := Twave$:# Wind period

> $\omega wind := \frac{2 \cdot \pi}{Twind + 0.0001}$;# Wind frequency [rad\s]

$$\omega wind := 0.6411348158 \quad \textbf{(16)}$$

> $vb := 50$:# Wind speed at refference height [m\s]

Damping properties

> zeta $:= 0.1$: #Damping ratio

>

The calculation of other used values

In this section the dependend parameters are expressed in either the building height or the platform width, other input values and/or eachother.

>

Building

> $n\_stories := \text{ceil}\left(\frac{hb}{4}\right)$:#Number of stories

> $wb := evalf\left(\frac{17}{3475290}\cdot hb^2 + \frac{421523}{3475290}\cdot hb + \frac{104225}{8911}\right)$;# Width of the building [m]

$$wb := 23.87428100 \quad (17)$$

> $wc := 0.2690207148\cdot 10^{-3}\cdot hb^2 - 0.06626948398\cdot hb + 15.01245651$;# Width of the core [m]

$$wc := 11.07571526 \quad (18)$$

> $L := \frac{hb}{n-0.5}$;#Length between the masses [m]

$$L := 40.00000000 \quad (19)$$

> $A\_core := wc^2 - (wc - tc)^2$; #Cross sectional area core [m2]

$$A\_core := 12.9308583 \quad (20)$$

> $EA := E\cdot A\_core$:
#Values for the tower, Note that the EI and EA of the building do not have a subscript

> $EI := evalf\left(0.7132958138\, vb^2\, wb\, hb^3\, \left(148.8202864 + 18.61828598\ln(hb) + \ln(hb)^2 + 18.61828598\ln(wb) + \ln(wb)^2\right)\right)$:

> $mass\_building := \frac{n\_stories\cdot wb^2\cdot 13.04\cdot 10^3}{9.81}$#mass of the building [kg]

$$mass\_building := 1.894127437\ 10^7 \quad (21)$$

>

>

Platform

> $EI\_platform := E\cdot\left(0.01198\cdot hp^3 - 0.05448\cdot hp^2 + 1.1877\cdot hp - 1.099\right)\cdot wp$
#Stiffness of the platform

$$EI\_platform := 5.835830000\ 10^{13} \quad (22)$$

> $mass\_platform := \frac{hp}{5}\cdot\frac{\left(\frac{wp^3}{6000} + 2.45\cdot wp^2 + 43.33\cdot wp - 2000\right)\cdot 10^3}{9.81}$: # Mass platform [kg]

> $extra\_ballast := \max\left(d\cdot wp^2\cdot \text{rho} - (mass\_platform + mass\_building), 0\right)$; #extra ballast [kg]

$$extra\_ballast := 7.530194683\ 10^7 \quad (23)$$

> $total\_mass := mass\_building + mass\_platform + extra\_ballast$; # total mass [kg]

$$total\_mass := 1.025000000\ 10^8 \quad (24)$$

>

> $COG := \frac{(mass\_platform + extra\_ballast)\cdot\frac{1}{2}\cdot hp + mass\_building\cdot\left(hp + \frac{1}{2}\cdot hb\right)}{mass\_platform + extra\_ballast + mass\_building}$;
Centre of gravity from the bottom of the platform [m]

$$COG := 18.12559294 \quad (25)$$

> $GM := \frac{\left(\frac{1}{12}\cdot wp^4\right)}{wp^2\cdot d} + \frac{1}{2}\cdot d - COG$# GM value [m]

$$GM := 70.20774039 \quad (26)$$

> $r := COG - d$:#COG from the bottom

>

MATRICES AND ITS VALUES

Here you can see the matrices as described in chapter 6. In addition to the matrices, the calculations of the values of the parameters in the matrices are shown as determined in the same chapter.

Matrices

Definition of the motions for the homogenious solution

$$u1 := uu1\cdot\cos(\omega\cdot t) :$$
$$u2 := uu2\cdot\cos(\omega\cdot t) :$$
$$u3 := uu3\cdot\cos(\omega\cdot t) :$$
$$w1 := ww1\cdot\cos(\omega\cdot t) :$$
$$w2 := ww2\cdot\cos(\omega\cdot t) :$$
$$w3 := ww3\cdot\cos(\omega\cdot t) :$$
$$\theta 1 := \theta\theta 1\cdot\cos(\omega\cdot t) :$$
$$\theta 2 := \theta\theta 2\cdot\cos(\omega\cdot t) :$$

$$\theta 3 := \theta\theta 3\cdot\cos(\omega\cdot t) :$$

Matrices

$$motion := \begin{bmatrix} w1 \\ w2 \\ w3 \\ u1 \\ u2 \\ u3 \\ \theta 1 \\ \theta 2 \\ \theta 3 \end{bmatrix} : motiondotdot := \begin{bmatrix} \frac{d^2}{dt^2}(w1) \\ \frac{d^2}{dt^2}(w2) \\ \frac{d^2}{dt^2}(w3) \\ \frac{d^2}{dt^2}(u1) \\ \frac{d^2}{dt^2}(u2) \\ \frac{d^2}{dt^2}(u3) \\ \frac{d^2}{dt^2}(\theta 1) \\ \frac{d^2}{dt^2}(\theta 2) \\ \frac{d^2}{dt^2}(\theta 3) \end{bmatrix} :$$

$$K\_beam :=$$

$$\begin{bmatrix} \frac{EA}{L} & -\frac{EA}{L} & 0 & 0 & 0 & 0 & 0 & 0 & 0 \\ -\frac{EA}{L} & \frac{2\cdot EA}{L} & -\frac{EA}{L} & 0 & 0 & 0 & 0 & 0 & 0 \\ 0 & -\frac{EA}{L} & \frac{EA}{L} & 0 & 0 & 0 & 0 & 0 & 0 \\ 0 & 0 & 0 & \frac{12\,EI}{L^3} & -\frac{12\,EI}{L^3} & 0 & \frac{6\,EI}{L^2} & \frac{6\,EI}{L^2} & 0 \\ 0 & 0 & 0 & -\frac{12\,EI}{L^3} & \frac{24\,EI}{L^3} & -\frac{12\,EI}{L^3} & -\frac{6\,EI}{L^2} & 0 & \frac{6\,EI}{L^2} \\ 0 & 0 & 0 & 0 & -\frac{12\,EI}{L^3} & \frac{12\,EI}{L^3} & 0 & -\frac{6\,EI}{L^2} & -\frac{6\,EI}{L^2} \\ 0 & 0 & 0 & \frac{6\,EI}{L^2} & -\frac{6\,EI}{L^2} & 0 & \frac{4\,EI}{L} & \frac{2\,EI}{L} & 0 \\ 0 & 0 & 0 & \frac{6\,EI}{L^2} & 0 & -\frac{6\,EI}{L^2} & \frac{2\,EI}{L} & \frac{2\cdot 4\cdot EI}{L} & \frac{2\,EI}{L} \\ 0 & 0 & 0 & 0 & \frac{6\,EI}{L^2} & -\frac{6\,EI}{L^2} & 0 & \frac{2\,EI}{L} & \frac{4\,EI}{L} \end{bmatrix} :$$

> $K\_spring :=$ $\begin{bmatrix} k1 & 0 & 0 & 0 & 0 & 0 & 0 & 0 & 0 \\ 0 & k2 & 0 & 0 & 0 & 0 & 0 & 0 & 0 \\ 0 & 0 & k3 & 0 & 0 & 0 & 0 & 0 & 0 \\ 0 & 0 & 0 & k4 & 0 & 0 & 0 & 0 & 0 \\ 0 & 0 & 0 & 0 & k5 & 0 & 0 & 0 & 0 \\ 0 & 0 & 0 & 0 & 0 & k6 & 0 & 0 & 0 \\ 0 & 0 & 0 & 0 & 0 & 0 & k7 & 0 & 0 \\ 0 & 0 & 0 & 0 & 0 & 0 & 0 & k8 & 0 \\ 0 & 0 & 0 & 0 & 0 & 0 & 0 & 0 & k9 \end{bmatrix} :$

> $K := K\_beam + K\_spring :$

> $M :=$
$[[m1 + a1, 0, 0, 0, 0, 0, 0, 0, 0],$
$[0, m2 + a2, 0, 0, 0, 0, 0, 0, 0],$
$[0, 0, m3 + a3, 0, 0, 0, 0, 0, 0],$
$[0, 0, 0, m4 + a4, 0, 0, 0, 0, 0],$
$[0, 0, 0, 0, m5 + a5, 0, 0, 0, 0],$
$[0, 0, 0, 0, 0, m6 + a6, 0, 0, 0],$
$[0, 0, 0, 0, 0, 0, J7 + a7, 0, 0],$
$[0, 0, 0, 0, 0, 0, 0, J8 + a8, 0],$
$[0, 0, 0, 0, 0, 0, 0, 0, J9 + a9]] :$

> $C :=$ $\begin{bmatrix} c1 & 0 & 0 & 0 & 0 & 0 & 0 & 0 & 0 \\ 0 & c2 & 0 & 0 & 0 & 0 & 0 & 0 & 0 \\ 0 & 0 & c3 & 0 & 0 & 0 & 0 & 0 & 0 \\ 0 & 0 & 0 & c4 & 0 & 0 & 0 & 0 & 0 \\ 0 & 0 & 0 & 0 & c5 & 0 & 0 & 0 & 0 \\ 0 & 0 & 0 & 0 & 0 & c6 & 0 & 0 & 0 \\ 0 & 0 & 0 & 0 & 0 & 0 & c7 & 0 & 0 \\ 0 & 0 & 0 & 0 & 0 & 0 & 0 & c8 & 0 \\ 0 & 0 & 0 & 0 & 0 & 0 & 0 & 0 & c9 \end{bmatrix}$:

>

The calculation of the values of the matrices

>

>

Spring stiffness

> $k1 := \mathrm{rho} \cdot g \cdot wp^2 : k2 := 0 : k3 := 0 : k4 := \mathrm{rho} \cdot g \cdot wp \cdot d : k5 := 0 : k6 := 0 : k8 := 0 : k9 := 0$:

>

The following formula is for the rotational stiffness including a deforming platform

> $k7 := \left(0.0329\, wp^4\, \rho\, g \left(9.91\, 10^{-11}\, g^3\, \rho^3\, wp^{15} + 0.0000228\, g^2\, \rho^2\, wp^{10}\, EI\_platform + 0.889\, g\, \rho\, wp^5\, EI\_platform^2 + 3240.\, EI\_platform^3\right) EI\_platform\right) \Big/ \left(5.23\, 10^{-14}\, g^4\, \rho^4\, wp^{20} + 1.53\, 10^{-8}\, g^3\, \rho^3\, wp^{15}\, EI\_platform + 0.000891\, g^2\, \rho^2\, wp^{10}\, EI\_platform^2 + 6.58\, g\, \rho\, wp^5\, EI\_platform^3 + 1300.\, EI\_platform^4\right) - d\, wp^2\, \rho\, g \left(COG - \frac{d}{2}\right)$

$$k7 := 6.564132130930336269675746078 54\, 10^{10} \quad \textbf{(15)}$$

>

Masses and rotational masses

> $m1 := mass\_platform + extra\_ballast + \frac{1}{5} \cdot mass\_building;\ m4 := m1$:

$$m1 := 1.898469805071421331397084708 74\, 10^{8} \quad \textbf{(16)}$$

> $m2 := \frac{2}{5} \cdot mass\_building;\ m3 := m2 : m5 := m2 : m6 := m2$:

$$m2 := 7.576509746428933430145764562 68\, 10^{6} \quad \textbf{(17)}$$

> $Aw := d \cdot wp : Izz := \frac{1}{12} \cdot wp \cdot d^3 : Ixx := \frac{1}{12} \cdot d \cdot wp^3 : Ipol := Ixx + Izz : \mathrm{Kappa} := evalf\left(\mathrm{sqrt}\left(\frac{Ipol}{Aw}\right)\right)$:

> Kappa

$$29.439202887759489515880142 4232 \quad \textbf{(18)}$$

> $J7 := m1 \cdot \mathrm{Kappa}^2$;

$$J7 := 1.645340497728565153877473414 24\, 10^{11} \quad \textbf{(19)}$$

> $J8 := n\_stories \cdot 1.31 \cdot 10^8 \cdot \frac{wb}{40} \cdot \frac{2}{5}$; $J9 := J8$:

$$J8 := 7.818827025946036158133565831 93\ 10^8 \quad (20)$$

> $J\_total := total\_mass \cdot \mathrm{Kappa}^2$;

$$J\_total := 1.776666666666666666666666666667\ 10^{11} \quad (21)$$

Added masses

> $a1 := \frac{1}{2} \cdot wp \cdot \mathrm{rho} \cdot 3.1415 \cdot \left(\frac{wp}{2} \right)^2$;

$$a1 := 4.025046875000000000000000000000\ 10^8 \quad (22)$$

> $a4 := \frac{1}{2} \cdot \mathrm{rho} \cdot 3.1415 \cdot d^2 \cdot wp$;

$$a4 := 6.440075000000000000000000000000\ 10^7 \quad (23)$$

> $a7 := evalf\left(\mathrm{rho} \cdot \pi \cdot \left(\left(\frac{wp}{4} \right)^2 \cdot \left(\frac{wp}{4} \right)^2 + \left(\frac{d}{2} \right)^2 \cdot \left(\frac{d}{2} + r \right)^2 \right) \right)$;

$$a7 := 1.279913125423580352546012014 52\ 10^9 \quad (24)$$

> $a2 := 0 : a3 := 0 : a5 := 0 : a6 := 0 : a8 := 0 : a9 := 0$:

>

Damping

> $c1 := 2 \cdot \mathrm{zeta}(m1 + a1) \cdot k1$

$$c1 := 2.0110500000\ 10^7 \quad (25)$$

> $c4 := 2 \cdot \mathrm{zeta}(m2 + a2) \cdot k4$

$$c4 := 4.022100000\ 10^6 \quad (26)$$

> $c7 := 2 \cdot \mathrm{zeta}(m3 + a3) \cdot k7$

$$c7 := 1.312826426186067253935149215 71\ 10^{10} \quad (27)$$

> $c2 := 0 : c3 := 0 : c5 := 0 : c6 := 0 : c8 := 0 : c9 := 0$:

>

EIGENFREQUENCIES CALCULATION

In this paragraph the calculation of the eigenfrequencies is shown. In chapter 6 it is explained that the eigenfrequencies can be determined by taking the determinant of $-\omega^2 * M + K$ and set it to zero, than solve for ω.

Here the determinant is determined. This determinant is than set to zero to solve for omega which will be the Eigenfrequencies.

```
> determi := -ω^2·M + K :
> with(linalg) :
> CharacteristicEQ := collect(det(determi), ω) :
> sol := solve(CharacteristicEQ, ω) :
>
```

Eigenfrequencies

The solutions are in radian/seconds

```
> with(ArrayTools) :
> for i to 18 do ωω[i] := sol[i]end do;
```

$$\omega\omega_{1} := 0.27252619232978036157507840565 4$$

$$\omega\omega_{2} := 0.40683431420875819807911334190 4$$

$$\omega\omega_{3} := 0.53942640332328346977233442640 7$$

$$\omega\omega_{4} := 3.61601368574117147003419523897$$

$$\omega\omega_{5} := 14.73085323500481979344905974 61$$

$$\omega\omega_{6} := 18.14375146815175759862023607 00$$

$$\omega\omega_{7} := 38.13314962795666847933094075 62$$

$$\omega\omega_{8} := 43.10522614645531634096580741 42$$

$$\omega\omega_{9} := 64.44099163348072449466441777 13$$

$$\omega\omega_{10} := -0.27252619232978033446248079 0913$$

$$\omega\omega_{11} := -0.40683431420875826266104627 6372$$

$$\omega\omega_{12} := -0.53942640332328343109865294 8174$$

$$\omega\omega_{13} := -3.61601368574117147390491069134$$

$$\omega\omega_{14} := -14.73085323500481940372665991 19$$

$$\omega\omega_{15} := -18.14375146815175851680972470 72$$

$$\omega\omega_{16} := -38.13314962795665337575946842 26$$

$$\omega\omega_{17} := -43.10522614645533674975127451 91$$

$$\omega\omega_{18} := -64.44099163348071753628034219 60 \quad (31)$$

FORCES

Here the calculations are shown of the different forces and moments due to the waves and wind. These are as described in chapter 2 and Appendix II. This ends with the force matrix. For the growing wave investigation the growth factor will be added here.

Calculation of the forces on the masses

```
> Digits := 10 :
```

Vertical force

```
> wave := 1/2 ·Hw·sin( 2·π·t/Twave + 2·π·x/Lwave ) :
> Fwater := rho·g :
> wave2D := wave·Fwater·wp :
> wave1D := int(wave2D, x = 0 .. wp) :
>
> maxwave := 0 :
> for t from 0 by 0.1 to Twave do
    if evalf(simplify(wave1D)) > maxwave then maxwave := evalf(simplify(wave1D)) end if
    end do:
> t :='t':
>
> F_ver_wave_1 := maxwave·sin(ωwave·t);
```

$$F\_ver\_wave\_1 := 3.699231334\ 10^{7} \sin(0.6404877988970016796050241352 24\, t) \quad (32)$$

```
>
```

Horizontal Force

```
>
```

Wave

```
> x := 0 : Hw1 := wave :
> x := wp : Hw2 := wave :
> x :='x':
> F1 := (d + Hw1)^2·1/2 ·rho·g :
> F2 := (d + Hw2)^2·1/2 ·rho·g :
>
> FF := F1 − F2 :
> maxwave := 0 :
> for t from 1 by 0.1 to Twave do
    if evalf(simplify(FF)) > maxwave then maxwave := evalf(simplify(FF)) end if
    end do:
> t :='t':
>
> F_hor_wave_1 := maxwave·sin(ωwave·t);
```

$$F\_hor\_wave\_1 := 348715.585 \sin(0.6404877988970016796050241352 24\, t) \quad (33)$$

```
> maxFv := maxwave
```

$$maxFv := 348715.585 \quad (34)$$

Wind

Wind speed calculation

```
>
> z0 := 0.003 : co := 1 : kl := 1 :
```

> $kr := 0.19 \cdot \left(\frac{z0}{0.05} \right)^{0.07}$:

> $cr := kr \cdot \log\left(\frac{z}{z0} \right)$:

> sigma := $kr \cdot vb \cdot kl$:

> $vm := cr \cdot co \cdot vb$:

> $Iv := \frac{\text{sigma}}{vm}$:

> $cpe := 0.7 + 0.8$

$$cpe := 1.5 \tag{35}$$

> $z := wb$:

> $qlow := (1 + 7 \cdot Iv) \cdot 0.5 \cdot 1.25 \cdot cpe \cdot vm^2 : \#\left[\frac{N}{m^2} \right]$

> $z := hb$:

> $qhigh := (1 + 7 \cdot Iv) \cdot 0.5 \cdot 1.25 \cdot cpe \cdot vm^2 : \#\left[\frac{N}{m^2} \right]$

> $z :='z'$:

>

Wind force calculation

> $Ffor1 := qlow \cdot wb$;

$$Ffor1 := 195564.4759 \tag{36}$$

> $Ffor2 := qlow \cdot wb + \frac{h - wb}{hb - 2 \cdot wb} \cdot (qhigh - qlow) \cdot wb$:

> $Ffor3 := qhigh \cdot wb$:

>

> $Fwind := piecewise(h \le wb, Ffor1, wb < h \le hb - wb, Ffor2, hb - wb < h < hb, Ffor3)$:

>

> $Fwind1 := \int_0^{\frac{1}{2} \cdot L} Fwind \, dh : Fwind2 := \int_{\frac{1}{2} \cdot L}^{\frac{3}{2} \cdot L} Fwind \, dh : Fwind3 := \int_{\frac{3}{2} \cdot L}^{\frac{5}{2} \cdot L} Fwind \, dh$:

> $A := 5$:

> $vb := A \cdot \sin(\omega wind \cdot t)$:

> $t := \frac{1}{4} \cdot Twind : FF1 := Fwind1 : FF2 := Fwind2 : FF3 := Fwind3$:

> $t :='t'$:

> $F\_hor\_wind\_1 := FF1 \cdot \sin(\omega wind \cdot t)$; $F\_hor\_wind\_2 := FF2 \cdot \sin(\omega wind \cdot t)$;
$F\_hor\_wind\_3 := FF3 \cdot \sin(\omega wind \cdot t)$;

$$F\_hor\_wind\_1 := 3.911289518\ 10^6 \sin(0.64048127003594117052071709 4278\ t)$$
$$F\_hor\_wind\_2 := 8.465846847\ 10^6 \sin(0.64048127003594117052071709 4278\ t)$$
$$F\_hor\_wind\_3 := 9.754784620\ 10^6 \sin(0.64048127003594117052071709 4278\ t) \tag{37}$$

> $Ftot := Fwind1 + Fwind2 + Fwind3$

$$Ftot := 2.213192098\ 10^7 \tag{38}$$

Moment

Wave

> $Fwater := \mathrm{rho} \cdot g$:

> $waveforce := wave \cdot Fwater \cdot wp$:

> $Area := \int_0^{wp} waveforce \, \mathrm{d}x$:

> $centre := \frac{1}{Area} \cdot \int_0^{wp} x \cdot waveforce \, \mathrm{d}x$:

> $arm := \frac{1}{2} \cdot wp - centre$:

> $Mwave := arm \cdot Area$:

> $maxwave := 0$:

> **for** t **from** 0 **by** 0.1 **to** $Twave$ **do**
if $evalf(simplify(Mwave)) > maxwave$ **then** $maxwave := evalf(simplify(Mwave))$ **end if**
end do:

> $t := 't'$:

> $M\_wave\_rot\_1 := maxwave \cdot \sin(\omega wave \cdot t)$;

$$M\_wave\_rot\_1 := 2.628259178\ 10^{9} \sin(0.64048779889700167960502413522 4\, t) \quad (39)$$

> $maxM := maxwave$

$$maxM := 2.628259178\ 10^{9} \quad (40)$$

Wind

> $t := \frac{1}{4} \cdot Twind$:

> $AAA := \int_0^{hb} Fwind \, \mathrm{d}h : mid := \frac{1}{AAA} \cdot \int_0^{hb} Fwind \cdot h \, \mathrm{d}h : M1 := AAA \cdot mid$:

> $AAA := \int_L^{hb} Fwind \, \mathrm{d}h : mid := \frac{1}{AAA} \cdot \int_L^{hb} Fwind \cdot h \, \mathrm{d}h : M2 := AAA \cdot (mid - L)$:

> $AAA := \int_{2 \cdot L}^{hb} Fwind \, \mathrm{d}h : mid := \frac{1}{AAA} \cdot \int_{2 \cdot L}^{hb} Fwind \cdot h \, \mathrm{d}h : M3 := AAA \cdot (mid - 2 \cdot L)$:

> $t := 't'$:

> $M\_wind\_rot\_1 := M1 \cdot \sin(\omega wind \cdot t)$

$$M\_wind\_rot\_1 := 1.165123225\ 10^{9} \sin(0.64048127003594117052071709427 8\, t) \quad (41)$$

> $M\_wind\_rot\_2 := M2 \cdot \sin(\omega wind \cdot t)$

(42)

$$M\_wind\_rot\_2 := 4.369869283\ 10^{8} \sin(0.64048127003594117052071709427 8\ t) \quad (42)$$

> $M\_wind\_rot\_3 := M3 \cdot \sin(\omega wind \cdot t)$

$$M\_wind\_rot\_3 := 4.941478871\ 10^{7} \sin(0.64048127003594117052071709427 8\ t) \quad (43)$$

> $M\_wind\_total := M1 + M2 + M3;$

$$M\_wind\_total := 1.651524942\ 10^{9} \quad (44)$$

Force matrix

> $F\_ver\_1 := F\_ver\_wave\_1$:
> $F\_hor\_1 := F\_hor\_wave\_1 + F\_hor\_wind\_1$:
> $F\_hor\_2 := F\_hor\_wind\_2 : F\_hor\_3 := F\_hor\_wind\_3$:
> $M\_rot\_1 := M\_wave\_rot\_1 + M\_wind\_rot\_1$:
> $M\_rot\_2 := M\_wind\_rot\_2 : M\_rot\_3 := M\_wind\_rot\_3$:

> $Fext := \begin{bmatrix} F\_ver\_1 \\ 0 \\ 0 \\ F\_hor\_1 \\ F\_hor\_2 \\ F\_hor\_3 \\ M\_rot\_1 \\ M\_rot\_2 \\ M\_rot\_3 \end{bmatrix};$

$$Fext := [[3.699231334\ 10^{7} \sin(0.64048779889700167960502413522 4\ t)], \quad (45)$$
$$[0],$$
$$[0],$$
$$[348715.585 \sin(0.64048779889700167960502413522 4\ t)$$
$$+ 3.911289518\ 10^{6} \sin(0.64048127003594117052071709427 8\ t)],$$
$$[8.465846847\ 10^{6} \sin(0.64048127003594117052071709427 8\ t)],$$
$$[9.754784620\ 10^{6} \sin(0.64048127003594117052071709427 8\ t)],$$
$$[2.628259178\ 10^{9} \sin(0.64048779889700167960502413522 4\ t)$$
$$+ 1.165123225\ 10^{9} \sin(0.64048127003594117052071709427 8\ t)],$$
$$[4.369869283\ 10^{8} \sin(0.64048127003594117052071709427 8\ t)],$$
$$[4.941478871\ 10^{7} \sin(0.64048127003594117052071709427 8\ t)]]$$

PARTICULAR SOLUTION, SOLVING THE EQUATION OF MOTION AND DETERMINING THE MAXIMUM ACCELERATION

Here the calculations of the particular solution can be seen. This is calculate by solving the equation of motion. To solve all unknowns, all nine DOF are set equal to the force at four different time values. This creates 36 equation to solve the 36 unknowns. When the particular solution is known, the maximum acceleration is determined by calculating the second derivative of the motions, and then calculating the acceleration for time values between 0 and the wave period. The highest acceleration is the maximum acceleration. These calculations are all based on the calculation shown in chapter 6.

Particular solution

>

> $w1\_part := C11\cdot\cos(\omega wave\cdot t) + C12\cdot\sin(\omega wave\cdot t) + C13\cdot\cos(\omega wind\cdot t) + C14\cdot\sin(\omega wind\cdot t)$:

> $w2\_part := C21\cdot\cos(\omega wave\cdot t) + C22\cdot\sin(\omega wave\cdot t) + C23\cdot\cos(\omega wind\cdot t) + C24\cdot\sin(\omega wind\cdot t)$:

> $w3\_part := C31\cdot\cos(\omega wave\cdot t) + C32\cdot\sin(\omega wave\cdot t) + C33\cdot\cos(\omega wind\cdot t) + C34\cdot\sin(\omega wind\cdot t)$:

> $u1\_part := C41\cdot\cos(\omega wave\cdot t) + C42\cdot\sin(\omega wave\cdot t) + C43\cdot\cos(\omega wind\cdot t) + C44\cdot\sin(\omega wind\cdot t)$:

> $u2\_part := C51\cdot\cos(\omega wave\cdot t) + C52\cdot\sin(\omega wave\cdot t) + C53\cdot\cos(\omega wind\cdot t) + C54\cdot\sin(\omega wind\cdot t)$:

> $u3\_part := C61\cdot\cos(\omega wave\cdot t) + C62\cdot\sin(\omega wave\cdot t) + C63\cdot\cos(\omega wind\cdot t) + C64\cdot\sin(\omega wind\cdot t)$:

> $\theta1\_part := C71\cdot\cos(\omega wave\cdot t) + C72\cdot\sin(\omega wave\cdot t) + C73\cdot\cos(\omega wind\cdot t) + C74\cdot\sin(\omega wind\cdot t)$:

> $\theta2\_part := C81\cdot\cos(\omega wave\cdot t) + C82\cdot\sin(\omega wave\cdot t) + C83\cdot\cos(\omega wind\cdot t) + C84\cdot\sin(\omega wind\cdot t)$:

> $\theta3\_part := C91\cdot\cos(\omega wave\cdot t) + C92\cdot\sin(\omega wave\cdot t) + C93\cdot\cos(\omega wind\cdot t) + C94\cdot\sin(\omega wind\cdot t)$:

> $$motion := \begin{bmatrix} w1\_part \\ w2\_part \\ w3\_part \\ u1\_part \\ u2\_part \\ u3\_part \\ \theta1\_part \\ \theta2\_part \\ \theta3\_part \end{bmatrix} : motiondot := \begin{bmatrix} \frac{d}{dt}(w1\_part) \\ \frac{d}{dt}(w2\_part) \\ \frac{d}{dt}(w3\_part) \\ \frac{d}{dt}(u1\_part) \\ \frac{d}{dt}(u2\_part) \\ \frac{d}{dt}(u3\_part) \\ \frac{d}{dt}(\theta1\_part) \\ \frac{d}{dt}(\theta2\_part) \\ \frac{d}{dt}(\theta3\_part) \end{bmatrix} : motiondotdot :=$$

$$\begin{bmatrix} \frac{d^2}{dt^2}(w1\_part) \\ \frac{d^2}{dt^2}(w2\_part) \\ \frac{d^2}{dt^2}(w3\_part) \\ \frac{d^2}{dt^2}(u1\_part) \\ \frac{d^2}{dt^2}(u2\_part) \\ \frac{d^2}{dt^2}(u3\_part) \\ \frac{d^2}{dt^2}(\theta 1\_part) \\ \frac{d^2}{dt^2}(\theta 2\_part) \\ \frac{d^2}{dt^2}(\theta 3\_part) \end{bmatrix} :$$

> $eq := M \cdot motiondotdot + C \cdot motiondot + K \cdot motion :$
> $t := 0 :$
> $eq1 := eq[1] = Fext[1] :$
> $eq2 := eq[2] = Fext[2] :$
> $eq3 := eq[3] = Fext[3] :$
> $eq4 := eq[4] = Fext[4] :$
> $eq5 := eq[5] = Fext[5] :$
> $eq6 := eq[6] = Fext[6] :$
> $eq7 := eq[7] = Fext[7] :$
> $eq8 := eq[8] = Fext[8] :$
> $eq9 := eq[9] = Fext[9] :$

> $t := \frac{0.5 \cdot \pi}{\omega wave} :$
> $eq10 := eq[1] = Fext[1] :$
> $eq11 := eq[2] = Fext[2] :$

```
> eq12 := eq[3] = Fext[3]:
> eq13 := eq[4] = Fext[4]:
> eq14 := eq[5] = Fext[5]:
> eq15 := eq[6] = Fext[6]:
> eq16 := eq[7] = Fext[7]:
> eq17 := eq[8] = Fext[8]:
> eq18 := eq[9] = Fext[9]:
>
> t := π / ωwave :
> eq19 := eq[1] = Fext[1]:
> eq20 := eq[2] = Fext[2]:
> eq21 := eq[3] = Fext[3]:
> eq22 := eq[4] = Fext[4]:
> eq23 := eq[5] = Fext[5]:
> eq24 := eq[6] = Fext[6]:
> eq25 := eq[7] = Fext[7]:
> eq26 := eq[8] = Fext[8]:
> eq27 := eq[9] = Fext[9]:
>
> t := 1.5·π / ωwave :
> eq28 := eq[1] = Fext[1]:
> eq29 := eq[2] = Fext[2]:
> eq30 := eq[3] = Fext[3]:
> eq31 := eq[4] = Fext[4]:
> eq32 := eq[5] = Fext[5]:
> eq33 := eq[6] = Fext[6]:
> eq34 := eq[7] = Fext[7]:
> eq35 := eq[8] = Fext[8]:
> eq36 := eq[9] = Fext[9]:
>
> t :='t':
> sol := solve( {eq1, eq2, eq3, eq4, eq5, eq6, eq7, eq8, eq9, eq10, eq11, eq12, eq13, eq14, eq15,
      eq16, eq17, eq18, eq19, eq20, eq21, eq22, eq23, eq24, eq25, eq26, eq27, eq28, eq29, eq30,
      eq31, eq32, eq33, eq34, eq35, eq36}, {C11, C12, C13, C14, C21, C22, C23, C24, C31, C32,
      C33, C34, C41, C42, C43, C44, C51, C52, C53, C54, C61, C62, C63, C64, C71, C72, C73,
      C74, C81, C82, C83, C84, C91, C92, C93, C94}) : assign(sol)
```

$$> \ motion := \begin{bmatrix} w1\_part \\ w2\_part \\ w3\_part \\ u1\_part \\ u2\_part \\ u3\_part \\ \theta 1\_part \\ \theta 2\_part \\ \theta 3\_part \end{bmatrix};$$

$$\begin{aligned} motion := [\,[\,&-0.02139532040\cos(0.6404877988970016796050241352 24\,t) \\ &-0.2469642657\sin(0.6404877988970016796050241352 24\,t) \\ &-8.930460338\,10^{-7}\cos(0.6404812700359411705207170942 78\,t) \\ &+3.358067610\,10^{-7}\sin(0.6404812700359411705207170942 78\,t)\,], \\ [\,&-0.02142702576\cos(0.6404877988970016796050241352 24\,t) \\ &-0.2473302378\sin(0.6404877988970016796050241352 24\,t) \\ &-8.943718803\,10^{-7}\cos(0.6404812700359411705207170942 78\,t) \\ &+3.363043984\,10^{-7}\sin(0.6404812700359411705207170942 78\,t)\,], \\ [\,&-0.02144288431\cos(0.6404877988970016796050241352 24\,t) \\ &-0.2475132916\sin(0.6404877988970016796050241352 24\,t) \\ &-8.950337988\,10^{-7}\cos(0.6404812700359411705207170942 78\,t) \\ &+3.365533087\,10^{-7}\sin(0.6404812700359411705207170942 78\,t)\,], \\ [\,&0.1287637545\cos(0.6404877988970016796050241352 24\,t) \\ &+0.3684648371\sin(0.6404877988970016796050241352 24\,t) \\ &+0.1226575744\cos(0.6404812700359411705207170942 78\,t) \\ &+0.1338862759\sin(0.6404812700359411705207170942 78\,t)\,], \\ [\,&-0.9947823085\cos(0.6404877988970016796050241352 24\,t) \\ &-3.236161298\sin(0.6404877988970016796050241352 24\,t) \\ &-1.029041734\cos(0.6404812700359411705207170942 78\,t) \\ &-3.562969003\sin(0.6404812700359411705207170942 78\,t)\,], \\ [\,&-2.152791026\cos(0.6404877988970016796050241352 24\,t) \\ &-6.953621170\sin(0.6404877988970016796050241352 24\,t) \\ &-2.217235812\cos(0.6404812700359411705207170942 78\,t) \\ &-7.295913404\sin(0.6404812700359411705207170942 78\,t)\,], \\ [\,&-0.02730371773\cos(0.6404877988970016796050241352 24\,t) \\ &-0.08756001786\sin(0.6404877988970016796050241352 24\,t) \\ &-0.02797139601\cos(0.6404812700359411705207170942 78\,t) \\ &-0.09169075661\sin(0.6404812700359411705207170942 78\,t)\,], \\ [\,&-0.02868397682\cos(0.6404877988970016796050241352 24\,t) \\ &-0.09206045667\sin(0.6404877988970016796050241352 24\,t) \end{aligned} \tag{46}$$

```
    − 0.02942007237 cos(0.64048127003594117052071709427 8 t)
    − 0.09285291309 sin(0.64048127003594117052071709427 8 t) ],
   [ -0.02908860497 cos(0.64048779889700167960502413522 4 t)
    − 0.09339624210 sin(0.64048779889700167960502413522 4 t)
    − 0.02985564317 cos(0.64048127003594117052071709427 8 t)
    − 0.09354485698 sin(0.64048127003594117052071709427 8 t) ]]
> t :='t':
>
```

$$> total\_vertical\_acceleration\_mass\_1 := \frac{d^2}{dt^2}(w1\_part) :$$

$$> total\_vertical\_acceleration\_mass\_2 := \frac{d^2}{dt^2}(w2\_part) :$$

$$> total\_vertical\_acceleration\_mass\_3 := \frac{d^2}{dt^2}(w3\_part) :$$

$$> total\_horizontal\_acceleration\_mass\_1 := \frac{d^2}{dt^2}(u1\_part) :$$

$$> total\_horizontal\_acceleration\_mass\_2 := \frac{d^2}{dt^2}(u2\_part) :$$

$$> total\_horizontal\_acceleration\_mass\_3 := \frac{d^2}{dt^2}(u3\_part) :$$

$$> total\_angularacceleration\_mass\_1 := \frac{d^2}{dt^2}(\theta 1\_part) :$$

$$> total\_angularacceleration\_mass\_2 := \frac{d^2}{dt^2}(\theta 2\_part) :$$

$$> total\_angularacceleration\_mass\_3 := \frac{d^2}{dt^2}(\theta 3\_part) :$$

```
>
> max_vertical_acceleration1_1 := 0 : max_vertical_acceleration2_1 := 0 :
      max_vertical_acceleration3_1 := 0 :
> for t from 0 by 0.01 to Twave do
  if evalf(simplify(total_vertical_acceleration_mass_1)) > max_vertical_acceleration1_1
      then max_vertical_acceleration1_1 :=
       evalf(simplify(total_vertical_acceleration_mass_1)) end if
  end do:
> for t from 0 by 0.01 to Twave do
  if evalf(simplify(total_vertical_acceleration_mass_2)) > max_vertical_acceleration2_1
      then max_vertical_acceleration2_1 :=
       evalf(simplify(total_vertical_acceleration_mass_2)) end if
  end do:

> for t from 0 by 0.01 to Twave do
  if evalf(simplify(total_vertical_acceleration_mass_3)) > max_vertical_acceleration3_1
```

```
        then max_vertical_acceleration3_1 :=
         evalf(simplify(total_vertical_acceleration_mass_3)) end if
    end do:
>
> max_horizontal_acceleration1_1 := 0 : max_horizontal_acceleration2_1 := 0 :
        max_horizontal_acceleration3_1 := 0 :
> for t from 0 by 0.01 to Twave do
    if evalf(simplify(total_horizontal_acceleration_mass_1)) > max_horizontal_acceleration1_1
        then max_horizontal_acceleration1_1 :=
         evalf(simplify(total_horizontal_acceleration_mass_1)) end if
    end do:
> for t from 0 by 0.01 to Twave do
    if evalf(simplify(total_horizontal_acceleration_mass_2)) > max_horizontal_acceleration2_1
        then max_horizontal_acceleration2_1 :=
         evalf(simplify(total_horizontal_acceleration_mass_2)) end if
    end do:

> for t from 0 by 0.01 to Twave do
    if evalf(simplify(total_horizontal_acceleration_mass_3)) > max_horizontal_acceleration3_1
        then max_horizontal_acceleration3_1 :=
         evalf(simplify(total_horizontal_acceleration_mass_3)) end if
    end do:
>
>
> maxangaccel1_1 := 0 : maxangaccel2_1 := 0 : maxangaccel3_1 := 0 :
> for t from 0 by 0.01 to Twave do
    if abs(evalf(simplify(total_angularacceleration_mass_1))) > maxangaccel1_1
        then maxangaccel1_1 := abs(evalf(simplify(total_angularacceleration_mass_1))) end if
    end do:
> for t from 0 by 0.01 to Twave do
    if abs(evalf(simplify(total_angularacceleration_mass_2))) > maxangaccel2_1
        then maxangaccel2_1 := abs(evalf(simplify(total_angularacceleration_mass_2))) end if
    end do:

> for t from 0 by 0.01 to Twave do
    if abs(evalf(simplify(total_angularacceleration_mass_3))) > maxangaccel3_1
        then maxangaccel3_1 := abs(evalf(simplify(total_angularacceleration_mass_3))) end if
    end do:
```

CALCULATION OF THE MAXIMUM ACCERLERATION AT THE TOP OF THE BUILDING

Due to the modelling the top mass is not at the same height as the top of the building. Therefore this extra calculation is added to calculate the horizontal displacement and acceleration at the top of the building.

Results for the top of the building

To calculate the translation and thus acceleration of the top of the building (mass 3 is not at the top of the building) the formula for the translation of the tower over the height is determined. This is done with the results from the three masses. the deflection of a beam is a third degree polynomal.

```
> x :='x': t :='t':
> u_tower := C1·x^3 + C2·x^2 + C3·x + C4
```

$$u\_tower := C1\,x^3 + C2\,x^2 + C3\,x + C4 \quad (53)$$

```
> u_tower_dot := d/dx (u_tower);
```

$$u\_tower\_dot := 3\,C1\,x^2 + 2\,C2\,x + C3 \quad (54)$$

```
> x := 0 :
> eq1 := u_tower = motion[4] :
> x := hb/(3 - 0.5) :
> eq2 := u_tower = motion[5] :
> x := 2·hb/(3 - 0.5) :
> eq3 := u_tower = motion[6] :
> eq4 := u_tower_dot = motion[9] :
> x :='x':
> sol := solve({eq1, eq2, eq3, eq4}, {C1, C2, C3, C4}) : assign(sol) :
> x := hb :
> u_tower_dotdot := d^2/dt^2 (u_tower) :
> total_horizontal_acceleration_topofbuilding := u_tower_dotdot :
> max_horizontal_acceleration_topofbuilding := 0 :
> max_horizontal_deflection := 0 :
> for t from 0 by 0.01 to Twave do
    if evalf(simplify(total_horizontal_acceleration_topofbuilding))
       > max_horizontal_acceleration_topofbuilding
      then max_horizontal_acceleration_topofbuilding :=
       evalf(simplify(total_horizontal_acceleration_topofbuilding)) end if
    end do:
> max_horizontal_acceleration_topofbuilding
```

$$7.721270720 \quad (55)$$

```
> for t from 0 by 0.01 to Twave do
    if evalf(simplify(u_tower)) > max_horizontal_deflection then max_horizontal_deflection :=
       evalf(simplify(u_tower)) end if
    end do:
> max_horizontal_deflection
```

$$18.82233096 \quad (56)$$

APPENDIX VIII - DIANA MULTIPLE MASS MODEL RESULTS

Diana has been used to check the calculations of the Eigen Frequencies. A Diana model with 3 point masses was created for this purpose. In addition, Diana was used to investigate the influence of multiple point masses. Models with 3, 5 and 9 point masses were made. For each of these, the values were calculated separately, such as the mass. In the figure below, you can see the three models as they appear in Diana. A schematic representation has also been made. Because the eigenfrequency calculations are made in such a way that the lowest mass is always at the bottom of the element, this is also done in Diana. Next, the result of the masses are equally distributed. This ensures that the masses are no longer at the same height. This may result in different values.

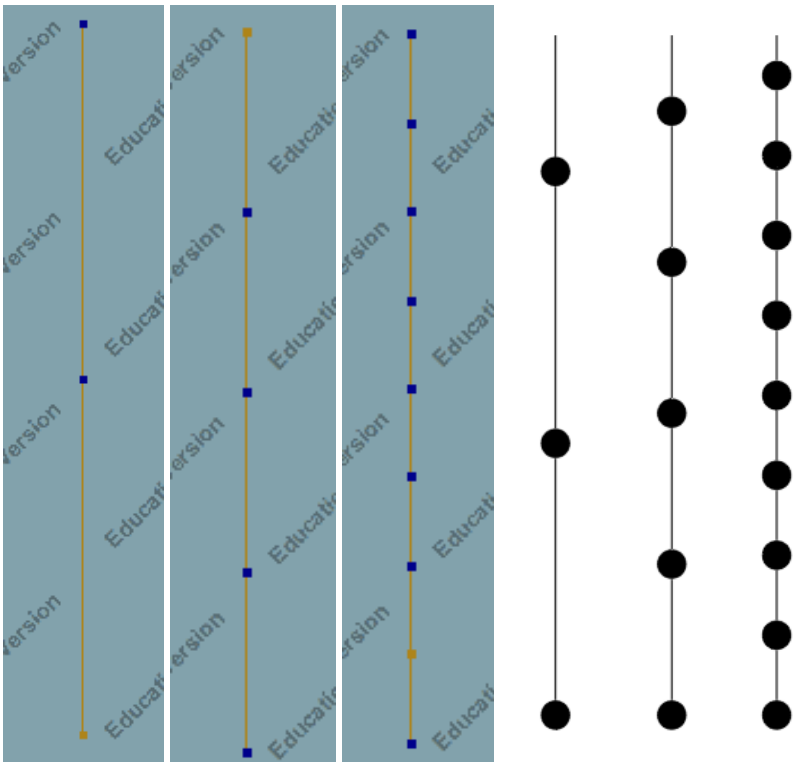

Figure 141 – 3, 5 and 9 mass model in Diana and schematic versions.

To compare the values of the calculations and the Diana model, the results of the calculations in Maple are shown below. On the left, the eigenfrequencies are expressed in rad/s and on the right in Hz. Diana always gives the frequencies in Hz.

$$\omega\omega_1 := 0.073908333545666483824153813713 0 \qquad \omega_{1,2} := 0.011763223546978590454266085263 9$$

$$\omega\omega_2 := 0.484655463332995775917604293405 \qquad \omega_{2,2} := 0.077137587670379719229286056566 3$$

$$\omega\omega_3 := 1.261700967679902966483581103 08 \qquad \omega_{3,2} := 0.200811868164873940232943037257$$

$$\omega\omega_4 := 6.685562426066749537734140068 67 \qquad \omega_{4,2} := 1.064071689649331455950046167 23$$

$$\omega\omega_5 := 14.80623246398086911170117747 19 \qquad \omega_{5,2} := 2.356554586022738995973448586 97$$

$$\omega\omega_6 := 15.69291489534778836985839694 43 \qquad \omega_{6,2} := 2.497678640036254714285913885 78$$

$$\omega\omega_7 := 38.14443768534959536855283046 99 \qquad \omega_{7,2} := 6.071054859995160809892221943 34$$

$$\omega\omega_8 := 39.43510973618315690052824182 86 \qquad \omega_{8,2} := 6.276477755241629301373267838 41$$

$$\omega\omega_9 := 64.71426997856409071621836103 78 \qquad \omega_{9,2} := 10.299899726016885359894693782 9$$

Figure 142 - Eigenfrequencies of the 3 mass model. Calculated with Maple.

The results of the Diana model are shown in the table below. The results of the 5 and 9 point mass models are also given. The DOF or leading motion is also shown. The figure below the table shows the eigenmodes of the Diana model for the different eigenfrequencies of the 3-mass model. These are used to determine the leading motion and to determine whether the calculations are correct. The table shows that there is little difference between the eigenfrequencies of the models. There is some difference, but this can be caused by different rounding (Diana works with 5 decimals, this can cause a difference) or by the fact that the masses are not at the same heights. The largest deviations are in the eigenfrequencies higher than 2 Hz. These are far away from the eigenfrequencies limits and will therefore have no influence on the further calculations. It can be concluded that 3 masses are enough to model the floating high-rise accurately.

Table 38 - Eigenfrequencies of the different DOF for the 3, 5 and 9 mass models in Diana.

Frequency Number:	1	2	3	4	5	6	7	8	9
3 masses									
Frequency [Hz]	0.0122	0.0771	0.149	1.238	2.357	3.121	6.071	6.900	10.266
DOF	u_1	w_1	θ_1	u_3	w_3	u_2	w_2	θ_3	θ_2
5 masses									
Frequency [Hz]	0.0122	0.0771	0.109	1.288	2.385	2.989	6.501	6.759	10.169
DOF	u_1	w_1	θ_1	u_5	w_5	u_3	w_3	θ_5	θ_3
9 masses									
Frequency [Hz]	0.0122	0.0771	0.0149	1.291	2.395	2.964	6.429	6.991	10.477
DOF	u_1	w_1	θ_1	u_9	w_9	u_5	w_5	θ_9	θ_5

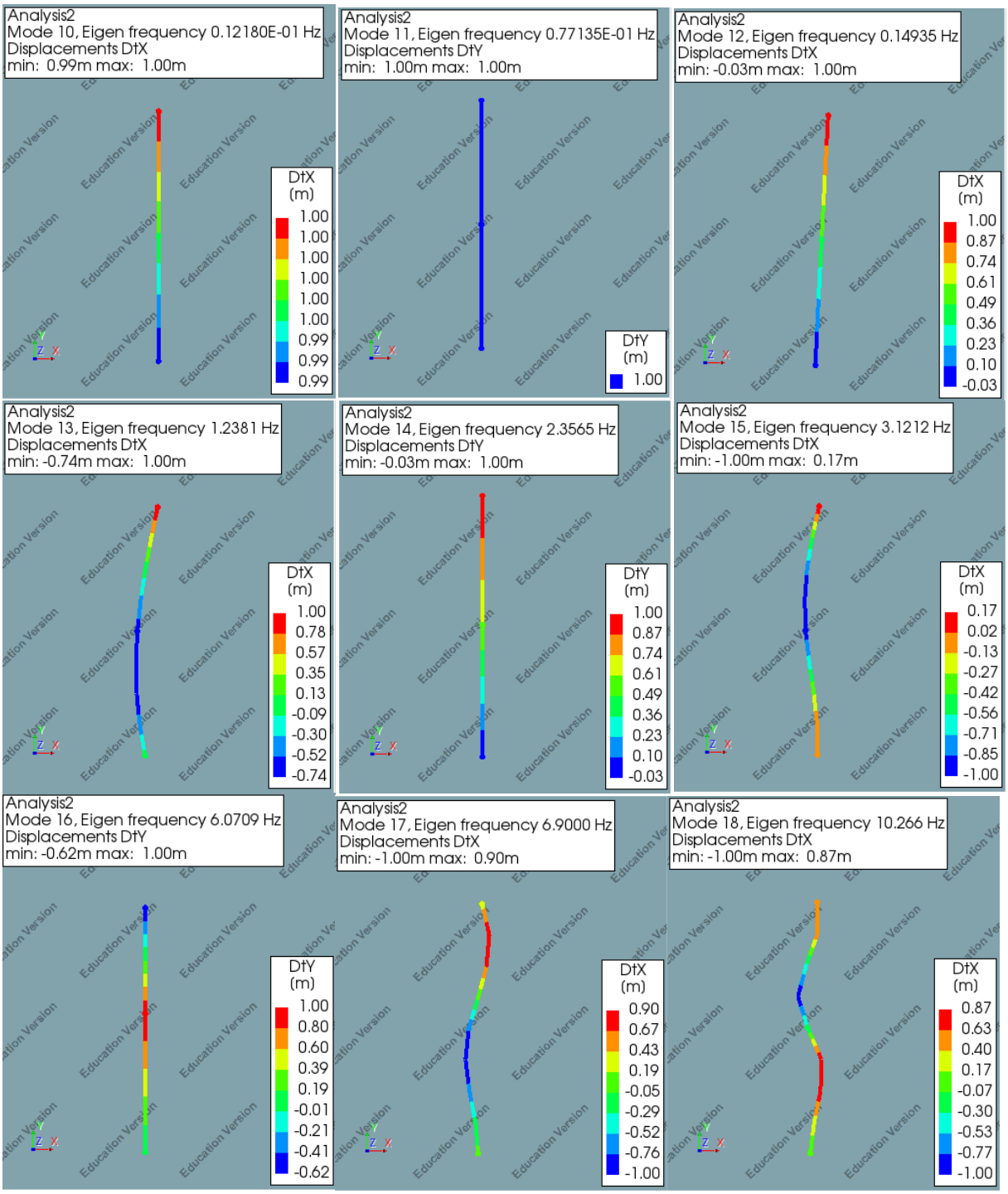

Figure 143 - eigenmodes in Diana of the example. The eigenfrequency is given in the top left corner. Note that some deformations are in x and some in y direction (u and w in the hand calculation).

Below are the eigenfrequencies of the 5 and 9 mass models in Diana. These match the table but also show the extra frequencies that can be calculated with multiple point masses. These frequencies are always higher than those found in the 3-mass model and are far out of range of the limiting frequencies.

```
0.00000E+00( 13)    0.00000E+00( 14)    0.00000E+00( 15)    0.12179E-01( 16)
0.77135E-01( 17)    0.10946E+00( 18)    0.12288E+01( 19)    0.23857E+01( 20)
0.29885E+01( 21)    0.65088E+01( 22)    0.67589E+01( 23)    0.10169E+02( 24)
0.10342E+02( 25)    0.12682E+02( 26)    0.15683E+02( 27)    0.19789E+02( 28)
0.20733E+02( 29)    0.20978E+02( 30)    0.41202E+06( 31)   -0.44399E+06( 32)
```

Figure 144 - Eigenfrequencies of the Diana model with 5 point masses. Note: The first 12 frequencies are all equal to 0 and thus not shown. Frequency 31 and higher are also not of interest

```
0.00000E+00( 25)    0.00000E+00( 26)    0.00000E+00( 27)    0.12180E-01( 28)
0.77135E-01( 29)    0.14863E+00( 30)    0.12908E+01( 31)    0.23954E+01( 32)
0.29638E+01( 33)    0.64294E+01( 34)    0.69905E+01( 35)    0.10477E+02( 36)
0.11371E+02( 37)    0.14439E+02( 38)    0.15368E+02( 39)    0.17884E+02( 40)
0.18843E+02( 41)    0.20533E+02( 42)    0.21677E+02( 43)    0.22197E+02( 44)
0.23773E+02( 45)    0.25060E+02( 46)    0.35778E+02( 47)    0.41522E+02( 48)
0.46129E+02( 49)    0.51563E+02( 50)    0.56897E+02( 51)    0.61545E+02( 52)
0.65117E+02( 53)    0.67358E+02( 54)   -0.36625E+06( 55)   -0.59437E+06( 56)
```

Figure 145 - Eigenfrequencies of the Diana model with 9 point masses. Note: The first 27 frequencies are all equal to 0 and thus not shown. Frequency 55 and higher are also not of interest

Limiting values have been set for the eigenfrequencies. These are between 0.3 and 1.44 rad/s. In order to determine which DOF must be examined to ensure that no resonance can occur, the eigenfrequencies are calculated for different values of the platform width and building height. This involves platform widths of 100, 300 and 500 m and building heights of 100, 300 and 500 m. The results are analysed and a conclusion is drawn about the importance of the eigenfrequency in connection with the resonance. This set yields 7 eigenfrequencies (two do not provide stability) and so it is anecdotal evidence. However, it is too complicated to do otherwise. The results of the 9 eigenfrequencies are shown in the following nine tables.

Table 39 - Eigenfrequencies of the horizontal motion of the bottom mass with different platform widths and building height in rad/s.

Horizontal motion bottom mass	Height building [m]		
Width platform [m]	**100**	**300**	**500**
100	0.300	x	x
300	0.180	0.165	0.109
500	0.140	0.137	0.056

The horizontal eigenfrequency decreases with increasing platform width. This is a consequence of the increased mass and added mass in this direction. Despite an also increasing spring stiffness. There is also a decrease in eigenfrequency for an increasing building height. Here the mass is also the reason. The results show that this DOF lies in the range of limiting frequencies and will therefore have to be investigated.

Table 40 - Eigenfrequencies of the vertical motion of the bottom mass with different platform widths and building height in rad/s.

Vertical motion bottom mass	Height building [m]		
Width platform [m]	**100**	**300**	**500**
100	0.485	x	x

300	0.286	0.285	0.276
500	0.222	0.222	0.221

With increasing platform width, the eigenfrequencies of the vertical motion of the lower mass decrease. This is because the mass increases considerably due to the extra counterweight required to reach the depth and because the added mass increases considerably. The spring stiffness also increases, but less than the mass and added mass together. The difference in height makes no difference to this motion. This is somewhat remarkable. The results show that this DOF lies in the range of limiting frequencies and will therefore have to be investigated.

Table 41 - Eigenfrequencies of the rotation of the bottom mass with different platform widths and building height in rad/s.

Rotation bottom mass	**Height building [m]**		
Width platform [m]	**100**	**300**	**500**
100	1.264	x	x
300	0.796	0.561	0.337
500	0.369	0.321	0.231

Also, the eigenfrequencies of the rotation of the lower mass decreases as the platform width increases and the height of the building increases. This has the same reasons as for the horizontal motion. The results show that this DOF lies in the range of limiting frequencies and will therefore have to be investigated.

The results of the other six DOF show that they are outside the range of the frequency limits and also do not come close to this range with an even larger platform width and/or building height. Only the horizontal motion of the upper mass can come close for extreme value. From these values it is concluded that they do not require further investigation into the limitation of the eigenfrequencies.

Table 42 - Eigenfrequencies of the horizontal motion of the top mass with different platform widths and building height in rad/s.

Horizontal motion top mass	**Height building [m]**		
Width platform [m]	**100**	**300**	**500**
100	7.828	x	x
300	3.174	3.199	2.073
500	3.076	1.884	2.025

Table 43 - Eigenfrequencies of the vertical motion of the top mass with different platform widths and building height in rad/s.

Vertical motion top mass	**Height building [m]**		
Width platform	**100**	**300**	**500**

[m]			
100	14.806	x	x
300	14.565	4.112	3.703
500	14.558	3.179	2.696

Table 44 - Eigenfrequencies of the horizontal motion of the middle mass with different platform widths and building height in rad/s.

Horizontal motion middle mass	Height building [m]		
Width platform [m]	**100**	**300**	**500**
100	21.596	x	x
300	18.085	8.312	5.275
500	17.993	8.309	5.267

Table 45 - Eigenfrequencies of the vertical motion of the middle mass with different platform widths and building height in rad/s.

Vertical motion middle mass	Height building [m]		
Width platform [m]	**100**	**300**	**500**
100	38.144	x	x
300	38.109	12.163	9.965
500	38.108	9.411	8.106

Table 46 - Eigenfrequencies of the rotation of the top mass with different platform widths and building height in rad/s.

Rotation top mass	Height building [m]		
Width platform [m]	**100**	**300**	**500**
100	44.333	x	x
300	43.098	70.291	93.317
500	43.064	70.206	93.306

Table 47 - Eigenfrequencies of the rotation of the middle mass with different platform widths and building height in rad/s.

Rotation motion middle mass	Height building [m]		
Width platform [m]	**100**	**300**	**500**
100	64.907	x	x
300	64.440	116.550	155.460
500	64.427	116.453	155.447

APPENDIX IX - ROTATIONAL STIFFNESS WITH A DEFORMING PLATFORM

The deformation of the platform is not included when the platform of the floating high-rise is modelled as only one point mass. To include the deformation, the formula of the rotational stiffness of rotation can no longer be used. This rotational stiffness calculation method is based on the GM value. As described earlier, using the GM value simplifies the calculation of the moment balance of the support springs, the moment due to the weight and an external moment. To calculate the rotational stiffness, this balance is used

There are two ways of determining the spring stiffness of the platform for the rotation. One is by using the GM value:

$$k_{rotation,GM} = \rho_{water} * g * V * GM \tag{A-IX.1}$$

In chapter 2 it is show that GM can be calculated with the following formula:

$$GM = \frac{1}{2} * d + \frac{I_i}{V_{sub}} - \overline{COG} \tag{A-IX.2}$$

Using $I_i = \frac{1}{12} * wp^4$ and $V_{sub} = d * wp^2$ this is simplified to:

$$GM = \frac{wp^2}{12d} + \frac{1}{2}d - \overline{COG} \tag{A-IX.3}$$

So k becomes:

$$k_{rotation,GM} = \rho_{water} * g * d * wp^2 * (\frac{wp^2}{12d} + \frac{1}{2}d - \overline{COG}) \tag{A-IX.4}$$

The other method is by using the moment, created by the force of the springs with a vertical displacement due to a rotation. This is first done for a beam with three springs.

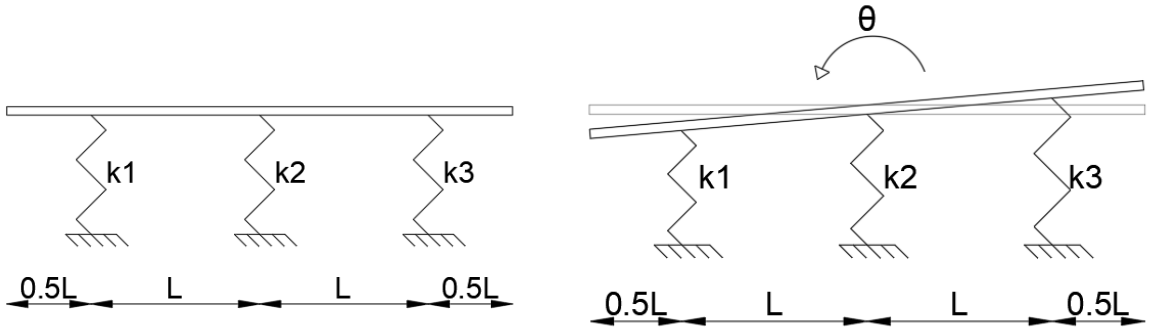

Figure 146 - Platform supported by three springs.

The middle spring does not displace and thus does not create a moment.

$$F_1 = k_1 * \theta * L \tag{A-IX.5}$$

$$F_3 = -k_3 * \theta * L \tag{A-IX.6}$$

The moments around the middle of the platform due to these forces are:

$$M_1 = k_1 * \theta * L^2 \tag{A-IX.7}$$

$$M_3 = k_3 * \theta * L^2 \tag{A-IX.8}$$

So the total moment due to the springs is:

$$M_1 + M_3 = k_1 * \theta * L^2 + k_3 * \theta * L^2 = (k_1 + k_3) * \theta * L^2 \tag{A-IX.9}$$

All the springs have the same spring stiffness so this can be simplified to:

$$M_{springs} = 2k * L^2 * \theta \tag{A-IX.10}$$

The rotational stiffness is than $2k * L^2$. When the same is done with five springs the length L between the springs is reduced, the spring stiffness k is reduced and the moments of spring one and five will have the factor $2 * L^2$.

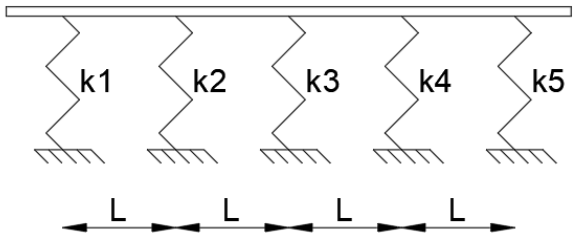

Figure 147 - Platform supported by five springs.

$$F_1 = k_1 * \theta * 2L \; and \; F_5 = k_5 * \theta * 2L \tag{A-IX.11}$$

$$M_1 = k_1 * \theta * (2L)^2 \; and \; M_5 = k_5 * \theta * (2L)^2 \tag{A-IX.12}$$

Spring two and four will have the same formula as springs one and three of the 3 spring model. All the moments are added again.

$$M_{springs} = (k_1 + k_5) * \theta * (2L)^2 + (k_2 + k_4) * \theta * L^2 \tag{A-IX.13}$$

When all springs have the same spring stiffness this is simplified to:

$$M_{springs} = 2k * \theta * (2L)^2 + 2k * \theta * L^2 \tag{A-IX.14}$$

$$M_{springs} = 2k * L^2 * \left(1 + 2^2\right) * \theta \tag{A-IX.15}$$

With now $2k * L^2 * \left(1 + 2^2\right)$ as rotational spring stiffness. The water actually forms a line-spring-support. In order to achieve this, an infinite number of springs must be used. To calculate this, the number of springs is set equal to n. Next, the lengths between the springs and the spring stiffness's can be determined in terms of n:

$$L = \frac{width\ of\ the\ platform}{n} \tag{A-IX.16}$$

$$k_{vertical} = \frac{\rho_{water} * g * width\ of\ the\ platform^2}{n} \tag{A-IX.17}$$

The rotational rigidity can also be described in terms of n using a summation:

$$k_{rotation,spring} = 2k * L^2 * \sum_{x=1}^{\frac{n-1}{2}} x^2 \tag{A-IX.18}$$

Combining the three gives:

$$k_{rotation,spring} = \frac{2 * \rho_{water} * g * wp^4}{n^3} * \sum_{x=1}^{\frac{n-1}{2}} x^2 \tag{A-IX.19}$$

When unlimited spring are used, $n \to \infty$. The limit will be:

$$k_{rotation,spring} = \lim_{n\to\infty}(\frac{2 * \rho_{water} * g * wp^4}{n^3} * \sum_{x=1}^{\frac{n-1}{2}} x^2) \tag{A-IX.20}$$

$$k_{rotation,spring} = \frac{1}{12} * \rho_{water} * g * wp^4 \tag{A-IX.21}$$

This is different from the formula with GM. That formula includes the displacement of the centre of gravity, this is not yet included in the multiple spring method. To include this the moment due to the weight needs to be calculated and added to the total moment sum. This moment due to the weight is:

$$M_{weight} = m * g * (\overline{COG} - \frac{1}{2}d) * \theta \tag{A-IX.22}$$

The mass m can be written as $d * wp^2 * \rho_{water}$. The moment due to the weight than becomes:

$$M_{weight} = d * wp^2 * \rho_{water} * g * (\overline{COG} - \frac{1}{2}d) * \theta \tag{A-IX.23}$$

The added part to the stiffness is than

$$k_{weight} = d * wp^2 * \rho_{water} * g * (\overline{COG} - \frac{1}{2}d) \tag{A-IX.24}$$

This “stiffness” is than subtracted of the results of the limit (subtraction as the moment works in the opposite direction of the moment due to the springs)

$$\lim_{n\to\infty}(k) = \frac{1}{12} * \rho_{water} * g * wp^4 - d * wp^2 * \rho_{water} * g * (\overline{COG} - \frac{1}{2}d) \tag{A-IX.25}$$

This formula does not look exactly like the GM method, but it is. So this spring method can be used to calculate the stiffness of the spring.

Now that the rotational stiffness can be determined with the vertical springs, the deformation of the platform can also be included in the determination of the rotational stiffness. To do this, Ordinary Differential Equations (ODEs) are used. These can be used to find a relation between moment and rotation in the centre of the platform. First the model with three masses is used. To solve an ODE, boundary conditions must be used. Figure 148 shows the schematisation with the different boundary condition. Two ODEs are used, one for each beam.

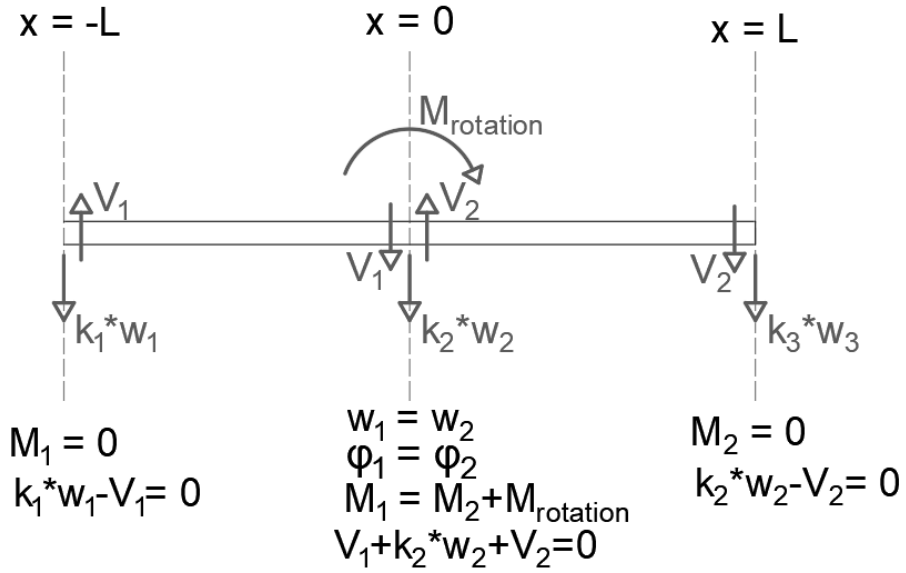

Figure 148 - Schematisation of the platform and the boundary conditions for the ODE.

The deflection has the form of:

$$w(x) = \frac{1}{6} * C1 * x^3 + \frac{1}{2} * C2 * x^2 + C3 * x + C4\ [m] \tag{A-IX.26}$$

With the eight boundary conditions the four unknowns of both deflection formulas can be solved. Solving this means expressing the unknown constants in terms of length, stiffness, spring stiffness and the moment in the middle. With the two formulas, the rotation in the middle can be determined and expressed in the same constants:

$$\theta = \frac{M_{rotation}(L^3 * k + 3EI)}{6L^2 * EI * k} \tag{A-IX.27}$$

Rewriting this to express the moment in terms of rotation:

$$M_{rotation} = \frac{6\theta * L^2 * EI * k}{L^3 * k + 3EI} \tag{A-IX.28}$$

Where:

EI Is the stiffness of the platform.

If the platform is infinitely stiff, this formula should give the same answer as the manual calculations above. To check this, the limit is taken from EI to infinity:

$$M_{rotation} = \lim_{EI \to \infty} \left(\frac{6\theta * L^2 * EI * k}{L^3 * k + 3EI} \right) \tag{A-IX.29}$$

This gives:

$$M_{rotation} = 2L^2 * k \tag{A-IX.30}$$

This is indeed the same as found earlier for a model with three springs/masses. Drawing up the boundary conditions is a manual job that cannot be scaled up to infinity, so the manual calculation (sum) method is used first to determine what a sufficient number of springs is. Therefore, the manual calculation (sum) method is first used to determine the adequate number of springs. The result of a given number of springs is then divided by the previous result (for example, the result of five springs is divided by that of three springs). To determine the difference in percentages, this number is subtracted by one and multiplied by 100. The results are shown in the table below.

Table 48 - Change in value for the rotational stiffness with a certain amount of spring compared to the previous value (in percentages).

Number of springs	3	5	7	9	11	13	15
Change in value (%)	N/A	8.00	2.04	0.82	0.41	0.24	0.15

With nine springs, the change is less than one per cent. Therefore, nine springs is determined as enough to determine the rotational stiffness. The ODE method is done again, now with 9 springs. This gives the following formula for the moment in the middle:

$$M_{rotation} = \frac{24 * L^2 * k * \left(28 * L^9 * k^3 + 981 * EI * L^6 * k^2 + 5832 * EI^2 * L^3 * k + 3240 * EI^3\right) * EI}{97 * L^{12} * k^4 + 4332 * EI * L^9 * k^3 + 38340 * EI^2 * L^6 * k^2 + 43200 * EI^3 * L^3 * k + 1296 * EI^4} * \theta \tag{A-IX.31}$$

When the expression for k and L are used in terms of n, with n equal to 9 the relationship between the moment and the rotation changes to:

$$M_{rotation} = \frac{0.0329 * wp^4 * rho * g * \left(9.91 * 10^{-11} * g^3 * rho^3 * wp^{15} + 2.28 * 10^{-5} * EI * g^2 * rho^2 * wp^{10} + 0.889 * EI^2 * g * rho * wp^5 + 3240. * EI^3\right) * EI}{5.23 * 10^{-14} * g^4 * rho^4 * wp^{20} + 1.53 * 10^{-8} * EI * g^3 * rho^3 * wp^{15} + 8.91 * 10^{-4} * EI^2 * g^2 * rho^2 * wp^{10} + 6.58 * EI^3 * g * rho * wp^5 + 1300. * E} * \theta \tag{A-IX.32}$$

And thus the rotational stiffness, including the deformation of the platform and the second order moment, can be calculated with the following formula:

$$k_{rotation} = \frac{0.0329 * wp^4 * rho * g * \left(9.91 * 10^{-11} * g^3 * rho^3 * wp^{15} + 2.28 * 10^{-5} * EI * g^2 * rho^2 * wp^{10} + 0.889 * EI^2 * g * rho * wp^5 + 3240. * EI^3\right) * EI}{5.23 * 10^{-14} * g^4 * rho^4 * wp^{20} + 1.53 * 10^{-8} * EI * g^3 * rho^3 * wp^{15} + 8.91 * 10^{-4} * EI^2 * g^2 * rho^2 * wp^{10} + 6.58 * EI^3 * g * rho * wp^5 + 1300. * EI^4 - d * wp^2 * \rho_{water} * g * \left(\overline{COG} - \frac{1}{2} d\right)} \tag{A-IX.33}$$

MAPLE CALCULATIONS

Most of the calculations for the rotational spring stiffness is done in Maple. The script is shown below

```
> restart :
>
```

Rotational stiffness with the GM value

```
> k_rotation_GM := rho·g·V·GM :
> GM := 1/2·d + Ii/V − COG :
> Ii := 1/12·wp^4 : V := d·wp^2 :
> k_rotation_GM
```

$$\rho\, g\, d\, wp^2 \left(\frac{d}{2} + \frac{wp^2}{12\, d} - COG \right) \tag{1}$$

```
>
```

Rotational stiffness with vertical spring method

Three springs

```
> F1 := k·θ·L; F3 := -k·θ·L;
```

$$F1 := k\,\theta\,L$$

$$F3 := -k\,\theta\,L \tag{2}$$

```
> M1 := F1·L; M3 := -F3·L;
```

$$M1 := k\,\theta\,L^2$$

$$M3 := k\,\theta\,L^2 \tag{3}$$

```
> Mtot := M1 + M3;
```

$$Mtot := 2\,k\,\theta\,L^2 \tag{4}$$

```
> k_rotation := Mtot/θ;
```

$$k\_rotation := 2\,k\,L^2 \tag{5}$$

```
>
```

Five springs

```
> F1 := k·θ·2· L; F2 := k·θ·L; F4 := -k·θ·L; F5 := -k·θ·2· L;
```

$$F1 := 2\,k\,\theta\,L$$

$$F2 := k\,\theta\,L$$

$$F4 := -k\,\theta\,L$$

$$F5 := -2\,k\,\theta\,L \tag{6}$$

```
> M1 := F1·(2· L); M2 := F2·L; M4 := -F4·L; M5 := -F5·(2· L);
```

$$M1 := 4\,k\,\theta\,L^2$$

$$M2 := k\,\theta\,L^2$$

$$M4 := k\,\theta\,L^2$$

$$M5 := 4\,k\,\theta\,L^2 \tag{7}$$

```
> Mtot := M1 + M2 + M4 + M5;
```

$$Mtot := 10\,k\,\theta\,L^2 \tag{8}$$

> $k\_rotation := \frac{Mtot}{\theta}$;

$$k\_rotation := 10\, k\, L^2 \tag{9}$$

>

n springs and limit

> $k := \frac{\mathrm{rho} \cdot g \cdot wp^2}{n}$; $L := \frac{wp}{n}$;

$$k := \frac{\rho\, g\, wp^2}{n}$$

$$L := \frac{wp}{n} \tag{10}$$

> $k\_rotationsum := 2 \cdot k \cdot L^2 \cdot sum\left(x^2, x = 0 .. \frac{n-1}{2}\right)$:

>

> $k\_rotationlim := limit(k\_rotationsum, n = \infty)$;

$$k\_rotationlim := \frac{\rho\, g\, wp^4}{12} \tag{11}$$

With weight moment

> $M\_weight := m \cdot g \cdot \left(COG - \frac{1}{2} d\right) \cdot \theta$:

> $m := V \cdot \mathrm{rho}$: $V := d \cdot wp^2$:

> $k\_weight := \frac{M\_weight}{\theta}$;

$$k\_weight := d\, wp^2\, \rho\, g \left(COG - \frac{d}{2}\right) \tag{12}$$

Rotation spring stiffness formula

> $k\_rotation\_springs := k\_rotationlim - k\_weight$

$$k\_rotation\_springs := \frac{\rho\, g\, wp^4}{12} - d\, wp^2\, \rho\, g \left(COG - \frac{d}{2}\right) \tag{13}$$

>

>

Accuracy of the amount of springs

> *restart* :

> $k := \frac{\mathrm{rho} \cdot g \cdot wp^2}{n}$: $L := \frac{wp}{n}$:

> **for** n **from** 3 **by** 2 **to** 15 **do** $k\_rotationsum[n] := 2 \cdot k \cdot L^2 \cdot sum\left(x^2, x = 0 .. \frac{n-1}{2}\right)$ **end**

$$k\_rotationsum_3 := \frac{2\, \rho\, g\, wp^4}{27}$$

$$k\_rotationsum_5 := \frac{2\, \rho\, g\, wp^4}{25}$$

$$k\_rotationsum_7 := \frac{4\,\rho\,g\,wp^4}{49}$$

$$k\_rotationsum_9 := \frac{20\,\rho\,g\,wp^4}{243}$$

$$k\_rotationsum_{11} := \frac{10\,\rho\,g\,wp^4}{121}$$

$$k\_rotationsum_{13} := \frac{14\,\rho\,g\,wp^4}{169}$$

$$k\_rotationsum_{15} := \frac{56\,\rho\,g\,wp^4}{675} \quad \textbf{(14)}$$

> **for** n **from** 3 **by** 2 **to** 15 **do** $change[n] := evalf\left(\left(\frac{k\_rotationsum[n]}{k\_rotationsum[n-2]} - 1\right)\cdot 100\right)$ **end**

$$change_3 := \frac{7.407407407\,\rho\,g\,wp^4}{k\_rotationsum_1} - 100.$$

$$change_5 := 8.$$

$$change_7 := 2.040816327$$

$$change_9 := 0.8230452675$$

$$change_{11} := 0.4132231405$$

$$change_{13} := 0.2366863905$$

$$change_{15} := 0.1481481481 \quad \textbf{(15)}$$

>

```
restart :
with(plots) :
```

Three springs ODE's

ODE's

```
ODE1 := EI·diff(w1(x), x$4) = 0 :
ODE2 := EI·diff(w2(x), x$4) = 0 :

sol := dsolve({ODE1, ODE2}, {w1(x), w2(x)}) : assign(sol) :
w1 := w1(x) : w2 := w2(x) :
```

Relations

```
phi1 := -diff(w1, x) : kappa1 := diff(phi1, x) : M1 := kappa1·EI : V1 := diff(M1, x) :
phi2 := -diff(w2, x) : kappa2 := diff(phi2, x) : M2 := kappa2·EI : V2 := diff(M2, x) :
```

Boundry conditions

```
x := -L : eq1 := 0 = V1 − k·w1 : eq2 := M1 = 0 :
x := 0 : eq3 := w1 = w2 : eq4 := phi1 = phi2 : eq5 := M1 = M2 + Mrotation : eq6 := 0 = -k·w1
     + V2 − V1 :
x := L : eq7 := 0 = -k·w2 − V2 : eq8 := M2 = 0 :
```

Solving the constants in the deformation formula's

```
sol1 := solve({eq1, eq2, eq3, eq4, eq5, eq6, eq7, eq8}, {_C1, _C2, _C3, _C4, _C5, _C6, _C7,
     _C8}) : assign(sol1) :
```

Finding the relation between the moment and the rotation in the middle of the platform

```
x := 0 : eq1 := θ = phi1
```

$$eq1 := \theta = \frac{Mrotation\,(L^3 k + 3\,EI)}{6\,L^2\,EI\,k} \tag{1}$$

```
sol := solve({eq1}, {Mrotation}); assign(sol) :
```

$$sol := \left\{ Mrotation = \frac{6\,\theta\,L^2\,EI\,k}{L^3 k + 3\,EI} \right\} \tag{2}$$

Checking if the limit of EI to infinity is equal to the hand calculation

```
limit(Mrotation/θ, EI = ∞);
```

$$2\,L^2 k \tag{3}$$

Five springs ODE's

```
restart :
```

ODE's

```
> ODE1 := EI·diff(w1(x), x$4) = 0 :
> ODE2 := EI·diff(w2(x), x$4) = 0 :
> ODE3 := EI·diff(w3(x), x$4) = 0 :
> ODE4 := EI·diff(w4(x), x$4) = 0 :
>
> sol := dsolve({ODE1, ODE2, ODE3, ODE4}, {w1(x), w2(x), w3(x), w4(x)}) : assign(sol) :
> w1 := w1(x) : w2 := w2(x) : w3 := w3(x) : w4 := w4(x) :
>
```

Relations

```
> phi1 := -diff(w1, x) : kappa1 := diff(phi1, x) : M1 := kappa1·EI : V1 := diff(M1, x) :
> phi2 := -diff(w2, x) : kappa2 := diff(phi2, x) : M2 := kappa2·EI : V2 := diff(M2, x) :
> phi3 := -diff(w3, x) : kappa3 := diff(phi3, x) : M3 := kappa3·EI : V3 := diff(M3, x) :
> phi4 := -diff(w4, x) : kappa4 := diff(phi4, x) : M4 := kappa4·EI : V4 := diff(M4, x) :
>
```

Boundry conditions

```
> x := -2·L : eq1 := 0 = V1 - k·w1 : eq2 := M1 = 0 :
> x := -L : eq3 := w1 = w2 : eq4 := phi1 = phi2 : eq5 := M1 = M2 : eq6 := 0 = -k·w1 + V2
      - V1 :
> x := 0 : eq7 := w2 = w3 : eq8 := phi2 = phi3 : eq9 := M2 = M3 + Mrotation : eq10 := 0 = -k
     ·w2 + V3 - V2 :
> x := L : eq11 := w3 = w4 : eq12 := phi3 = phi4 : eq13 := M3 = M4 : eq14 := 0 = -k·w3 + V4
      - V3 :
> x := 2·L : eq15 := 0 = -k·w4 - V4 : eq16 := M4 = 0 :
>
```

Solving the constants in the deformation formula's

```
> sol1 := solve({eq1, eq2, eq3, eq4, eq5, eq6, eq7, eq8, eq9, eq10, eq11, eq12, eq13, eq14, eq15,
      eq16}, {_C1, _C2, _C3, _C4, _C5, _C6, _C7, _C8, _C9, _C10, _C11, _C12, _C13, _C14,
      _C15, _C16}) : assign(sol1) :
>
```

Finding the relation between the moment and the rotation in the middle of the platform

```
> x := 0 : eq1 := θ = phi2
```

$$eq1 := \theta = \frac{Mrotation\left(7\,L^6\,k^2 + 108\,EI\,L^3\,k + 36\,EI^2\right)}{24\,EI\,L^2\left(2\,L^3\,k + 15\,EI\right)k} \tag{4}$$

```
> sol := solve({eq1}, {Mrotation}); assign(sol) :
```

$$sol := \left\{Mrotation = \frac{24\,\theta\,EI\,L^2\left(2\,L^3\,k + 15\,EI\right)k}{7\,L^6\,k^2 + 108\,EI\,L^3\,k + 36\,EI^2}\right\} \tag{5}$$

Checking if the limit of EI to infinity is equal to the hand calculation

```
> limit(Mrotation/θ, EI = ∞);
```

$$10\,L^2\,k \tag{6}$$

```
>
```

Nine springs ODE's

```
> restart :
```

ODE's

```
> ODE1 := EI·diff(w1(x), x$4) = 0 :
> ODE2 := EI·diff(w2(x), x$4) = 0 :
> ODE3 := EI·diff(w3(x), x$4) = 0 :
> ODE4 := EI·diff(w4(x), x$4) = 0 :
> ODE5 := EI·diff(w5(x), x$4) = 0 :
> ODE6 := EI·diff(w6(x), x$4) = 0 :
> ODE7 := EI·diff(w7(x), x$4) = 0 :
> ODE8 := EI·diff(w8(x), x$4) = 0 :
>
> sol := dsolve({ODE1, ODE2, ODE3, ODE4, ODE5, ODE6, ODE7, ODE8}, {w1(x), w2(x),
      w3(x), w4(x), w5(x), w6(x), w7(x), w8(x)}) : assign(sol) :
> w1 := w1(x) : w2 := w2(x) : w3 := w3(x) : w4 := w4(x) : w5 := w5(x) : w6 := w6(x) :
      w7 := w7(x) : w8 := w8(x) :
>
```

Relations

```
> phi1 := -diff(w1, x) : kappa1 := diff(phi1, x) : M1 := kappa1·EI : V1 := diff(M1, x) :
> phi2 := -diff(w2, x) : kappa2 := diff(phi2, x) : M2 := kappa2·EI : V2 := diff(M2, x) :
> phi3 := -diff(w3, x) : kappa3 := diff(phi3, x) : M3 := kappa3·EI : V3 := diff(M3, x) :
> phi4 := -diff(w4, x) : kappa4 := diff(phi4, x) : M4 := kappa4·EI : V4 := diff(M4, x) :
> phi5 := -diff(w5, x) : kappa5 := diff(phi5, x) : M5 := kappa5·EI : V5 := diff(M5, x) :
> phi6 := -diff(w6, x) : kappa6 := diff(phi6, x) : M6 := kappa6·EI : V6 := diff(M6, x) :
> phi7 := -diff(w7, x) : kappa7 := diff(phi7, x) : M7 := kappa7·EI : V7 := diff(M7, x) :
> phi8 := -diff(w8, x) : kappa8 := diff(phi8, x) : M8 := kappa8·EI : V8 := diff(M8, x) :
>
```

Boundry conditions

```
> x := -4·L : eq1 := 0 = V1 - k·w1 : eq2 := M1 = 0 :
> x := -3·L : eq3 := w1 = w2 : eq4 := phi1 = phi2 : eq5 := M1 = M2 : eq6 := 0 = -k·w1 + V2
      - V1 :
> x := -2·L : eq7 := w2 = w3 : eq8 := phi2 = phi3 : eq9 := M2 = M3 : eq10 := 0 = -k·w2 + V3
      - V2 :
> x := -L : eq11 := w3 = w4 : eq12 := phi3 = phi4 : eq13 := M3 = M4 : eq14 := 0 = -k·w3 + V4
      - V3 :
> x := 0 : eq15 := w4 = w5 : eq16 := phi4 = phi5 : eq17 := M4 = M5 + Mrotation : eq18 := 0 =
      -k·w4 + V5 - V4 :
> x := L : eq19 := w5 = w6 : eq20 := phi5 = phi6 : eq21 := M5 = M6 : eq22 := 0 = -k·w5 + V6
      - V5 :
> x := 2·L : eq23 := w6 = w7 : eq24 := phi6 = phi7 : eq25 := M6 = M7 : eq26 := 0 = -k·w6 + V7
      - V6 :
> x := 3·L : eq27 := w7 = w8 : eq28 := phi7 = phi8 : eq29 := M7 = M8 : eq30 := 0 = -k·w7 + V8
      - V7 :
> x := 4·L : eq31 := 0 = -k·w8 - V8 : eq32 := M8 = 0 :
>
```

Solving the constants in the deformation formula's

```
> sol1 := solve({eq1, eq2, eq3, eq4, eq5, eq6, eq7, eq8, eq9, eq10, eq11, eq12, eq13, eq14, eq15,
      eq16, eq17, eq18, eq19, eq20, eq21, eq22, eq23, eq24, eq25, eq26, eq27, eq28, eq29, eq30,
      eq31, eq32}, {_C1, _C2, _C3, _C4, _C5, _C6, _C7, _C8, _C9, _C10, _C11, _C12, _C13,
```

$$\_C14, \_C15, \_C16, \_C17, \_C18, \_C19, \_C20, \_C21, \_C22, \_C23, \_C24, \_C25, \_C26, \_C27, \_C28, \_C29, \_C30, \_C31, \_C32\}) : assign(sol1) :$$

Finding the relation between the moment and the rotation in the middle of the platform

> $x := 0 : eq1 := \theta = phi4$

$$eq1 := \theta = \frac{Mrotation\left(97\,L^{12}k^4 + 4332\,EI\,L^9k^3 + 38340\,EI^2L^6k^2 + 43200\,EI^3L^3k + 1296\,EI^4\right)}{24\,L^2k\left(28\,L^9k^3 + 981\,EI\,L^6k^2 + 5832\,EI^2L^3k + 3240\,EI^3\right)EI} \tag{7}$$

> $sol := solve(\{eq1\}, \{Mrotation\}); assign(sol) :$

$$sol := \left\{Mrotation = \frac{24\,\theta\,L^2k\left(28\,L^9k^3 + 981\,EI\,L^6k^2 + 5832\,EI^2L^3k + 3240\,EI^3\right)EI}{97\,L^{12}k^4 + 4332\,EI\,L^9k^3 + 38340\,EI^2L^6k^2 + 43200\,EI^3L^3k + 1296\,EI^4}\right\} \tag{8}$$

Checking if the limit of EI to infinity is equal to the hand calculation

> $limit\left(\frac{Mrotation}{\theta}, EI = \infty\right);$

$$60\,L^2k \tag{9}$$

> $k := \frac{rho \cdot g \cdot wp^2}{9} : L := \frac{wp}{9} :$

> $Mrotation$

$$\left(8\,\theta\,wp^4\rho\,g\left(\frac{28}{282429536481}\,g^3\rho^3\,wp^{15} + \frac{109}{4782969}\,EI\,g^2\rho^2\,wp^{10} + \frac{8}{9}\,EI^2g\,\rho\,wp^5 + 3240\,EI^3\right)EI\right) \Big/ \left(243\left(\frac{97}{1853020188851841}\,g^4\rho^4\,wp^{20} + \frac{1444}{94143178827}\,EI\,g^3\rho^3\,wp^{15} + \frac{1420}{1594323}\,EI^2g^2\rho^2\,wp^{10} + \frac{1600}{243}\,EI^3g\,\rho\,wp^5 + 1296\,EI^4\right)\right) \tag{10}$$

> $Digits := 3 :$

> $evalf\left(\frac{Mrotation}{\theta}\right)$

$$\left(0.0329\,wp^4\rho\,g\left(9.91\,10^{-11}g^3\rho^3\,wp^{15} + 0.0000228\,EI\,g^2\rho^2\,wp^{10} + 0.889\,EI^2g\,\rho\,wp^5 + 3240.\,EI^3\right)EI\right) \Big/ \left(5.23\,10^{-14}g^4\rho^4\,wp^{20} + 1.53\,10^{-8}EI\,g^3\rho^3\,wp^{15} + 0.000891\,EI^2g^2\rho^2\,wp^{10} + 6.58\,EI^3g\,\rho\,wp^5 + 1300.\,EI^4\right) \tag{11}$$

APPENDIX X – GROWING WAVES

To investigate the motion for a growing wave the total solution is calculated for an extreme case: A building of 500 m high and a platform width of 500m at the Atlantic Ocean. In this research a devolving time of 40 hours is determined for a devolving storm. However, as the building can also sail into a storm the same calculations are done with an 1 hour developing time. In the first paragraph the determination of the growth factor of the wave is shown (same as in chapter 6), then the results are shown for the developing time of 40 hours and then of 1 hour.

GROWTH FACTOR

To investigate the response to a wave with a growing wave, a growth factor must be added to the formula of the wave. A normal exponential function was not used for this growth because this would mean that after reaching the full height (growth factor = 1), the wave would continue to grow. Instead, a formula for the growth factor was sought that starts "slowly" and does not exceed 1. In mathematical terms, the function must have a limit of $\lim_{t\to-\infty}(g(t)) = 0$ and $\lim_{t\to\infty}(g(t)) = 1$ This can be achieved with a so-called "S" curve. The standard formula for an S curve is as follows

$$\frac{1}{1+e^{-t}} \tag{A-X.1}$$

However, a typical S curve has a value of 0.5 at t = 0. The growth factor at t = 0 should actually be 0. In addition, the value 1 is approached very quickly. Therefore, a few adjustments have been made to the formula. The formula has been shifted and a factor has been added so that the formula has a value of 0.001 (=0.1%) at t = 0 and a value of 0.999 (=99.9%) at t = develop time. In this case, the develop time is equal to 40 hours * 60 * 60 = 144000 seconds or 1 hours *60*60. The formula becomes:

$$growth\ factor\ (t) = \frac{1}{1+e^{-0.0000959271*(t-\frac{1}{2}*144000)}} \tag{A-X..2}$$

For 40 hours. The growth factor for the develop time of 40 hours looks as follows:

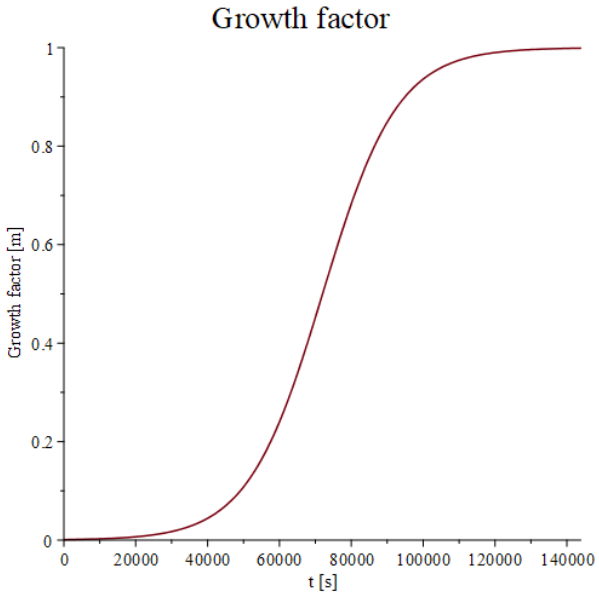

Figure 149 - Growth factor of the growing wave, developing time is 40 hours.

This growth factor is added to sine and cosine part of both the wave load and to the standard formula used to solve the particular part of the equation of motion, see the equations below.

$$\boldsymbol{F} = \begin{bmatrix} Growth\ factor * \widehat{F}_{ver,1,wave} * \sin(\omega_{wave} t) \\ 0 \\ 0 \\ Growth\ factor * \widehat{F}_{hor,1,wave} * \sin(\omega_{wave} t) + \widehat{F}_{hor,1,wind} * \sin(\omega_{wind} t) \\ \widehat{F}_{hor,2,wind} * \sin(\omega_{wind} t) \\ \widehat{F}_{hor,3,wind} * \sin(\omega_{wind} t) \\ Growth\ factor * \widehat{M}_{rot,1,wave} * \sin(\omega_{wave} t) + \widehat{M}_{rot,1,wind} * \sin(\omega_{wind} t) \\ \widehat{M}_{rot,2,wind} * \sin(\omega_{wind} t) \\ \widehat{M}_{rot,3,wind} * \sin(\omega_{wind} t) \end{bmatrix} \quad \text{(A-X.3)}$$

$$w_i(t) = C_{i,1} * Growth\ factor * sin(\omega_{wave} t) + C_{i,2} * Growth\ factor * cos(\omega_{wave} t) + C_{i,3} * sin(\omega_{wind} t) + C_{i,4} * cos(\omega_{wind} t)\ [m] \quad \text{(A-X.4)}$$

DEVELOPING TIME = 40 HOURS

Four graphs have been produced for each of the three different motions. Graph one is the displacement/rotation from t = 0 to t = 40 hours. This is the "Developing wave". Graph two is the displacement/rotation from t = 40 hours to t = 40 hours + 300 seconds. This is the "Fully developed wave". The third and fourth graphs have the same time intervals but deal only with the homogeneous solution.

VERTICAL MOTION

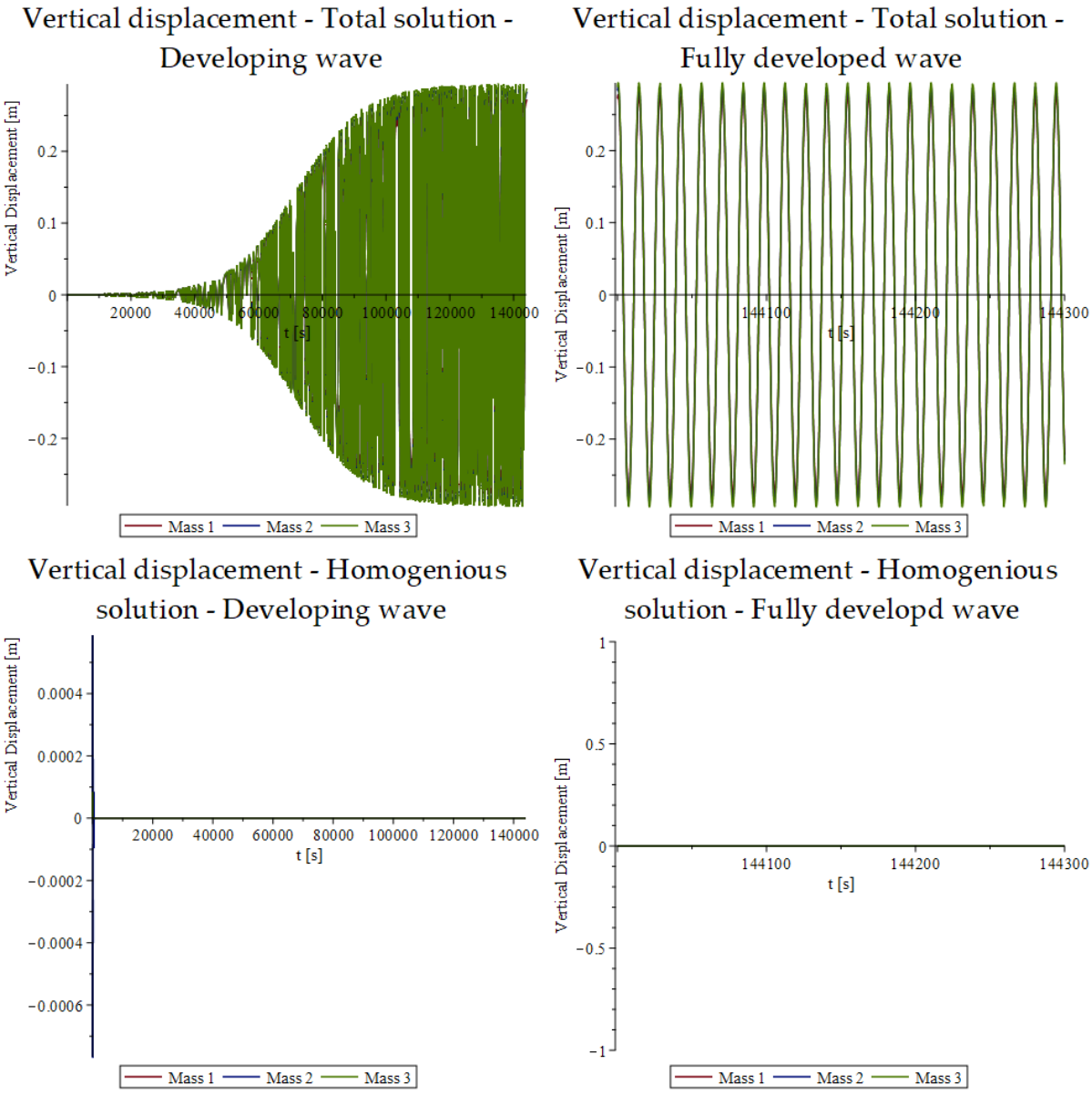

Figure 150 - Growing wave result of the vertical motion with a developing time of 40 hours. a) displacement from t = 0 to t = 40 hours. b) the displacement from t = 40 hours to t = 40 hours + 300 seconds. c) homogeneous part of the displacement from t = 0 to t = 40 hours. d) homogeneous part of the displacement from t = 40 hours to t = 40 hours + 300 seconds.

HORIZONTAL MOTION

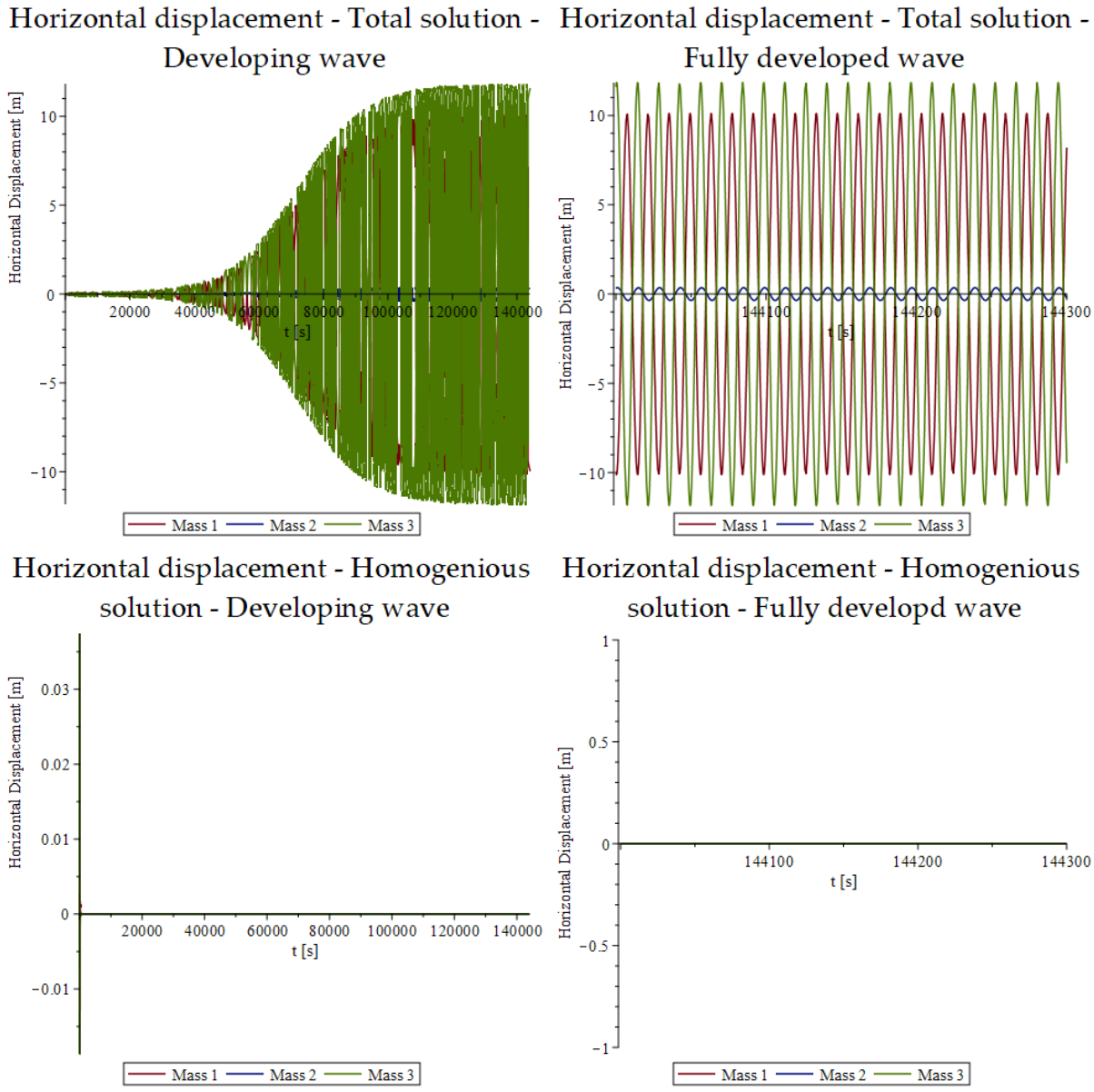

Figure 151 - Growing wave result of the horizontal motion with a developing time of 40 hours. a) displacement from t = 0 to t = 40 hours. b) the displacement from t = 40 hours to t = 40 hours + 300 seconds. c) homogeneous part of the displacement from t = 0 to t = 40 hours. d) homogeneous part of the displacement from t = 40 hours to t = 40 hours + 300 seconds.

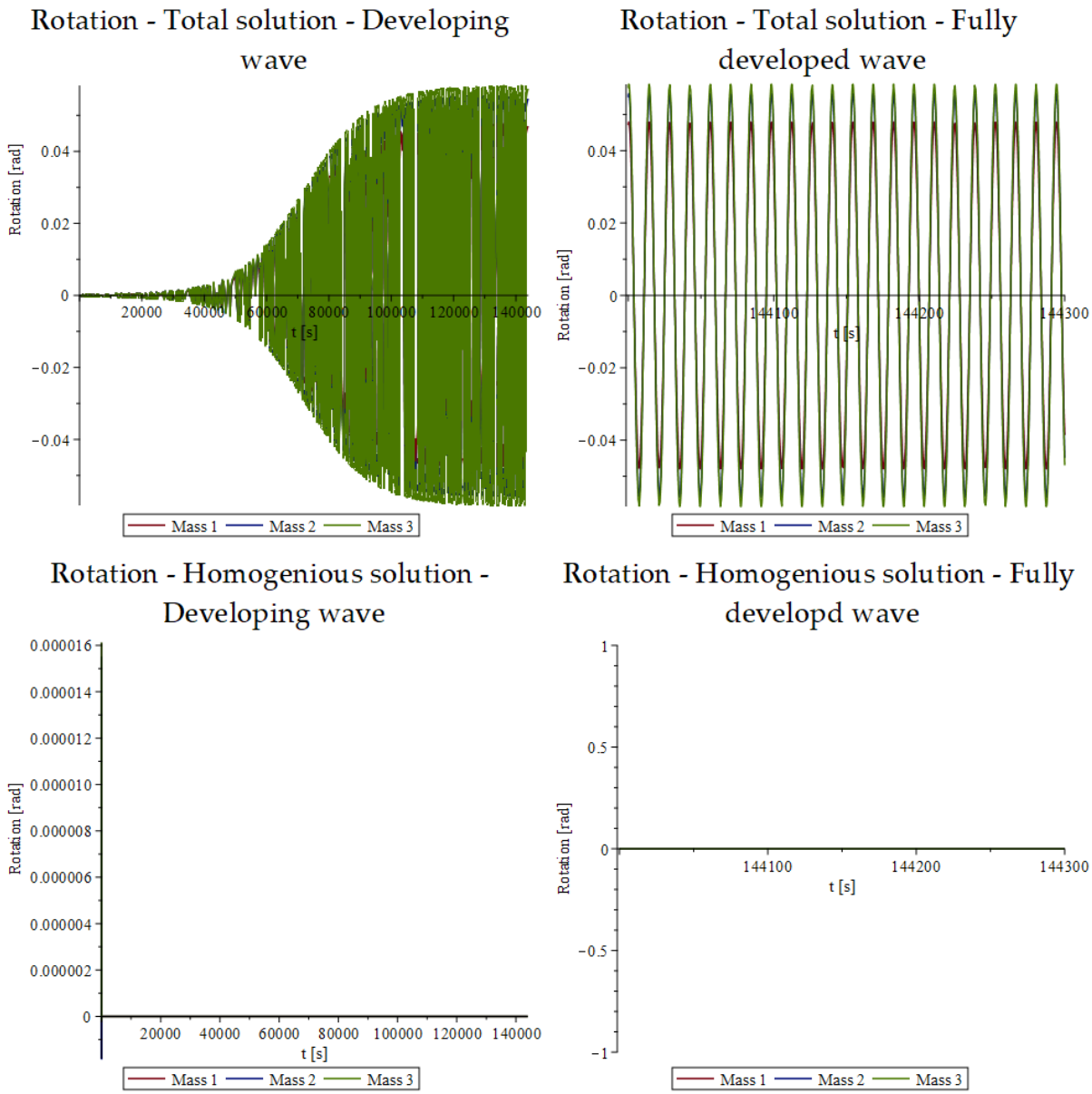

Figure 152 - Growing wave result of the rotational motion with a developing time of 40 hours. a) the rotation from t = 0 to t = 40 hours. b) the rotation from t = 40 hours to t = 40 hours + 300 seconds. c) homogeneous part of the rotation from t = 0 to t = 40 hours. d) homogeneous part of the rotation from t = 40 hours to t = 40 hours + 300 seconds.

DEVELOPING TIME = 1 HOUR

The graphs have the same setup as for the developing time of 40 hours.

VERTICAL MOTION

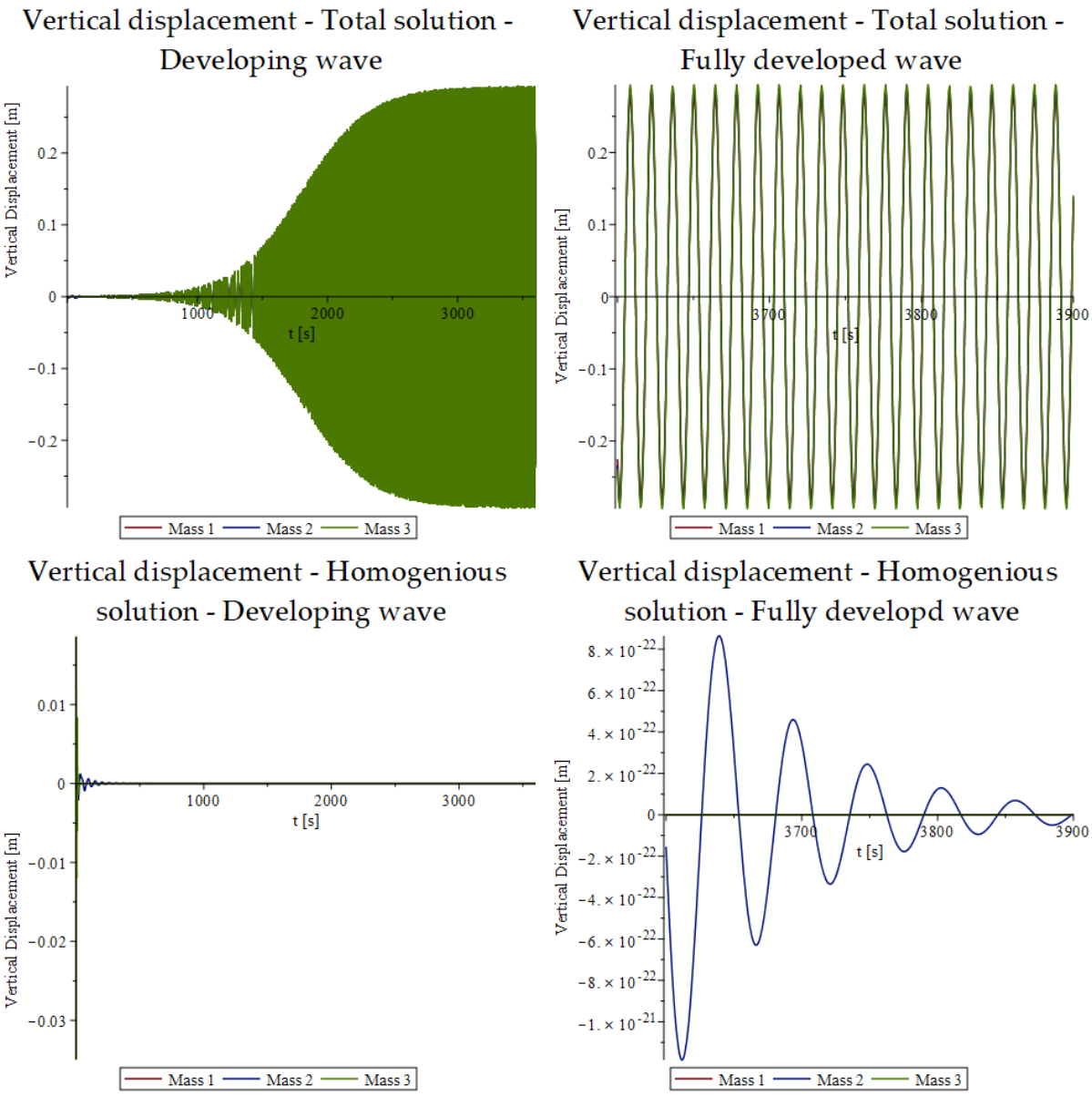

Figure 153 - Growing wave result of the vertical motion with a developing time of 1 hour. a) displacement from t = 0 to t = 1 hour. b) the displacement from t = 1 hour to t = 1 hour + 300 seconds. c) homogeneous part of the displacement from t = 0 to t = 1 hour. d) homogeneous part of the displacement from t = 1 hour to t = 1 hour + 300 seconds.

HORIZONTAL MOTION

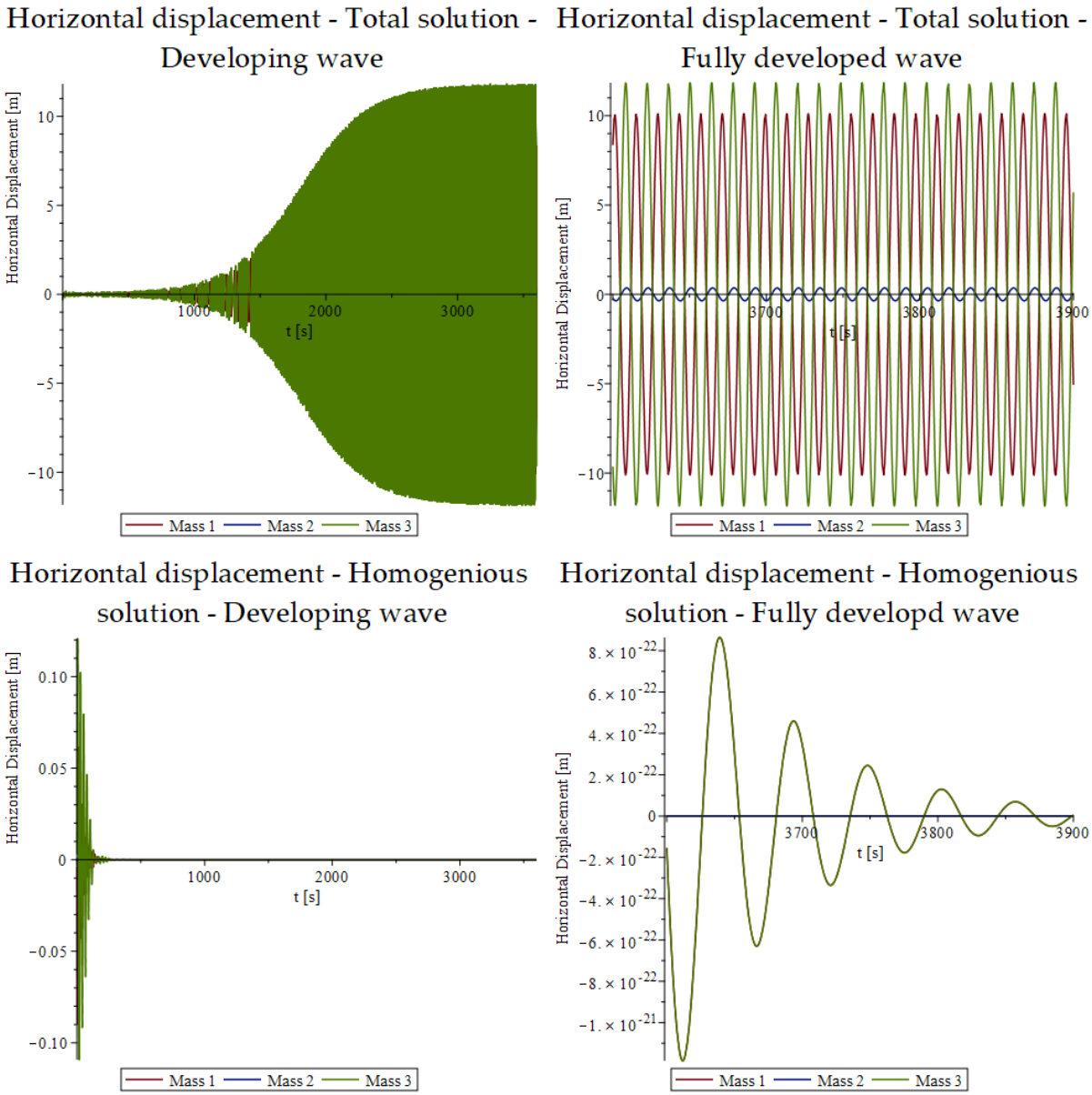

Figure 154 - Growing wave result of the horizontal motion with a developing time of 1 hour. a) displacement from t = 0 to t = 1 hour. b) the displacement from t = 1 hour to t = 1 hour + 300 seconds. c) homogeneous part of the displacement from t = 0 to t = 1 hour. d) homogeneous part of the displacement from t = 1 hour to t = 1 hour + 300 seconds.

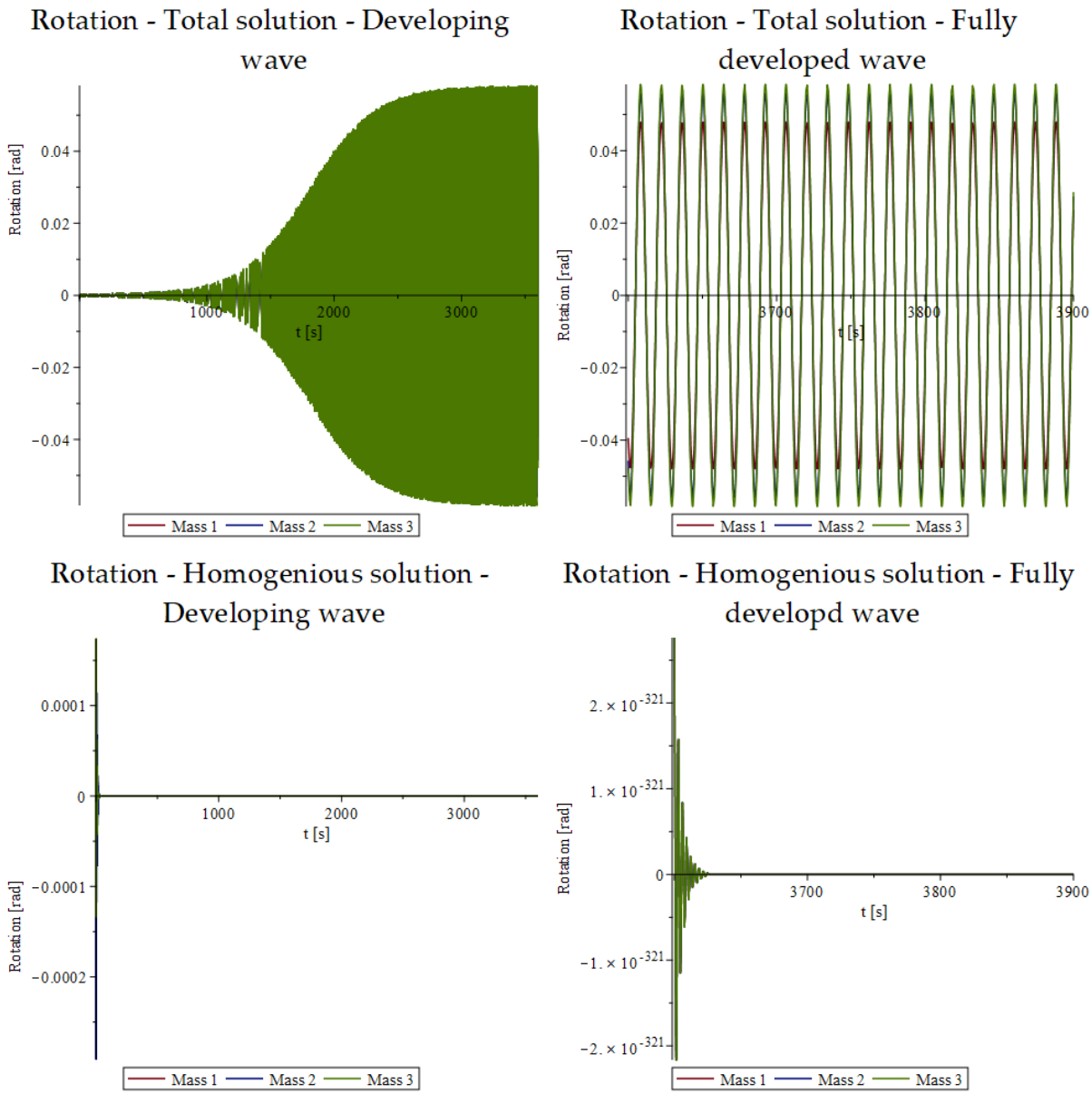

Figure 155 - Growing wave result of the rotational motion with a developing time of 1 hour. a) the rotation from t = 0 to t = 1 hour. b) the rotation from t = 1 hour to t = 1 hour + 300 seconds. c) homogeneous part of the rotation from t = 0 to t = 1 hour. d) homogeneous part of the rotation from t = 1 hour to t = 1 hour + 300 seconds.

APPENDIX XI – INFLUENCING PARAMETERS

This appendix discuss the influencing parameters: Height of the centre of gravity and damping.

Height of the centre of gravity

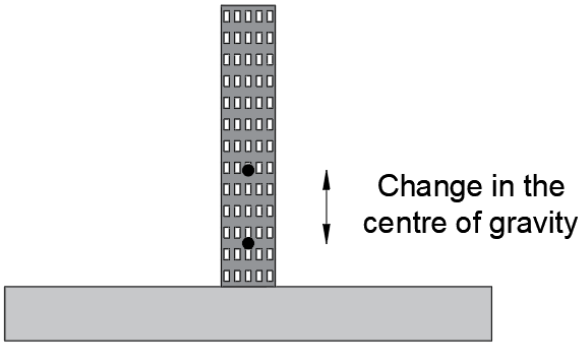

Figure 156 - Change in the height of the centre of gravity.

The results for the maximum accelerations for different height of the centre of gravity (COG) of the floating high-rise are shown in Figure 157. These are the horizontal and angular acceleration of all three masses. The COG has no direct influence on the vertical acceleration and this acceleration is thus not included.

The figure shows that the COG height has almost no influence on the horizontal acceleration and the angular acceleration (In the figure, the angular acceleration seems to decrease strongly. However, if one looks at the values on the vertical axis, one can see that the decrease is minimal.) Thus, changing the COG has a minimal influence on all accelerations. This is interesting because the GM value, which has a big influence, is determined by this COG value.

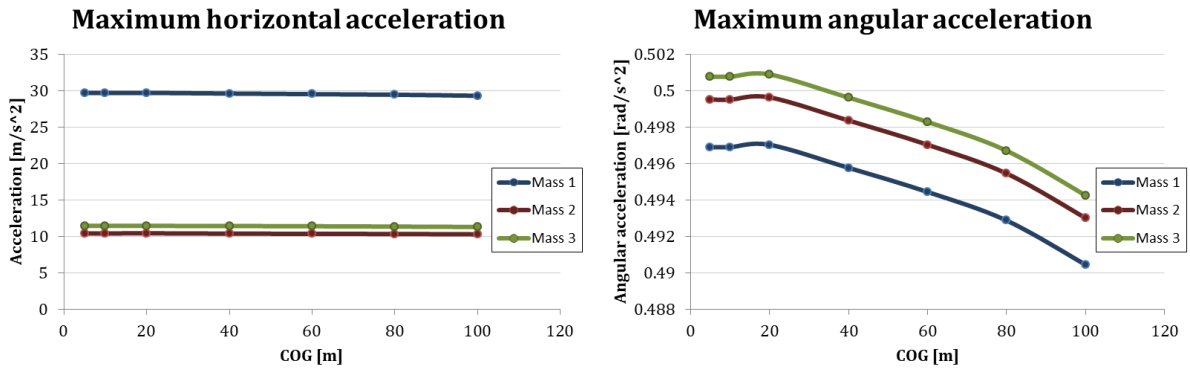

Figure 157 - Maximum accelerations for different centre of gravity heights. a) Horizontal acceleration. b) Angular acceleration.

Damping

The results for the maximum accelerations for different height of the centre of gravity (COG) of the floating high-rise are shown in Figure 158. These are the vertical, horizontal and angular acceleration of all three masses.

The accelerations of the masses all decrease with increasing damping as in the single-mass models. The damping has a greater influence on the horizontal acceleration, especially of the lower

mass, and on the angular acceleration. Increasing the damping constant can thus bring about a significant reduction in the acceleration.

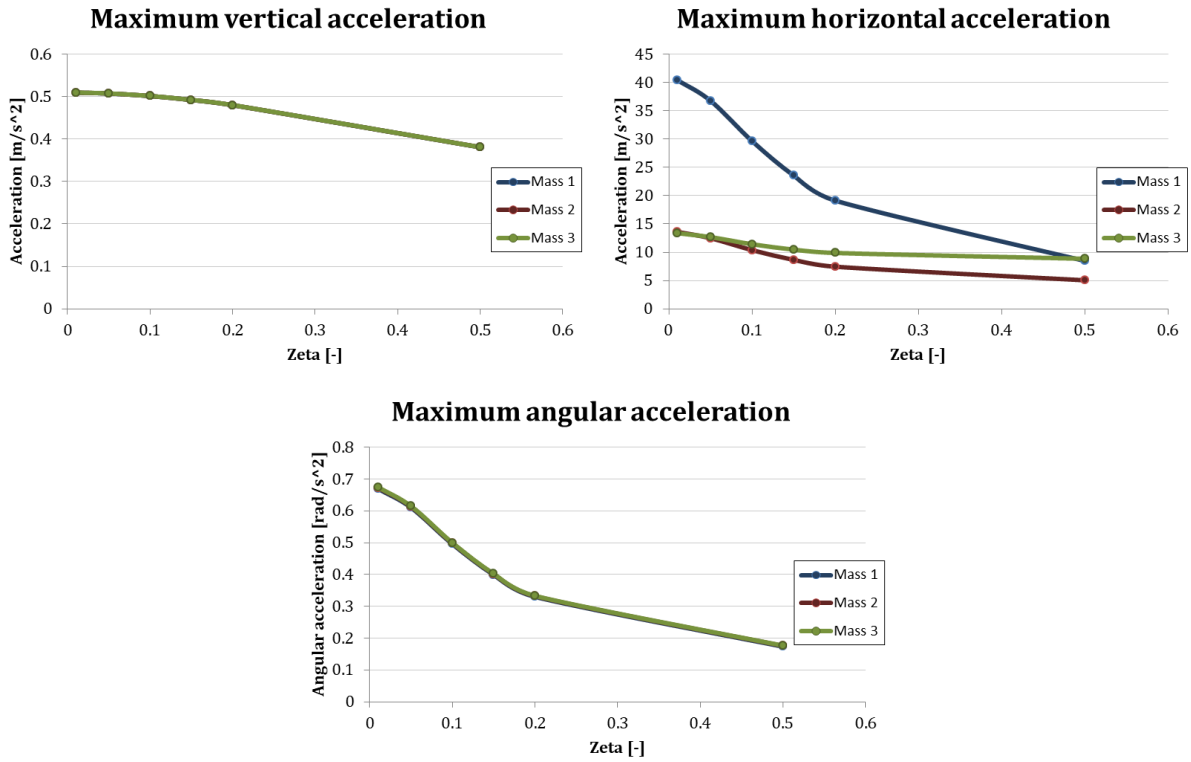

Figure 158 - Maximum accelerations for different damping values zeta. a) Vertical acceleration. b) Horizontal acceleration. c) Angular acceleration.

APPENDIX XII – MOTION AT THE TOP OF THE BUILDING

This appendix shows the determination of the motion and acceleration at the top of the building.

In this study, the building and the platform were modelled as three point masses connected with a 1d element, see Figure 159, to determine the dynamic stability. The figure shows that the position of the point masses is chosen such that the top two have the same amount of mass. This ensures that the top mass is not at the top of the building but at $4/5$ of the height. Due to the rotation of the platform, the building will translate horizontally, the higher the building, the greater this translation. So there is a big chance that the top of the building is normative for the accelerations. Therefore a calculation has been made to use the results for the motions of the three masses to calculate the motion of the top of the building. This calculation is shown here.

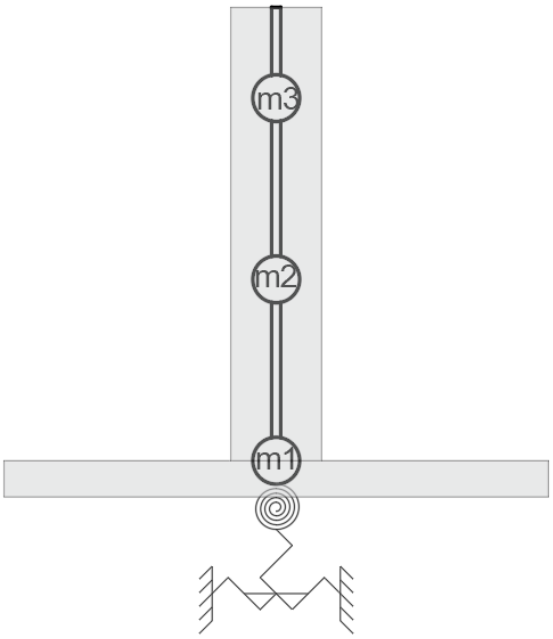

Figure 159 - Multiple-mass model for the dynamic stability.

For the calculations, the building is modelled as a beam, as in the static and dynamic stability. The deformation of a beam has the following expression:

$$EI * \frac{d^4u}{dx^4} = q \tag{A-XII.1}$$

Where

EI is the bending stiffness of the building

u is the deformation

x is the relative position

q is the external load

The external load is equal to zero in this case. The formula shows that the deformation itself is a third degree polynomial. It can be written as:

$$u(x) = c_1x^3 + c_2x^2 + c_3x + c_4 \quad \text{(A-XII.2)}$$

Where

c_i are unknown constants

In this case the "x" is the height from the bottom of the building. That means that the point masses are at the heights:

$$h_1 = 0,\ h_2 = \frac{hb}{3-\frac{1}{2}}\ and\ h_3 = \frac{2*hb}{3-\frac{1}{2}} \quad \text{(A-XII.3)}$$

Where

h_i is the height of point mass i

hb is the height of the building

This is illustrated in the figure below:

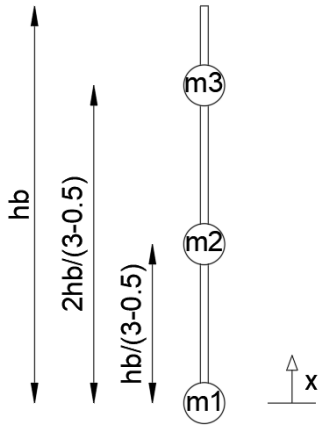

Figure 160 - Relative position of the point masses.

The deformation at these three points are known. These are the horizontal motions of the three point masses. These depend on the time. To keep the equations simple the dependency on the time has been omitted. The polynomial needs four equations to solve the unknowns. The fourth equation will be the rotation at $h_1 = 0$. This rotation is also know. The rotation can be calculated by taking the derivative of the deflection. This gives the following four equations:

$$u(0) = c_4 = u_1 \quad \text{(A-XII.4)}$$

$$u\left(\frac{hb}{3-\frac{1}{2}}\right) = \frac{8}{125} * c_1 * hb^3 + \frac{4}{25} * c_2 * hb^2 + \frac{2}{5} * c_3 * hb\ +\ c_4 = u_2 \quad \text{(A-XII.5)}$$

$$u\left(\frac{2*hb}{3-\frac{1}{2}}\right) = \frac{64}{125} * c_1 * hb^3 + \frac{16}{25} * c_2 * hb^2 + \frac{4}{5} * c_3 * hb\ +\ c_4 = u_3 \quad \text{(A-XII.6)}$$

$$\frac{du}{dx}(0) = c_3 = \theta_1 \tag{A-XII.7}$$

Where

u_i is the horizontal displacement of the point masses.

θ_1 is the rotation of the bottom mass.

Solving these equations gives the following result:

$$c_1 = 25 * \frac{4 * hb * \theta + 15 * u_1 - 20 * u_2 + 5 * u_3}{32 * hb^3} \tag{A-XII.8}$$

$$c_2 = -5 * \frac{12 * hb * \theta + 35 * u_1 - 40 * u_2 + 5 * u_3}{16 * hb^2} \tag{A-XII.9}$$

$$c_3 = \theta \tag{A-XII.10}$$

$$c_4 = u_1 \tag{A-XII.11}$$

The expression for de deformation becomes:

$$u(x) = 25 * \frac{4 * hb * \theta + 15 * u_1 - 20 * u_2 + 5 * u_3}{32 * hb^3} x^3 - 5 * \frac{12 * hb * \theta + 35 * u_1 - 40 * u_2 + 5 * u_3}{16 * hb^2} x^2 + \theta x + u_1 \tag{A-XII.12}$$

The deformation at the top of the building can be calculated by using $x = hb$:

$$u(hb) = \frac{3 * hb * \theta(t)}{8} + \frac{57 * u_1(t)}{32} - \frac{25 * u_2(t)}{8} + \frac{75 * u_3(t)}{32} \tag{A-XII.13}$$

In this equation the dependency on the variable time is shown for the horizontal translation and the rotation. To calculate the rotation at the top of the building, the derivative of $u(x)$ to x must be calculated and then $x = hb$ must be entered. For the acceleration of the horizontal motion, the double derivative of $u(hb)$ to time (t) must be calculated.

APPENDIX XIII – MAXIMUM ACCELERATION CALCULATIONS MULTIPLE MASS MODEL

In this appendix the results of the multiple mass model are shown. These will consist of results from the three locations: North Sea, Atlantic Ocean and equator. For the North Sea results are shown for a 100, 300 and 500 m building and for a 100 m building with a set depth of 20 m. For the Atlantic Ocean only a building of 100m and a building of 100 m with a set depth of 20 m is shown. Finally for the equator only the results for a 100 m building is shown.

NORTH SEA

HEIGHT BUILDING = 100 M

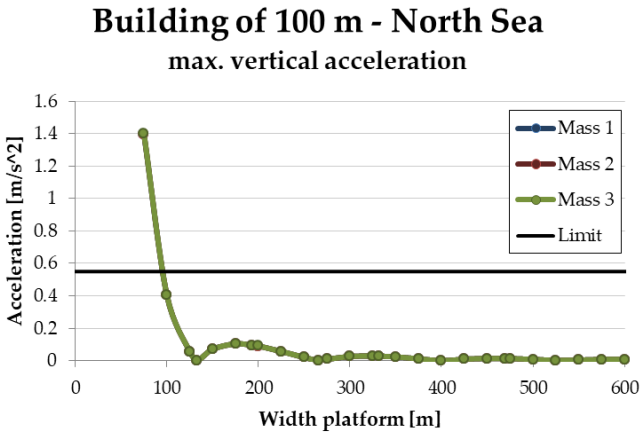

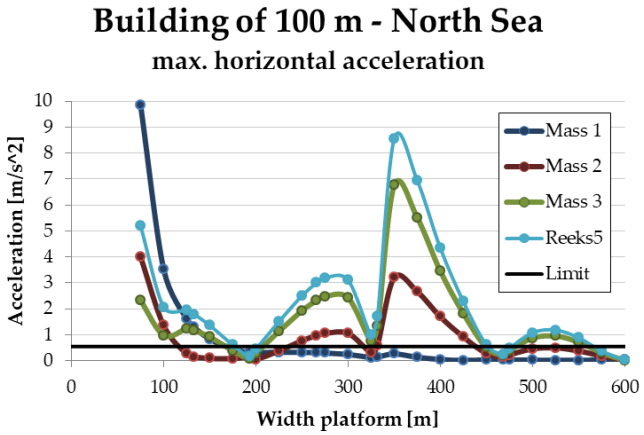

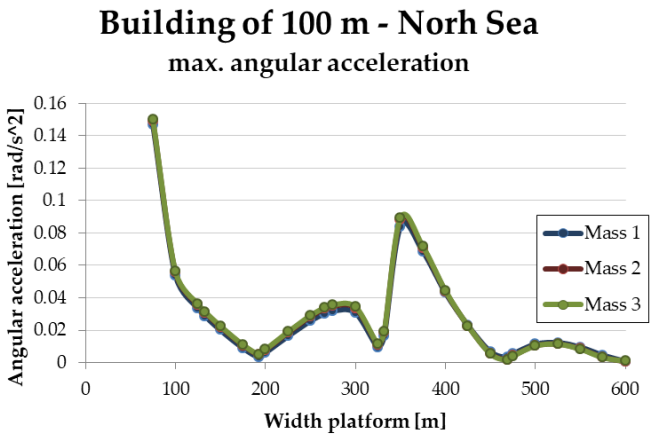

Figure 161 - Maximum acceleration of the three motions for a building of 100 m at the North Sea.

HEIGHT BUILDING = 300 M

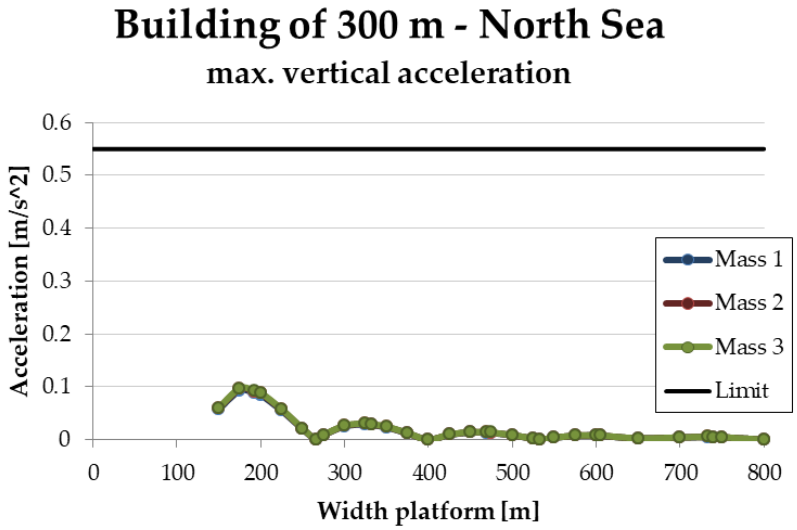

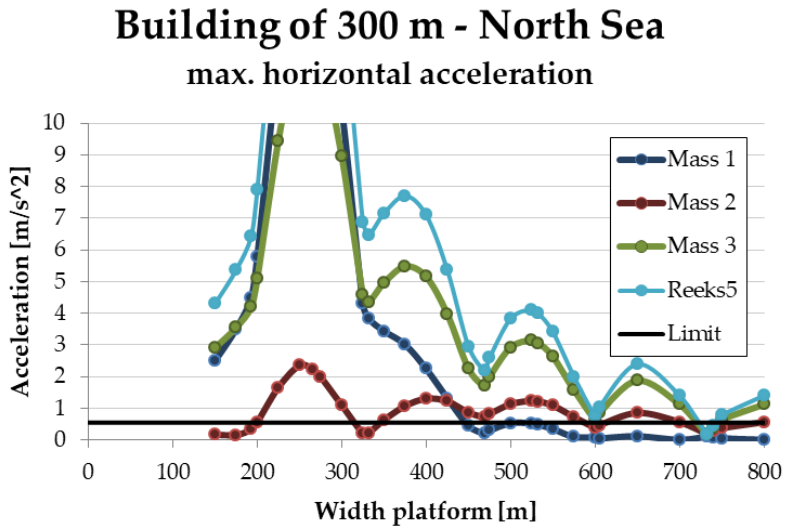

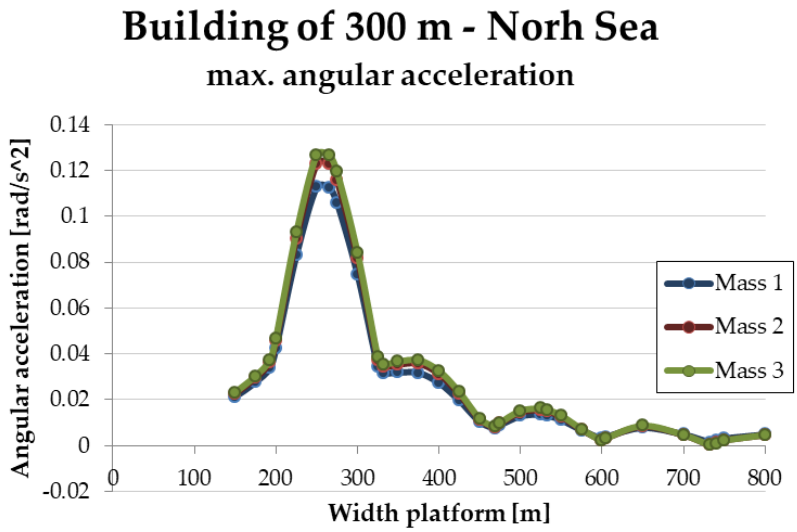

Figure 162 - Maximum acceleration of the three motions for a building of 300 m at the North Sea.

HEIGHT BUILDING = 500 M

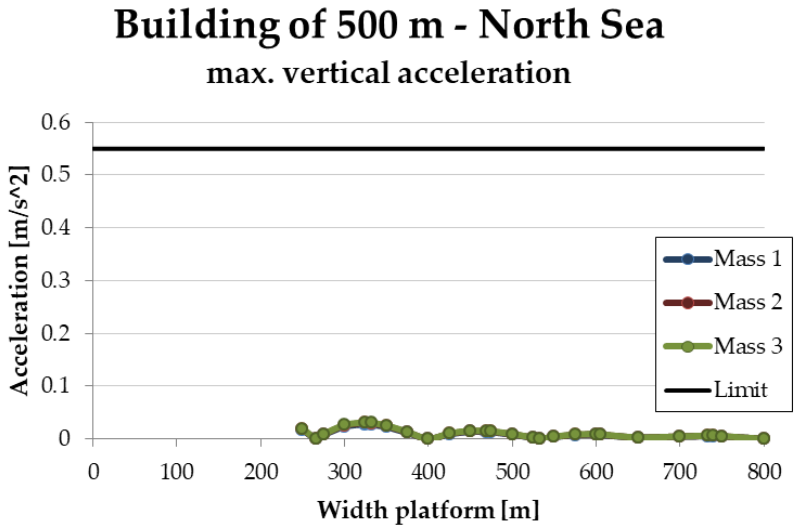

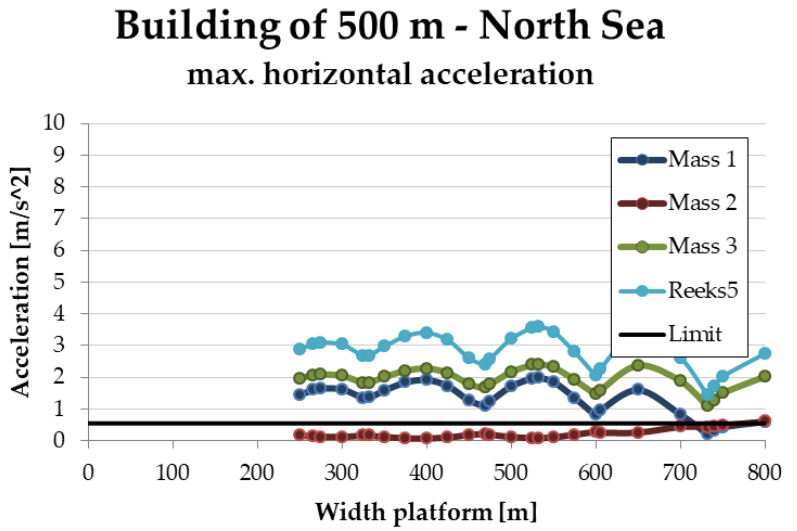

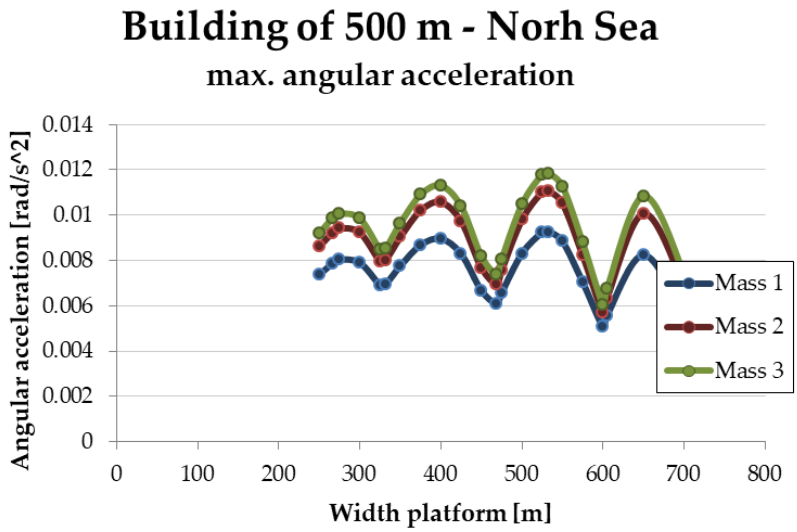

Figure 163 - Maximum acceleration of the three motions for a building of 500 m at the North Sea.

HEIGHT BUILDING = 100 M AND DEPTH = 20 M

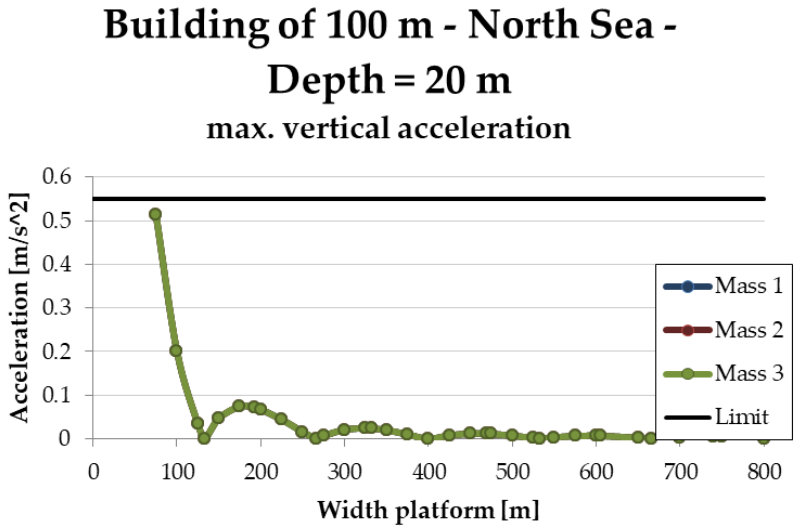

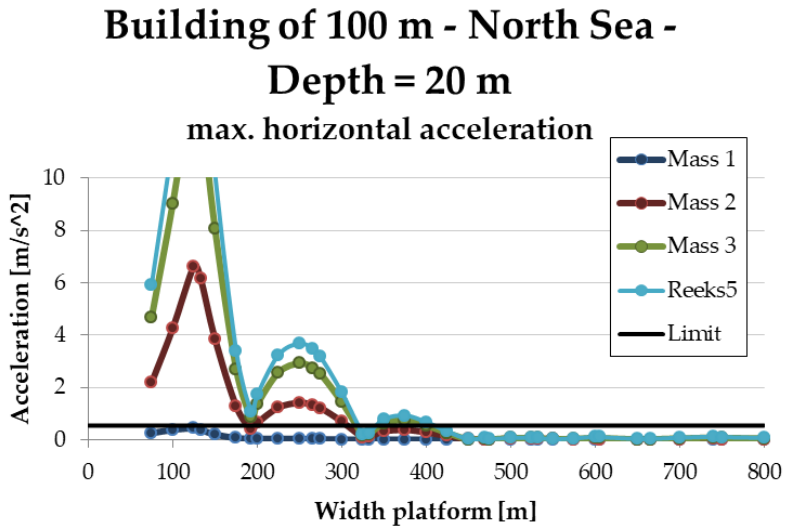

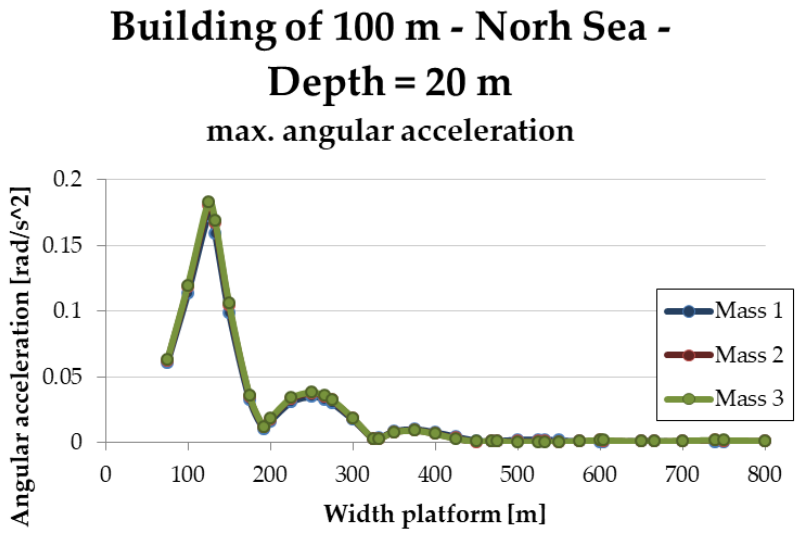

Figure 164 - Maximum acceleration of the three motions for a building of 100 m and a depth of 20 m at the North Sea.

ATLANTIC OCEAN

HEIGHT BUILDING = 100 M

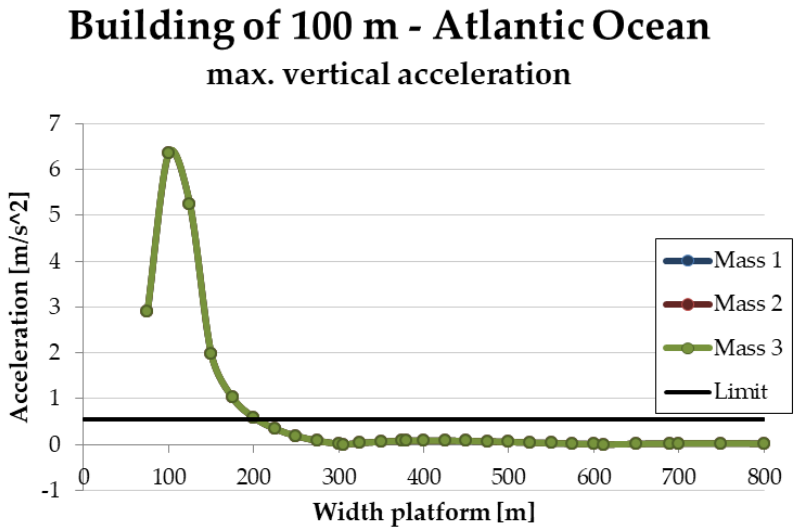

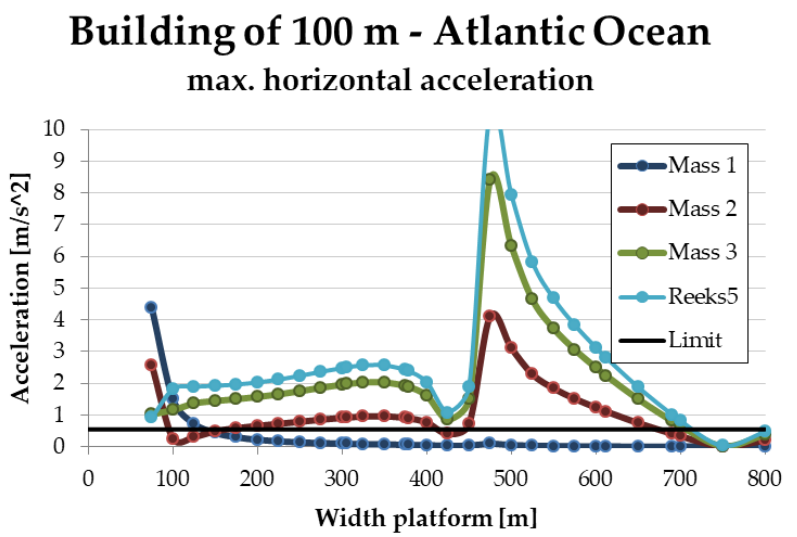

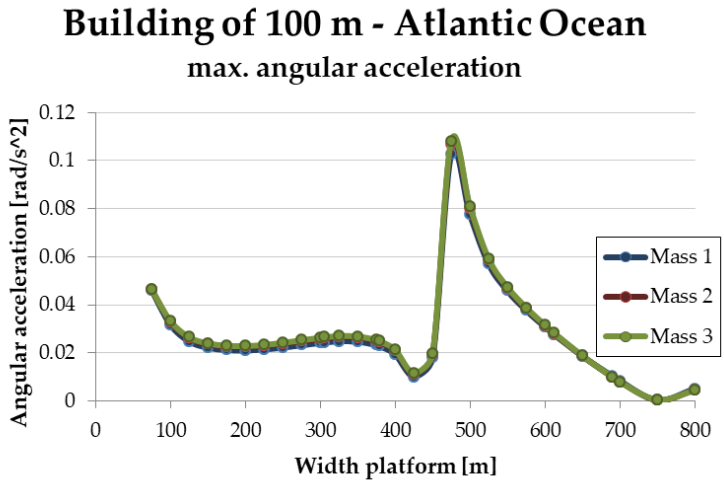

Figure 165 - Maximum acceleration of the three motions for a building of 100 m at the Atlantic ocean.

HEIGHT BUILDING = 100 M AND DEPTH = 20 M

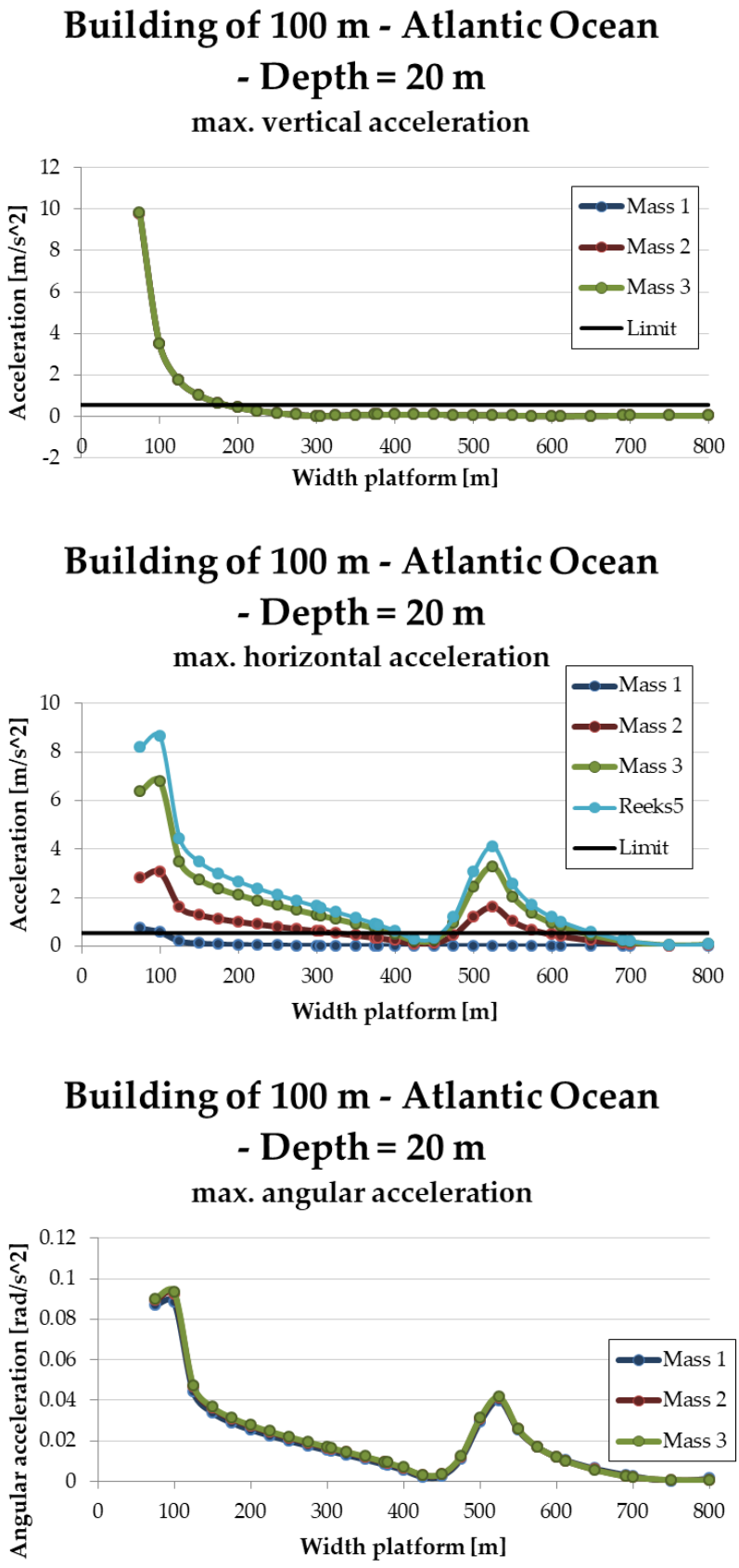

Figure 166 - Maximum acceleration of the three motions for a building of 100 m and a depth of 20 m at the Atlantic ocean.

EQUATOR

HEIGHT BUILDING = 100 M

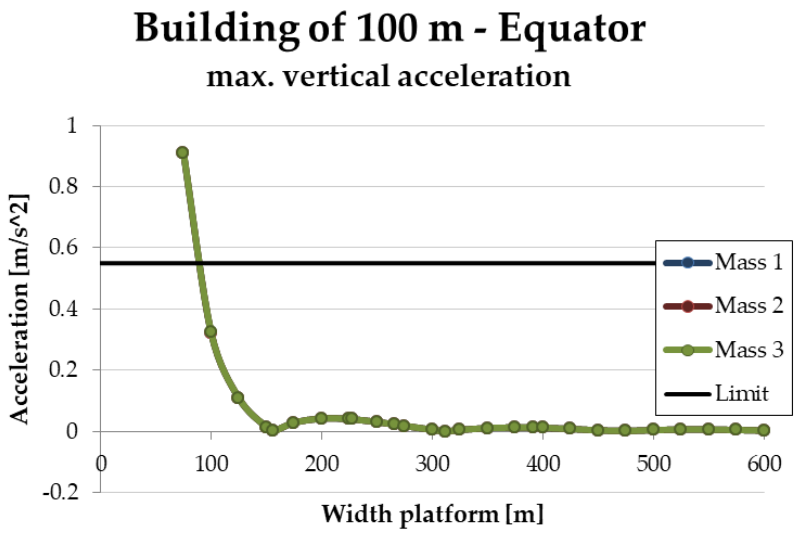

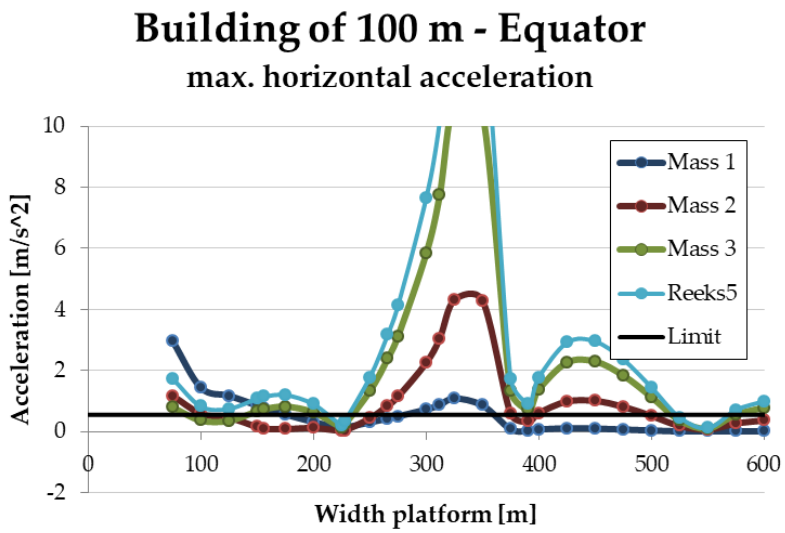

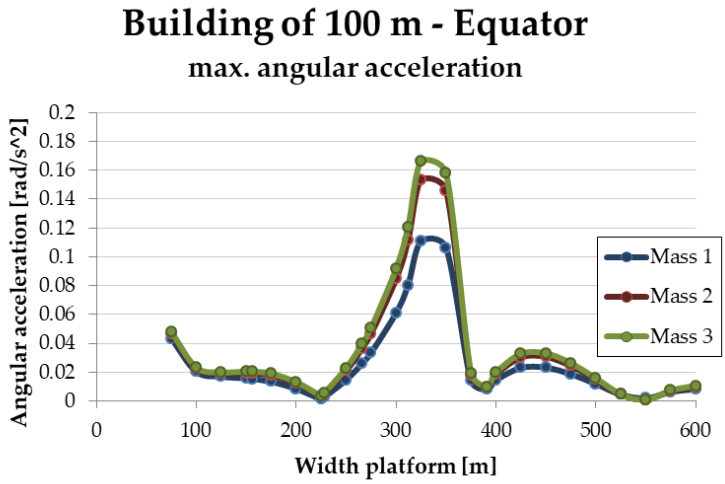

Figure 167 - Maximum acceleration of the three motions for a building of 100 m at the Equator.

APPENDIX XIV – LIMITATION DUE TO THE FREQUENCY

This appendix shows the results and the calculation of the limits of frequencies for the three different motions for the three locations in the first paragraph. First the results are shown for the North Sea. For the equator the results are almost the same and thus are not shown extensively. At last the result for the Atlantic ocean are shown.

In the second paragraph the results are shown of the calculation of the eigenfrequencies of both the single-mass models and the multi-mass models. These are compared in graphs. These are all results for the North Sea.

RESULTS

NORTH SEA

In the program Maple, the eigenfrequency is expressed in the two independent parameters; height of the building and width of the platform for a predetermined depth and height of the platform. With this expression, a 3D graph can be made. This is used to visualise what is done and to check whether the following steps taken are correct. The 3D graphs of the three motion can be seen below for a depth of 20 m. The red surface is the limiting frequency of 0.43 rad/s

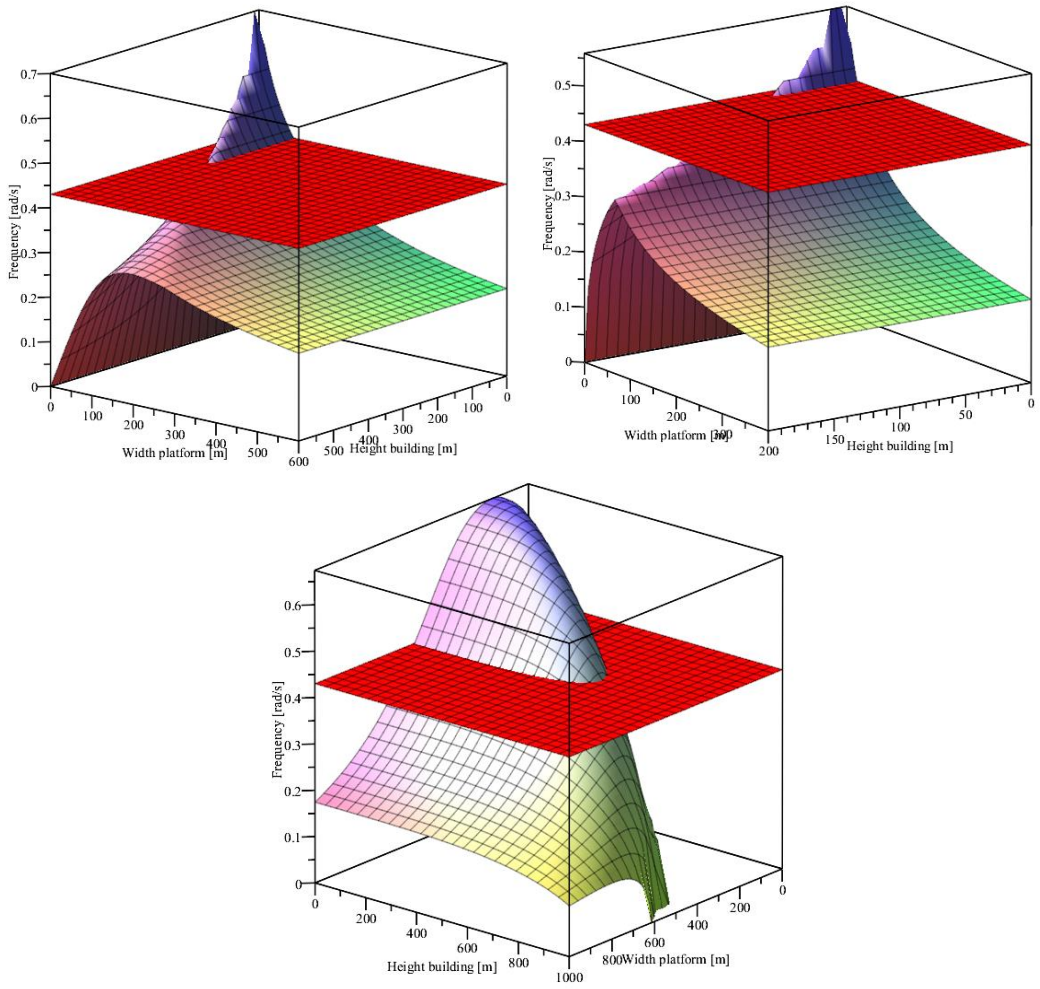

Figure 168 - 3D graph of the eigenfrequency of a) the vertical motion and b) horizontal motion. c) rotational motion with a depth of 20 m for the conditions at the North Sea.

The three limits are calculated for different depths. In addition to these three limits, the depth limit and the static stability limit were also calculated/added to obtain the following graphs:

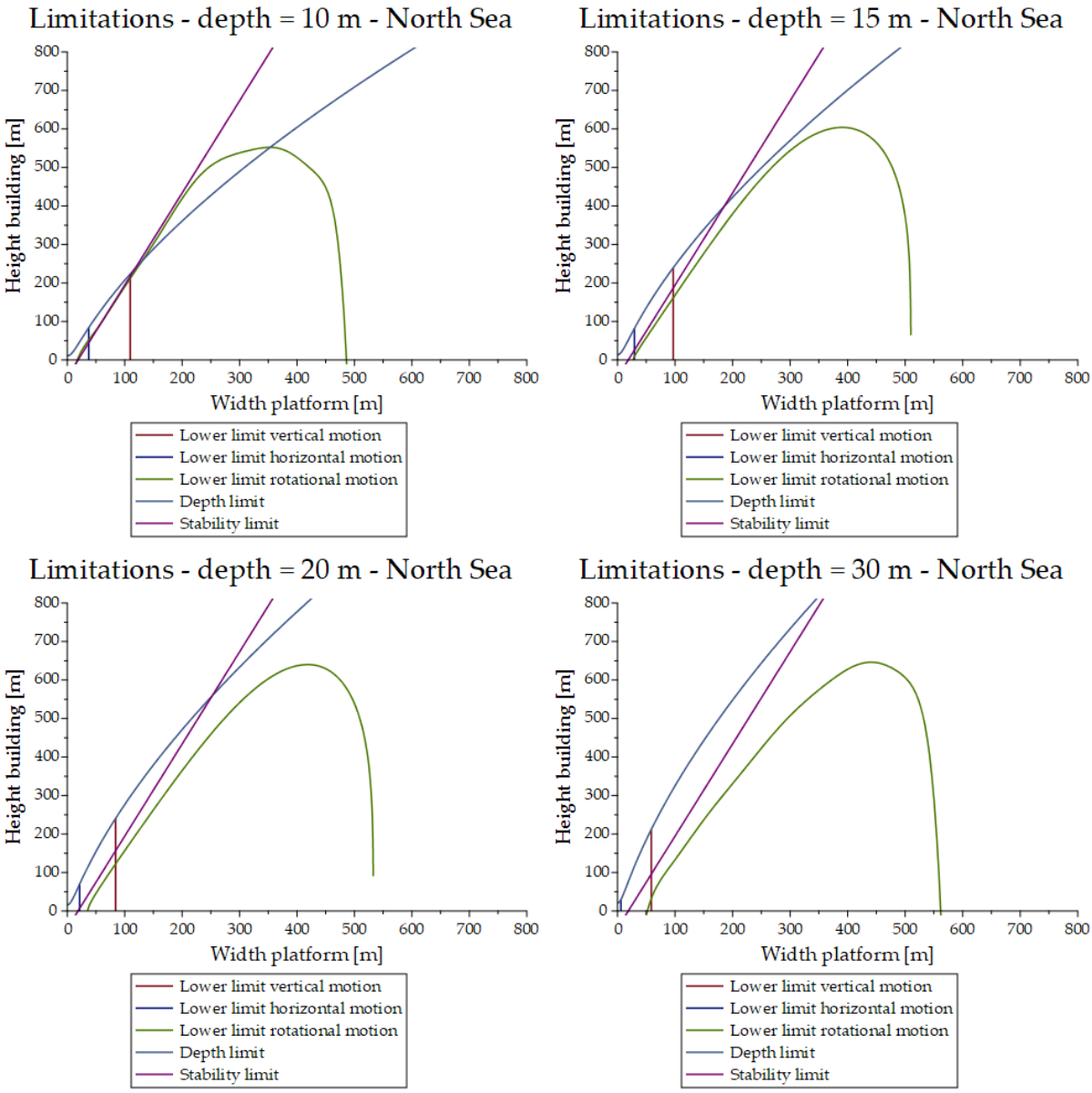

Figure 169 - Limitations for the North Sea for a platform depth of a) 10 m. b) 15 m. c) 20 m. d) 30 m.

Both the vertical and horizontal frequency limit have a vertical boundary. This can be seen as the minimum platform width required to avoid resonance. Because these can therefore be used in the design of a floating high-rise building, the values have been precisely determined. The results are shown in the table below.

Table 49 - Platform width values of the vertical limiting frequency boundaries for the vertical and horizontal motion at the North Sea for different depths.

Depth [m]	15	20	30*
Limit platform width vertical motion [m]	97	84	59
Limit platform width horizontal motion [m]	29	22	6

* Note that at the North Sea this depth is actually not possible or the chosen input.

EQUATOR

For the equator, the results are the same as for the North Sea. Since the only location condition that has an influence is the frequency limit and this is almost the same for these locations, the North Sea can be looked at for the equator when it comes to these limits.

ATLANTIC OCEAN

The same calculations and graphs were made for the Atlantic Ocean location. These can be seen below.

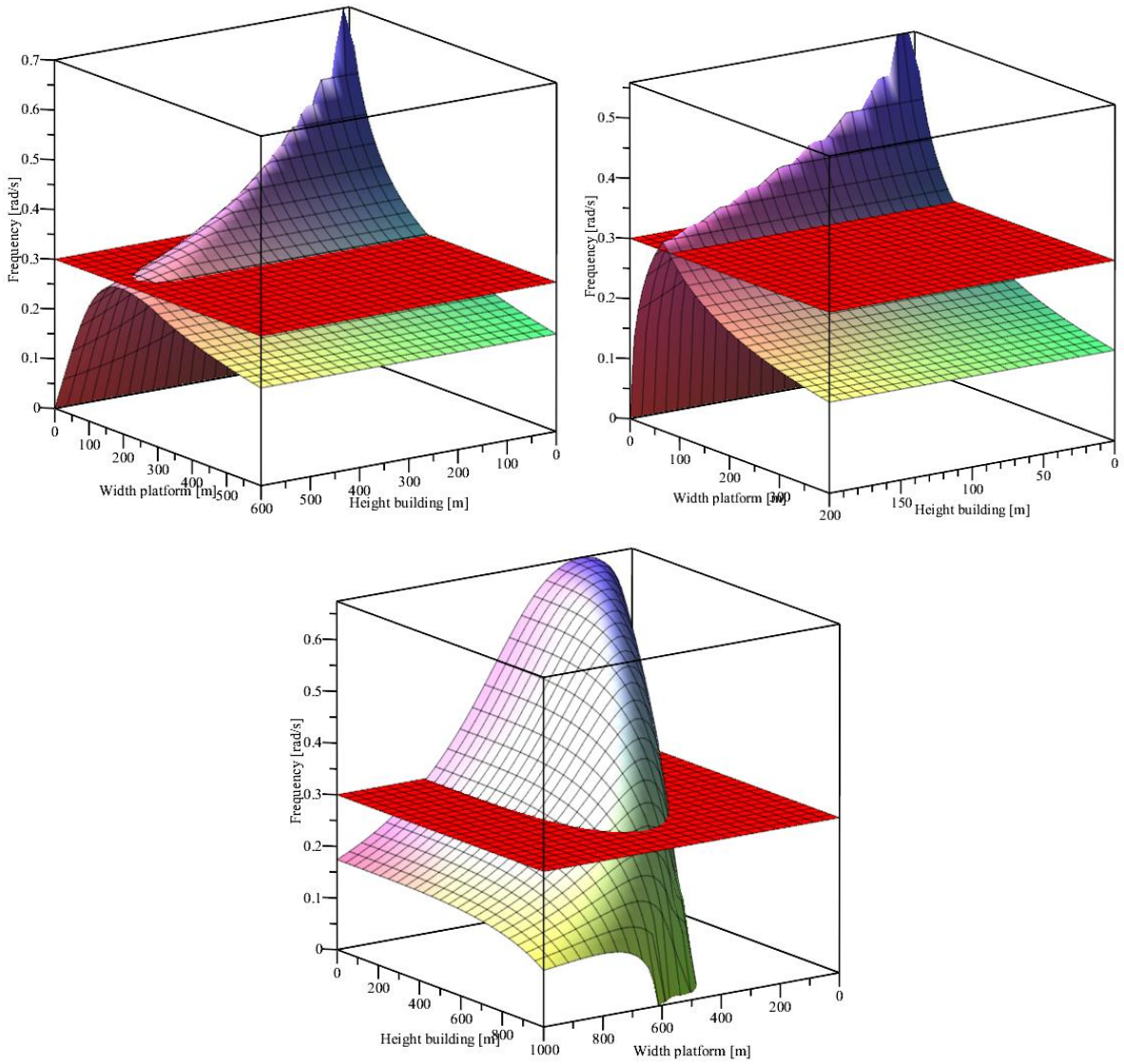

Figure 170 - 3D graph of the eigenfrequency of a) the vertical motion and b) horizontal motion. c) rotational motion with a depth of 20 m for the conditions at the Atlantic ocean.

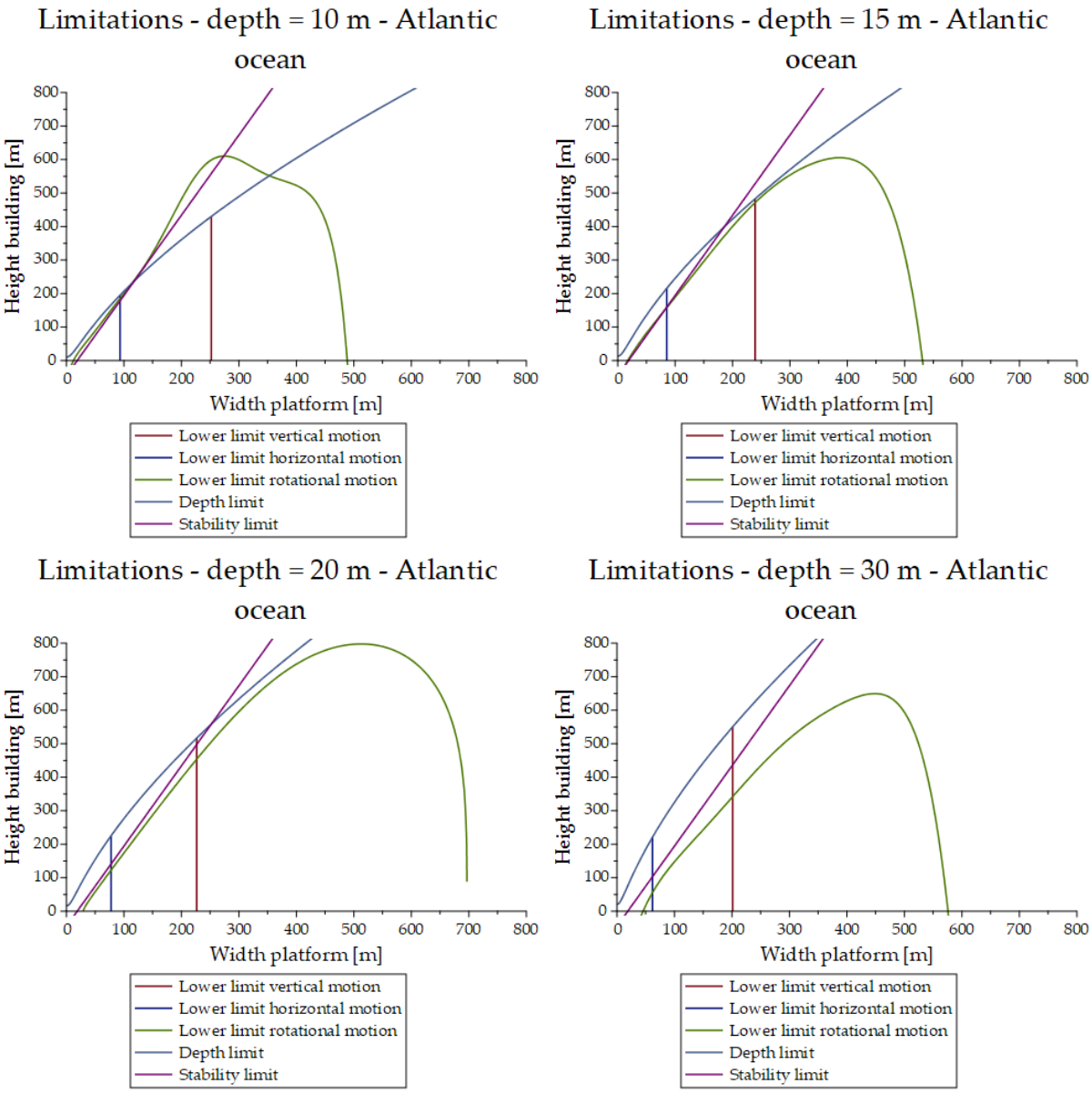

Figure 171 - Limitations for the Atlantic ocean for a platform depth of a) 10 m. b) 15 m. c) 20 m. d) 30 m.

Table 50 - Platform width values of the vertical limiting frequency boundaries for the vertical and horizontal motion at the Atlantic ocean for different depths.

Depth [m]	15	20	30
Limit platform width vertical motion [m]	239	226	201
Limit platform width horizontal motion [m]	85	78	62

SINGLE MASS VS MULTIPLE MASS MODEL

BUILDING HEIGHT = 100 M

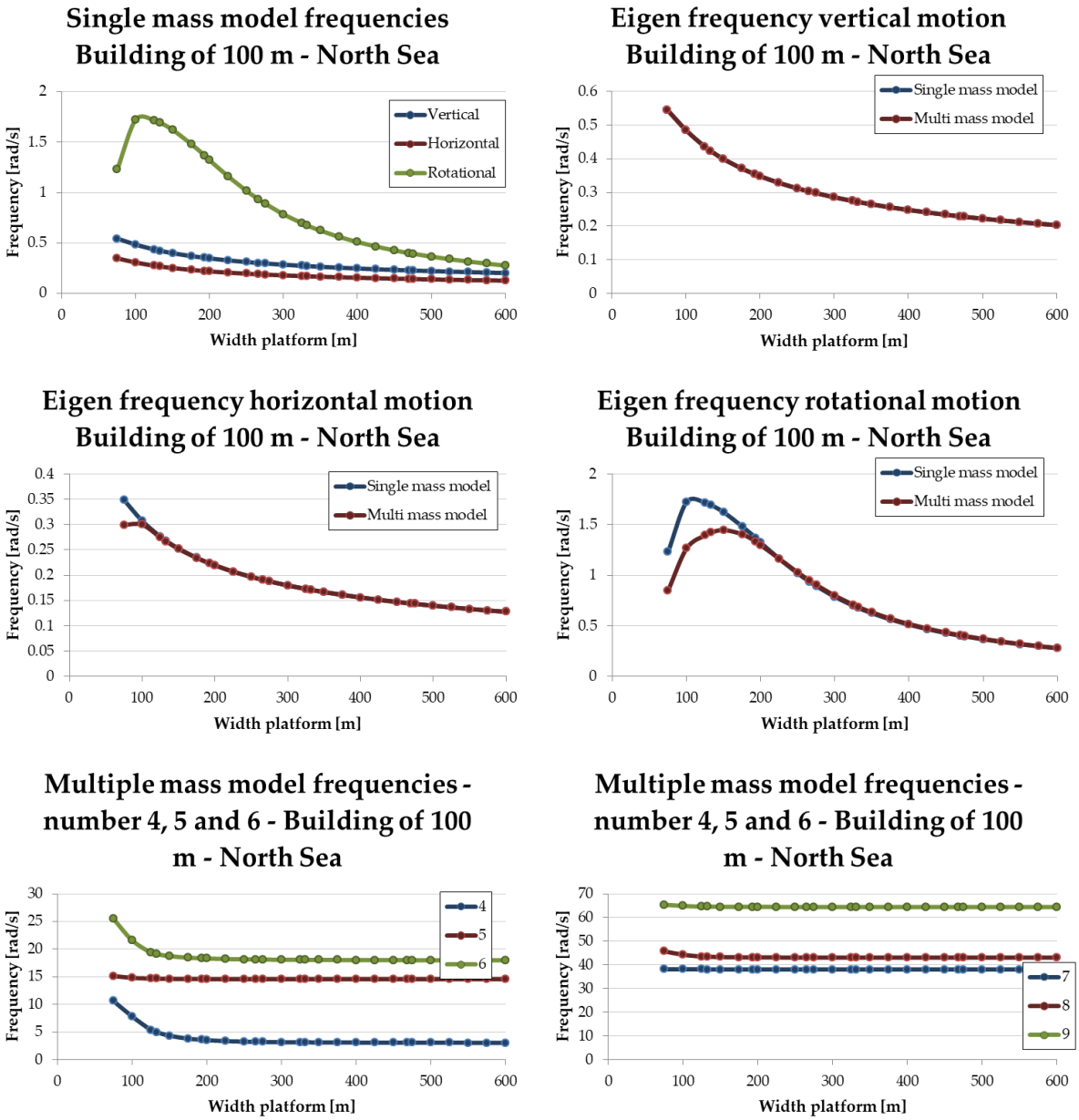

Figure 172 - Eigenfrequencies of both the single-mass model and the multi-mass model for a building of 100m. Numerically calculated

BUILDING HEIGHT = 300 M

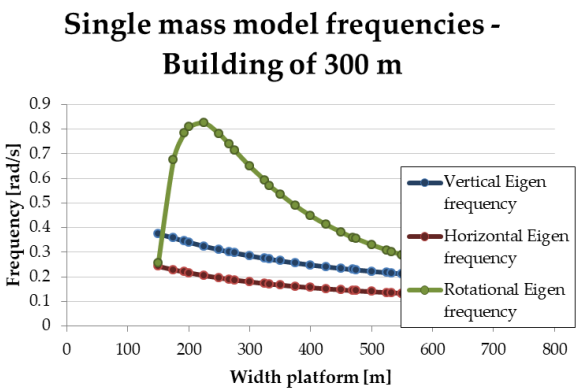

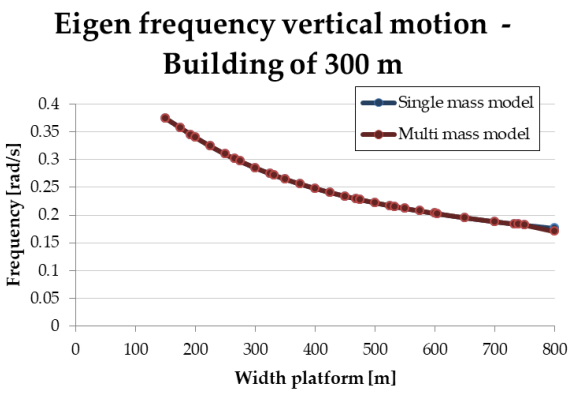

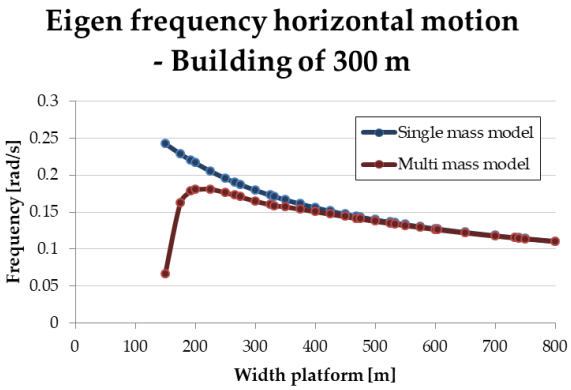

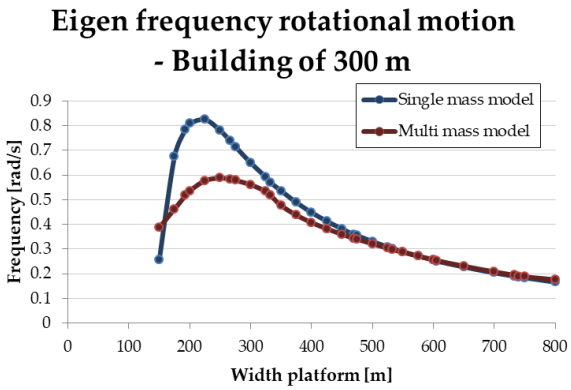

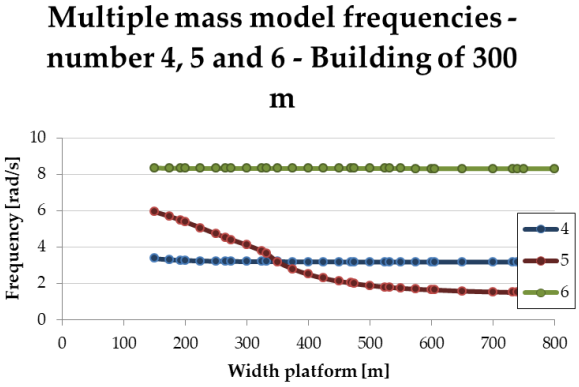

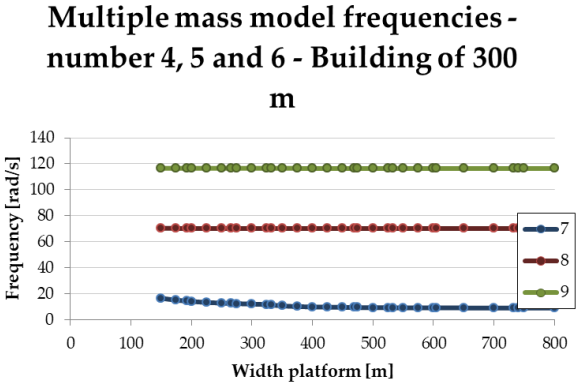

BUILDING HEIGHT = 500 M

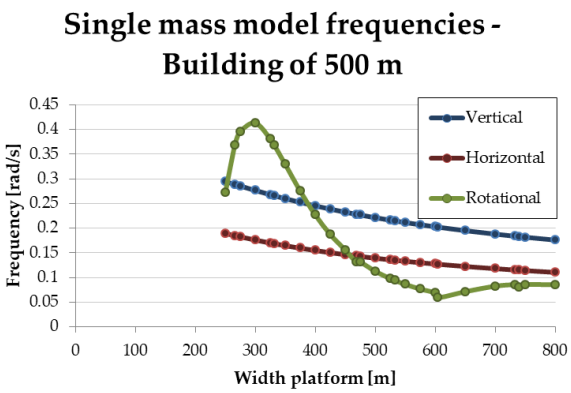

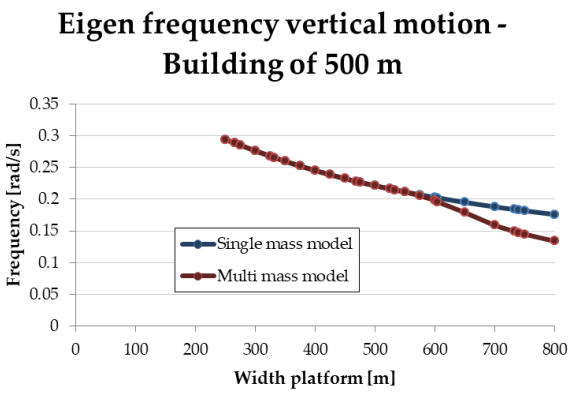

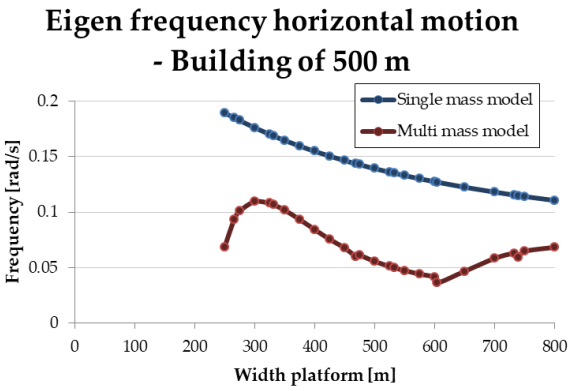

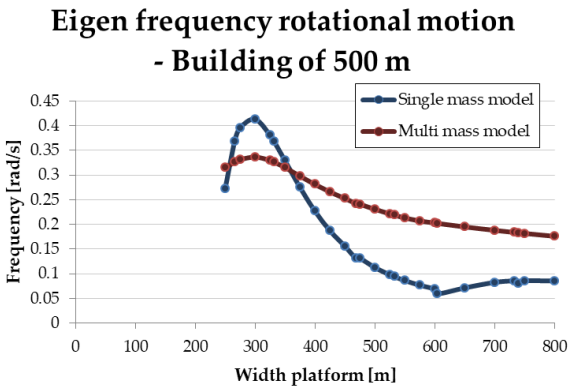

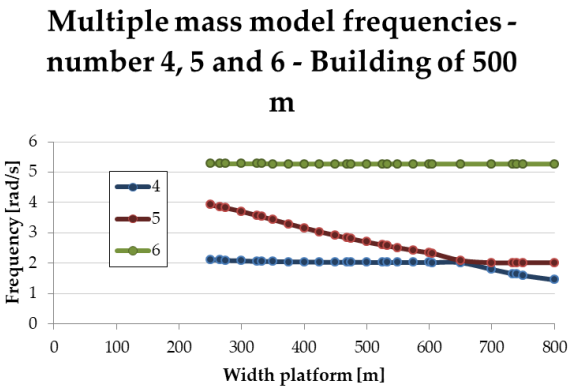

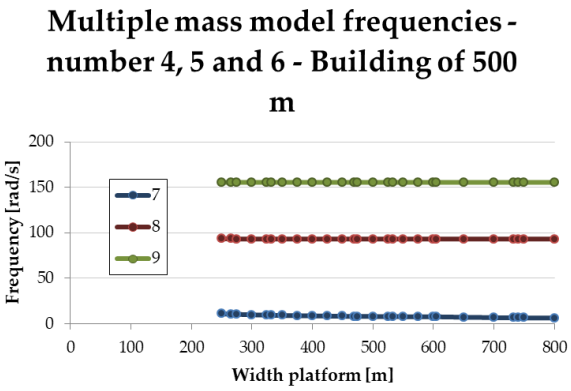

CALCULATIONS

Most of the calculation are done in maple. In the following figures the standard script is shown to calculate the different limits.

```
> restart :
>
```

Limits of the frequencies

```
>
> limitlow := 0.43 :#0.43 or 0.30 depending on the location
> limithigh := 1.44 : #1.44 or 1.01 depending on the location
>
```

Input values

This first part gives the undependend parameters a value. The name is writen after the value. The red values are changed during the study to investigate different options.

```
>
```

Input values

```
> n := 3 : #number of masses
> g := 9.81 :

> d := 20 : #Depth platform
> hp := 25 : #Height platform
>
> E := 1/3 ·3.9·10^10 :#[N/m^2] Youngs modules concrete
> rho := 1025 :
>
>
```

The calculation of other used values

In this section the dependend parameters are expressed in either the building height or the platform width, other input values and/or eachother.

```
>
```

Building

```
> n_stories := hb/4 :#Number of stories

> wb := evalf((17/3475290)·hb^2 + (421523/3475290)·hb + 104225/8911);# Width of the building [m]
```

$$wb := 4.891678105\ 10^{-6}\ hb^2 + 0.1212914606\ hb + 11.69621816 \quad (1)$$

```
> mass_building := n_stories·wb^2·13.04·10^3/9.81 #mass of the building [kg]
```

$$mass\_building := 332.3139652\ hb\ (4.891678105\ 10^{-6}\ hb^2 + 0.1212914606\ hb + 11.69621816)^2 \quad (2)$$

```
>
>
```

Platform

```
> EI_platform := E·(0.01198·hp^3 - 0.05448·hp^2 + 1.1877·hp - 1.099)·wp
      #Stiffness of the platform
```

(3)

$$EI\_platform := 2.362503000\ 10^{12}\ wp \tag{3}$$

> $$mass\_platform := \frac{hp}{5} \cdot \frac{\left(\frac{wp^3}{6000} + 2.45 \cdot wp^2 + 43.33 \cdot wp - 2000\right) \cdot 10^3}{9.81} : \#\ Mass\ platform\ [kg]$$

For the extraballst a max command is added in order for it not to have a negative extra ballast. This is the case if the mass of the platform and the mass of the building is enough to reach the aquired depth.

> $$extra\_ballast := \max\left(d \cdot wp^2 \cdot \mathrm{rho} - (mass\_platform + mass\_building), 0\right); \#extra\ ballast\ [kg]$$

$$extra\_ballast := \max\left(0,\ 19251.27421\ wp^2 - 332.3139652\ hb\ \left(4.891678105\ 10^{-6}\ hb^2 + 0.1212914606\ hb + 11.69621816\right)^2 - 0.08494733267\ wp^3 - 22084.60755\ wp + 1.019367992\ 10^6\right) \tag{4}$$

> $$total\_mass := mass\_building + mass\_platform + extra\_ballast; \#\ total\ mass\ [kg]$$

$$total\_mass := 332.3139652\ hb\ \left(4.891678105\ 10^{-6}\ hb^2 + 0.1212914606\ hb + 11.69621816\right)^2 + 0.08494733267\ wp^3 + 1248.725790\ wp^2 + 22084.60755\ wp - 1.019367992\ 10^6 + \max\left(0,\ 19251.27421\ wp^2 - 332.3139652\ hb\ \left(4.891678105\ 10^{-6}\ hb^2 + 0.1212914606\ hb + 11.69621816\right)^2 - 0.08494733267\ wp^3 - 22084.60755\ wp + 1.019367992\ 10^6\right) \tag{5}$$

>

> $$COG := \frac{(mass\_platform + extra\_ballast) \cdot \frac{1}{2} \cdot hp + mass\_building \cdot \left(hp + \frac{1}{2} \cdot hb\right)}{mass\_platform + extra\_ballast + mass\_building};$$
> $$\#\ Centre\ of\ gravity\ from\ the\ bottom\ of\ the\ platform\ [m]$$

$$COG := \left(1.061841658\ wp^3 + 15609.07238\ wp^2 + 276057.5944\ wp - 1.274209990\ 10^7 + \frac{1}{2}\left(25 \max\left(0,\ 19251.27421\ wp^2 - 332.3139652\ hb\ \left(4.891678105\ 10^{-6}\ hb^2 + 0.1212914606\ hb + 11.69621816\right)^2 - 0.08494733267\ wp^3 - 22084.60755\ wp + 1.019367992\ 10^6\right)\right) + 332.3139652\ hb\ \left(4.891678105\ 10^{-6}\ hb^2 + 0.1212914606\ hb + 11.69621816\right)^2 \left(25 + \frac{hb}{2}\right)\right) \Big/ \left(332.3139652\ hb\ \left(4.891678105\ 10^{-6}\ hb^2 + 0.1212914606\ hb + 11.69621816\right)^2 + 0.08494733267\ wp^3 + 1248.725790\ wp^2 + 22084.60755\ wp - 1.019367992\ 10^6 + \max\left(0,\ 19251.27421\ wp^2 - 332.3139652\ hb\ \left(4.891678105\ 10^{-6}\ hb^2 + 0.1212914606\ hb + 11.69621816\right)^2 - 0.08494733267\ wp^3 - 22084.60755\ wp + 1.019367992\ 10^6\right)\right) \tag{6}$$

> $$GM := \frac{\left(\frac{1}{12} \cdot wp^4\right)}{wp^2 \cdot d} + \frac{1}{2} \cdot d - COG\#\ GM\ value\ [m]$$

$$GM := \frac{wp^2}{240} + 10 - \left(1.061841658\, wp^3 + 15609.07238\, wp^2 + 276057.5944\, wp - 1.274209990\, 10^7 + \frac{1}{2}\left(25 \max\left(0, 19251.27421\, wp^2 - 332.3139652\, hb\, \left(4.891678105\, 10^{-6}\, hb^2 + 0.1212914606\, hb + 11.69621816\right)^2 - 0.08494733267\, wp^3 - 22084.60755\, wp + 1.019367992\, 10^6\right)\right) + 332.3139652\, hb\, \left(4.891678105\, 10^{-6}\, hb^2 + 0.1212914606\, hb + 11.69621816\right)^2 \left(25 + \frac{hb}{2}\right)\right) \Big/ \left(332.3139652\, hb\, \left(4.891678105\, 10^{-6}\, hb^2 + 0.1212914606\, hb + 11.69621816\right)^2 + 0.08494733267\, wp^3 + 1248.725790\, wp^2 + 22084.60755\, wp - 1.019367992\, 10^6 + \max\left(0, 19251.27421\, wp^2 - 332.3139652\, hb\, \left(4.891678105\, 10^{-6}\, hb^2 + 0.1212914606\, hb + 11.69621816\right)^2 - 0.08494733267\, wp^3 - 22084.60755\, wp + 1.019367992\, 10^6\right)\right) \tag{7}$$

> $r := COG - d$;#COG from the bottom

$$r := \left(1.061841658\, wp^3 + 15609.07238\, wp^2 + 276057.5944\, wp - 1.274209990\, 10^7 + \frac{1}{2}\left(25 \max\left(0, 19251.27421\, wp^2 - 332.3139652\, hb\, \left(4.891678105\, 10^{-6}\, hb^2 + 0.1212914606\, hb + 11.69621816\right)^2 - 0.08494733267\, wp^3 - 22084.60755\, wp + 1.019367992\, 10^6\right)\right) + 332.3139652\, hb\, \left(4.891678105\, 10^{-6}\, hb^2 + 0.1212914606\, hb + 11.69621816\right)^2 \left(25 + \frac{hb}{2}\right)\right) \Big/ \left(332.3139652\, hb\, \left(4.891678105\, 10^{-6}\, hb^2 + 0.1212914606\, hb + 11.69621816\right)^2 + 0.08494733267\, wp^3 + 1248.725790\, wp^2 + 22084.60755\, wp - 1.019367992\, 10^6 + \max\left(0, 19251.27421\, wp^2 - 332.3139652\, hb\, \left(4.891678105\, 10^{-6}\, hb^2 + 0.1212914606\, hb + 11.69621816\right)^2 - 0.08494733267\, wp^3 - 22084.60755\, wp + 1.019367992\, 10^6\right)\right) - 20 \tag{8}$$

>

Depth limit

>

For the depth limit the relation between the height of the building and the width of the building is calculated for which the extra ballast is zero and thus the mass of the platform and building make sure that the depth is equal to the input depth "d"

> $d\_uit := \frac{mass\_platform + mass\_building}{wp^2 \cdot \mathrm{rho}}$:

> $eq1 := d\_uit = d$:

> $sol := solve(\{eq1\}, \{hb\})$: $assign(sol)$

> $depthlimit := hb$;

$$depthlimit := 2000.\ RootOf\left(795177959563301288089544233\ \_Z^5 + 19716811712074122953812432760\ \_Z^4 + 123172559037120508204541033768\ \_Z^3 + 265460414593750000\ wp^3 + 1178594166735660788939288848 0\ \_Z^2 - 60160231906250000000000\ wp^2 + 284131595663291559850991632\ \_Z + 690143985937500000000000\ wp - 3185524975000000000000000\right) \quad (9)$$

> $hb := 'hb'$:

Stability limit

The stability limit was determind in the stability chapter.

> $stability\_limit := 2.3936 \cdot wp - 44.817$;

$$stability\_limit := 2.3936\ wp - 44.817 \quad (10)$$

>

>

Vertical motion

Firs the input parameters for the Eigen frequencie are calculated

> $a := \frac{1}{2} \cdot wp \cdot \mathrm{rho} \cdot \pi \cdot \left(\frac{wp}{2}\right)^2$: $k := \mathrm{rho} \cdot g \cdot wp^2$: $m := total\_mass$:

Than the Eigen frequencie is calculated and ploted.

> $\omega\_vertical := \mathrm{sqrt}\left(\frac{k}{m + a}\right)$;

$$\omega\_vertical := 100.2758695 \left(wp^2 \Big/ \left(332.3139652\ hb\ \left(4.891678105\ 10^{-6}\ hb^2 + 0.1212914606\ hb + 11.69621816\right)^2 + 0.08494733267\ wp^3 + 1248.725790\ wp^2 + 22084.60755\ wp - 1.019367992\ 10^6 + \max\left(0, 19251.27421\ wp^2 - 332.3139652\ hb\ \left(4.891678105\ 10^{-6}\ hb^2 + 0.1212914606\ hb + 11.69621816\right)^2 - 0.08494733267\ wp^3 - 22084.60755\ wp + 1.019367992\ 10^6\right) + \frac{1025\ wp^3\ \pi}{8}\right)\right)^{1/2} \quad (11)$$

> $plot3d([\omega\_vertical, limitlow], hb = 0 \ldots 600, wp = 0 \ldots 600, labels = [$"Height building [m]",

"Width platform [m]", "Frequency [rad/s]"], *labeldirections* = [*horizontal*, *horizontal*, *vertical*])

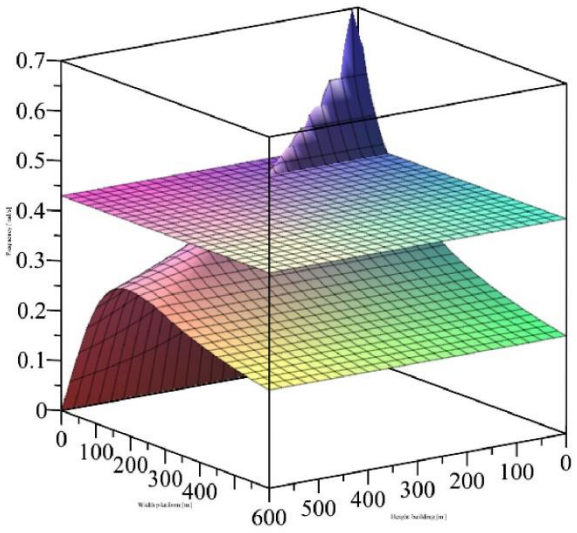

Than the equation is set up in which the frequency is set equal to the limiting frequency. This is done for both the limits.

```
> eq1 := ω_vertical = limitlow :
> sol := solve({eq1}, {hb}) : assign(sol)
> vertical_limitlow := hb :
> hb :='hb':
> eq1 := ω_vertical = limithigh :
> sol := solve({eq1}, {hb}) : assign(sol)
> vertical_limitup := hb :
> hb :='hb':
>
>
> hb :='hb':
>
>
```

Now the vertical depth limit is calculated. This is the width of the platform for which the resulting frequency limit is vertical. This can be seen in the graph after.

```
> eq1 := vertical_limitlow = depthlimit :
```

```
> sol := solve({eq1}, {wp}); assign(sol[2])
```

$$sol := \{wp = 0.\}, \{wp = 84.17566363\} \quad \textbf{(12)}$$

```
> with(plots) :

> border_vertical := wp
```

$$border\_vertical := 84.17566363 \quad \textbf{(13)}$$

```
> wp := border_vertical : vertical_limitlow2 := vertical_limitlow : wp :='wp':
> AA := plot(vertical_limitlow, wp = 0 .. border_vertical, ) :
> BB := plot([[border_vertical, 0], [border_vertical, vertical_limitlow2]]) :
> CC := plot(0, wp = border_vertical .. 300, y = 0 .. 300) :
> display({AA, BB, CC}, labels = ["Width platform [m]", "Height building [m]"], labeldirections
    = [horizontal, vertical], title = "Limitations vertical motion - depth = 20 m - North Sea",
    axesfont = ["Palatino Linotype", 12], titlefont = ["Palatino Linotype", 20], labelfont
    = ["Palatino Linotype", 14]);
```

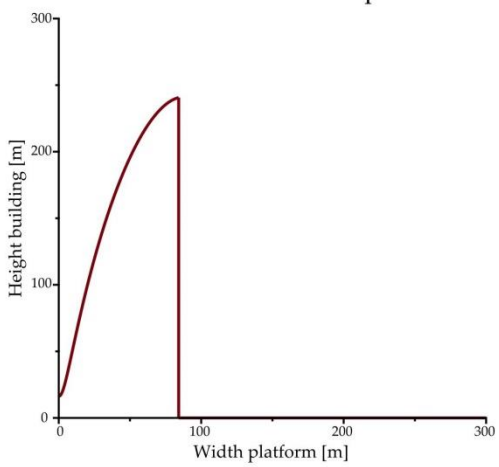


```
>
>
>
>
>
```

Horizontal motion

The calculations for the horizontal motion is the same as for the vertical motion.

```
> a := 1/2 ·rho·3.1415 ·d^2·wp : k := rho·g·wp·(d) : m := total_mass :

> ω_horizontal := sqrt(k/(m + a));
```

$$\omega\_horizontal := 448.4473213 \quad \textbf{(14)}$$

$$\left(wp \Big/ \left(332.3139652\, hb \left(4.891678105\, 10^{-6}\, hb^2 + 0.1212914606\, hb + 11.69621816\right)^2 + 0.08494733267\, wp^3 + 1248.725790\, wp^2 + 666092.1076\, wp - 1.019367992\, 10^6 + \max\left(0,\ 19251.27421\, wp^2 - 332.3139652\, hb \left(4.891678105\, 10^{-6}\, hb^2 + 0.1212914606\, hb + 11.69621816\right)^2 - 0.08494733267\, wp^3 - 22084.60755\, wp + 1.019367992\, 10^6\right)\right)\right)^{1/2}$$

```
> plot3d( [ω_horizontal, limitlow], hb = 0 ... 200, wp = 0 ... 400, labels = ["Height building [m]",
      "Width platform [m]", "Frequency [rad/s]"], labeldirections = [horizontal, horizontal,
      vertical])
```

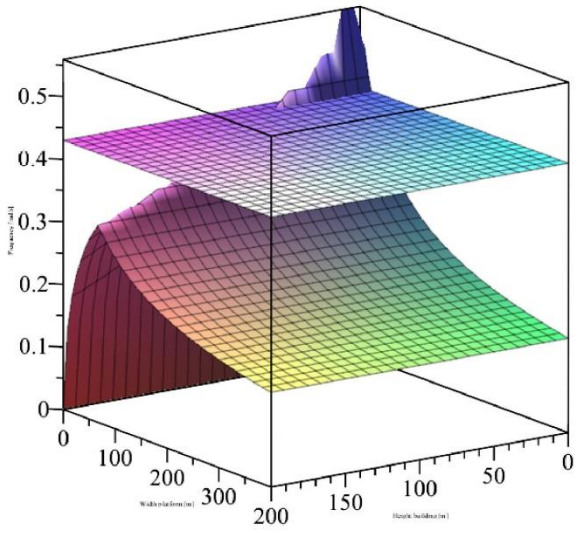


```
> eq1 := ω_horizontal = limitlow :

> sol := solve( {eq1}, {hb} ) : assign(sol)
> horizontal_limitlow := hb :
> hb :='hb':
>
> eq1 := ω_horizontal = limithigh :

> sol := solve( {eq1}, {hb} ) : assign(sol)
> horizontal_limitup := hb :
>
```

```
> hb := horizontal_limitlow :
> #for wp from 0 by 10 to 800 do simplify(evalf(ω_horizontal)) end do
> hb :='hb':
>
> eq1 := horizontal_limitlow = depthlimit :
> sol := solve({eq1}, {wp}); assign(sol[2])
```

$$sol := \{wp = 0.\}, \{wp = 21.64070578\} \quad \textbf{(15)}$$

```
> border_horizontal := wp
```

$$border\_horizontal := 21.64070578 \quad \textbf{(16)}$$

```
> wp := border_horizontal : horizontal_limitlow2 := horizontal_limitlow : wp :='wp':
>
> DD := plot(horizontal_limitlow, wp = 0 .. border_horizontal) :
> EE := plot([[border_horizontal, 0], [border_horizontal, horizontal_limitlow2]]) :
> CC := plot(0, wp = border_horizontal .. 300, y = 0 .. 300) :
> display({DD, EE, CC });
```

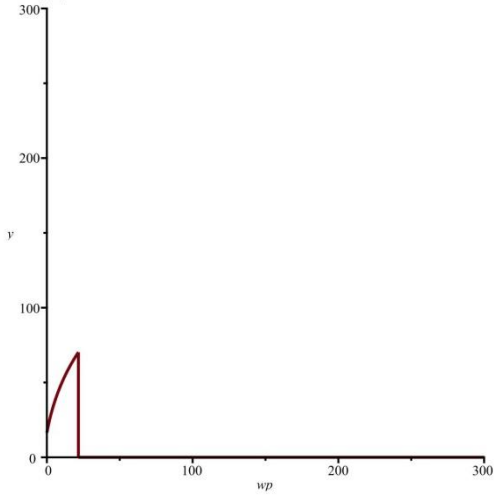


```
>
>
>
```

Rotational motion

The calculations for the horizontal motion is the same as for the vertical motion. In this case the extra ballast is not limited in order for the programe to be able to calculate. As the depth limit is used this is not a problem for the final graphs

```
> extra_ballast := d·wp^2·rho - (mass_platform + mass_building) :
> total_mass := mass_building + mass_platform + extra_ballast :
>
> k := simplify(evalf((0.0329 wp^4 ρ g (9.91 10^-11 g^3 ρ^3 wp^15
```

$$+ 0.0000228\, g^2\, \rho^2\, wp^{10}\, EI\_platform + 0.889\, g\, \rho\, wp^5\, EI\_platform^2 + 3240.\, EI\_platform^3\Big)$$

$$EI\_platform\Big) \Big/ \Big(5.23\ 10^{-14}\, g^4\, \rho^4\, wp^{20} + 1.53\ 10^{-8}\, g^3\, \rho^3\, wp^{15}\, EI\_platform$$

$$+ 0.000891\, g^2\, \rho^2\, wp^{10}\, EI\_platform^2 + 6.58\, g\, \rho\, wp^5\, EI\_platform^3 + 1300.\, EI\_platform^4\Big)$$

$$- d\, wp^2\, \rho\, g\left(COG - \frac{d}{2}\right)\Big)\Big) :$$

>

> $a := \mathrm{rho}\cdot\pi\cdot\left(\left(\frac{wp}{4}\right)^2\cdot\left(\frac{wp}{4}\right)^2 + \left(\frac{d}{2}\right)^2\cdot\left(\frac{d}{2} + r\right)^2\right) : m := total\_mass :$

> $Imm := m\cdot K^2 : K := \mathrm{sqrt}\left(\frac{Ipol}{Aw}\right) : Ipol := Ixx + Izz : Ixx := \frac{1}{12}\cdot d\cdot wp^3 : Izz := \frac{1}{12}\cdot wp\cdot d^3 :$
$Aw := d\cdot wp :$

> $\omega\_rotational := simplify\left(evalf\left(\mathrm{sqrt}\left(\frac{k}{Imm + a}\right)\right)\right) :$

>

> $plot3d([\omega\_rotational, limitlow], wp = 0 \ldots 1000, hb = 0 \ldots 1000, labels = [\text{"Width platform [m]"}, \text{"Height building [m]"}, \text{"Frequency [rad/s]"}], labeldirections = [horizontal, horizontal, vertical])$

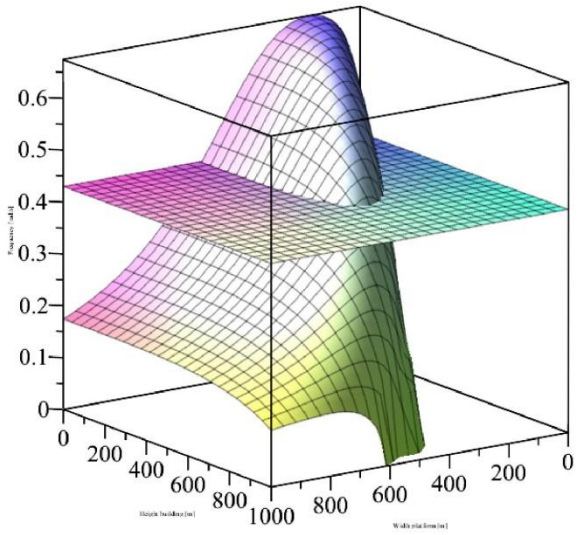

>

> $eq1 := simplify(evalf(\omega\_rotational)) = limitlow :$

```
> sol := solve({eq1}, {hb}) : assign(sol)
> rotational_limitlow := hb :
> hb :='hb':
>
> eq1 := simplify(evalf(ω_rotational)) = limithigh :

> sol := solve({eq1}, {hb}) : assign(sol)
> rotational_limitup := hb :
> hb :='hb':
> plot([rotational_limitlow], wp = 0 .. 800, labels = ["Width platform [m]",
      "Height building [m]"], labeldirections = [horizontal, vertical], title
      = "Limitations rotational motion - depth = 20 m - North Sea", axesfont
      = ["Palatino Linotype", 12], titlefont = ["Palatino Linotype", 20], labelfont
      = ["Palatino Linotype", 14])
```

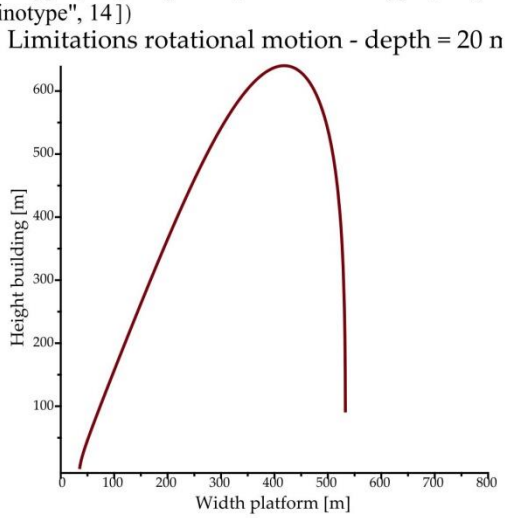


```
>
```

Total graphs

```
> plot([[[border_vertical, 0], [border_vertical, vertical_limitlow2]], [[border_horizontal, 0],
      [border_horizontal, horizontal_limitlow2]], rotational_limitlow, depthlimit, stability_limit],
      wp = 0 ..800, y = 0 ..800, labels = ["Width platform [m]", "Height building [m]"],
      labeldirections = [horizontal, vertical], legend = ["Lower limit vertical motion",
      "Lower limit horizontal motion", "Lower limit rotational motion", "Depth limit",
      "Stability limit"], title = "Limitations - depth = 20 m - North Sea", axesfont
      = ["Palatino Linotype", 12], titlefont = ["Palatino Linotype", 20], labelfont
      = ["Palatino Linotype", 14],
   legendstyle = [font = ["Palatino Linotype", 12]])
```

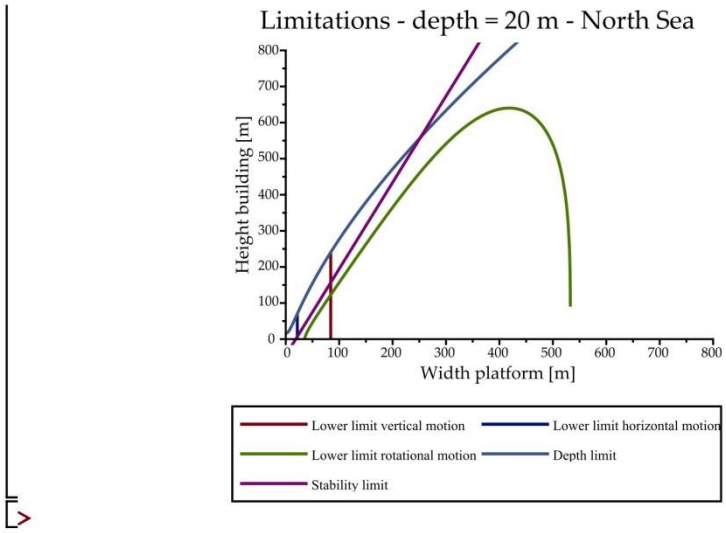

For the rotational frequency limit, sometimes a numerical approach had to be used. For this Python has been used. First, a function is defined to determine the eigenfrequency with as input the height of the building and the width of the platform. The expression used for the eigenfrequency comes from the Maple script shown above. Next, for 100 platform widths (from 0m to 1000 m) the eigenfrequency is calculated for building heights of 0 to 1000 with steps of 1. This determines for which building height at this platform width, the eigenfrequency is closest to the limit. The 100 resulting points are then used in the curve fitting. A polynomial of degree ten is used. The curve fit is the rotation frequency limit used to create the graphs in this appendix.

In [44]:
```
import numpy as np
import matplotlib.pyplot as plt
from scipy.optimize import curve_fit
```

In [45]:
```
def func (hb,wp):
    omega = np.sqrt(-(7.951779595*10**(-9)*hb**5 + 0.0003943362341*hb**4 + 4.92690236*hb**3 + 942.8753333*hb**2 + 45461.05529*hb
    return omega
```

In [46]:
```
limit = 0.43
```

In [47]:
```
hblim = np.zeros(100)
for wp in range (100):
    count = 999999
    for hb in range (1000):
        #print(func(hb,wp))
        if np.isnan(func(hb,(wp+1)*10)) == False:
            value = abs(func(hb,(wp+1)*10) - limit)
        else:
            value = 9999999

        if value < count:
            count = value
            hblim[wp] = hb
    if hblim[wp] == 0:
        if hblim[wp-1] != 0:
            break
    #print(hblim[wp],(wp+1)*10)

print(hblim)
```

```
C:\Users\boris\anaconda3new\lib\site-packages\ipykernel_launcher.py:2: RuntimeWarning: invalid value encountered in sqrt
```

```
[  0.   0.   0.   0.   0.  17.  54.  79. 102. 124. 145. 165. 186. 206.
 226. 245. 265. 284. 303. 322. 341. 360. 378. 396. 414. 432. 449. 466.
 482. 498. 514. 529. 543. 557. 570. 582. 594. 605. 614. 623. 630. 636.
 641. 644. 646. 645. 642. 636. 627. 614. 596. 571. 535. 481. 385.   0.
   0.   0.   0.   0.   0.   0.   0.   0.   0.   0.   0.   0.   0.   0.
   0.   0.   0.   0.   0.   0.   0.   0.   0.   0.   0.   0.   0.   0.
   0.   0.   0.   0.   0.   0.   0.   0.   0.   0.   0.   0.   0.   0.
   0.   0.]
```

In [48]:
```
wp = np.arange(100)*10
plt.plot(wp,hblim,'ro')
```

Out[48]:
```
[<matplotlib.lines.Line2D at 0x1aee2dbb048>]
```

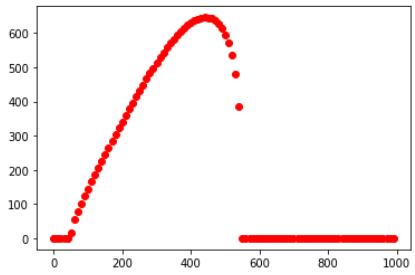

In [49]:
```
hblimnozeros = []
wpnozeros = []
for i in range (len(hblim)):
    if hblim[i] != 0.0:
        hblimnozeros.append(hblim[i])
        wpnozeros.append(wp[i])
xdata = wpnozeros
ydata = hblimnozeros
poly = np.polyfit(xdata, ydata, deg=10)

fig, ax = plt.subplots()
ax.plot(xdata,ydata, label='data')
ax.plot(xdata,np.polyval(poly, xdata), label='fit')
ax.legend()

for i in range(len(poly)):
    print(poly[i] ,"*x^",10-i)
```

```
-1.2827903361475623e-21 *x^ 10
3.6553492753362004e-18 *x^ 9
-4.534278333633919e-15 *x^ 8
3.213034234441481e-12 *x^ 7
-1.4350137967919754e-09 *x^ 6
4.204800200411345e-07 *x^ 5
-8.15686974834685e-05 *x^ 4
0.01031307730455926 *x^ 3
-0.8126414140442336 *x^ 2
38.14254195421076 *x^ 1
-748.9176217440454 *x^ 0
```